Multiple Vehicle Design Fire Scenarios in Car Parking Buildings

by

Mohd Zahirasri bin Mohd Tohir

Supervised by

Associate Professor Michael Spearpoint

and

Professor Charles Fleischmann

2015

A thesis submitted in partial fulfilment of the requirements
for the PhD Degree in Fire Engineering

Department of Civil and Natural Resources Engineering
University of Canterbury
Private Bag 4800
Christchurch, New Zealand

Abstract

Over recent years, there is considerable interest in the research of vehicle fires in car parking buildings. The acceptance towards performance-based design engineering approach around the world has led the use of engineering approaches to the assessment of fire safety in structures. In fire safety context of performance-based design, one of the fundamental components is design scenario.

The aim of this thesis is to formulate an approach that is able to develop appropriate design fire scenarios for vehicle fires in car parking buildings using probabilistic assessment methods as part of a risk-based approach. This is achieved by creating a probabilistic model to investigate the risks associated with vehicle fires in car parking buildings, such that fire risk is equal to probability multiplied by consequence. The probability component depends on a number of factors which are the vehicle parking distribution probability, i.e. the probability of vehicles being distributed in a particular pattern throughout the building at a given time; the vehicle classification i.e. the composition of different vehicle types in a fleet; and the vehicle fire involvement, i.e. the likely number of vehicles involved in a fire. The consequence component is defined as the severity of the fire in terms of fire growth, energy released, and number of vehicles involved in burning.

The thesis consists of three tasks; the first task is the collation of results for single passenger vehicle experiments and the application of probabilistic assessment model for vehicle fire scenarios in car parking buildings. In the first task, probability distributions for fire severity characteristics for a single passenger vehicle are introduced and a probabilistic quantitative fire risk analysis is performed. The second task enhances specific probabilistic assessment components based on the findings made in the first task. Two main focuses in this task are to introduce probability distributions of characteristics for the design fire curves for a single vehicle, and to develop an approach of predicting the time to ignition for subsequent vehicle given the first vehicle is already burnings as there is a need to assess the fire spreading between vehicles. The final task applies the enhanced components obtained from the second task into the probabilistic assessment model. As a result, a conclusion is drawn following the completed work in the final task.

Example demonstrations of the application of the probabilistic model are also shown in the thesis. One is using probabilistic model to determine the fire load energy densities for risk-based design of car parking buildings. The other work is about the analysis of the probability of fire spread from a vehicle to another vehicle in car parks.

Acknowledgement

This thesis would not have been possible without the tireless assistance, guidance and motivation provided by my main supervisor, Associate Professor Michael Spearpoint. His patience, encouragement, and on-going support throughout the whole journey were invaluable to me. I will be forever indebted to him.

I would like to extend my appreciation to Professor Charles Fleischmann as my associate supervsior; Dr. Anthony Abu from Fire Engineering teaching staff; Greg Baker from BRANZ; Colleen Wade from BRANZ; Neil Challands from the NZFS; the Fire Engineering research group; and other postgraduates students for all their help and guidance. I apologise to anyone whom I forget to mention here.

I would like to also take this opportunity to thank the Ministry of Education, Malaysia and Universiti Putra Malaysia for funding my PhD studies at University of Canterbury.

I could not have completed this thesis without the unwavering support and assistance given by my parents; Mohd Tohir and Siti Zalehah, my in-laws, my brothers and my sisters.

My deepest appreciation goes out to my wife, Hafisha and our 2 children – Nusayba and Usayd. Thank you for your patience, faith and presence during this last four years. Thank you for simply being the joy that brightens my life.

Most importantly I thank God for giving me the opportunity to partake in this academic endeavour and for reminding me that this thesis is only a start of another journey.

List of publications, presentations and supervised project

The thesis is based on the following papers:

1. Tohir, M.Z.M., and Spearpoint, M., (2013) Distribution analysis of the fire severity characteristics of single passenger road vehicles using heat release rate data, Fire Science Reviews 2:5, http://dx.doi.org/10.1186/2193-0414-2-5
2. Tohir, M.Z.M, and Spearpoint, M., (2014a) Development of Fire Scenarios for Car Parking Buildings using Risk Analysis. Fire Safety Science (in press). http://www.iafss.org/publications/fss/11/141/view
3. Tohir, M.Z.M, and Spearpoint, M., (2014b) Simplified approach to predict heat release rate curves from multiple vehicle fires in car parking buildings. Published in the Proceedings from the 3rd International Fires in Vehicles Conference, Berlin, Germany.
4. Spearpoint, M., Tohir, M.Z.M., Abu, A.K., and Xie, P. (2015) Fire load energy densities for the risk-based design of car parking buildings. Case Studies in Fire Safety (in press). http://dx.doi.org/10.1016/j.csfs.2015.04.001
5. Tohir, M.Z.M., Spearpoint, M., and Fleischmann, C.M., Prediction of time of ignition in a multiple vehicle fire spread experiment. Submitted to Fire & Materials.

In addition, the author gave a presentation related to one chapter in the thesis:

1. "The capability of B-RISK zone modelling software to simulate BRE multiple vehicle fire spread test" Presented at Society of Fire Protection Engineers' 2014 Engineering Technology Conference, Long Beach, California.

The author also involved in the supervisory team for an undergraduate fire engineering research project related to the thesis. The project is:

1. Anderson C. M., and Bell N. M., (2014) Analysis of vehicle distribution in parking buildings. Proc. Civil and Natural Resources Engineering Research Conference, 18 Oct, University of Canterbury, New Zealand, vol. 2, 65-72.

Table of Contents

List of Figures

List of Tables

Nomenclature

Symbol	Description	Unit
A	Estimate of the surface area	m²
B	Constant	g/kJ
C	Constant	g/s/m²
E_{tot}	Total energy content	MJ
FTP	Flux-time product	$\frac{kW \cdot s^n}{m^2}$
$HRRPUA$	Heat release rate per unit area	kW/m²
ΔH_c	Heat of combustion	kJ/g
k_{ing}	The time width coefficient	-
L_g	Heat of gasification of fuel	kJ/g
$\dot{m}''$	Characteristic burning rate per unit area	-
n	Power law index	-
n_{ing}	The retard index	-
$n_{samples}$	The number of samples (i.e. experiments)	-
n_{space}	Number of parking spaces	-
$P(x)$	Probability of multiple vehicle fires	-
$\dot{Q}(t)$	The heat release rate	kW
$\dot{Q}(t)_{tot}$	Combined total heat release rate	kW
$\dot{Q}_f$	Heat release rate of free burning fuel item	kW
$\dot{Q}_{max}$	Peak heat release rate	kW
$\Delta\dot{Q}$	Additional heat release rate	kW
$\dot{q}''$	Incident radiation flux	kW/m²
$\dot{q}''_{cr}$	Critical heat flux	kW/m²
$\dot{q}''_e$	Radiant heat from the gas layers and the room surfaces	kW/m²
$\dot{q}''_{fl}$	Radiation heat flux received by the target ignition	kW/m²
$\dot{q}''_i$	Heat flux at ith time increment	kW/m²
r	Radial distance from the centre of the burning item to the nearest point of the target item	m
r_{ing}	The amplitude coefficient	-
t	Time	min, s

t_i	Time at ith time increment	min, s
t_{ig}	Time to ignition	min, s
t_{max}	Time to reach peak heat release rate	min, s
X	Coefficient in each classification	-
$\bar{X}$	Average of the coefficients in the data set	-
$x_{vehicle}$	Number of vehicles	-

Greek symbol	**Description**	**Unit**
κ	Shape parameter for probability distribution	-
α_{exp}	Exponential method fire growth coefficient	min^{-1}
α_{mowrer}	Mowrer 20-80 method fire growth coefficient	kW/min^2
α_{peak}	Peak method fire growth coefficient	kW/min^2
θ	Scale parameter for probability distribution	-
β_{exp}	Exponential decay coefficient	min^{-1}
β_{peak}	t-squared decay coefficient	kW/min^2
β_{power}	Power law decay coefficient	min^{-1}
λ_r	Radiative fraction	-
σ	Standard deviation of a growth/decay combination	-

Abbreviations	**Description**
ABS	Acrylonitrile butadiene styrene
ANSI	American National Standards Institute
BG	Beta general distribution
BHP	Broken Hill Proprietary Company Limited
BRANZ	Building Research Association New Zealand
BRE	Building Research Establishment, United Kingdom
BSPP	Fire Brigade of Paris, France
C/AS	Acceptable Solutions
C/VM2	New Zealand verification method for fire
CDF	Cumulative density function
CFD	Computational Fluid Dynamics
CIB	Conseil International du Bâtiment (English: International Council for Building)

CLG	Communities and Local Government, United Kingdom
CTICM	Centre Technique Industriel de la Construction Metallique, France
DFG	Design Fire Generator
DBH	Department of Building and Housing, New Zealand
DP	Date published
E	Exponential distribution
ECCS	European Convention for Constructional Steelwork
ED	Experiment date
EU	European Union
FDS	Fire Dynamics Simulator
FIRS	Fire incident reporting system
FLED	Fire load energy density
FRS	Fire Research Station, United Kingdom
FTP	Flux-time product
G	Gamma distribution
GPE	Greatest possible error
HFM	Heat flux measurement
HRR	Heat release rate
HVAC	Heating, ventilation and air conditioning
INERIS	National Competence Centre for Industrial Safety and Environmental Protection, France
LL	Log logistic distribution
LN	Log normal distribution
LOS	Level of service
LPG	Liquefied petroleum gas
MFPA	Leipzig Institute for Materials Research and Testing, Germany
MPV	Multi-purpose vehicle
MSI	Ministry of Science and Innovation, New Zealand
MVFRI	Motor Vehicle Fire Research Institute, USA
N/A	Not applicable
NBN	Bureau for Standardisation, Belgium
NZBC	New Zealand Building Codes
NZFS	New Zealand Fire Service

NZTA	New Zealand Transport Authority
PSM	Point source model
PVB	Polyvinyl Butyral
PVC	Polyvinyl Chloride
RS	Report submitted
SBO	Strategic Basic Research
SFPE	Society of Fire Protection Engineers
SHEVS	Smoke and heat exhaust ventilation system
SUV	Sport utility vehicle
T	Triangular distribution
UCVFire	University of Canterbury Vehicle Fire simulation tool
USA	United States of America
VBA	Visual Basic Application
W	Weibull distribution

Classification identifier	**Description**
M*x*	Passenger Car: Mini classification
L*x*	Passenger Car: Light classification
C*x*	Passenger Car: Compact classification
MED*x*	Passenger Car: Medium classification
H*x*	Passenger Car: Heavy classification
MPV*x*	Passenger Car: MPV classification
SUV*x*	Passenger Car: SUV classification
U*x*	Unknown classification

Method combination	**Description**
Ing	Ingason exponential curve
P.t	Peak growth and t-squared decay
P.p	Peak growth and Power law decay
P.e	Peak growth and Exponential decay
M.t	Mowrer 20-80 growth and t-squared decay

M.p	Mowrer 20-80 growth and Power law decay
M.e	Mowrer 20-80 gorwth and Exponential decay
E.t	Exponential growth and t-squared decay
E.p	Exponential growth and Power law decay
E.e	Exponential growth and exponential decay

Chapter 1 INTRODUCTION

1.1 Background

Vehicle fires in car parking buildings are relatively rare events compared to other types of fires in occupied buildings in New Zealand and the United Kingdom [1, 2]. However, even though it is a rare event, there have been several significant vehicle fires in car parking buildings around the world, some of them fatal. One notable incident in 2006 resulted in seven fire fighters killed when the roof of an underground car park collapsed due to a vehicle fire in Gretchenbach, Switzerland. Another notable incident, also in 2006, was in Bristol, United Kingdom where 22 vehicles were destroyed in an underground car park. This incident resulted in one fatality as a result of the fire spreading above ground [1]. These two examples show that vehicle fires in car parking buildings, despite being rare, can be calamitous to the occupants of the parking building itself or the occupants of neighbouring buildings.

An assessment of a major fire in an underground car park in Gothenburg in March 2011 concluded that the fire had caused severe damage to the concrete structure [3]. The fire lasted for about three and a half hours and destroyed 20 cars. This incident shows that despite no fatalities being reported, vehicle fires in car park could pose threat of structural failure. Recently (27th of February 2015) incident locally in New Zealand, a vehicle has caught fire in a shopping mall car park which eventually led to the evacuation of hundreds of shoppers [4]. The incident which took place in a car park attached to the shopping area produces smoke and spreads throughout the mall. This incident shows that fires in car parking buildings may cause significant disruption to the occupants in neighbouring buildings.

All of the incidents mentioned above show that vehicle fires in car parking buildings could potentially pose different sorts of problems. At the same time, the rapid development of new materials in automotive construction as well new types of fuels for vehicles pose new challenges regarding containment of vehicle fires. As a result, research on fires in vehicles is becoming more critical, therefore, these have led to considerable interest in the research of vehicle fires in car parking buildings over recent years.

Austroads [5] defines that a car parking building is a structure that is built specifically to park vehicles while they are not in use. This structure is normally built to cater to passenger vehicles, and NZTA [6] characterises that a passenger vehicle is constructed primarily for the carriage of passengers which has not more than nine seating positions (including the driver's

seating position). As this structure is built to park vehicles and not for the means of habitation for humans, the main occupants of the structure are usually the vehicle passengers and parking operator workers. Car parking buildings is commonly found as a form of a stand-alone building or mixed use with other building structures and can be designed to be single-storey, multi-storey or underground structure. These different forms of car parking buildings are constructed based on the functionalities and the design demands of a particular building, for instance, in shopping malls where the structure is built next to the shopping area for convenient access by shoppers.

The parking area inside a car parking building structure can be classified into two types; the first type is open; and the other one is fully enclosed. There is no uniformly used classification for car parks. One example, in the International Building Code [7], an open car park is defined by the exterior side of the structure having uniformly distributed openings on two or more sides. The area of such openings in exterior walls on a tier must be at least 20% of the total perimeter wall area of each tier. The aggregate length of the openings provides natural ventilation and constitutes a minimum of 40% of the perimeter of the tier. Interior walls are at least 20% open with uniformly distributed openings. In another example, the European Convention for Constructional Steelwork [8, 9] defines an open car park if the ventilation areas in the walls are situated in at least two opposite facades, equal at least to one-third of the total surface area of all the walls and corresponds to at least 5% of the floor area of one parking level. These two examples show that different jurisdictions or authorities have different definitions of classifications for car parks.

From a fire engineering point of view, there are two effects on fire growth in vehicle fires in car parking buildings; one is the local effect within a vehicle i.e. in the case of fire initiated in a vehicle and spreading to the whole vehicle, and another one is the global effect to the parking area in the sense of a vehicle is burning. This thesis focuses on the global effect in which, the two classifications of car park areas will have different effects on fire growth, occupant behaviours and structures if a fire occurs. For an open car park area where there is always fresh air present, a fire can burn freely as long as combustible materials are available. However, wind velocity and direction would have an effect on the fire spread and fire growth. In an enclosed car park where the immediate air supply is limited, the compartment fire effect will cause the fire to fully develop and produce a substantial amount of heat. From a life safety point of view, fires occurring in an enclosed car park will lead to incomplete

combustion, thus releasing a higher proportion of toxic gases compared to a car park with sufficient ventilation. These toxic gases will endanger the lives of anyone who may be present. These two classifications of car park areas present different problems and challenges in fire engineering.

For the fire protection of car parking buildings, any fire safety system may act to address life and for property safety, both in the building concerned and for the surrounding area. The system usually consists of passive and active fire control. Passive fire control is generally a type of fire control that is built into the structure of the building (e.g. fire resistant doors and protected beams and columns). Whereas active fire control is a type of fire control that requires manual or automatic motion and response in order to work (e.g. automatic sprinklers and fire extinguishers).

Fire safety is a regulatory requirement in New Zealand and compliance documents are one means of complying with the fire safety clauses of New Zealand Building Code (NZBC) [10]. The compliance documents consists of sets of prescriptive rules that contain at least Acceptable Solutions (AS) and/or Verification Methods (VM) [11]. The fire safety regulatory requirements for the design of car parking buildings can be found in Acceptable Solution C/AS7 [12]. Another way to comply with the fire safety clauses of NZBC is by offering an alternative solution based on specific fire engineering design. This enables the building owner to propose their own design as long as they demonstrate compliance with the NZBC.

The role of fire fighters when a fire occurs is also important for the safety of occupants inside car parking buildings. There is a requirement in the New Zealand Building Code to safeguard New Zealand Fire Service (NZFS) personnel while fire suppression and rescue operations take place. Thus, a design with a fire fighter's operation in mind will provide more efficient fire fighter intervention and this will result in a safer outcome for the occupants.

1.2 Initiative for the research

Over recent years, the performance-based design approach has gained acceptance in the engineering community around the world. This has prompted an expanded demand in engineering approaches to the assessment of fire safety in structures. Performance-based design is an approach which gives flexibility to achieve targeted objectives (i.e. health, safety, amenity and sustainability) of building a structure as long as safety can be

demonstrated. In fire safety engineering, the approach will provide a rational means of efficient and effective fire safety design to achieve the performance objectives. The common tasks required for the design process include defining the project scope, establishing objectives, developing performance criteria, and identifying and selecting appropriate design scenarios. In a fire safety context, a design scenario is fundamental to any fire safety evaluation process. The design scenario includes aspects such as fire loads, location of the fire, building characteristics, occupant response, fire protection systems, design fires, ventilation openings, and the like [13].

According to Fleischmann [13], there are unlimited numbers of potential design fire scenarios in achieving the performance criteria for a proposed building. Depending on the objective for the fire safety design e.g. life safety, property, and/or structure, different design fire scenarios may be required. There is the need for further research into how to determine reasonable fire scenarios and raises the possibility that a single set of scenarios may not be applicable to all types of car parking buildings given the variations in design and use. These scenarios need to consider the relative number, layout and type of vehicles that could be present in a parking building; the likelihood that multiple vehicles could burn simultaneously and the potential total energy that could be released by the burning vehicles.

Design fire scenarios for car parking buildings found from the literature focuses on satisfying the objectives for structure. According to the European Convention for Constructional Steelwork (ECCS) (1993) [8, 9], there are two critical scenarios in an open car park:

- Scenario 1: Implies only one vehicle burning at mid-span under the beam. It corresponds to the maximum bending moment position and so the most critical situation for the beams.
- Scenario 2: Two burning vehicles are considered, parked at each side of a beam.

Joyeux et al. [14] in their experimental tests, introduced another two scenarios which are defined as:

- Scenario 3: Three vehicles of parked on consecutive bays. The vehicle in the middle is ignited.
- Scenario 4: Two vehicles parked on parking bays located in front each other.

The National Competence Centre for Industrial Safety and Environmental Protection (INERIS), France suggests three scenarios for design fire scenarios in car parks [15]. One scenario is identical to Scenario 1 mentioned earlier and the vehicle is assumed to be a small van full of inflammable products, commonly known as a utility vehicle. The other scenarios are defined as:

- Scenario 5: Seven vehicles, including a utility vehicle, parked in a single row with the vehicle in the middle to be ignited first.
- Scenario 6: Four cars, including a utility vehicle, with two vehicles at each row facing each other.

For Scenario 5 and 6, the time of propagation of fire from one vehicle to another is 12 minutes [15]. Scenarios 1 to 6 are best represented visually in Figure 1-1.

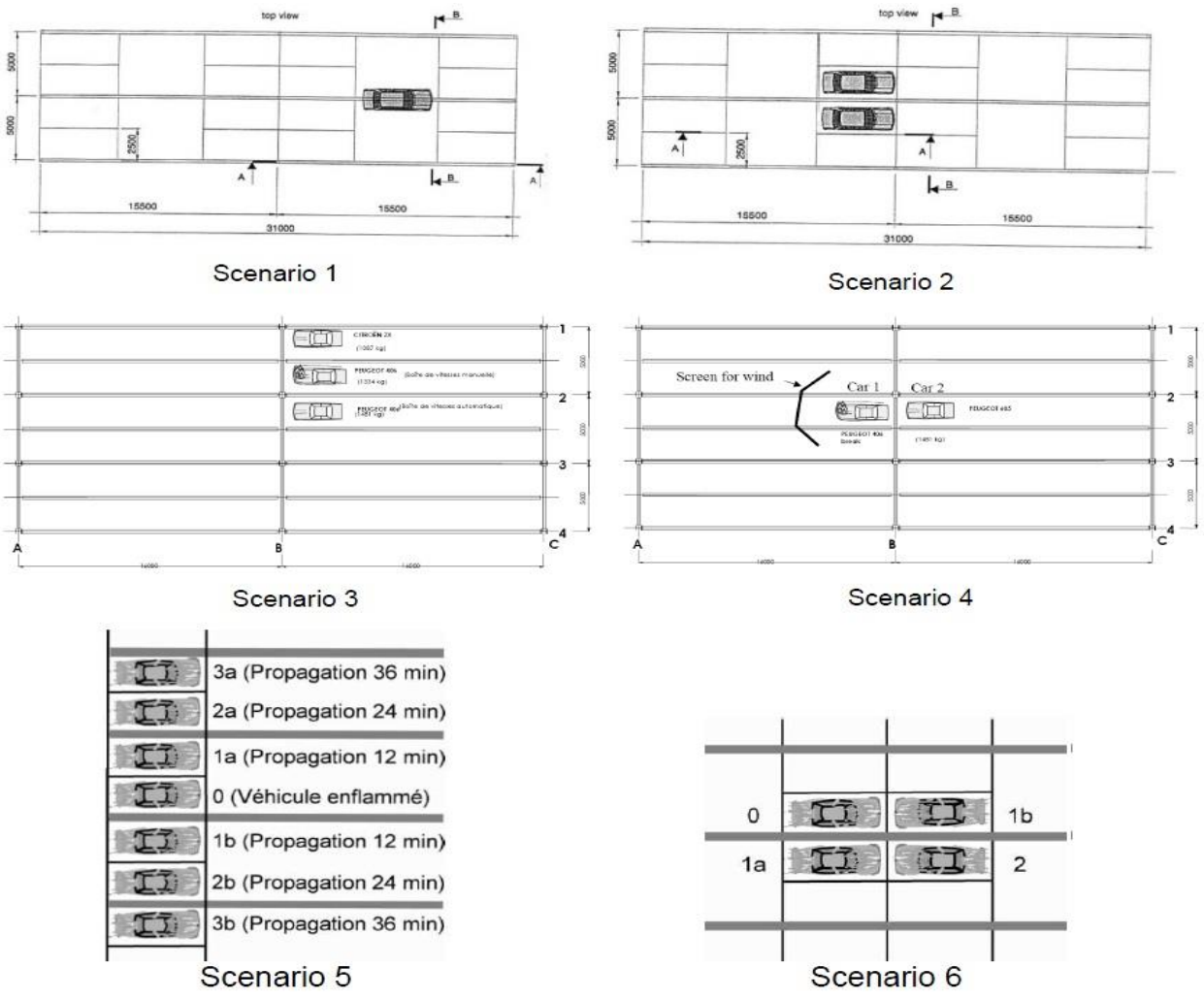

Figure 1-1: Scenario 1 to 6 for design scenarios of car parking buildings from literature (Reproduced from Jaspart et al. [9])

It was unclear from the literature on how these design fire scenarios were formed. It was also unclear how the propagation time from one vehicle to another vehicle was decided. From these scenarios, some questions arise, are the six scenarios mentioned in the literature suitable to be used for any design objectives? Are the six scenarios can be depicted as the worst-case scenario for any design of car parks? These uncertainties and questions show there is a need in the research of determining suitable design fire scenarios for car parking buildings.

In car parking buildings, to determine the suitable design fire scenarios, there are several questions have to be answered. The questions are:

a) How many vehicles burn in a scenario?
b) What are the distances between these vehicles?
c) What type of vehicles involved in the scenario?
d) How fast the fire will spread between vehicles?

There is no easy answer for each of these questions. For example, the number of vehicles burn in scenario depends on certain variables such as, how big is the car park, what is the function and type of car park, how the vehicles are distributed, etc. Therefore, this has led to the prospect of risk-based research on vehicle fires in car parking buildings.

There is emerging interest in using probabilistic assessment methods as part of a risk-based approach to performance-based fire safety design. These methods provide an objective quantification of risk which could lead to an optimization of the selection of fire protection measures in a cost-effective manner. Work by Cheong et al. [16] has presented a method to identify the possible fire scenarios that can occur in a road tunnel using probabilistic assessment. This method has been found to be successful for identifying possible fire scenarios for road tunnels. However, by using the same principle, is it able to identify possible design fire scenarios for vehicle fires in car parking buildings?

Up until now, there have been very few, if any extensive studies carried out on the probabilistic assessment methods for identifying possible fire scenarios for vehicle fires in car parking buildings. Therefore, this thesis attempts to use the similar principle by Cheong et al.

[16] and formulate an approach which is able to identify suitable fire scenarios for vehicle fires in car parking buildings.

1.3 Objective of the research

The main objective of this research project is to formulate an approach that is able to develop appropriate design fire scenarios for vehicles in car parking buildings using probabilistic assessment method as part of risk-based approach. In order to achieve the objective, the research involves a series of analyses of results from past experiments, analyses of various statistics, and simulations of vehicle fires, which will be explained in much detail in the subsequent chapters. Furthermore, the flexibility of the introduced approach enables the author to answer the other questions related to vehicle fires in car parking buildings posed in Section 2.2.9.

The measure of fire severity which is used throughout this research will be in the context of heat release rate, which is one of the most important fire severity characteristics relating to fire safety [17]. Therefore, the term fire severity does not measure the actual impact of the fire on structure, or people, in terms of fire temperatures, consequent structure temperatures or structure response, smoke production, etc. which are beyond the scope of this research.

Another scope of the research is limited to only for passenger vehicles and in enclosed car park areas. Therefore, this research eliminates the possibility of having a free-burning open air environment.

To achieve the objective, the research is divided into the following tasks:

<u>Task 1 – Collation of experimental results and application of initial probabilistic assessment method.</u>

i) The methodology requires a substantial amount of data and collating sufficient experimental data. Thus, the first step is collating results of previous single vehicle fire experiments from available resources to establish probability distributions for heat release rate, time to reach peak heat release rate and total heat released for different classifications of vehicles. These distributions are then used in as the input for the analysis in ii).

ii) Identify potential design fire scenarios in car parks using probabilistic quantitative risk analysis approach by incorporating a relatively simple vehicle parking model,

statistical data on vehicle fleets, measurements of passenger vehicle heat release and vehicle fire incident data.

Task 2 – Enhancement of probabilistic assessment components

i) Analyse heat release rate curves from single vehicle fire experiments results to characterise design fire for multiple vehicle fire scenarios. Introduce probability distribution of characteristics of design fire curves for a single vehicle.
ii) Develop a simplified approach to predict heat release rate curves using a probabilistic design fire for a single vehicle. This is as a means of examining the usability of the probability distribution of characteristics of design fire curves for a single vehicle introduced earlier.
iii) Develop an approach to predict time of ignition for subsequent vehicle given the first vehicle is already burning. This approach is then compared with the B-RISK software [18], which has the capability of performing fire spread between items in an enclosed condition.

Task 3 – Application of enhanced components to the probabilistic assessment method

i) Create a simulation tool for multiple vehicle fire spread using a combination of probabilistic approaches acquired from previous tasks.
ii) Carry out a case study by doing assessment of the capability of the probabilistic approach by performing comparisons with a real life vehicle fire in a car park incident. This is also a means of examining the ability of the simulation tool introduced.
iii) Perform analysis to determine appropriate fire scenarios using enhanced analytical data for two components, i.e. fire severity component and vehicle fire involvement probability component.

The research also has been able to answer some of specific questions regarding vehicle fires in car parking buildings by:

i) Performing a probabilistic analysis to determine the fire load energy densities for risk-based design of car parking buildings.
ii) Using the simulation tool mentioned previously in Task 3 to analyse the probability of fire spread from a vehicle to another vehicle in car parks.

1.4 Limitations of the research

Due to high cost of setting up vehicle fire experiments, this research requires experimental results from previous research for the purpose of analyses. One of the main limitations is that there are not much available resources on measured results (at least heat release rate data) of vehicle fire experiments. This is further addressed in Chapter 3.

Another limitation is the research requires sets of statistics on certain tasks which are at times difficult to obtain. For example, in order to get the statistical data of passenger vehicles on the road for different classifications, the author has to combine information from several sources. This is further discussed in Chapter 4.

For the real incident case study, the limitation is the reported incident of real fire. In the event of a real fire, there were obviously no measurements taken and only limited observations are recorded. Even one could argue about the validity of recorded observations by the fire brigade and/or public witness due to the main focus during the incident being to save lives and property. Thus, the comparison with real fire incident is based on what other people attempted along with the limited observed data from the literature.

All other limitations from the specific tasks are discussed in its corresponding chapters. Since this thesis is built upon several different tasks that have their own limitations, the author endeavoured to maintain consistent level of crudeness for all tasks.

1.5 Structure of the thesis

This thesis consists of 14 chapters of which 6 chapters were published or submitted to journals, published as conference proceedings, or presented in a conference. It is to be noted that these papers, even though they were written to address specific tasks in achieving the overall research outcome, will involve some repetitions, especially in the introduction section of the papers. These were meant to provide a brief introduction or general overview about the research to the readers of the journal or conference proceedings. However, there are some minor modifications in terms of formatting and contents from the original papers to better suit the flow of the thesis. Also, for the chapters using the author's journal papers and conference proceedings, there will be other supplementary information which was not included in the original submission of the papers since the tasks in the research were attempted in sequence.

Chapter 2 presents the general and key literature review of the thesis.

Chapter 3 explores available single passenger vehicle fire experiments results from the literature and collates them according to specific vehicle classification. Distribution analysis was conducted on the collation of results and the analysis will be one of the key input parameters throughout the research.

The initial attempt to develop vehicle fire scenarios for car parking buildings using fire risk analysis is presented in Chapter 4.

Chapter 5 provides the results of characterisation of design fires for a single passenger vehicle from the collated experiments results in Chapter 3. A simplified approach is introduced to predict heat release rate curves from multiple vehicle fires in car parking buildings which is presented in Chapter 6. It is noted that the work in Chapter 5 and Chapter 6 were done in parallel, therefore there are some parts in Chapter 5 which rely from the results in Chapter 6.

Chapter 7 outlines the analysis on the prediction of time of ignition in a multiple vehicle experiment. The outcome of the work is an approach to predict time of ignition of a vehicle given a heat source is already present. Chapter 8 compares the analysis in Chapter 7 using B-RISK simulation software.

As an application of what was learned in previous chapters, Chapter 9 presents the analysis of fire load energy densities for risk-based design of car parking buildings.

Chapter 10 describes the creation of a multiple vehicle fire spread simulation program which will be used in the coming chapters as a means application of the findings of the research.

Chapter 11 discusses the probability of fire spread from a vehicle to another vehicle in car parks by applying the simulation program introduced.

The findings on the application of the simulation program for a case study of real incident of vehicle fires in car park are presented in Chapter 12.

Another attempt at developing vehicle fire scenarios for car parking buildings using enhanced analytical input is discussed in Chapter 13.

Finally, Chapter 14 provides a set of conclusions and recommendations for future work.

Chapter 2 LITERATURE REVIEW

2.1 Overview

The literature review in this thesis consists of two parts. First part is the general review of literature on vehicle fires in car parking buildings. This is presented in ascending order by year of publication. The second part is the review of the key literature related to the tasks in the thesis.

Further reviews on specific topics are presented in corresponding chapters. Specific topics such as:

a) Single passenger vehicle fire experiments are reviewed in Chapter 3.
b) Design fires for single passenger vehicle are reviewed in Chapter 5.
c) Multiple passenger vehicle fire experiments are reviewed in Chapter 6, Chapter 7, and Chapter 8.
d) Fire load energy density for car parking buildings are reviewed in Chapter 9.
e) A case study on vehicle fires in car parking buildings is reviewed in Chapter 12.

2.2 General review

The issues related to vehicle fires is a vast topic as it ranges from fire incidents and investigation; case studies; statistics; fire development; alternative fuels; materials; regulations and standards; smoke and heat control; structural; and detecting and suppression. The types of vehicles in a fire also range from road vehicles, rail, and ships. For road vehicles, it could range from trucks, passenger vehicles, and coaches. These fires could occur in a tunnel, open road, car parking buildings, bridges, or premises. Hence, the scope is limited to the issue of vehicle fires for passenger vehicles in car parking buildings.

There were many significant literatures on vehicle fires in car parking buildings, dating back to as early as 1960s. However, in this review, the first literature begins with Li (2004) [19] since in his thesis, he has presented an extensive literature review on vehicle fires in car parking buildings prior to his work. It is to note that in this chapter, the term ‘car parking building’ is sometimes referred as car parks, parking, or parking building depending on the literature.

2.2.1 Li (2004) [19]

In his thesis, Li attempted to answer several questions regarding the topic of vehicle fires in car parking buildings. These questions included:

- What is the likelihood of vehicle fires in parking buildings and does the likelihood vary with the type of parking building (e.g. private or public)?
- How likely is the fire to spread to neighbouring vehicles, and why?
- What are the causes of vehicle fires in parking buildings (e.g. arson, ignition, etc.)?
- What materials are involved in vehicle fires in parking buildings?
- What is the severity of vehicle fires in parking buildings?
- How appropriate is the installation of sprinklers in parking buildings to protect the life safety and/or property?

However, in the thesis Li limits the scope to examining the characteristics of historical data for vehicle fires in New Zealand parking buildings from 1995 to 2003, evaluating the probabilities of such fires using event tree analysis, and presenting a cost-benefit analysis model for the provision of sprinklers in parking buildings. While other questions remain unanswered, there is a vast opportunity for research to be done in the topic.

Also, Li discussed most vehicle fires in car park buildings literature in the recent past. This review mainly discusses experiments on the severity of vehicles fires, experiments of vehicle fires in parking structures, simulation and modelling based on experimental results, experiments on performance of the sprinkler system in parking buildings, and statistical studies of vehicle fires. The preceding works discussed by Li were Butcher et al. [20], Gewain [21], Bennetts et al. [22], Schleich et al. [23], and Joyeux et al. [14], which reported on vehicle fire tests in open structures. Burgi [24], BHP [25], Bennetts et al. [26], and Kitano et al. [27] researched fire tests in closed structures. Their findings give an indication that a fire can spread between vehicles, especially in closed parking structures. The review also found that the main hazard to human life and safety in closed parking structure fires was due to large amounts of they smoke produced. In addition, some of the literature demonstrated the effectiveness of sprinklers in controlling the development of car fires although one research [24] showed that the water from sprinklers shifted the burning petrol to adjacent vehicles.

Li organized his work by collecting historical data, which were filtered from New Zealand Fire Service (NZFS) incident reporting systems data. This provided the relevant probabilities for the construction of event tree model that considered the type of parking buildings and different vehicle fire spread scenarios. The results from these event tree models were applied

to a cost-benefit analysis model, whereby the cost-benefit ratio measure is used and annual cost avoidance of vehicle fire damage by sprinklers in the parking building is identified as the benefit. A case study was finally performed for a public parking building with a total floor area of 30,000 m² using Monte Carlo simulation in the @RISK add-on for Microsoft Excel.

It was found that on average, there were 12 vehicle fire incidents each year in New Zealand parking buildings. Multiple vehicle fire incidents accounted for approximately 3% of such fires. Arson is found to be the leading cause of vehicle fires in New Zealand parking buildings (26.7% of all fires). It was concluded that annual vehicle fire frequencies in New Zealand parking buildings are generally lower than those in buildings of other occupancies. Based on available data collected during this research, it was further found that an economically installed automatic sprinkler system does not justify itself in a parking building situation from the building owner's point of view.

This work by Li provides a useful foundation for future work for research on vehicle fires in car park buildings. The historical data for vehicle fires can be extended from 2005 until present as these data are useful for fire risk analysis. The method of constructing an event tree also proved to be very useful for the research on fire risk analysis.

2.2.2 Jaspart et al. (2009) [9]

The report is a part of a research programme of the Research Fund for Coal and Steel conducted in University of Coimbra, Portugal. The report is divided into three main parts in which only the first part is related to this thesis. The first part presents an extensive review of vehicle fires in car parking building research from the early 1960s up until the work was published. The work is somehow similar to what has been presented by Li [19] but to a certain extent is much more extensive.

The report has reviewed vehicle fire experiments in the past, numerical and analytical studies in car parks, presented cases of real fires in car parks buildings, fire tests in car park buildings or on sub-structures, real vehicle fires in car parks statistics, and outlines design requirements of car parks in different countries.

2.2.3 BRE (2010) [1]

In this report, Building Research Establishment (BRE) finished a project that aimed to gather information on the nature of fires involving the current design of cars and to use this new knowledge as a basis, if necessary, for updating current guidance used in the United Kingdom on fire safety strategies for car park buildings. The project was commissioned by Communities and Local Government (CLG) Sustainable Buildings Division to carry out a three year project titled Fire Spread in Car Parks. This report was intended to be of value to designers, fire engineers, computer modellers and enforcers, involved in the design of car parks and the fire safety provisions that are appropriate.

This report includes a world-wide literature review of the related topic of vehicle fires, laboratory tests on car materials, a review of United Kingdom fire statistics, computer modelling of vehicle fires in car park buildings, and a series of eleven full-scale fire tests that included burning a total of sixteen cars.

This research provides information that will complement previous works that were done in the related topic. The burning of the 16 cars proved to be useful because these tests provided important parameters for fire risk research. These vehicle burning tests are useful input for this research work. These are further discussed in Chapter 7.

2.2.4 van der Heijden (2010) [28]

The thesis discussed heat and smoke removal in semi-open car parks which is defined as a car park in which there are wall openings directly linked to the outside air. The car park definition is somewhat similar to open car park explained in the previous chapter. In order to discuss the topic, an assessment of the fire safety level was conducted when semi-open car parks were designed using current guidelines on the bases of worst case scenarios and wind effects were attempted. Thus, a research question was identified and this was answered in the thesis. The research question was: *"To what extent is there a risk in the safe deployment of the fire brigade during a car fire in a semi-open car park, when the amount of natural ventilation is in line with the conditions as stated in current Dutch guidelines, and when wind-effects as well as potentially worst-case scenarios are taken into account"*

The research began by doing literature reviews of vehicle fires and car park building codes around the world. Then, the researcher looked at general car park dimensions in the

Netherlands, the influence of wind in semi-open car parks, the distribution and location of the opening area of the car park building have significant influence on the fire safety level, and the effect of different locations for structural beams.

The fire safety levels of semi-open car parking buildings were assessed using Computational Fluid Dynamics (CFD) simulations. This study uses a fixed design fire for passenger vehicles as well as fixed time of ignition in the CFD simulation based on measurements performed by van Oerle et al. [29]. The study concludes that the effect of the presence of wind does not make much difference as compared to the same situation without the presence of wind. It was also concluded that from this study, it is possible to design a semi-open car parking building that complies with current existing Dutch guidelines, but still has an insufficient safety level when assessed with the criteria for safe deployment of the fire department.

2.2.5 Collier (2011) [30]

Collier from Building Research Association New Zealand (BRANZ) compiled a report in 2011 on vehicle fires in car parking buildings. The main objective of this report was to gather information regarding traditional fire design assumptions for car parking buildings to account for modern cars with modern materials, which are believed to contribute significantly to increased fire loads as compared to old cars. This report also gathers information about vehicle stacking systems in car park buildings that may also have limited natural ventilation and/or mechanical ventilation systems. This project has advanced the work to date in the New Zealand context and proposes necessary changes.

This research began with the collated statistics from previous research on vehicle fires in car park buildings. The research then focused on modelling vehicle fire experiments in car park buildings using zone model fire software, BRANZFIRE (a precursor to B-RISK) [31] and computational-fluid dynamics simulation based software, Fire Dynamics Simulator (FDS). In the both of the simulations, the author uses a fixed design fire and made assumption on the time of ignition of subsequent vehicles. From the research, it was found that fire modelling with the new car fire input parameters indicates that existing New Zealand Building Codes (NZBC) requirements for open natural ventilation in above-ground car parks remain satisfactory. However, for closed underground car parks and/or car parks that may include stacking systems, tenability becomes a serious concern. Also, to a lesser extent, the performance of structural steel members may be an issue.

2.2.6 Fire safety & explosion safety in car parks research group, Belgium

This multi-disciplinary research team was formed to focus on the development of fundamental design approaches for the improvement of fire safety and explosion safety in car parks. The research team comprised of representatives from several universities and agencies in Belgium. The project is funded by IWT-Vlaanderen, Belgium (Agency for Innovation by Science and Technology) in the Strategic Basic Research (SBO) framework.

Deckers (2007) [32]. The research discussed the simulation of smoke and heat exhaust ventilation system (SHEVS) in large enclosed car parks. This was done by comparing with standard (NBN 208-20-2) of the Dutch standards. This type of solution was tested by simulating various scenarios using the FDS simulation software.

Tilley (2007) [33]. This report was a summary of a study regarding a fire in a small underground car park. From the research, it was found that there was quite a trend in Belgium to have more small underground car parks. The definition of small was enough space for about ten cars. The thesis also discussed types of measures taken in Belgium to protect these underground car parks against fire. These measures were investigated using the FDS simulation software.

Jansen (2010) [34]. The thesis discussed the selection of car fire scenarios in car park buildings, the modelling of the fire scenarios and the resulting thermal load on structures as well as the local heating and strength reduction of the structure. The scenarios were chosen based on past realistic scenarios that have happened in the past. These scenarios were then simulated using the FDS simulation software.

Baert (2011) [35]. The research mainly discussed fire safety of smoke and heat extraction systems in underground car parks. Topics discussed in the thesis were back layering of smoke, influence of beam configurations on back layering and delay of detection systems. A survey of regulations, standards and experiments on heat release rates of cars also were reported in the thesis. One topic which is of interest for this thesis is the compilation of the design fire of passenger vehicle which have been regularly used in car parks. The simulation used in this thesis was performed using the FDS simulation software.

It can be concluded from the work that there were no attempts on risk-based approach to tackle the problem of vehicle fires in car parking buildings. It was also found that in the work that the researchers have used fixed design fires for passenger vehicles which are from Bureau for Standardisation (NBN) [36], Joyeux [37], and van Oerle et al. [29] in their FDS simulations. When there were two or more vehicles involved in the simulation, the researchers also used assumed ignition time for the each of the vehicles.

2.2.7 Fire Safety Journal Special Issue on car park fire safety

The work by the fire safety & explosion safety in car parks research group, Belgium has gained attention of the editor-in-Chief for Fire Safety Journal to publish a special issue on car park fire safety. The issue focuses on the topic of car park fire safety where there were nine research articles published. The articles ranging from the topics of fluid mechanics(smoke and heat control), diagnostic technique, risk analysis, and structural stability.

There are two articles of interests for this thesis. Firstly, Merci and Shipp [38] discusses about the lessons learnt from the research of smoke and heat control for fires in large car parks. The research is divided into two parts where the first part discussed about statistics of vehicle fires in car parks and experiments conducted by BRE which is of particular interest for this thesis. The contents of the first part of this article are mainly previously published in BRE [1]. The second part discusses about smoke and heat control by means of horizontal mechanical ventilation in which related to other articles in this issue.

Second is the article by Annerel et al. [39] which discusses on thermo-mechanical analysis of an underground car park structure exposed to fire. This work recreates two real car park fire incidents i.e. Gretchenbach fire and Harbour edge using FDS. For both incidents, there was sufficient information for the purpose of simulation. Therefore, with enough of information of the recreation of the incidents, this article is useful as an input for the work in Chapter 12.

2.2.8 Other research reports

Noordijk and Lemaire [40]. This study focuses on how to model fire spread between cars in a car parking building in which was triggered by a fire incident at Schiphol Airport, Netherlands involving 30 cars where it was believed that the fire spread during the incident was much faster than assumed. The study recognised that fire between vehicles can occur by

emission of radiation, heat transfer through air and absorption of the radiation. The work then introduces a fire spread model using CFD. In the conclusion, driven by uncertainties, the fire spread model was capable of predicting fire spread between cars even though it was not clear from the paper what the measure of the capability was. Noordijk and Lemaire also reiterated that the model is still in a development phase and needs further validation and improvement.

Jug et al. [41]. This study attempted to provide a baseline for performance-based design of car park buildings using probabilistic methods. However, the main objective was unclear and there was no clear method on how the authors attempted to address the problem.

Olthof and Scheerder [42]. The objective of this study was to understand underground car parks fire scenarios that may occur at the time the fire brigade arrives at the scene. The outcome of this research could be used to develop a fire fighting strategy for underground car parks. The outcome of the research could also give authority bodies much needed information to adjust fire safety measurements in the designing process. For this research, the outcomes were "used by fire department of Apeldoorn for their fire fighting strategies". The outcome of the research has been based on literature research, statistics, fire investigation and field tests. Two fire scenarios were determined and used from the analysis of research data in combination with a probabilistic and physical approach.

2.2.9 Conclusions drawn from the review

From the review of the literature, it was found that there were real tests and experiments on vehicle fires in car park buildings in the past. While these isolated tests may have proven to be useful for previous studies, there remains room to integrate all of the outcomes from all tests and develop a statistical study as a part of probabilistic assessment method of vehicle fires in car parking buildings.

Also, from the review it was found that much of the research attempted to perform vehicle fires in car park buildings simulation numerically using FDS or other CFD software in which, most of the research used fixed design fires for a single vehicle obtained from previous studies e.g. Bureau for Standardisation (NBN) [36], Joyeux [37], and van Oerle et al. [29], and assumes the time of ignition of subsequent vehicles in the simulation. Also, from what were reviewed in the literature, there was no attempt on performing a risk-based analysis on vehicle fires in car park buildings, hence giving much room for research in the area.

The discussions from the literature review also suggest that the design fire used for a single passenger vehicle for all the numerical analyses is also based on a single deterministic curve. The question is, are all vehicles having the same identical design fire every time it burns? This question leads to another question, if there are two vehicles in which both of the vehicles are of same manufacturer and same model, are both of the vehicles going to have the same design fire? These questions also have led to the prospect of performing risk-based analysis on design fires of vehicles.

Another discussion from the literature was regarding the time of ignition of subsequent vehicle if the first vehicle is ignited when performing simulation of a vehicle fire. This leads to questions such as, is the time of ignition already predetermined prior to performing the simulations? Is this time of ignition fixed for all vehicles? These questions have led to the prospect of research in this area.

There are also other questions related to vehicle fires in car park buildings research which has been going around the fire engineering community. One question is, what is the fire load energy density inside a car park area? Another question arises is, what is the probability of fire spread from vehicle to another vehicle if a vehicle is burned?

All the questions asked in this section are understood to be closely related to one another and are made known that there are opportunities to conduct research using the risk-based approach. The main question of the research would be, what is the most suitable design fire scenario in order to design a car parking building? Other related questions will be the sub-questions en route to answering the main question which will be attempted to be answered in this thesis.

2.3 Review of key literature to the thesis

There are several key literatures which were published prior to Li's [19] work that are thoroughly used in this thesis. Therefore these are reviewed in this section.

2.3.1 Joyeux (1997) [37]

This report aimed to perform vehicle fire with different configuration from previous experiments conducted by other researchers. The idea of the work was to simulate vehicle

fires in a car park. Ten experiments were conducted in which some of the experiments involve single and two vehicles. Further explanations about the experiments are found in Chapter 3 and Chapter 7.

The key points that are used throughout the thesis are firstly the introduction of vehicle classification which is based on its calorific potential. The definition of the classification system proposed by the author is shown in Table 2-1, while the mean car mass, mass loss and energy available to be released versus category are shown in Table 2-2. These classifications are then reproduced again in in the work by Schleich et al. [23] and Joyeux [14]. The origin of the development of the classifications was unclear and the only information found was from Joyeux [14] where the classifications are said to classify registration number in France (data available on 3615 AUTOM). The classification system is important in this thesis in the sense of comparison with what obtained in the following chapters. It is suggested from Joyeux [14] that in order to use the classification, coefficients of potential energy released during the fire which varies between 0.5 and 0.8 have to be used.

Table 2-1: Definition of classification (Reproduced from Joyeux [37])

Trademarks	Category 1	Category 2	Category 3	Category 4	Category 5
Peugeout	106	306	406	605	806
Renault	Twingo-Clio	Megane	Laguna	Safrane	Espace
Citroen	Saxo	ZX	Xantia	XM	Evasion
Ford	Fiesta	Escort	Mondeo	Scorpio	Galaxy
Opel	Corsa	Astra	Vectra	Omega	Frontera
Fiat	Punto	Bravo	Tempra	Croma	Ulysse
Wolkswagen	Polo	Golf	Passat	N/A	Sharan

Table 2-2: Mean car mass, mass loss and energy available to be released versus category (Reproduced from Joyeux [37])

Category	Car mass (kg)	Mass loss (kg)	Released energy (MJ)
1	850	200	6000
2	1000	250	7500
3	1250	320	9500
4	1400	400	12000
5	1400	400	12000

As a comparison, the classification system proposed by Joyeux is compared with the classification system introduced by American National Standards Institute (ANSI) which is based on the curb weight of a passenger vehicle. Curb weight is defined as total weight of a

vehicle with standard equipment while not loaded with passengers and cargo. The comparison is shown in Table 2-3.

Table 2-3: Comparison of Joyeux classification and ANSI classification

ANSI Classification	Curb weight	Category
Passenger car: Mini	1500 – 1999 lbs (680 – 906 kg)	1
Passenger car: Light	2000 – 2499 lbs (907 – 1134 kg)	2
Passenger car: Compact	2500 – 2999 lbs (1135 – 1360 kg)	3
Passenger car: Medium	3000 – 3499 lbs (1361 – 1587 kg)	4 and 5
Passenger car: Heavy	≥ 3500 lbs (≥ 1588 kg)	-
Van / MPV	Not defined	-
SUV	Not defined	-

Another key point to be drawn from this report is the introduction of reference curve for vehicle fire. It was concluded that a reference curve is deduced from one of the vehicle fire experiments reported i.e. Test 7 (Figure 2-1). This decision was due to the experiment gave the highest values of heat release rate as compared to other available single vehicle fire experiments at that time. The comparison is shown in Figure 2-2 and Figure 2-3. This reference curve has been widely used in vehicle fire simulation such as in Collier [30], de Feijter and Breunese [43], Jansen [34], and Baert [35].

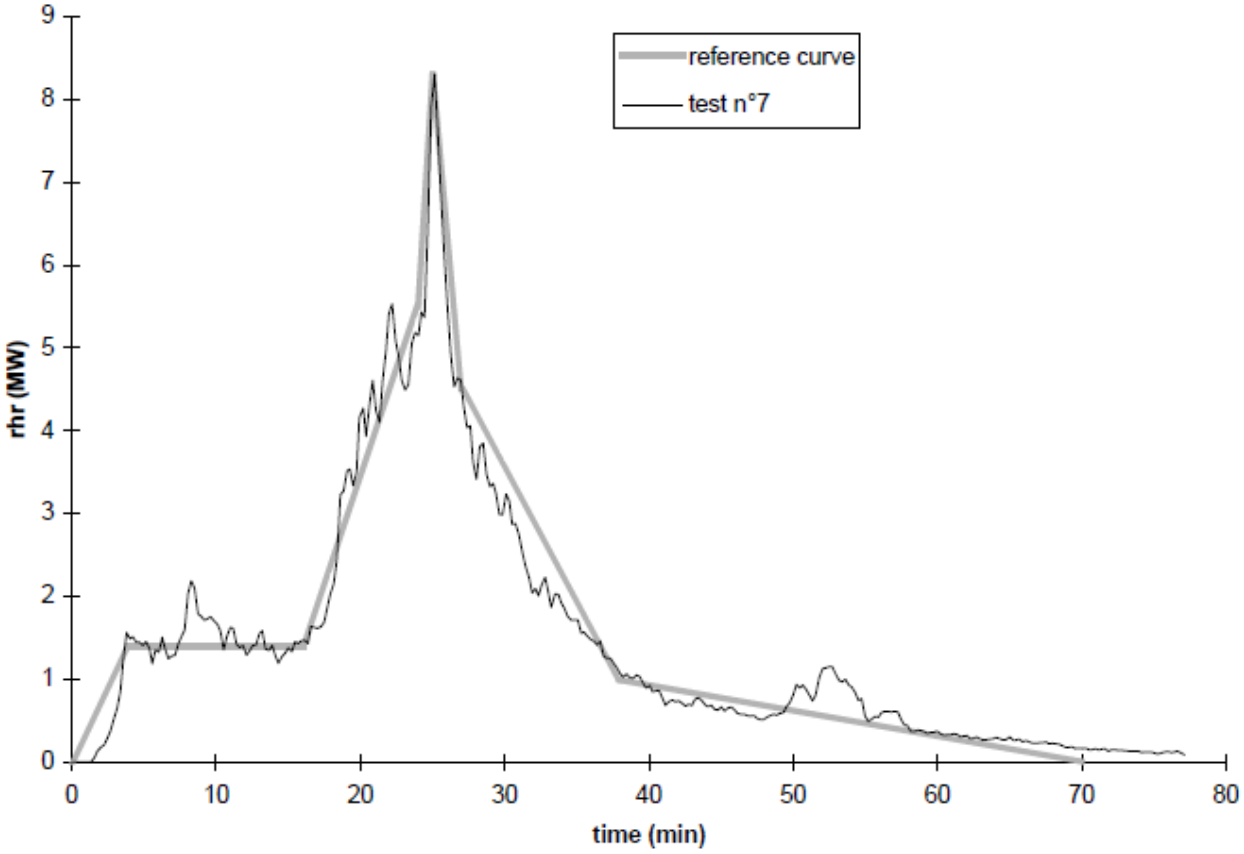

Figure 2-1: Reference curve of heat release rate of single vehicle fire and Test 7 curve (Reproduced from Joyeux [37])

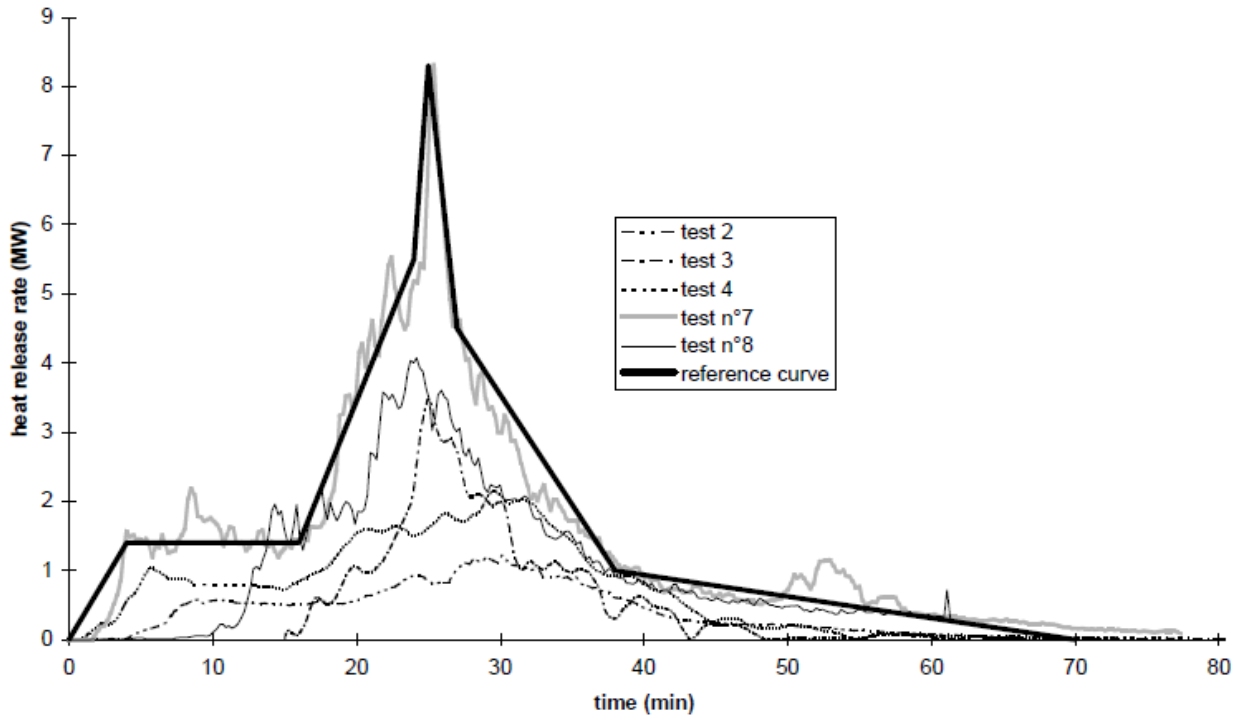

Figure 2-2: Comparisons of the reference curve with the heat release rate of one car fire measured during CTICM car fire tests (Reproduced from Joyeux [37])

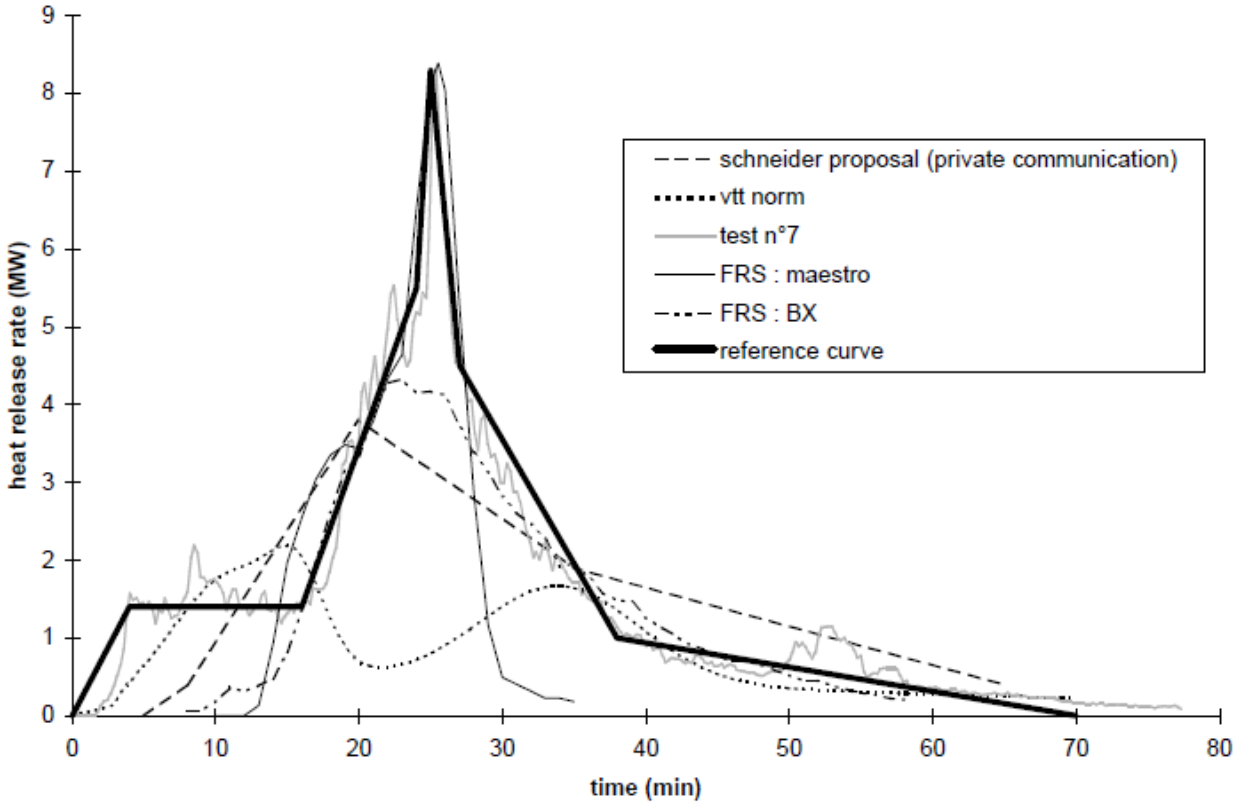

Figure 2-3: Comparisons of the reference curve with all heat release rate of one car fire of the literature (Reproduced from Joyeux [37])

2.3.2 Joyeux (2002) [14]

This report compiles the vehicle fire experiments results of different scenarios as a means to convince national authorities that car parking buildings are not required to have a large duration of fire resistance requirements. The report is divided into several sections which include the set up and results of the experiments in an open and closed car park and also review on statistics of fires in car parks.

This review is focused on the collection of statistics of fires in car parks in which are used in Chapter 4. It was reported that the statistics of vehicle fires mainly come from Fire Brigade of Paris (BSPP); and town councils of Marseille, Toulouse, Brussels and Berlin.

2.3.2.1 Underground car parks

The report presented the statistics collected as several different functions such as the distribution of number of vehicles involved, vehicle classification involved, time to extinction for all cases, injured people, and fire brigade call time. This review selects statistics that are deemed to be important to the thesis.

Figure 2-4 shows the distribution of the number of cars involved in a fire. From the figure, it can be seen clearly that a single vehicle fire occurred the most of the times. The distribution shows both percentages of all fires and the ones that involve vehicles since it was given in the statistics that not all reported fires in underground car parks involve vehicles. Figure 2-5 shows the distribution of vehicles involved in underground car parks. Most of the reports mentioned the class of the vehicles i.e. 91% of cars were used to develop the distribution. It can be seen from the distribution that the lower the classification of the vehicles, the higher the percentage of involvement in vehicle fires.

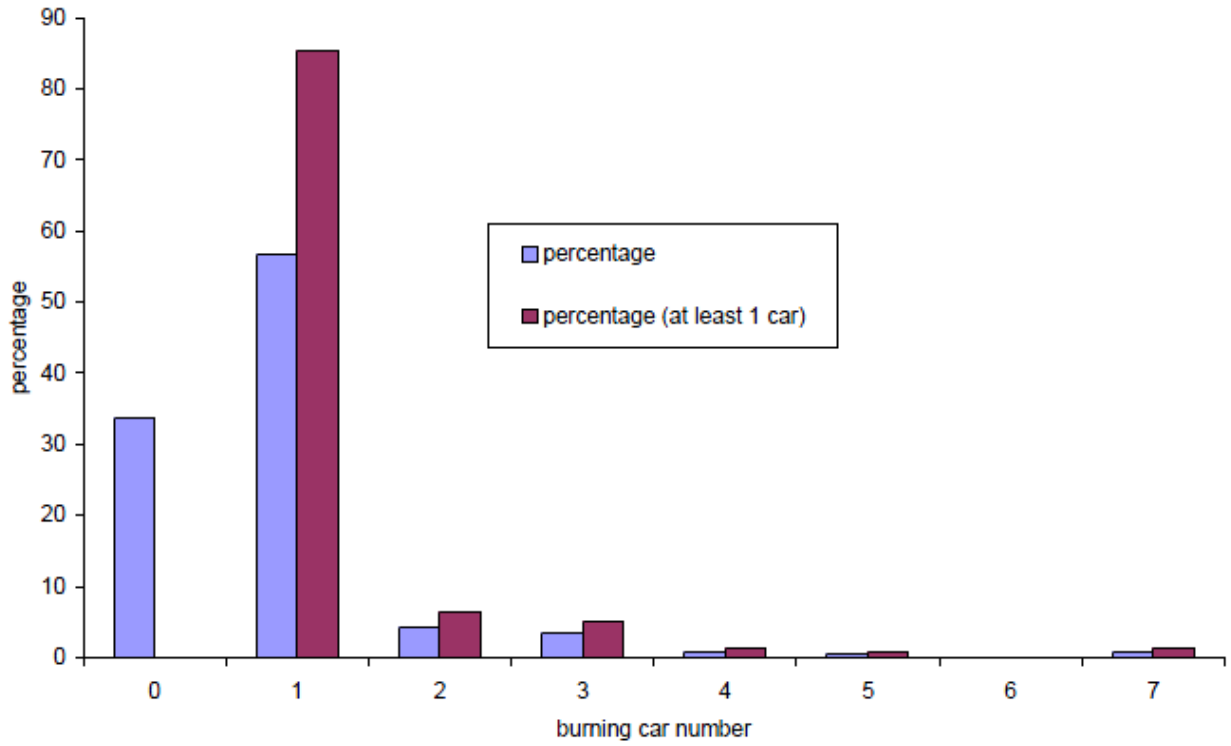

Figure 2-4: Distribution of number of cars involved in underground car park fires (Reproduced from Joyeux [14])

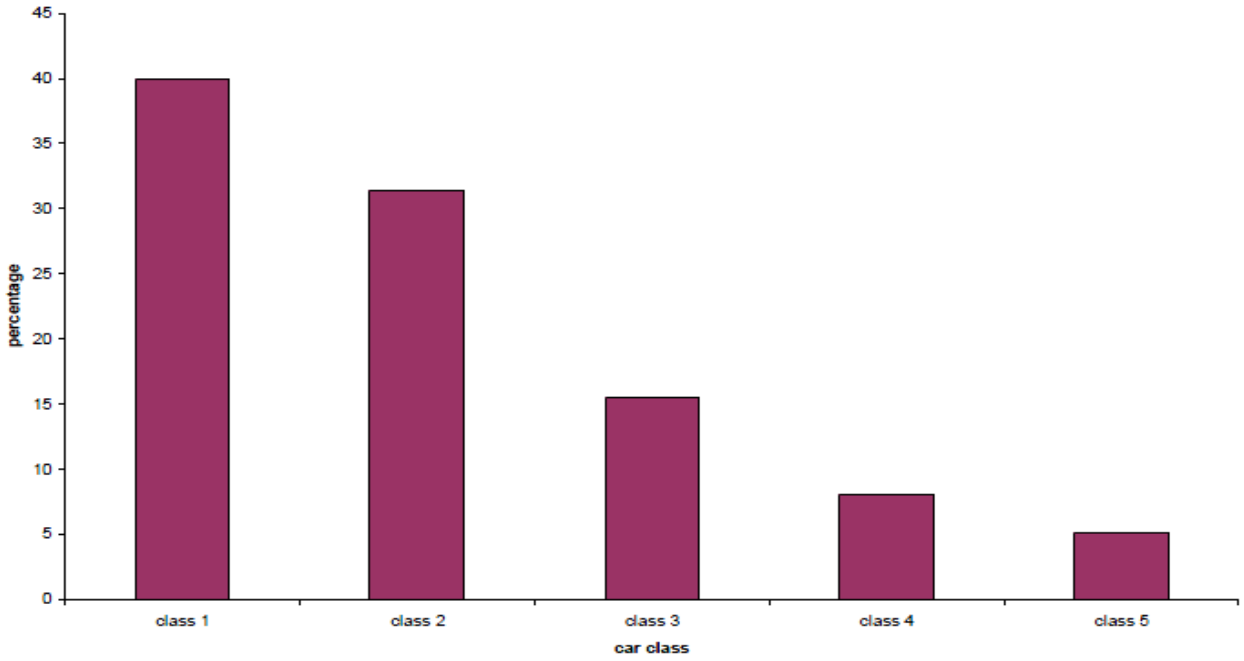

Figure 2-5: Classification of cars involved in vehicle fires in underground car parks (Reproduced from Joyeux [14])

2.3.2.2 Open car parks

Figure 2-6 shows the distribution of vehicles involved in open car parks fires. Similar to discussion in previous section, the distribution shows both percentages of all fires and the ones that involve vehicles. It can be seen that for the open car parks, the highest percentage of vehicle fire involved is also for a single vehicle which is similar to the underground car park vehicle fires distribution.

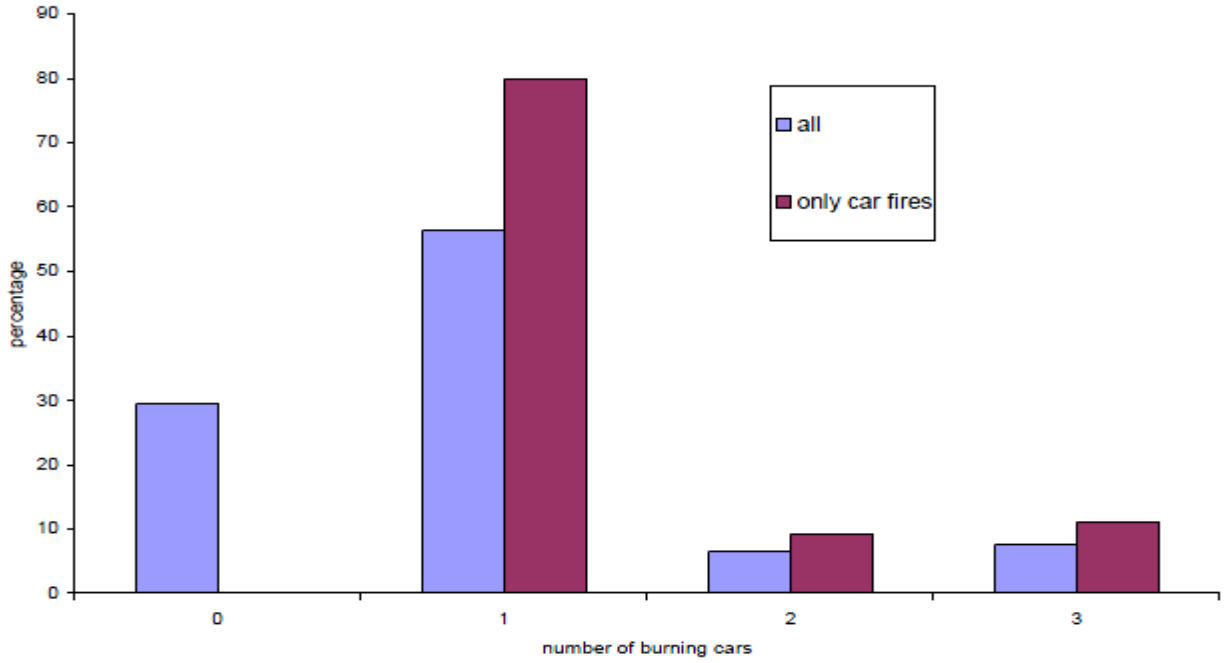

Figure 2-6: Distribution of number of cars involved in open car park fires (Reproduced from Joyeux [14])

The distribution of the vehicle classification of the open car parks fires is shown in Figure 2-7. The distribution shows similar trend from what have been obtained in underground car park fire where the lower the classification of the vehicles shows higher the percentage of involvement in vehicle fires.

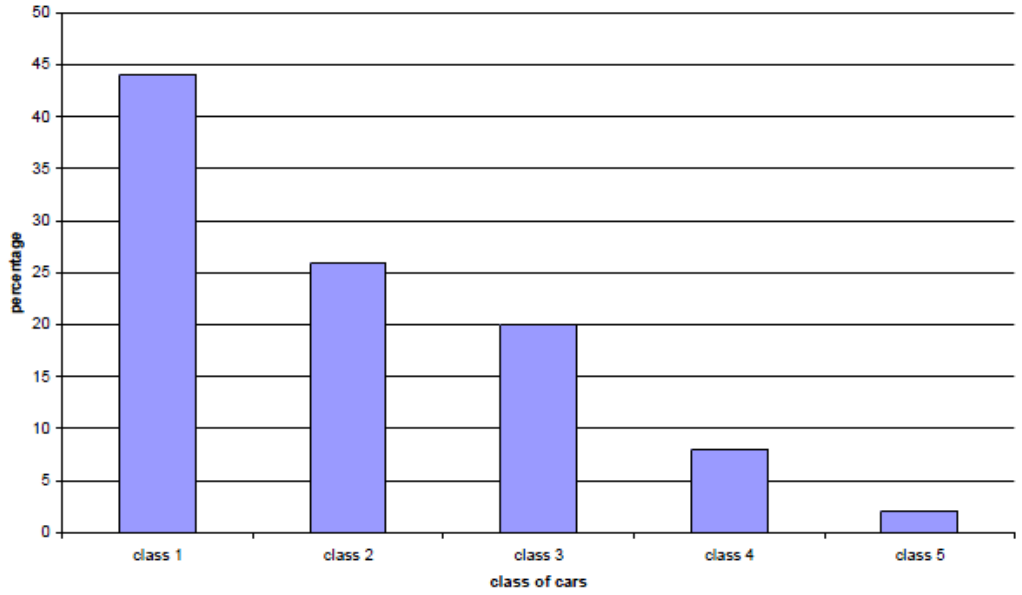

Figure 2-7: Classification of cars involved in vehicle fires in open car parks (Reproduced from Joyeux [14])

The comparison of the statistics of both the underground car park and open car park is shown in Figure 2-8. Overall it can be concluded that most vehicle fires reported in the statistics involved only a single vehicle and the percentage becoming much lesser as number of burning vehicles increasing. These findings are useful and used for the work in Chapter 4.

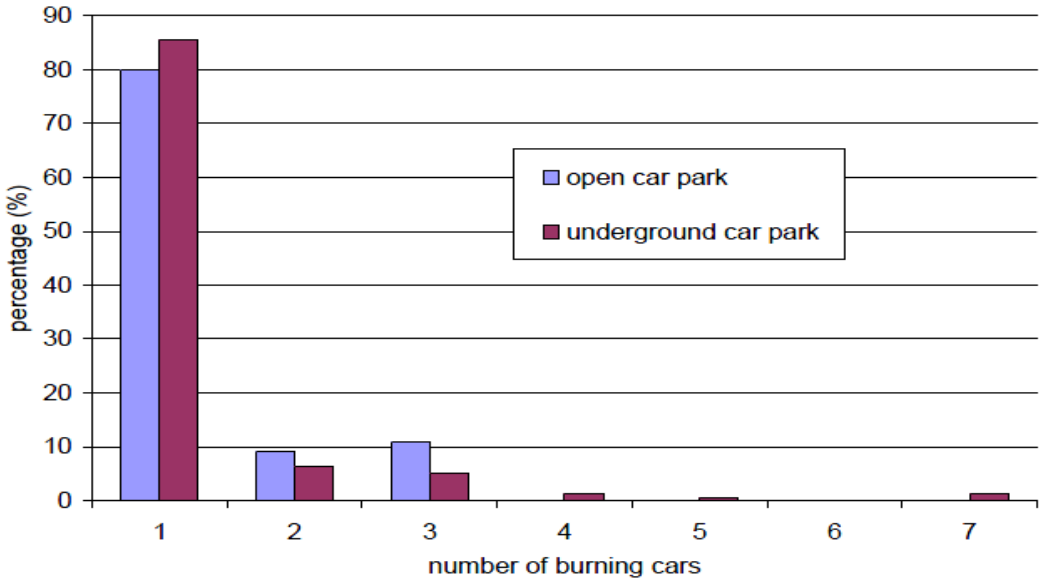

Figure 2-8: Distribution of vehicle fires in underground and open car parks (Reproduced from Joyeux [14])

Chapter 3 SINGLE PASSENGER ROAD VEHICLES FIRE SEVERITY CHARACTERISTICS ANALYSIS

Published as Tohir, M.Z.M., and Spearpoint, M. “Distribution analysis of the fire severity characteristics of single passenger road vehicles using heat release rate data” in *Fire Science Reviews* 2:5, 2013. [44]

Abstract

Fires associated with vehicles have the potential to impact on life safety and property protection. The fire severity characteristics of single passenger vehicle fires are presented in this chapter by the total energy released, peak rate of heat release and the time to peak rate of heat release using experimental data collated from the literature. Risk-based fire design can be supported by data presented in a statistical form such that passenger vehicles are categorized by their curb weight and probability distribution curves are obtained for each fire severity characteristic. Analysis of the data shows that the total energy released and the time to peak rate of heat release are generally shown to exhibit an increasing trend with curb weight.

3.1 Introduction

Fires in vehicles can impact on the life safety of the vehicle occupants and the people in the vicinity of the fire. Vehicle fires can also result in material losses both in terms of the vehicle itself but also to neighbouring property. Therefore it is prudent to understand the risks of vehicle fires and the need to potentially reduce their probability of occurring and/or mitigate the severity if a fire does occur. This review is part of a larger research investigation into risk-based fire safety of passenger road vehicles in parking buildings being undertaken at the University of Canterbury.

Heat release rate is an important fire severity characteristic relating to fire safety [17]. The heat release rate time-history defines the growth of the fire and other related characteristics such as the peak heat release rate, the time to the peak and the total energy release which in turn determine some measures of the severity of the fire particularly when considering the impacts to people and property remote from the vehicle itself. Moreover, the fire environment can be assessed using the heat release rate information as input to a calculation. For example, the smoke layer height as a measure of tenability can be predicted by a computational model once the heat release rate is determined. In addition, the tenability components of smoke such as obscuration, toxic species and heat may need to be determined and these components can often be obtained as a function of the heat release rate. Thus, this review compiles the available heat release rates curves for a single passenger road vehicles from the current literature to form a resource for calculations such as the fire spread between vehicles, fire and smoke conditions in enclosures (such as car parks or tunnels), etc.

With the increased consideration of performance-based fire safety analysis in New Zealand and elsewhere, the design fire concept is a critical component for the design of buildings [45]. There is developing interest in using probabilistic assessment methods as part of a risk-based approach to performance-based fire safety design. These methods provide an objective quantification of risk which could lead to an optimization of the selection of fire protection measures in a cost-effective manner. Hence, there is a need to compile data in a statistical form and this review introduces a set of probability distributions for the heat release rate characteristics of passenger road vehicles. These distributions provide researchers and designers with a starting point for risk-based design of parking buildings or other similar structures that involve vehicles.

3.1.1 Vehicle classification

The definition of passenger vehicle used in this review is based on the New Zealand Transport Authority (NZTA) which states that it is a motor vehicle constructed primarily for the carriage of passengers, with not more than nine seating positions which include the driver's seating position, and either has at least four wheels or it has three wheels and a gross vehicle mass exceeding one tonne [6]. Therefore, the passenger vehicle data collected here are limited by this definition, which excludes other ground-based passenger vehicles such as buses, trains etc.

However even within the NZTA definition of a passenger vehicle there is likely to be a wide range of vehicle sizes and types so it is useful to consider classifying vehicles into smaller groups. There are numerous of ways to categorize passenger vehicles and different regulations and jurisdictions have a variety of definitions for the purposes of classification. Some of the most common classifications are the vehicle engine size, the vehicle dimensions (e.g. length, interior volume size), the vehicle seating capacity, the vehicle curb weight, age, or wheelbase [46]. For this review the American National Standards Institute (ANSI) [47] classification system based on the curb weight of the vehicle is adopted (Table 3-1) as the mass is identified in this chapter as a key parameter related to the potential fire load of vehicles. For example, previous work by [14] provides total energy release values for five car categories such that the higher the average mass of the vehicles the higher the total energy released. Similarly research by [48] shows an increasing linear trend for the correlation of body weight against total energy released from four vehicle fire experiments. As such, it seems reasonable to investigate further how the heavier the vehicle the more total energy that will likely be released during the fire. It is also useful to consider how the peak heat release rate and the time to peak heat release rate for vehicles changes as the vehicle mass increases.

Table 3-1: ANSI classification of vehicles by curb weight.

Classification	Curb weight
Passenger car: Mini	1500 – 1999 lbs (680 – 906 kg)
Passenger car: Light	2000 – 2499 lbs (907 – 1134 kg)
Passenger car: Compact	2500 – 2999 lbs (1135 – 1360 kg)
Passenger car: Medium	3000 – 3499 lbs (1361 – 1587 kg)
Passenger car: Heavy	≥ 3500 lbs (≥ 1588 kg)
Van / MPV	Not defined
SUV	Not defined

To further argue for the classification of passenger vehicle by mass, data from the EU [49] shown in Table 3-2 illustrates how vehicles are divided into bands determined on mass and also shows that the population of vehicles varies between different countries. Therefore a risk-based assessment on vehicle fires might need to account for this variation particularly if it is accepted that the vehicle mass relates to the severity of a vehicle fire.

Table 3-2: Percentage of passenger vehicle population classified by weight in some European countries.

	< 1000 kg	**1000 - 1249 kg**	**1250 - 1499 kg**	**≥ 1500 kg**
Netherlands	33.7	31.0	24.8	10.4
Estonia	8.1	31.5	32.3	28.1
Spain	22.6	34.1	31.8	11.5
Finland	11.7	28.9	36.4	23.1
Cyprus	27.4	33.6	23.8	15.1
Latvia	7.4	30.7	32.9	29.1
Norway	10.1	27.6	36.2	26.1
Switzerland	8.6	23.5	30.6	37.4
Poland	33.3	31.0	20.0	15.7
Portugal	0.6	5.7	28.0	65.7
Average, %	**16.3**	**27.8**	**29.7**	**26.2**

However, this selection of classification has its own weaknesses considering that different weight classes do not necessarily directly relate to the amount of combustible material in a vehicle. Based on the report by [50], the usage of plastics/composites in light vehicles has been increasing steadily from 1960s up to 2010s. Thus, the age of the vehicles is also an important factor which may affect the severity of the fire and this is further investigated below.

3.1.2 Vehicle fires

In order for fire to occur in a passenger vehicle there are three main elements that must be present. First are the combustible materials which include fluids such as engine fuels and oils, transmission oils, power steering fluids, brake fluids and lubricants; upholsteries; tyres; plastic materials such as in dashboards and bumpers; possibly the body work of the vehicle itself; and finally, any contents being carried in the vehicle. Second is the availability of oxygen depends on whether vehicle doors and windows are open (and/or break during the fire), the ease that air can reach other internal parts of the car plus the external ventilation if the vehicle is in an enclosure. Some of the experiments collated in this review include the difference in vehicle burning characteristics as a result of the degree of opening of the vehicle

windows. The third element is the source of ignition. Common sources of ignition for vehicles are electrical faults, hot surfaces, mechanical failure and deliberate actions [16].

The heat release rate curves for single passenger vehicles are obtained from several publications of large-scale calorimeter fire experiments dating back from 1980s to the late 2000s. The review is limited to single vehicles since multiple vehicle experimental data is sparse. From the heat release rate curves the focus is on three characteristics which can be directly obtained from the heat release rate curves; the peak heat release rate, the time to reach peak heat release rate and the total energy released. There is inevitably an overlap with previous work, in particular the study of design fires for vehicles in tunnels by [51] and the database of vehicle fires available from [52]. However, these studies did not consider any form of vehicle classification and corresponding statistical analysis of severity characteristics and there are experiments that are included in this study that post-date the work by [51] and [52].

To achieve the objectives of the review, two components are presented. First is a collation and summary of the passenger vehicle fire experiments including an associated reproduction of the rate of heat release curve. Second is the distribution analysis which gathers the experiments into the specified weight-related classifications and suggests a distribution shape for each burning severity characteristic of interest. For this purpose the BestFit capability of the @RISK software [53] is used to process the data sets.

3.2 Collation of experiments – summary descriptions

A total of 41 single passenger vehicle fire experiments are collated where details are obtained from the corresponding reference sources. For the ANSI classification, the mass of the vehicle is required but if a source did not explicitly declare the mass then other information is used. For example, where the make, model and the year of manufacture are quoted in the original source, then the mass is obtained from the manufacturer's vehicle specification manual. In some cases the make, model and/or year were not given, thus the mass of the vehicles were obtained using the make and models information from several car specification database websites [54-56]. For the references which only specify the general model, a range for the mass of vehicles is collated. In some instances these ranges cross different classification groups and so these experiments are placed into groups which have the majority of the possible mass values for the vehicle model. Table 3-3 shows the frequency of vehicles

when they are grouped using the ANSI classification, however one vehicle is unclassified as there is insufficient detail provided in the original source material. From this point on, the experiments are compiled within its classification for the purpose of comparison and analysis.

Table 3-3: Number of experiments by ANSI classification.

ANSI classification	No. of experiments
Passenger car: Mini	6
Passenger car: Light	7
Passenger car: Compact	7
Passenger car: Medium	5
Passenger car: Heavy	7
Van / MPV	6
SUV	2
Unclassified vehicle	1

Table 3-4, Table 3-5,Table 3-6, Table 3-7, Table 3-8, Table 3-9, Table 3-10 and Table 3-11 provides a summary of the 41 experiments where each is given a unique identification code related to its ANSI classification which is used throughout this chapter rather than the referring to the details of the experiment itself. The exact year of vehicle manufacture not always given in the source reference but typically the decade is identified. In some cases the year of manufacture could only be estimated from the year of the publication of the original source and the years for which the vehicle was available. Values for the mass are that of the vehicle without contents but in some cases the heat release rate data includes the contribution of additional contents included in the experiment. Mass values for experiments M6, M7, L5, L7, MED5, MPV3, MPV4, MPV5 and MPV6 are shown as ranges for reasons explained previously.

The ‘Facility type’ column is the type of calorimeter used which is most cases was either an open calorimeter that did not restrict air flow to the vehicle or a room calorimeter with limited ventilation paths. The ‘Heat release rate evaluation method’ column provides information on how the heat release rate curve was obtained from the experiment. However not all references were clear on the exact technique used and so the information provided here is limited by what can be interpreted from the original publication. ‘Mass loss’ indicates that a mass loss measurement technique was used; ‘Convective calorimetry’ means the heat release rate was established by using temperature measurements; ‘Species-based calorimetry’ means that the heat release rate was obtained using either O_2 depletion, CO_2 and/or CO generation while ‘Oxygen depletion’ means that the use of O_2 depletion was clearly stated in

the reference. ‘Other methods’ means that the heat release rate was obtained either using chemical or radiative methods. ‘Not mentioned’ in the column means that it was unclear what method was used to evaluate the heat release rate curve.

The ‘Condition’ column provides some detail regarding the vehicle before the fire was started, in particular the degree of openness of any doors and/or windows. The ‘Ignition source’ column is the additional fuel used to start the fire while the ‘Ignition location’ column is the point of fire origin. Some of the resources have included the incipient stage in the heat release rate curves and this is clearly identified while for others the inclusion of an incipient stage is not clearly stated or no mention of the incipient stage is made. The status of the incipient stage is indicated in the specified column.

‘Mass loss rate’ relates to the rate of mass loss during the burning of the vehicle. ‘Toxic product emission’ relates to information regarding the toxic products produced or emitted during the experiment. The ‘smoke production’ relates to information regarding the production of smoke from the experiment. For these three items of information ‘Y’ in the column means that information is available in the resource while ‘N’ means that no information is available. The ‘Reference and experiment date (ED), report submitted (RS) or date published (DP)’ column is the information about the primary reference and about when the experiment was performed, or where no information is given then the date of the report was submitted is listed. If no experiment date and report submission date is available then the published date of the resource is shown.

Table 3-4:Passenger car: Mini

ID	Vehicle make and model	Vehicle year	Curb weight (kg)	Facility type	Condition	Ignition source	Ignition location	Incipient stage	Mass loss rate	Toxic product emission/Product consumption	Heat release rate evaluation method	Smoke production	Reference and experiment date (ED)/report submitted (RS)/date published (DP)
M1	Trabant Limousine	Undetermined, available from 1963 - 1990	695	Room calorimeter	Slight gap at top of windows	250 mL isopropanol	Front seat	Unclear	N	N	Convective calorimetry	N	[57] ED 1998
M2	Renault 5	1980s	757	Corner calorimeter	N/A	1.5 L gasoline in open tray	Under left front seat	Not mentioned	Y	N	Species-based calorimetry	N	[37] ED 24 Jul 1995
M3	Unknown	1995	830	Open calorimeter	N/A	1 L gasoline in open tray	Under gear box	Not mentioned	Y	N	Species based calorimetry	N	[37] ED 5 Jul 1996
M4	Rover-Austin Metro LS	1990s	893	Room calorimeter	Slight gap at top of windows	250 mL isopropanol	Front seat	Unclear	N	N	Convective calorimetry	N	[57] ED 1998
M5	Opel Kadett	Undetermined, available from 1962 - 1991	737-1007	Parking garage	N/A	N/A	N/A	Unclear	Y	N	Mass loss	N	[29] DP 5 Nov 1999
M6	Fiat 127	Undetermined, available from 1971 - 1983	705-870	Road tunnel	N/A	N/A	N/A	Unclear	N	N	Not mentioned	N	[58] ED 1997

Table 3-5: Passenger car: Light

ID	Vehicle make and model	Vehicle year	Curb weight (kg)	Facility type	Condition	Ignition source	Ignition location	Incipient stage	Mass loss rate	Carbon emission/Product consumption	Heat release rate evaluation method	Smoke production	Reference and experiment date (ED)/report submitted (RS)/date published (DP)
L1	Datsun 160 J Sedan	Late 1970s	918	Open calorimeter	All doors closed, left front window completely open, other windows rolled down 5 cm	3 L of heptane in open tray	Under the engine	Included	Y	Y (CO & CO_2 production)	Oxygen depletion	Y	[59] RS 6 May 1993
L2	Ford Taurus	Late 1970s	990	Open Calorimeter	Left door 10 cm ajar with the window completely open, right door closed with window rolled down 5 cm	1.5 L of heptane in open tray	Under left front seat	Included	Y	Y (CO & CO_2 production)	Oxygen depletion	Y	[59] RS 6 May 1993
L3	Citroen BX 16 RE	1970s or 1980s	1067	Room Calorimeter	Slight gap at top of windows	250 mL isopropanol	Front seat	Unclear	N	N	Convective calorimetry	N	[57] ED 1998
L4	Datsun 180B Sedan	Late 1970s	1102	Open Calorimeter	All doors closed, left front window completely open, other windows rolled down 5 cm	3 L of heptane in open tray	Under the engine	Included	Y	Y (CO & CO_2 production)	Oxygen depletion	Y	[59] RS 6 May 1993

L5	Austin Maestro	1982	915-950	Rail shuttle car	Driver and front passenger side windows completely open	No.7 wood crib (peak HRR of about 10 kW)	On front seat	Included	N	N	Oxygen depletion	N	[60] ED 18 Feb 1991
L6	Citroen BX 14 RE	1986	930	Rail shuttle car	Driver and front passenger side windows completely open	400 mL gasoline in foil tray (100 mL spilled)	Engine compartment under hood	Unclear	N	N	Oxygen depletion	N	[60] ED 18 Feb 1991
L7	Peugeot 309	Undetermined, available from 1985 - 1993	880-975	Parking garage	N/A	N/A	N/A	Unclear	Y	N	Mass loss	N	[29] DP 5 Nov 1999

Table 3-6: Passenger car: Compact

ID	Vehicle make and model	Vehicle year	Curb weight (kg)	Facility type	Condition	Ignition source	Ignition location	Incipient stage	Mass loss rate	Carbon emission/Product consumption	Heat release rate evaluation method	Smoke production	Reference and experiment date (ED)/report submitted (RS)/date published (DP)
C1	Unknown	Undetermined, available from 1970 – late 1990s	1182	Open Calorimeter	Driver and passenger windows rolled down 10 cm	Cloth soaked with methanol	Driver's seat	Included	N	N	Oxygen depletion	N	[48] DP March 2004
C2	Unknown	1995	1303	Open Calorimeter	N/A	1.5 L gasoline in open tray	Under left front seat	Not mentioned	Y	N	Species-based calorimetry	N	[37] ED 19 Jun 1996
C3	Unknown	1990s	1360	Room Calorimeter	1 m^2 windows opened; tank has 10 L of gasoline fuel.	80 g of alcohol gel fuel	Right rear wheel	Included	N	N	Mass loss	N	[61] RS 11 Sep 2007
C4	Unknown	1990s	1360	Room Calorimeter	Windows closed; tank has 10 L of gasoline fuel.	80 g of alcohol gel fuel	Right rear wheel	Included	N	N	Mass loss	N	[61] RS 11 Sep 2008
C5	Unknown	1990s	1360	Room Calorimeter	Windows closed; Tank has 20 L of gasoline fuel.	80 g of alcohol gel fuel	Right rear wheel	Included	N	N	Mass loss	N	[61] RS 11 Sep 2009
C6	Unknown	1990s	1360	Room	0.28 m^2 left front	2 L of	Left front	Included	N	N	Mass loss	N	[61]

				Calorimeter	window opened; Tank has 10 L of gasoline fuel.	gasoline spilled on left front seat	seat						RS 11 Sep 2010
C7	Ford Focus	2002	1197	Room Calorimeter	All passenger windows closed, bonnet closed after fire has established.	IMS soaked fibre-board	Engine compartment	Included	N	N	Species-based calorimetry	N	[1] ED 27 Aug 2008

Table 3-7: Passenger car: Medium

ID	Vehicle make and model	Vehicle year	Curb weight (kg)	Facility type	Condition	Ignition source	Ignition location	Incipient stage	Mass loss rate	Carbon emission/Product consumption	Heat release rate evaluation method	Smoke production	Reference and experiment date (ED)/report submitted (RS)/date published (DP)
MED1	Unknown	Undetermined, available from 1970 – late 1990s	1380	Open Calorimeter	Driver and passenger windows rolled down 10 cm	Cloth soaked with methanol	Driver's seat	Included	N	N	Oxygen depletion	N	[48] DP March 2004
MED2	Peugeot 406 Berline	1994	1382	Corner Calorimeter	N/A	1.5 L gasoline in open tray	Under gear box	Included	Y	N	Oxygen depletion	N	[14] ED 1995
MED3	Peugeot 406 Break	1994	1454	Corner Calorimeter	N/A	1.5 L gasoline in open tray	Under gear box	Included	Y	N	Oxygen depletion	N	[14] ED 1995
MED4	Unknown	Undetermined, available from 1970 – late 1990s	1470	Open Calorimeter	Driver and passenger windows rolled down 10 cm	Cloth soaked with methanol	Driver's seat	Included	N	N	Oxygen depletion	N	[48] DP March 2004
MED5	Renault Laguna	Undetermined, available from 1993 - 1999	1380 - 1550	N/A	60 l of fuel was in the fuel tank	N/A	N/A	Unclear	N	N	Not mentioned	N	[62] ED June 1999

Table 3-8: Passenger car: Heavy

ID	Vehicle make and model	Vehicle year	Curb weight (kg)	Facility type	Condition	Ignition source	Ignition location	Incipient stage	Mass loss rate	Carbon emission/Product consumption	Heat release rate evaluation method	Smoke production	Reference and experiment date (ED)/report submitted (RS)/date published (DP)
H1	Honda Accord	1998	1649	Open Calorimeter	All doors closed and front door windows raised, left and right rear door glass broken	Pool from 400 mL/min fuel tank leak ignited at 35 s	Under vehicle	Included	Y	Y (CO & CO_2 production)	Species-based calorimetry & other methods	Y	[63] ED 25 Feb 1999
H2	Honda Accord	1998	1738	Open Calorimeter	Windshield and right front door glass broken	Methanol vapour	Windshield washer fluid reservoir	Included	Y	Y (CO & CO_2 production)	Species-based calorimetry & other methods	Y	[64] ED 23 Feb 1999
H3	Chevrolet Camaro	1997	1811	Open Calorimeter	Left side door window and rear compartment lift window were shattered, gap between the bottom of the left door and frame	Pool from 515 mL/min fuel tank leak ignited at 30 s	Under vehicle	Included	Y	Y (CO & CO_2 production)	Species-based calorimetry & other methods	Y	[65] ED 30 Sep 1997
H4	Chevrolet	1999	1848	Open	Doors closed with	Nichrome	In air cleaner	Included	Y	Y (CO & CO_2	Species-	Y	[66]

	Camaro (Modified)			Calorimeter	windows raised to full closed position, right window glass (passenger door) of the vehicle broken	wires wrapped around PP sheet (1.2 kW)	housing in engine compartment			production)	based calorimetry & other methods		ED 21 Feb 2000
H5	Chevrolet Camaro	1999	1848	Open Calorimeter	Doors closed with windows raised to full closed position, right window glass (passenger door) of the vehicle broken	Nichrome wires wrapped around PP sheet (1.2 kW)	In air cleaner housing in engine compartment	Included	Y	Y (CO & CO_2 production)	Species-based calorimetry & other methods	Y	[66] ED 21 Feb 2000
H6	Chevrolet Camaro	1997	1849	Open Calorimeter	Windshield and right door window were broken and a section of the weld seam between the floor pan and inner rocker panel was separated	Propane torch flame impinging on HVAC module	Engine compartment	Included	Y	Y (CO & CO_2 production)	Species-based calorimetry & other methods	Y	[67] ED 1 Oct 1997
H7	Unknown	Undetermined, available from 1970 – late 1990s	1920	Open Calorimeter	Driver and passenger windows rolled down 10 cm	Cloth soaked with methanol	Driver's seat	Included	N	N	Oxygen depletion	N	[48] DP March 2004

Table 3-9: Sport-utility vehicle (SUV)

ID	Vehicle make and model	Vehicle year	Curb weight (kg)	Facility type	Condition	Ignition source	Ignition location	Incipient stage	Mass loss rate	Carbon emission/Product consumption	Heat release rate evalution method	Smoke production	Reference and experiment date (ED)/report submitted (RS)/date published (DP)
SUV1	Ford Explorer	1998	2232	Open Calorimeter	Pass through openings under left front seat; shift lever; drain holes, left door and door sills	Pool from 350 mL/min fuel tank leak ignited at 30 s	Under vehicle (mid-body)	Included	Y	Y (CO & CO_2 production)	Species-based calorimetry & other methods	Y	[68] ED 11 Jun 1998
SUV2	Ford Explorer	1998	2249	Open Calorimeter	Window openings on the left and right quarter panels; additional opening on the rear lift gate, left rear door, door frames and seams along the rear compartment floor panels	Pool from 750 mL/min fuel tank leak ignited at 30 s	Under vehicle	Included	Y	Y (CO & CO_2 production)	Species-based calorimetry & other methods	Y	[69] ED 9 Jun 1998

Table 3-10: Multi-purpose vehicle (MPV)

ID	Vehicle make and model	Vehicle year	Curb weight (kg)	Facility type	Condition	Ignition source	Ignition location	Incipient stage	Mass loss rate	Carbon emission/Product consumption	Heat release rate evaluation method	Smoke production	Reference and experiment date (ED)/report submitted (RS)/date published (DP)
MPV1	Plymouth Voyager	1996	1946	Open Calorimeter	Rear hatch window broken, left rear vent window open, left rear quarter panel cracked from crash	Pool from 243 ML/min fuel tank leak ignited at 30s	Under vehicle	Included	Y	Y (CO & CO_2 production)	Species-based calorimetry & other methods	Y	[70] ED 15 Nov 1996
MPV2	Dodge Caravan Sport	1996	1981	Open Calorimeter	Driver and passenger window slightly open	Electrical wire igniter	Around battery and power distributor housing	Included	Y	Y (CO & CO_2 production)	Species-based calorimetry & other methods	Y	[71] ED 13 Nov 1996
MPV3	Unknown (Minivan)	1995	N/A	Open Calorimeter	Driver and passenger window open	2 L of gasoline	Poured on driver's seat	Included (prior experiment not included)	N	Y (O_2 consumption, CO & CO_2 production)	Temperature difference	N	[72] ED 7 Dec 1999
MPV4	Renault Espace	Undetermined, available from 1984 – Late 1990s	1170 - 1780	Parking Garage	N/A	N/A	N/A	Unclear	Y	N	Mass loss	N	[29] DP 5 Nov 1999
MPV5	Renault	2001	1170 -	Room	All passenger	IMS soaked	Engine	Included	N	N	Species-based	N	[1]

	Espace		1780	Calorimeter	windows closed, bonnet closed after fire has established.	fibre-board	compartment				calorimetry		ED 1 Sep 2008
MPV6	Renault Espace	Undetermined, available from 1984 - 1994	1170 - 1780	Tunnel	N/A	N/A	N/A	Unclear	N	N	Species-based calorimetry	N	[73] DP 1994

Table 3-11: Unclassified vehicle

ID	Vehicle make and model	Vehicle year	Curb weight (kg)	Facility type	Condition	Ignition source	Ignition location	Incipient stage	Mass loss rate	Carbon emission/Product consumption	Heat release rate evaluation method	Smoke production	Reference and experiment date (ED)/report submitted (RS)/date published (DP)
U1	Unknown	1998	N/A	Open Calorimeter	Battery removed, petrol tank emptied, air bags, belt stretchers, side impact protection inactivated.	0.21 L of mineral spirits	On driver's seat and right rear passenger seat	Included	N	Y (CO, HCN, HCl & SO_2 production)	Oxygen depletion	N	[74] RS 21 Dec 2004

3.3 Heat release rate data

The heat release rate curves presented in this cahpter are gathered by their classification group Figure 3-1, Figure 3-2, Figure 3-3, Figure 3-4, Figure 3-5, Figure 3-6, Figure 3-7, and Figure 3-8. The unit for heat release rate and the time are standardized to kilowatts (kW) and minutes respectively. So that the reader can easily get a sense of the relative magnitude of the data for each classification, the scales of the plots are fixed corresponding to the maximum of the heat release rate and time. However for heavy passenger cars, the first six plots (H1 – 6) are scaled to 3,500 kW for heat release rate and 20 min for the time while the final plot (H7) is scaled to 3,500 kW for heat release rate and 100 min for the time. Similarly for MPVs, all the plots are fixed at the heat release rate of 6,500 kW however; for the time scale, the first three plots (MPV1 – 3) are scaled to 10 min while the other three plots (MPV4 – 6) are scaled to 70 min.

In experiment MPV3 the fire was extinguished after 4 min and for experiment MED3 it is not mentioned in the source why the fire stopped at 56 min thus making the data incomplete. Experiments H1, H2, H3, H4, H5, H6, SUV1, SUV2, MPV1, MPV2 come from a related set of sources in which were all suppressed after a specific time. These experiments were all representative of post-accident fires carried out for the NHTSA. Experiment M5, L7, H2, H6, MPV4 and U1 have been adjusted to exclude the incipient stage of the fire, which shows no values or values too small to record. The adjusted time for experiments M5, L7, H2, H6, MPV4 and MPV6 were 1 min 18 s; 5 min; 17 min 47 s; 1 min 51 s; 7 min 42 s; and 3 min and 6 s respectively.

A summary of the peak heat release rate, the time to reach the peak heat release rate and the total energy released is given in Table 3-12, Table 3-13, Table 3-14, Table 3-15, Table 3-16, Table 3-17, Table 3-18, and Table 3-19. If the information is not explicitly stated in the corresponding reference sources then it is obtained from the curves. The total mass loss of the vehicles during the experiment is also stated if it is available from the references otherwise the tables indicates “N/A”.

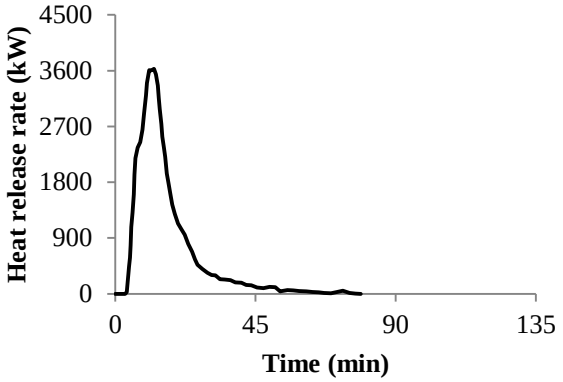

a) Experiment M1

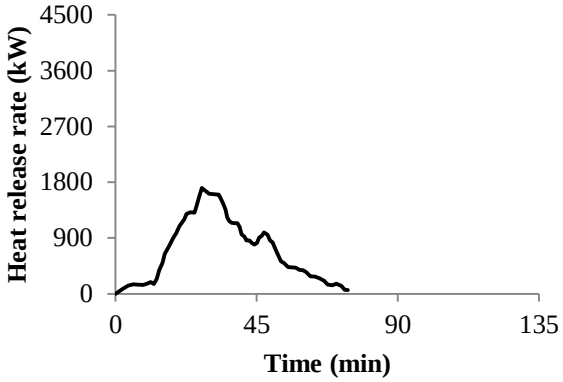

d) Experiment M4

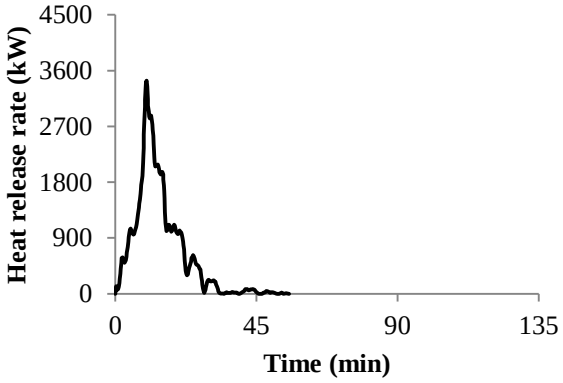

b) Experiment M2

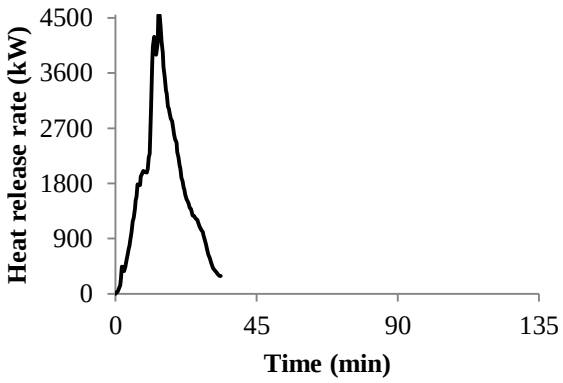

e) Experiment M5

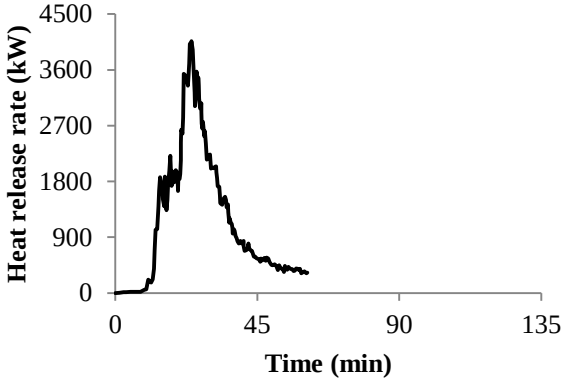

c) Experiment M3

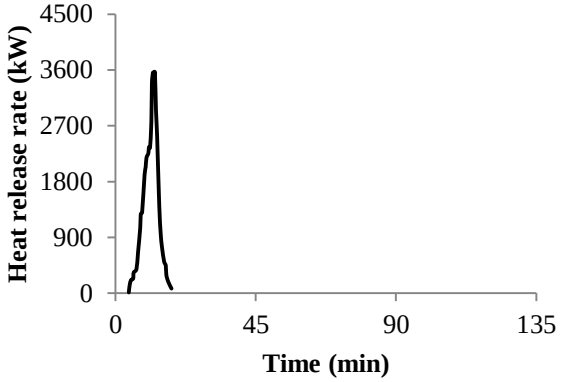

f) Experiment M6

Figure 3-1: List of Experiments; (a) Experiment M1 (b) Experiment M2 (c) Experiment M3 (d) Experiment M4 (e) Experiment M5 (f) Experiment M6.

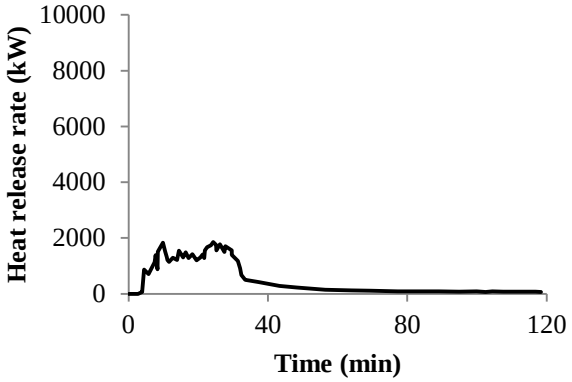

a) Experiment L1

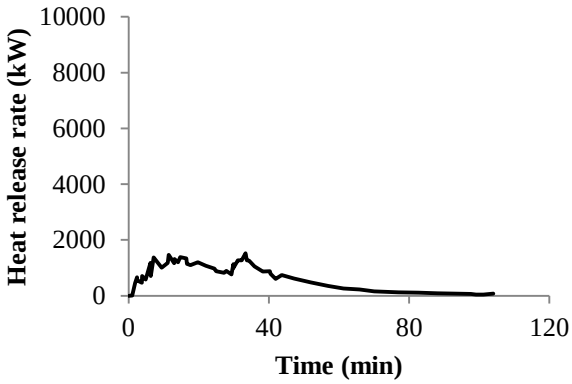

b) Experiment L2

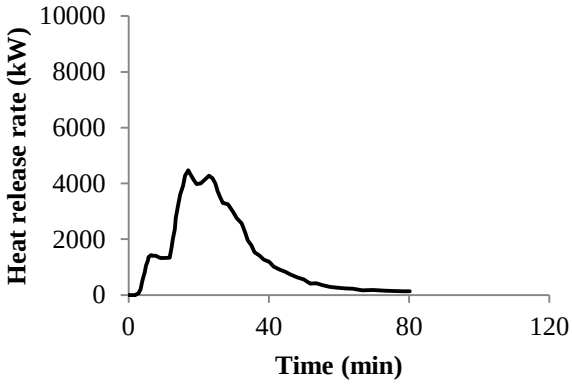

c) Experiment L3

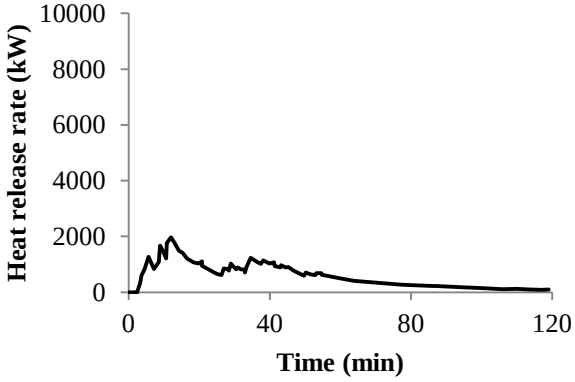

d) Experiment L4

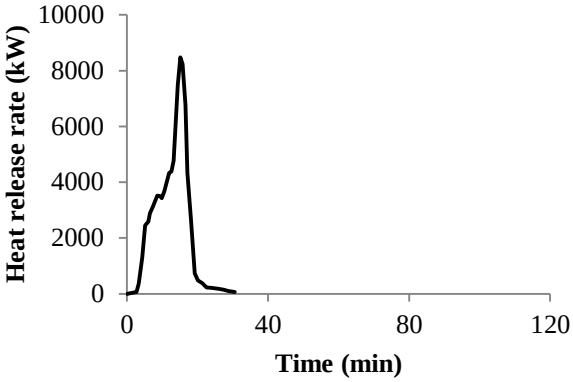

d) Experiment L5

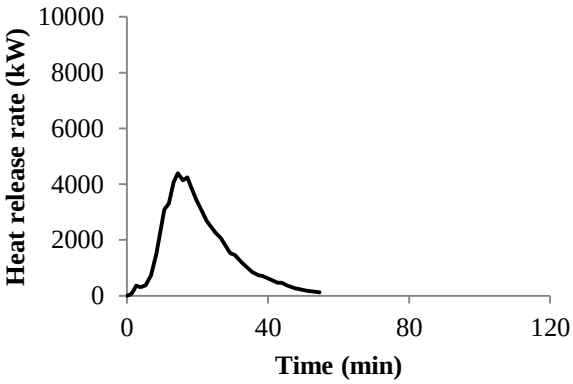

e) Experiment L6

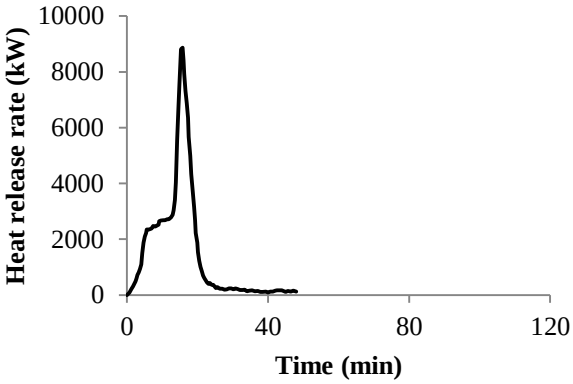

f) Experiment L7

Figure 3-2: List of Experiments; (a) Experiment L1 (b) Experiment L2 (c) Experiment L3 (d) Experiment L4 (e) Experiment L5 (f) Experiment L6 (g) Experiment L7.

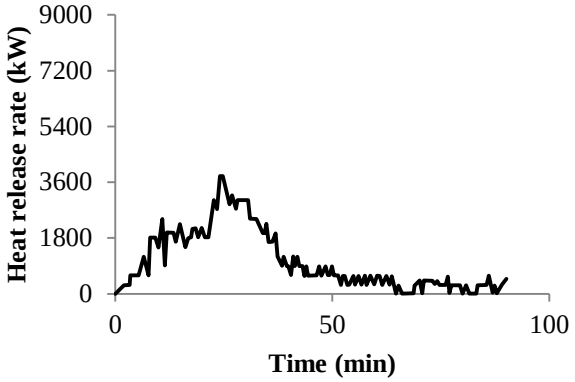

a) Experiment C1

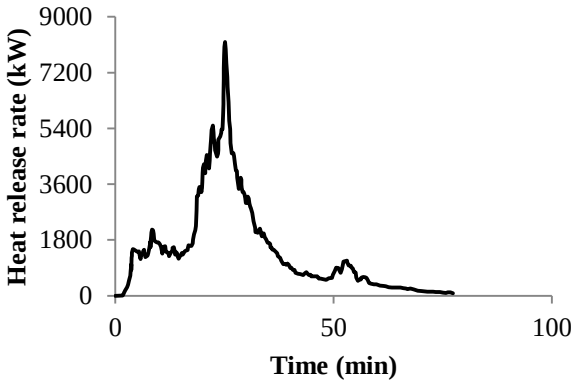

b) Experiment C2

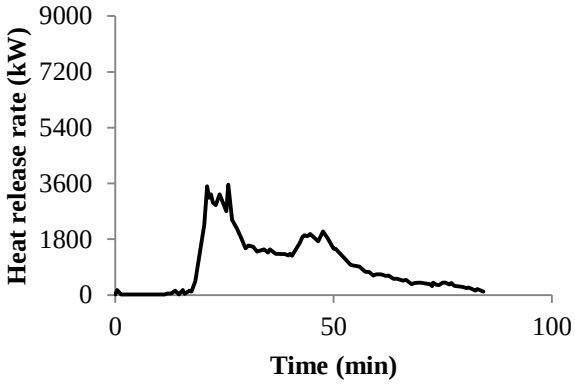

c) Experiment C3

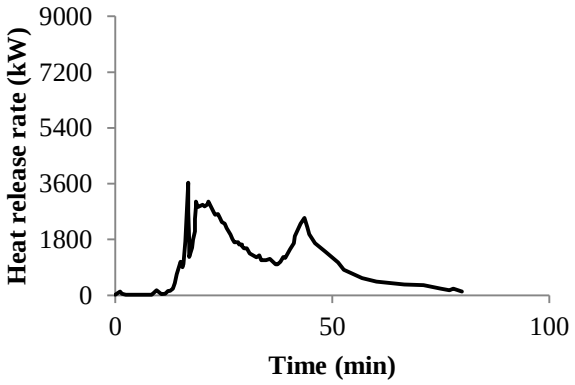

d) Experiment C4

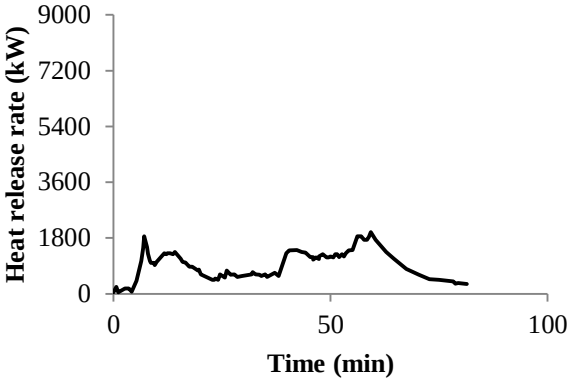

e) Experiment C5

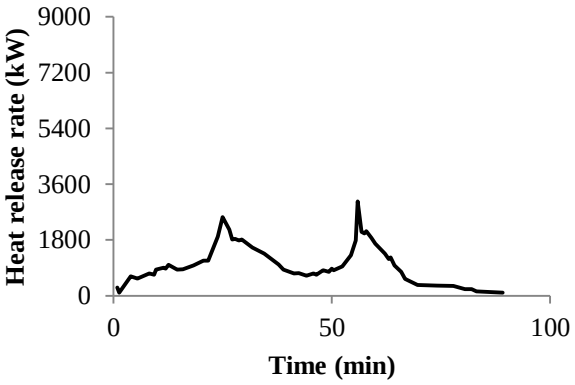

f) Experiment C6

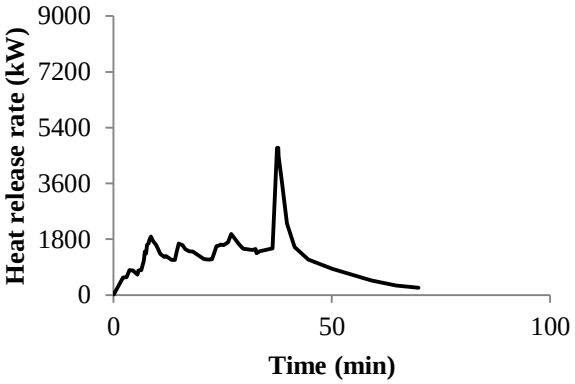

g) Experiment C7

Figure 3-3: List of Experiments; (a) Experiment C1 (b) Experiment C2 (c) Experiment C3 (d) Experiment C4 (e) Experiment C5 (f) Experiment C6 (g) Experiment C7.

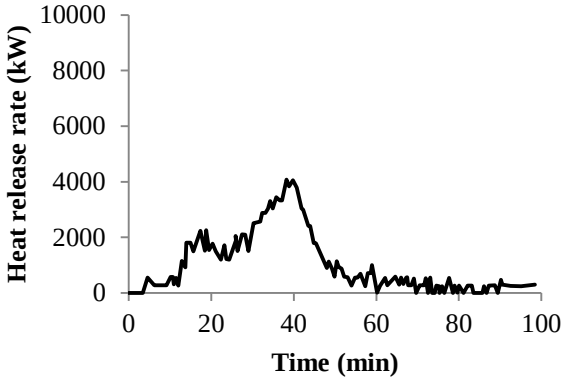

a) Experiment MED1

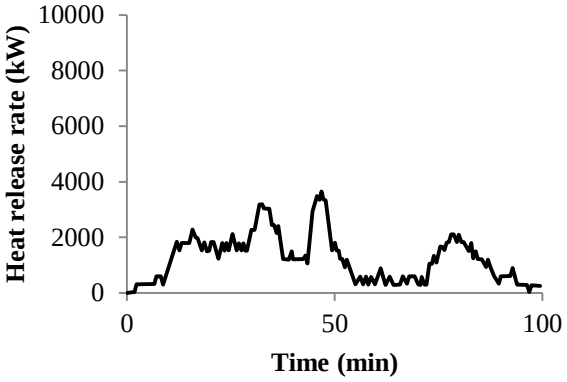

d) Experiment MED4

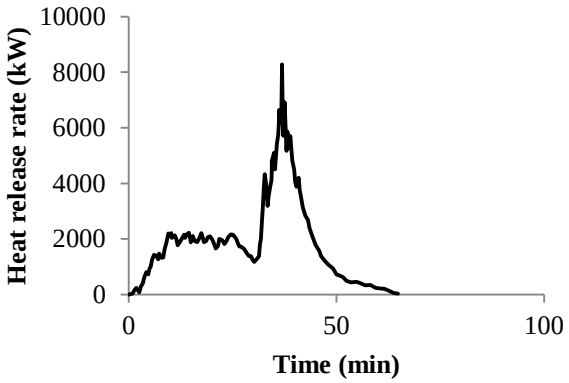

b) Experiment MED2

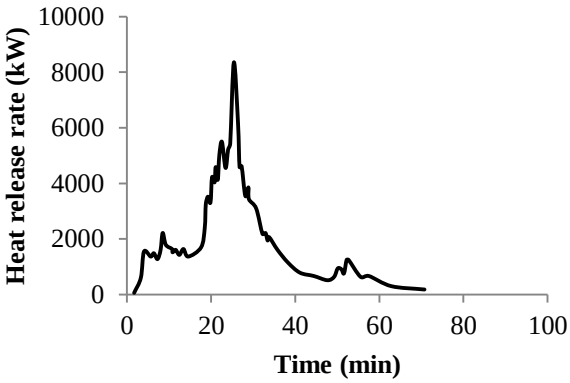

e) Experiment MED5

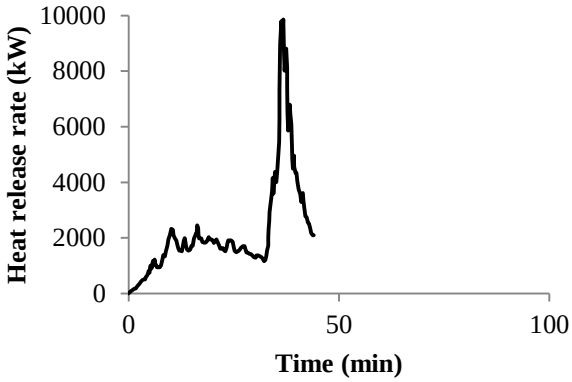

c) Experiment MED3

Figure 3-4: List of Experiments; (a) Experiment MED1 (b) Experiment MED2 (c) Experiment MED3 (d) Experiment MED4 (e) Experiment MED5.

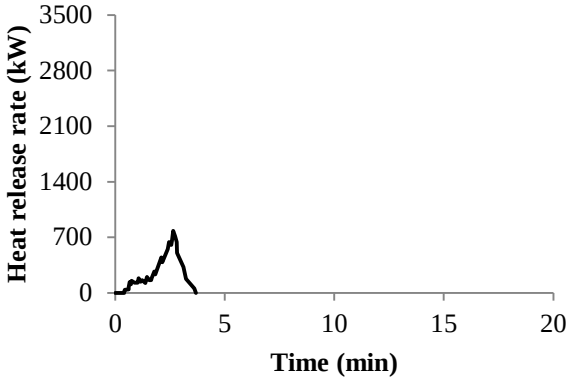

a) Experiment H1

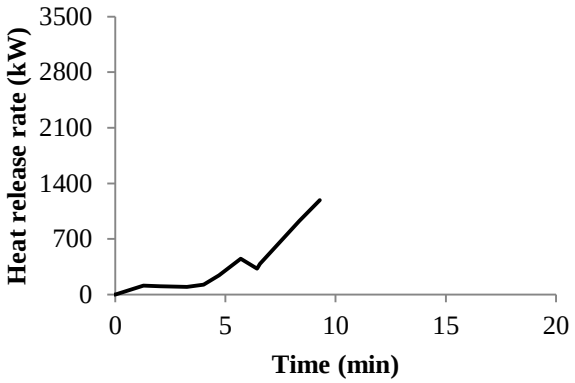

b) Experiment H2

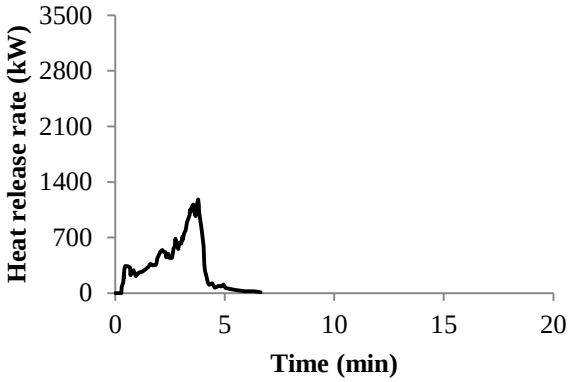

c) Experiment H3

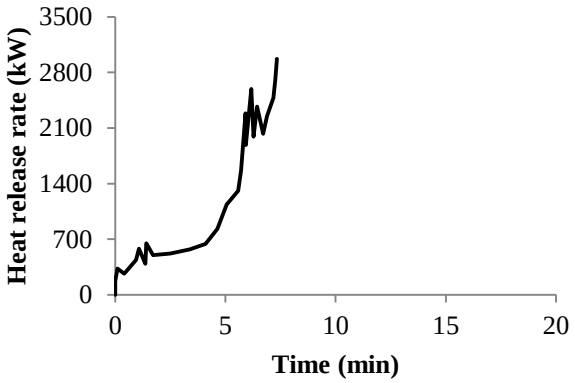

d) Experiment H4

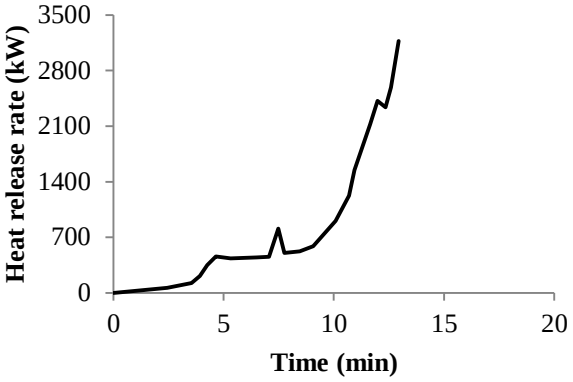

e) Experiment H5

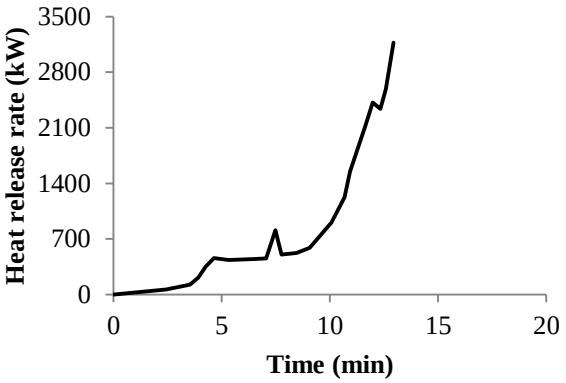

f) Experiment H6

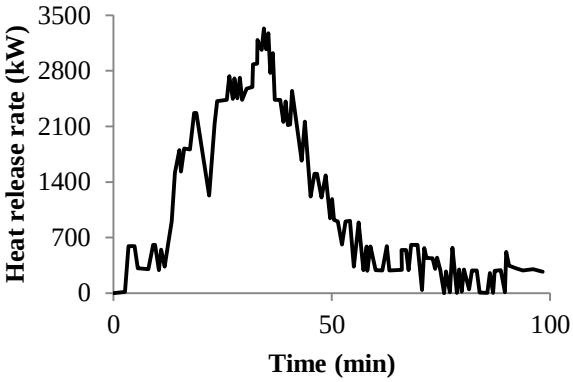

g) Experiment H7

Figure 3-5: List of Experiments; (a) Experiment H1 (b) Experiment H2 (c) Experiment H3 (d) Experiment H4 (e) Experiment H5 (f) Experiment H6 (g) Experiment H7.

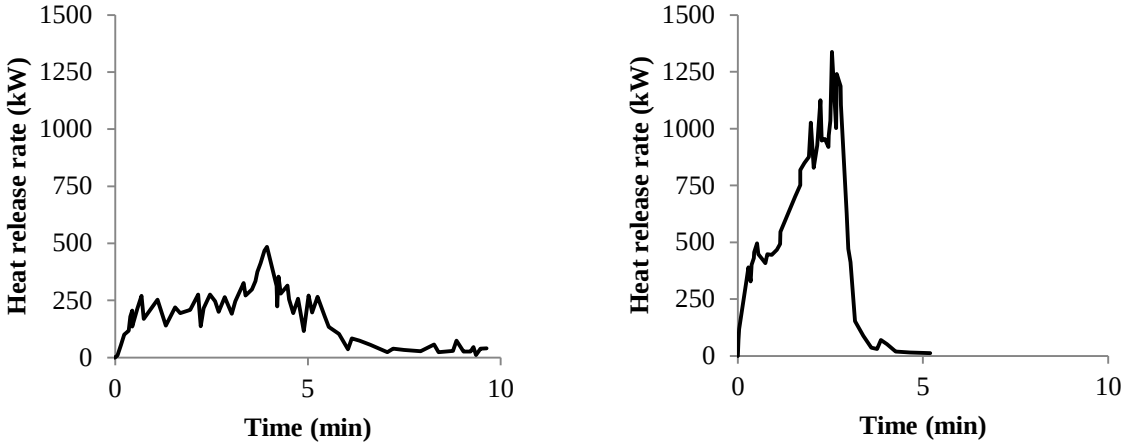

a) Experiment SUV1 b) Experiment SUV2

Figure 3-6: List of Experiments; (a) Experiment SUV1 (b) Experiment SUV2.

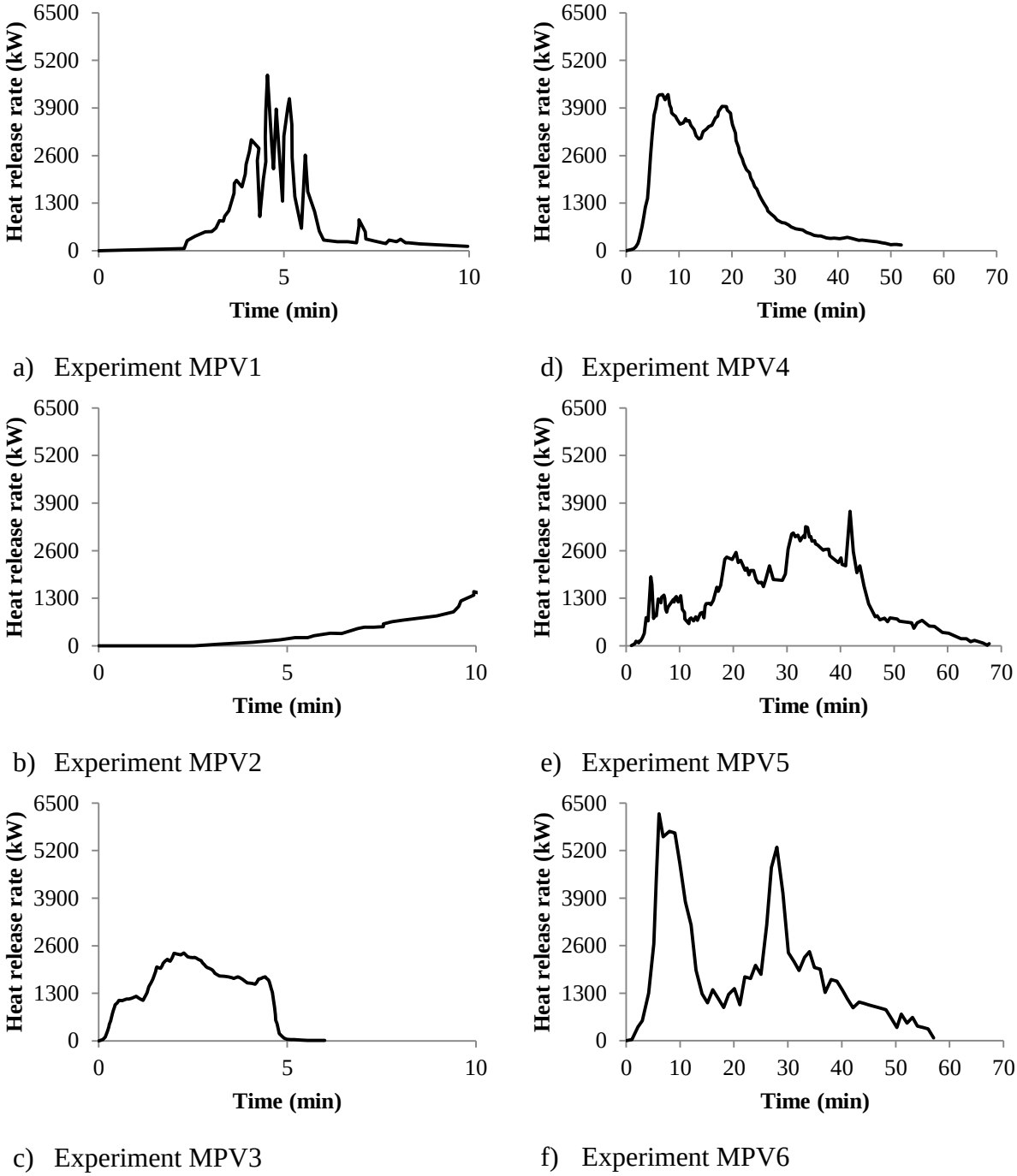

Figure 3-7: List of Experiments; (a) Experiment MPV1 (b) Experiment MPV2 (c) Experiment MPV3 (d) Experiment MPV4 (e) Experiment MPV5 (f) Experiment MPV6.

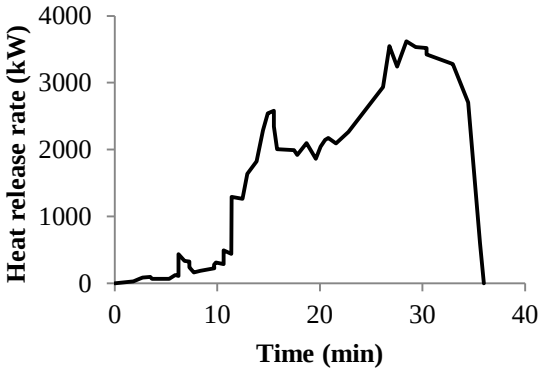

Figure 3-8: Heat release rate for unclassified vehicle experiment U1.

Table 3-12:Passenger car : Mini

Experiments	Peak heat release rate (kW)	Time to peak (min)	Total energy released (MJ)	Total mass loss (kg)
M1	3630	12.4	3100	100
M2	3439	10.0	2100	138
M3	4063	24.1	4090	184
M4	1710	27.6	3200	108
M5	4549	15.4	3466	139
M6	3560	12.0	1500	N/A

Table 3-13: Passenger car : Light

Experiments	Peak heat release rate (kW)	Time to peak (min)	Total energy released (MJ)	Total mass loss (kg)
L1	1859	24.3	3000	143
L2	1521	33.4	3300	141
L3	4470	17.0	8000	270
L4	1972	12.0	3900	176
L5	8482	15.2	4008	N/A
L6	4390	14.4	4957	N/A
L7	8872	20.8	4134	165

Table 3-14: Passenger car : Compact

Experiments	Peak heat release rate (kW)	Time to peak (min)	Total energy released (MJ)	Total mass loss (kg)
C1	3801	24.1	5280	165
C2	8188	25.2	6670	275
C3	3560	31.0	4950	225
C4	3633	25.0	4860	221
C5	1990	67.0	4930	224
C6	3039	55.0	5040	229
C7	4800	37.5	N/A	N/A

Table 3-15: Passenger car : Medium

Experiments	Peak heat release rate (kW)	Time to peak (min)	Total energy released (MJ)	Total mass loss (kg)
MED1	4073	38.3	6144	192
MED2	8283	36.9	7000	255
MED3	9854	37.8	6806	262
MED4	3650	46.9	5960	186
MED5	8354	26.0	6700	N/A

Table 3-16: Passenger car : Heavy

Experiments	Peak heat release rate (kW)	Time to peak (min)	Total energy released (MJ)	Total mass loss (kg)
H1	780	2.6	1816	N/A
H2	1189	27.1	199	N/A
H3	1181	3.8	130	N/A
H4	2973	12.7	445	N/A
H5	3173	12.9	540	N/A
H6	1161	16.0	233	N/A
H7	3332	34.4	7648	239

Table 3-17: Sport-utility vehicle (SUV)

Experiments	Peak heat release rate (kW)	Time to peak (min)	Total energy released (MJ)	Total mass loss (kg)
SUV1	484	4.3	90	N/A
SUV2	1337	2.5	131	N/A

Table 3-18: Multi-purpose vehicle (MPV)

Experiments	Peak heat release rate (kW)	Time to peak (min)	Total energy released (MJ)	Total mass loss (kg)
MPV1	4797	4.6	421	N/A
MPV2	1545	10.7	254	N/A
MPV3	2405	2.3	459	N/A
MPV4	4270	15.8	5028	201
MPV5	3800	54.0	N/A	N/A
MPV6	6206	9.2	7000	N/A

Table 3-19: Unclassified vehicle

Experiments	Peak heat release rate (kW)	Time to peak (min)	Total energy released (MJ)	Total mass loss (kg)
U1	3618	28.4	3800	N/A

3.4 Analysis and discussion

To perform further analysis of the data collected there are several factors that need to be considered. Firstly it is already noted that there has been a change in the types of materials used in vehicles over the 40-year span of experiments assessed in this work. These changes in materials have been notably in the plastics and composite content which have increased up to 181.4 kg (400 lbs) per vehicle in 2010s compared to less than 9.1 kg (20 lbs) per vehicle in the 1960s [50]. These changes could result in differences in the fire severity characteristics of a vehicle even if the weight is the same due to changing amount and calorific value of the combustible materials. In addition it is also noted that the procedures, standards and/or protocols varied between each experiment which likely lead to different effects on the fire spread, availability of air etc. Finally it is important to note that the various heat release rate measurement techniques, namely mass loss rate, convective calorimetry and species-based calorimetry, could result in variability in the heat release rate measurements [75] thus affecting the fire severity analyses.

As already discussed, this work will consider curb weight which is deemed sufficient for the purposes of the wider research objectives associated with a risk-based fire safety of passenger road vehicles in parking buildings. However even this grouping already reduces the data set size to a maximum of seven experiments which challenges any statistical analysis. The factors that include the age of the vehicle, the heat release rate measurement technique, the ignition conditions, the availability of air etc. mean that any analysis that groups the vehicle data together will result in heterogeneous data sets to some degree. It is not possible to create absolutely homogenous data sets that also provide sufficient items of data to be meaningful.

3.4.1 Vehicle age

Since it is noted that the amount of combustible materials in vehicles has changed over time, a vehicle age analysis for the 41 experiments is carried out. The data collated in this chapter includes passenger vehicles manufactured of a span of 40 years however not all of the references provided the exact year of vehicle manufacture thus the experiments were divided into three age categories; experiments with the known year of vehicle manufacture; experiments with the known decade of vehicle manufacture and experiments with an estimated decade of vehicle manufacture based on the date of experiment, date of submission

or publication of the source reference. Clearly the third age category introduces more uncertainty to the year of vehicle manufacture than the other two age categories.

There are 20 experiments that give a known year of manufacture. However, from these 20 experiments there are limitations on the results from the 12 experiments H1, H2, H3, H4, H5, H6, SUV1, SUV2, MPV1, MPV2, MPV3 and U1 (all manufactured during the 1990s) such that they are not suitable for complete analysis. There are 11 experiments with a known decade of manufacture while the remaining 10 experiments only have an estimated decade of manufacture based on the date of the experiment, and/or publication. For these 10 cases, five could only be dated somewhere between 1970 and the end of the 1990s, while three could only be dated somewhere between 1980 and the end of the 1990s, and the remaining two could only be dated somewhere between 1960 and the end of the 1990s. Figure 3-9 shows those dates for the first two age categories described above since data including the third age category gave widely dispersed results. It can be seen that 70% of the vehicles examined in this study were manufactured during the 1990s.

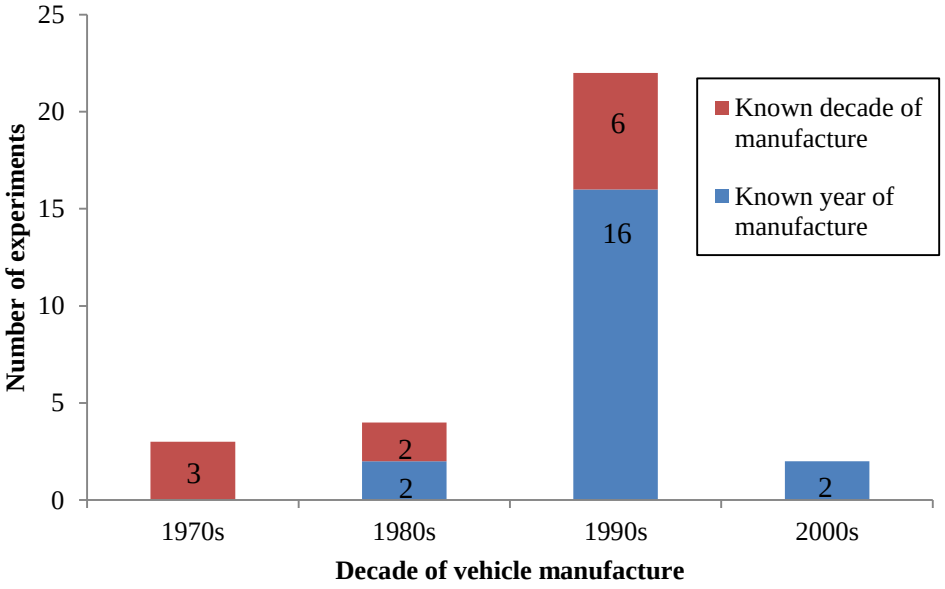

Figure 3-9:The experiments' vehicle age distribution over four decades.

3.4.2 Fire severity analysis

Table 3-20 gathers the results for the 41 experiments for the mean and standard deviation of peak heat release rate (kW), time to reach peak heat release rate (min) and total energy released (MJ) for each classification. Table 3-20 suggests that the three fire severity characteristics generally increase with curb weight up to the Passenger car: Medium class

where it is assumed that the combustible material content can be regarded as likely being reasonably homogeneous given a large majority of vehicles were manufactured during the 1990s. An assessment of these findings is provided later.

Table 3-20:Mean and standard deviation fire severity characteristics for all experiments by curb weight classification

Vehicle classification	Peak heat release rate (kW)				Time to peak (min)				Total energy released (MJ)			
	Mean	Standard deviation	Max value	Min value	Mean	Standard deviation	Max value	Min value	Mean	Standard deviation	Max value	Min value
Passenger car: Mini	3492	964	4063	1710	16.9	7.2	27.6	10.0	2909	945	4090	1500
Passenger car: Light	4509	3088	8872	1521	19.6	7.4	33.4	12.0	4471	1677	8000	3000
Passenger car: Compact	4144	1973	8188	1990	37.8	16.9	67.0	25.0	5288	692	6670	4860
Passenger car: Medium	6843	2797	9854	3650	37.2	7.4	46.9	26.0	6386	695	7000	5960
Passenger car:	1969	1126	3332	780	15.6	11.6	34.4	2.6	1573	2740	7648	130
Heavy	(3332)	(−)	(−)	(−)	(34.4)	(−)	(−)	(−)	(7648)	(−)	(−)	(−)
SUV	910	603	1337	484	3.4	1.2	4.3	2.5	110	28	131	90
	(−)	(−)	(−)	(−)	(−)	(−)	(−)	(−)	(−)	(−)	(−)	(−)
MPV	3837	1675	6206	1545	16.1	19.2	54.0	2.3	2632	3166	7000	254
	(4759)	(1041)	(6206)	(3800)	(26.3)	(19.7)	(54.0)	(9.2)	(6014)	(986)	(7000)	(5028)
Unclassified vehicle	3618	-	-	-	28.4	-	-	-	3800	-	-	-
	(−)	(−)	(−)	(−)	(−)	(−)	(−)	(−)	(−)	(−)	(−)	(−)

(-) not applicable

Values shown enclosed in braces do not include those experiments that have been excluded from further analysis.

However as noted earlier, there are limitations on the results from experiments H1, H2, H3, H4, H5, H6, SUV1, SUV2, MPV1, MPV2 and MPV3 as these experiments were suppressed prior to complete vehicle burnout or the data are otherwise incomplete. These limitations affect the usefulness of the statistics for Passenger Car: Heavy, SUV and MPV classifications and as a result, these curb weight classes are predominately excluded from the further analysis as the results would not likely represent the behaviour of vehicle fires for its class. Thus Table 3-20 also provides an analysis that excludes the 11 experiments listed above along with experiment U1 due to the lack of details.

Graphs of the total energy released, the time to reach the peak heat release rate and peak heat release rate are constructed for the four classifications with sufficient complete data, namely: Passenger Car: Mini, Light, Compact and Medium data sets. Additionally, four data points; three from MPV4, MPV5 and MPV6 and one from Passenger Car: Heavy (H7) are also included in the graphs. For experiments M5, M7, L5, L7 and MED5, horizontal bars are shown to represent the range of possible vehicle curb weights.

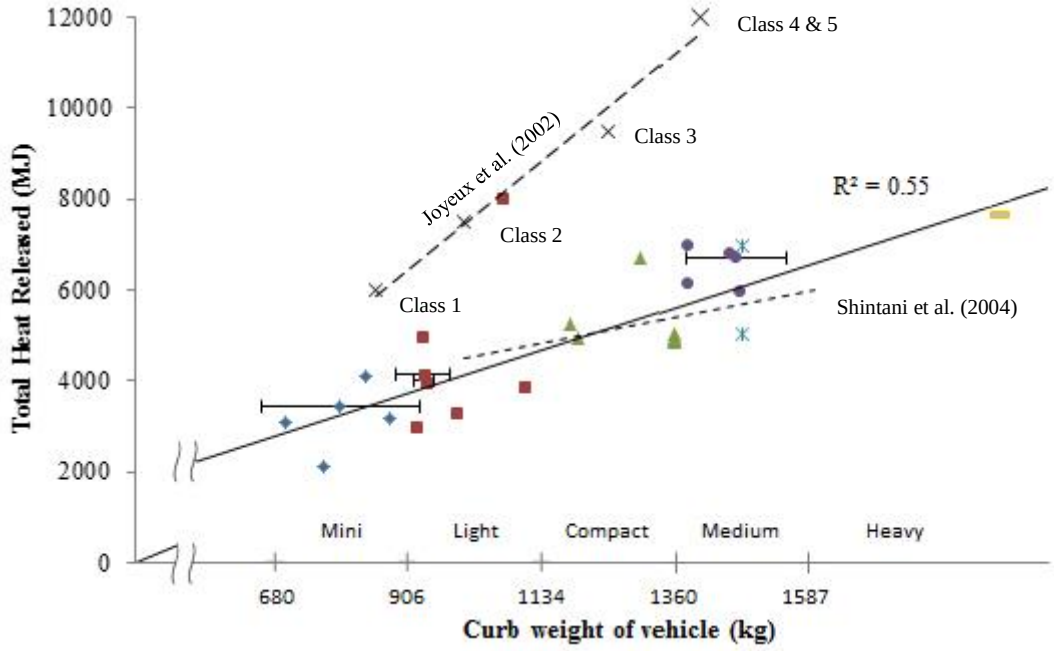

Figure 3-10: The total energy released against curb weight of vehicles and associated classifications. (Solid symbols correspond to ANSI vehicle curb weight classifications; ✳ symbol for ANSI MPV classification; and × symbol for Joyeux's European Car classification, 1 – 5).

Figure 3-10 shows there is a proportional increase in total energy released with the increment of curb weight where the average total energy released increases from around 3500 to 6800 MJ. A linear trend through the origin is fitted to the data with a relatively weak R^2 correlation value of 0.55. It is noted that the result from L3 appears as an outlier when compared to the remaining data and if this is excluded then the R^2 value increases to 0.72. The total energy release over the experiments considered can be approximated as 4.14 times the curb weight whether L3 is included or not. In comparison the vehicle mass categories proposed by [14] and the linear fit proposed by [48] are shown in Figure 10. It is clear that Joyeux et al.'s values for total energy release are noticeably higher for a given vehicle mass as compared to the experimental data with only the outlier from L3 being comparable. Shintani et al.'s linear

fit (where their four experiments are included in this analysis as experiments C1, MED1, MED4 and H7) is similar to the proposed linear fit across the majority of the data but an extrapolation to lower curb weights would give disproportionately lower energy release values.

It is useful to use the data to investigate whether the total energy released for a given vehicle category decreases as the vehicle age increases because of the changes in combustible materials over time. However since the majority of vehicles identified in this study are grouped in the 1990s age category and only the Passenger Car: Light curb weight classification spans more than two decades, it is not possible to get much in the way of firm conclusions on this issue. Figure 3-11 shows a graph of the average total energy release for the Passenger Car: Light curb weight classification for the best estimate of the decade of vehicle manufacture. Data for the 1980s consists of L3, L5 and L6 where the highest energy release is from L3 at 8000 MJ which is more than 60% greater than any other value recorded for this curb weight classification. If L3 is treated as an outlier, as previously, then the average total energy release reduces to 4483 MJ which still exceeds the 1990s result from the single L7 experiment. Using the information given by [50] for the increase in the amount of plastics per decade, then a vehicle manufactured in the late 1970s would have around 150 kg and one manufactured in the 1990s would have around 200 kg, i.e. an increase of 50 kg.

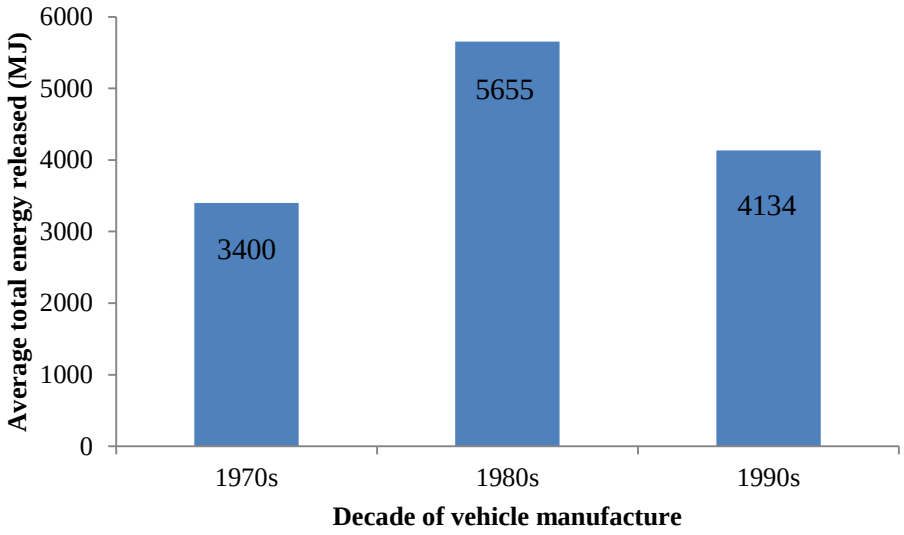

Figure 3-11: Total energy release for the passenger Car: light curb weight classification over the best estimate of the decade.

Heats of combustion for most typical thermoplastic and thermosetting polymers are in the range ~16 – 46 MJ/kg [76] and if it is then assumed that only the increase in plastics contributes to the change in the total energy release then this would result in an increase in the range 800 – 2300 MJ. From Figure 3-11 the change in total energy release is from an average value of 3400 MJ (L1, L2 and L4) expected value would be 4200 – 5700 MJ compared to around 4134 MJ (for experiment L7) which is less than the lower estimated bound.

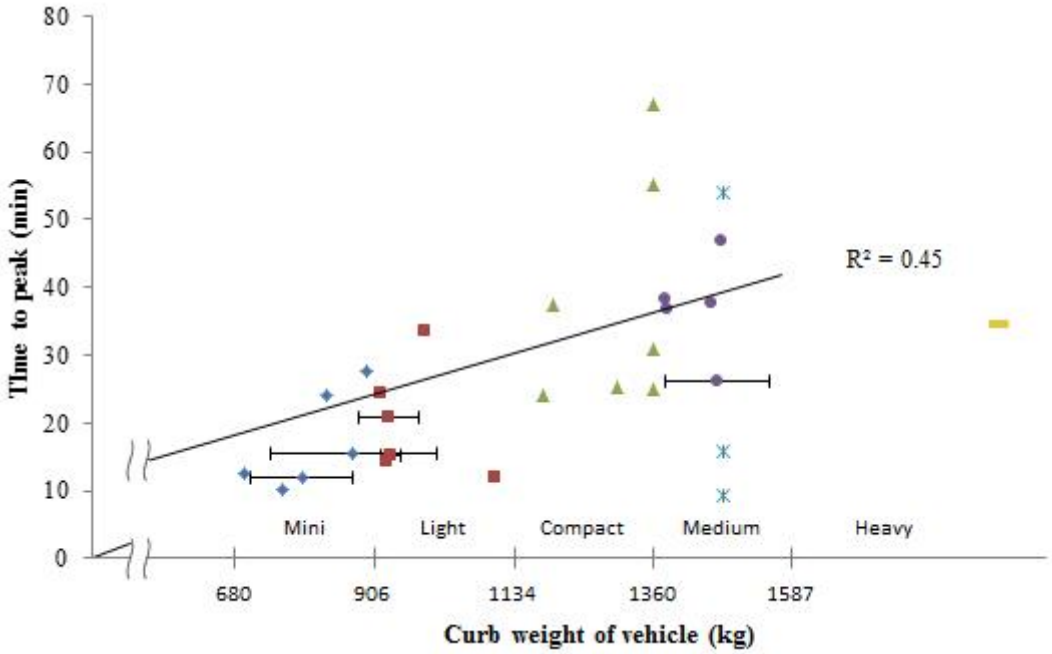

Figure 3-12: The time to reach peak heat release rate against curb weight of vehicles and associated classifications. (Solid symbols correspond to ANSI vehicle curb weight classifications; and ✳ symbol for ANSI MPV classification).

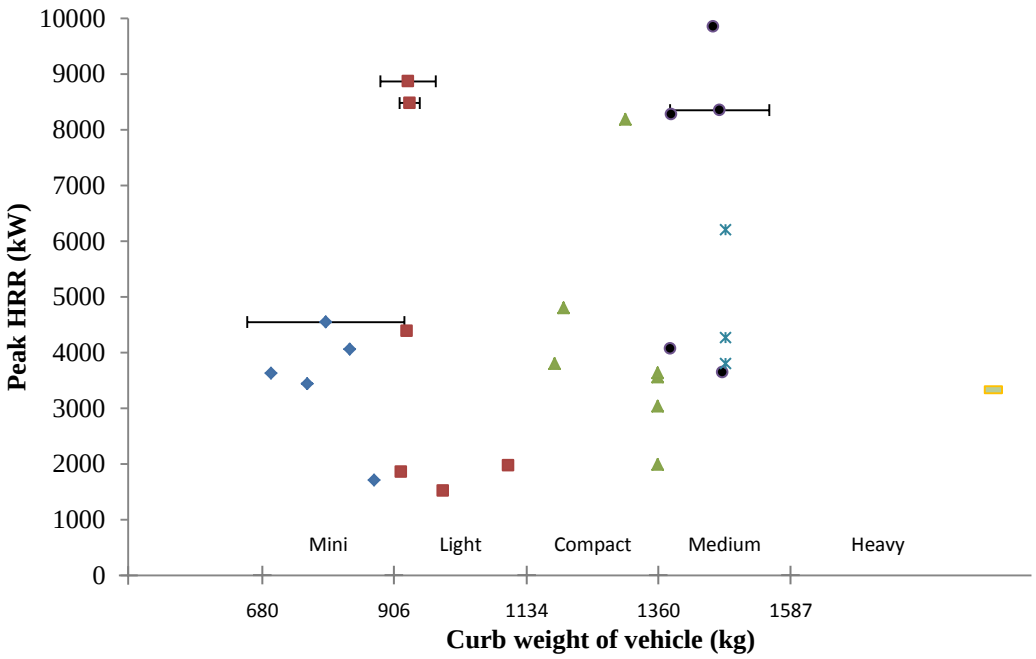

Figure 3-13: The peak heat release rates against curb weight of vehicles and associated classifications. (Solid symbols correspond to ANSI vehicle curb weight classifications; and ✳ symbol for ANSI MPV classification).

The time to reach peak heat release rate in Figure 3-12 shows a generally increasing trend as the curb weight class of the vehicles increases. A linear trend is fitted to the data up to the Passenger Car: Medium class due to limited adequate data sets for greater curb weights. However the fit only achieves an R^2 value of 0.45 with scatter in the data increasing as the curb weight increases. The peak heat release rate in Figure 3-13 exhibits a very weak correlation with curb weight such that there is a reduction for the Passenger car: Compact class when compared to the preceding lighter class. Although other classes show an increasing trend against the increase of curb weight there is noticeable scatter in the data and so there is no attempt to fit a trend line.

It is also worth to note that ventilation configuration of the vehicle i.e. the windows are open or not. However, from the data collation it seems that only 17 experiments were given quantifiable information regarding the ventilation configuration in the vehicle. Furthermore, from the 17 experiments, all of them were distributed in different classes and there were also different range of configuration of ventilation openings for different experiments i.e. windows were fully opened, windows were fully closed, 10 cm^2 front windows were opened, etc. Another important point to note is the ventilation configuration of the experimental facilities. It was recorded that, the vehicle in each experiment was exposed to open air, enclosed where there was limited supply of air, or partially enclosed. However, there were

limited information on the dimensions of the facility which restricts further analyses on this particular matter. Therefore, at this stage, no further analyses were conducted on the effect of the ventilation configuration of the vehicle or the experimental facilities.

3.4.3 Distribution analysis

Given the somewhat weak correlation for the linear fits to the total rate of heat release and time to peak rate of heat release it is worthwhile to further examine the data using statistical distributions. For this distribution analysis the curb weight classes Passenger car: Mini, Light, Compact and Medium are investigated as these groups had sufficient data available. In addition, a distribution that combines the passenger vehicles for these four curb weight classes is obtained in order to utilize a larger data set and provide a more generic distribution that encompasses the four classifications.

There are three methods used by the @RISK software for obtaining the best-fit probability distributions: the Chi-squared method, the Anderson-Darling method and the Kolmogorov-Smirnov method. Chi-squared method is best known as the goodness-of-fit statistic where it can be used with both continuous and discrete sample data. To use the chi-squared method, @RISK will break up the *x*-axis domain into several "bins" and then use a specific to obtain the best-fit probability [53]. A weakness of the chi-squared method is that there are no clear guidelines for selecting the number and location of the bins. Therefore, the number and location of the bins has to be selected arbitrarily. Another fit statistic method that can be used in @RISK is the Kolmogorov-Smirnov method it does not require binning, which makes it less arbitrary than the chi-squared method [53]. The method is much focused on the middle distribution and does not detect tail discrepancies very well. The other fit statistic method that can be used in @RISK is the Anderson-Darling method. Unlike the Kolmogorov-Smirnov method, which focuses in the middle of the distribution, the Anderson-Darling method highlights differences between the tails of the fitted distribution and input data [53].

For this particular analysis, the Kolmogorov-Smirnov method was chosen as this method is focused on the middle of the distribution. This is because the analysis is focusing on the average values of the distribution. The outcome of the @RISK distribution fitting process is a ranked order of fitting statistics for each potential distribution shape where a smaller value indicates a better fit. Nevertheless, for this particular analysis, the selections of distribution shapes were not only based on the ranking of the fitting statistics values but also based on the

distribution shapes that are commonly used and likely to be available in other software tools for further analysis, and also on selecting a consistent distribution shape for the various severity characteristics. For the fire risk analysis in parking building research the B-RISK model [18] is planned to be used for the analysis of fire spread between vehicles and so distribution shapes that have the potential to be used in this model have been selected. The distributions selected for the ranking in @RISK are Weibull, Beta General, Gamma, Lognormal, Log-Logistic and Triangular all with the lower bound fixed at zero where relevant.

Table 3-21, Table 3-22, and Table 3-23 shows the ranked order of distributions given by @RISK along with the associated fitting statistic. From this ranking it is decided that the Weibull distribution gives an acceptable overall result. It is clear that in some cases there is very little to choose between the fitting statistics for a given severity characteristic, for example although the Weibull distribution for the time to peak rate of heat release for Passenger car: Mini is the 3rd ranked in the list, the fitting statistic only decrease from 0.21 to 0.24 between the top ranked Log-Logistic and the Weibull distributions. Furthermore although the Weibull distribution is ranked 4th for the time to peak rate of heat release for Passenger car: Light the fitting statistic is still higher than the top-ranked distribution for the four other curb weight classifications. Each of the probability distributions are available in Appendix A.

Table 3-21: Ranked order distributions for peak heat released rate for combined vehicles.

	Mini		**Light**		**Compact**		**Medium**	
Rank	**Distribution shape**	**Value**	**Distribution shape**	**Value**	**Distribution shape**	**Value**	**Distribution shape**	**Value**
1	*Weibull*	*0.28*	Log-Logistic	0.24	Lognormal	0.22	Beta General	0.30
2	Beta General	0.29	*Weibull*	*0.24*	Gamma	0.24	Triangular	0.31
3	Gamma	0.35	Triangular	0.25	*Weibull*	0.26	*Weibull*	*0.32*
4	Lognormal	0.37	Lognormal	0.25	Triangular	0.28	Gamma	0.34
5	Triangular	0.41	Gamma	0.25	Beta General	0.35	Lognormal	0.34

Table 3-22: Ranked order distributions for time to reach peak heat release rate for combined vehicles.

	Mini		**Light**		**Compact**		**Medium**	
Rank	**Distribution shape**	**Value**	**Distribution shape**	**Value**	**Distribution shape**	**Value**	**Distribution shape**	**Value**
1	Log-Logistic	0.21	Log-Logistic	0.15	Log-Logistic	0.21	*Weibull*	*0.27*
2	Lognormal	0.24	Lognormal	0.18	*Weibull*	*0.22*	Gamma	0.31
3	*Weibull*	*0.24*	Gamma	0.19	Gamma	0.23	Lognormal	0.32
4	Gamma	0.25	*Weibull*	*0.20*	Lognormal	0.24	Triangular	0.42
5	Beta General	0.27	Triangular	0.24	Triangular	0.29		

Table 3-23: Ranked order distributions for total energy released for combined vehicles.

	Mini		Light		Compact		Medium	
Rank	**Distribution shape**	**Value**	**Distribution shape**	**Value**	**Distribution shape**	**Value**	**Distribution shape**	**Value**
1	Triangular	0.21	Triangular	0.25	Lognormal	0.32	Beta General	0.25
2	*Weibull*	*0.24*	Lognormal	0.25	Gamma	0.32	*Weibull*	*0.27*
3	Gamma	0.29	Gamma	0.27	*Weibull*	*0.36*	Gamma	0.30
4	Lognormal	0.30	*Weibull*	*0.28*	Beta General	0.45	Lognormal	0.30
5	Beta General	0.32	Beta General	0.45	Triangular	0.53	Triangular	0.57

Table 3-24 shows the summary of the distribution analysis for four vehicle classifications and all vehicles with the suggested distribution statistics for peak heat release rate, time to reach peak heat release rate and total energy released. Also in the table, κ is the shape parameter for probability distribution and θ is the scale parameter for probability distribution. Figure 3-14 shows the frequency data and best-fit distributions for peak heat release rate, time to reach peak heat release rate and total energy released for the combined passenger vehicle data. The 5^{th} and 95^{th} percentile values for each distribution are also indicated in Figure 3-14.

Table 3-24: Summary of the distribution analyses.

		Peak heat release rate (kW)		Time to peak (min)		Total energy released (MJ)	
Curb weight class	**Distribution parameter**	**κ**	**θ**	**κ**	**θ**	**κ**	**θ**
	Mini	5.19	3809	2.79	19.1	4.02	3222
	Light	1.66	5078	3.03	22.0	2.93	5009
	Compact	2.40	4691	2.60	42.8	7.49	5591
	Medium	3.18	7688	6.55	39.9	14.53	6648
	Combined	2.03	5256	2.12	31.3	3.23	5233

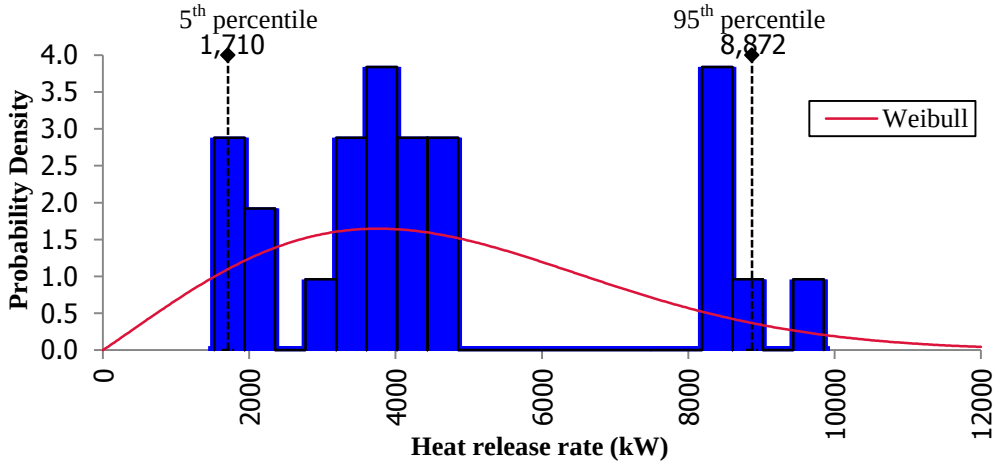

(a)

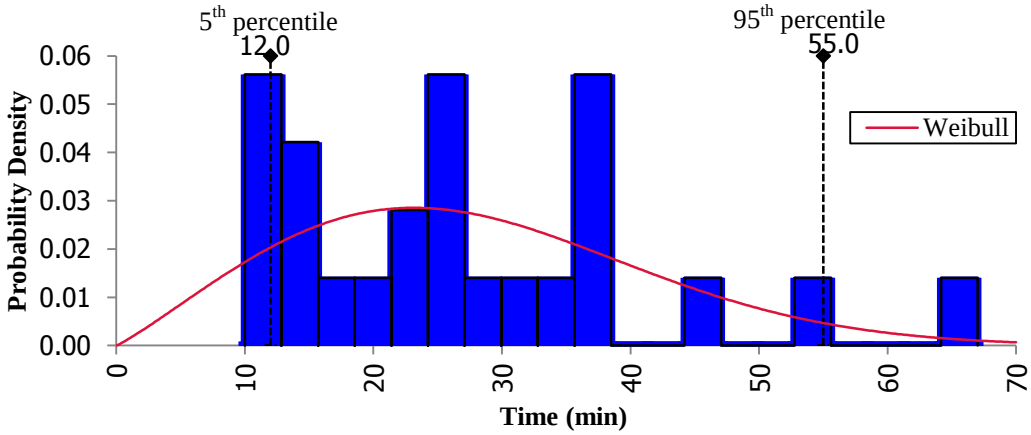

(b)

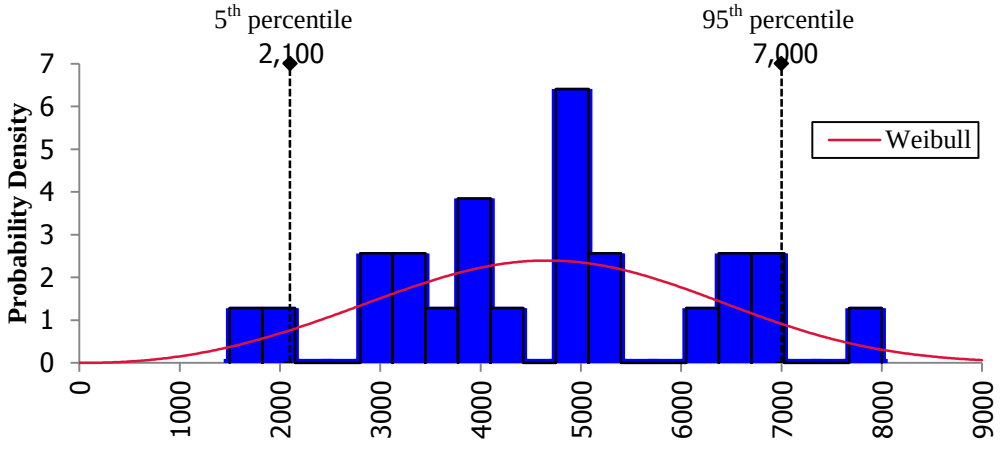

(c)

Figure 3-14: All passenger vehicle frequency data and best-fit distributions: (a) peak heat release rate, (b) of time to peak heat release rate, (c) total energy released.

3.5 Conclusions and recommendations

Experimental data for 41 single passenger vehicles have been obtained from the literature. Grouping these experiments by the curb weight of the vehicles forms a useful classification system that can be related to vehicle population and severity where the severity is defined here as the peak heat release rate, the time to reach peak heat release rate and total energy released.

For curb weight classes up to Passenger car: Medium it is found that the average values for the three fire severity characteristics generally increase as the curb weight increases. Previous studies have suggested there is a linear the increase in total energy released with curb weight. This study has also obtained a linear fit albeit with a relatively weak correlation. Similarly for the time to reach peak heat release rate a trend is also replicated in the plot of individual data. However, plotting individual results for the peak heat release rate do not clearly exhibit a strong trend that is suggested by the average values because of the scatter in the data.

The literature has found that the amount of combustible materials such as plastics in vehicles has increased since the 1960s. Although the age of the vehicles assessed in this review spans around four decades, it is found that it is sometimes difficult to even ascertain the decade in which an individual vehicle had been manufactured. Of those vehicles for which the decade could be determined with reasonable confidence it is found that around 70% were manufactured in the 1990s and data that spans multiple decades is not generally available for each curb weight class. As a result it is not possible to fully investigate the impact of vehicle age on the fire severity characteristics and thus the findings presented in this review should be treated with some care.

Weibull distribution functions have been obtained for the curb weights up to the Passenger car: Medium class and the combination of these classes. These distributions can be used to assess single-vehicle peak heat release rate, time to reach peak heat release rate and total energy released in a probabilistic manner which can aid designers wishing to perform probabilistic assessment analysis for cost-risk-optimized fire protection design.

It is recommended that the heat release rate for single passenger vehicles is examined again in the future to account for changes in vehicle design, construction and use. Technological

advancements will likely include changes in materials used in which could affect the fire behaviour of vehicles. All of the vehicles examined in this review are either petrol (gasoline) or diesel fuelled. For future experiments, it is recommended that research be conducted on vehicles using alternative fuels such as liquefied petroleum gas (LPG), hydrogen, electric power and solar power.

3.6 Supplementary information

Following the publication of the journal article in *Fire Science Reviews* in September 2013, the author has found additional single vehicle fire experimental data in the literature. Therefore, this section will present the additional data in the form of the summary of the experiments, the heat release rate curve, and the summary of the results consistent to the presentation approach in the journal.

To date, there are four additional data in which one of it is of Passenger car: Mini classification and three are of Van/MPV classification. This gives the total number of vehicle experiments collated to be 45. Table 3-25 provides a summary of the 4 additional experiments where each is given a unique identification code related to its ANSI classification which will be used throughout the research. All explanations about the summary table follow what have been explained in Section 3.2.

The heat release rate curves for the four additional data are shown in Figure 3-15. While the summary of the peak heat release rate, time to reach peak heat release rate, total energy released and total mass loss are shown in Table 3-26.

Table 3-25:Additional data for the collation of experiments

ID	Vehicle make and model	Vehicle year	Curb weight (kg)	Facility type	Condition	Ignition source	Ignition location	Incipient stage	Mass loss rate	Toxic product emission/Product consumption	Heat release rate evaluation method	Smoke production	Reference and experiment date (ED)/report submitted (RS)/date published (DP)
M7	Citroen BX	1989	874	Room calorimeter	Passenger front window open, all other windows closed	1.5 L gasoline in open tray	Under driver's seat	Included	N	Y	Oxygen depletion	N	[77] DP 2004
MPV7	Unknown	1990s	1440	Room calorimeter	All windows closed, 10 L fuel in tank	80 g alcohol gel fuel	Splashguard of right rear wheel	Included	N	N	Mass loss	N	[78] DP 16 Oct 2013
MPV8	Unknown	1990s	1440	Room calorimeter	All windows closed, 10 L fuel in tank	80 g alcohol gel fuel	Right front bumper	Included	N	N	Mass loss	N	[78] DP 16 Oct 2013
MPV9	Unknown	1990s	1440	Room calorimeter	All windows closed except left front window which is 20 cm opened, 10 L fuel in tank	80 g alcohol gel fuel	Centre of back row seat	Included	N	N	Mass loss	N	[78] DP 16 Oct 2013

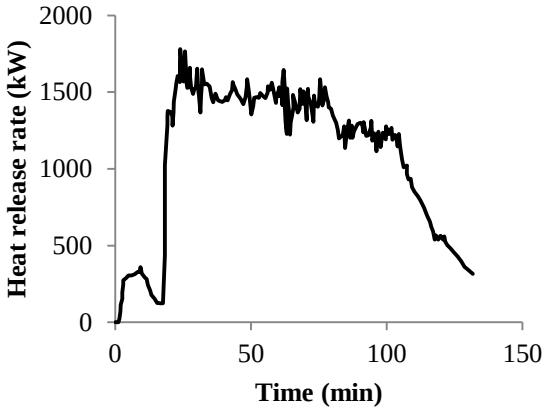

d) Experiment M7

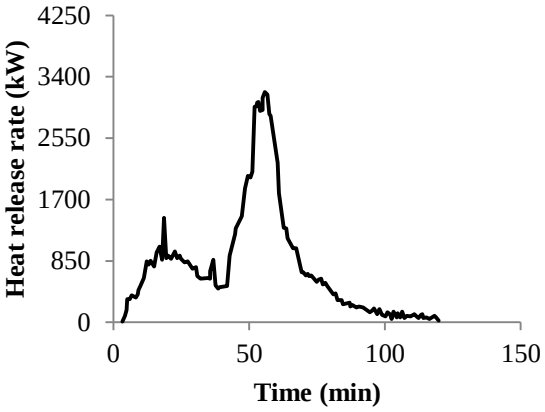

f) Experiment MPV8

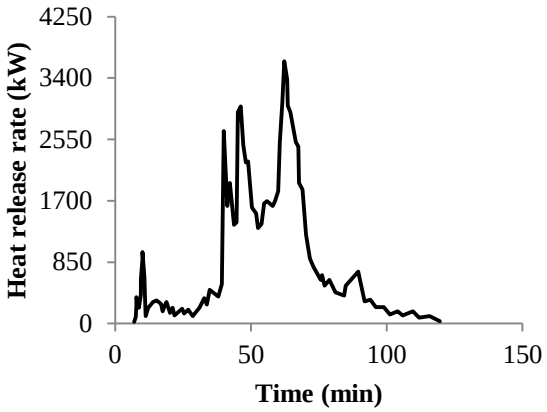

e) Experiment MPV7

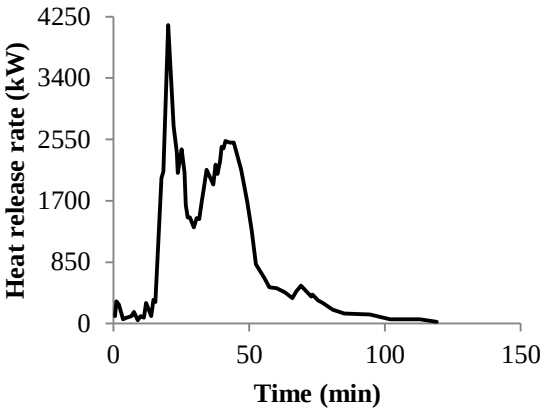

g) Experiment MPV9

Figure 3-15:List of Experiments; (a) Experiment M7 (b) Experiment MPV7 (c) Experiment MPV8 (d) Experiment MPV9

Table 3-26: Summary of the results for the four additional data

Experiments	Peak heat release rate (kW)	Time to peak (min)	Total energy released (MJ)	Total mass loss (kg)
M7	1780	24.0	8500	N/A
MPV7	3633	62.2	N/A	N/A
MPV8	3109	59.4	N/A	N/A
MPV9	4134	20.2	N/A	N/A

Chapter 4 DEVELOPMENT OF FIRE SCENARIOS USING FIRE RISK ANALYSIS

Published as Tohir, M.Z.M., and Spearpoint, M. "Development of Fire Scenarios for Car Parking Buildings using Risk Analysis" in *Fire Safety Science (in press)*, 2014.[79]

Abstract

This chapter describes a relatively simple probabilistic risk analysis model to determine appropriate fire scenarios for car parking buildings. The approach introduces a dimensionless measurement defined as fire risk level by multiplying probability by consequence. For the development of fire scenarios for car parking buildings, the key variables for the fire risk analysis are identified as vehicle parking distribution probability and how vehicles then form clusters of neighbours, vehicle classification, vehicle fire involvement probability, and the severity of vehicle fires. The selection of clusters of neighbouring vehicles and whether all vehicles in the cluster catch fire has the probability to affect the fire risk level. An example analysis is performed where a simple two-row, 100 space parking model with a 75% vehicle occupancy and 0.90 tendency factor weighting is used to obtain the vehicle distribution probability combined with various data sourced from the literature. It is found from the example analysis that fire risk level is largely driven by the vehicle fire involvement probability such that a single vehicle fire presents the worst case scenario in terms of fire risk.

4.1 Introduction

Vehicle parking buildings are commonly found in most modern urban environments. Such buildings can be stand-alone structures or attached to other occupancy types. The buildings can be multi-storey; above ground or below ground; be fully or partially enclosed; and be used to park a range of vehicle types (cars, vans, buses etc.). The usage characteristics of such buildings will depend on the service they provide: parking for patrons of a shopping mall, long-stay parking at an airport, parking for the residents of household units etc. This particular research is focussed on car parking buildings rather than for other vehicle types such as trucks or buses and the approach is similar to previous vehicle-fire related research [16], such that fire risk is equal to probability multiplied by consequence.

There have recently been several significant vehicle fires in car parking buildings and in some cases these have led to fatalities. For example, in 2006 seven fire fighters were killed in a fire in an underground car park in Gretchenbach, Switzerland [1]. Also in 2006 there was a car park fire in Bristol, United Kingdom where 22 vehicles were destroyed in the incident and one person died in the occupancy above the car park [1]. For example, in terms of design Zhao et al. [15, 80]state that there are standard fire scenarios for car parking buildings required by the French authorities. The scenarios are seven cars including a utility vehicle in the same parking row, four cars including a utility vehicle situated in two adjacent parking rows and one car located at any position on the floor. These fire scenarios are applied so as to derive the most severe scenarios in terms of meeting fire resistance objectives. However, Zhao et al. note that the greatest number of vehicles involved in a car parking fire was not more than three from incident statistics.

The life safety concerns of occupants and fire fighters and the appropriate design scenarios for structural design have led to consideration of the impacts of fires in car parking buildings. There is the need for further research into how to determine reasonable fire scenarios and raises the possibility that a single set of scenarios may not be applicable to all types of car parking buildings given the variations in design and use. The work presented in this chapter is part of a larger risk-based research project where the first step is to create design scenarios which will be used for subsequent analysis. These scenarios need to consider the relative number, layout and type of vehicles that could be present in a parking building; the likelihood that multiple vehicles could burn simultaneously and the potential total energy that could be

released by the burning vehicles. The focus in this chapter is on a vehicle parking model that can identify the likelihood and magnitude of multiple vehicle clusters.

Fire risk analysis is used to identify the impact of having a range of different vehicle fire scenarios in parking buildings. As a quantitative approach, the analysis establishes a dimensionless measurement for comparison, defined here as the fire risk level. For this research it is found that the probability component depends on a number of factors which are explained in the remainder of the chapter. The consequence component is defined as the severity of the fire and is represented by the vehicle peak rate of heat release, and this is also discussed further in the chapter. Clearly the most severe fire scenario does not necessarily have the highest risk level as it is compensated by the likelihood of the scenario occurring. Essentially the question becomes: for a given fire incident that starts in a specific vehicle what is the likely probability of a certain number of other vehicles being parked in neighbouring spaces, what are the likely types of vehicles in those spaces in terms of their combustible mass, will the fire spread to all of the neighbouring vehicles and what are the likely rate of heat release available from each vehicle that will contribute to the total heat release? Then how likely is this incident compared to the population of other similar incidents and which one of this population presents the greatest fire risk level?

The objective of this chapter is to present an approach to establish vehicle parking scenarios using a probabilistic quantitative risk analysis method by incorporating a relatively simple vehicle parking model, statistical data on vehicle fleets, measurements of passenger vehicle heat release and vehicle fire incident data. The resulting risk analysis method could be used for the future specification of regulatory requirements for the design of car parking buildings but it has also been developed to be sufficiently flexible as such that it can benefit designers and regulators for the assessment of specific car parking buildings.

4.2 Fire risk analysis

In order to perform the fire risk analysis, the first step is to be able to understand the day-to-day situation in a parking building and then list all the key variables that are potentially associated with vehicle fires in the building. This approach follows the generalized concept for any fire risk analysis, i.e. to identify the hazards and then to quantify consequence and probability of those hazards [81].

The key variables identified are the vehicle parking distribution probability, i.e. the probability of vehicles being distributed in a particular pattern throughout the building at a given time; the vehicle classification i.e. the composition of different vehicle types in a fleet; the vehicle fire involvement, i.e. the likely number of vehicles involved in a fire using past incident data; and the severity of vehicle fires, where each of these variables is further explained in this chapter. These variables are then used to create the necessary risk analysis components and the combination of these component variables determines a specific vehicle parking fire scenario.

Since the approach provides a numerical assessment, all of the key variables are quantitatively determined for each scenario. A probabilistic approach is used to demonstrate the severity of the fire as it relates to the likelihood of a given vehicle population and classification. The fire risk level is obtained by multiplying vehicle parking probability, vehicles classification, vehicle fire involvement probability and vehicle fire severity. Thus, this approach is used as a basis of a comparison to determine which scenario provides the highest fire risk.

Since there are almost limitless parking configurations; numbers of parking spaces; and parking space arrangements the approach used here attempts to be as generic as possible. Scenarios provide a general resemblance of the problem which can be related to most typical vehicle parking buildings. This generic approach is defined a simple two-row parking space arrangement as shown in Figure 4-1 as a starting point for the research. For this approach, the number of parking spaces n_{space} can be up to any desired value and the number of vehicles $x_{vehicle}$ can be up to n_{space} spaces. As an example, in Figure 4-1, the value for parking spaces n_{space} is 12 and the number of vehicles x is 5.

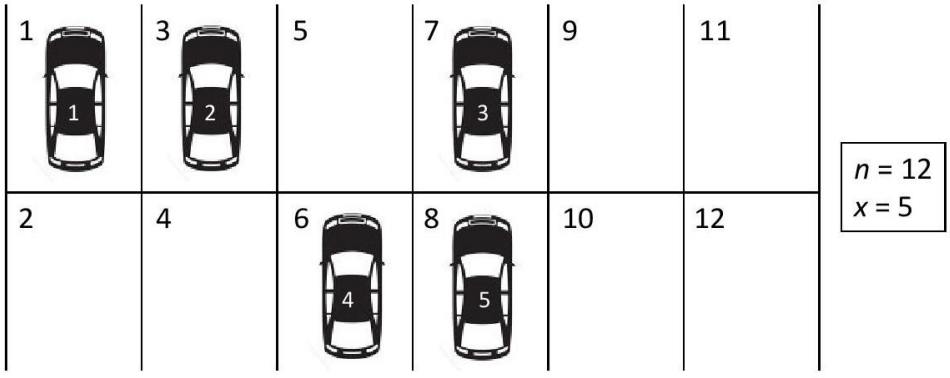

Figure 4-1:Generic scenario

The potential for an open-ended level of depth for each component has led to the need to retain a consistent level of detail when deciding on how to obtain numerical inputs to the risk analysis. However even with the somewhat simplified approach described here, the calculations applied in the fire risk analysis are automated with the creation of a parking simulation model using Visual Basic for Applications in Microsoft Excel.

4.2.1 Vehicle parking probability

The vehicle parking probability is used to determine the relative location of parked vehicles at a given time, i.e. the distribution of a given number of vehicles, $x_{vehicle}$ across the available parking spaces, n_{space}. The distribution of vehicles is then used to identify clusters of neighbouring vehicles as discussed later. For this research the parking location distribution is managed by using a Monte Carlo approach. For example, considering the two-row model introduced in Figure 4-1, there are 12 parking spaces available for vehicle parking, however there are only 5 vehicles to fill the spaces. Each Monte Carlo run distributes the 5 vehicles into the 12 spaces randomly and therefore a particular scenario is formed. A successive application of the Monte Carlo method is then used to construct the foundation for the vehicle parking distribution input to the risk analysis.

In reality the distribution of parked vehicles is influenced by human behaviour factors. The study of these factors in the search for a parking space is interesting field of study as the topic itself is very broad. From the work by Waerden et al. [82], it is found that distance variables between parking spaces and other aspects (i.e. ticket machines, car park entrance, stairways and/or exit to final destinations) have an impact on parking space search behaviour. Thus a random approach to the Monte Carlo car placement is unlikely to resemble the reality of the parking distribution. The car placement procedure has been modified to include a 'parking tendency factor' where it is assumed that vehicles tend to park at one end of the model to represent a distance variable. This parking tendency factor is governed by a user-defined weighting which controls the probability of vehicles being parked at one end of the model. The parking domain is equally split into a pair of two-row sections where a higher weighting results in a greater likelihood that a vehicle is placed in one of the pair over the other. As an example, this parking tendency factor can be visualized in Figure 4-2 where a weighting of 80% is applied. In this example, the dotted lines represent the separation for the pair of two-row sections; Section 1 and Section 2 with Section 1 being nearer to the distance variable. A run of simulation will have 80% chance of a car to be randomly placed in Section 1 while

there is 20% chance of the car to be randomly placed in Section 2. This simplification, however, has its own limitations where the distributions within the sections are still random, thus if Section 1 is full, then vehicles in Section 2 will not be further affected by the distance variable. This can be improved by dividing the two-row parking model into many smaller sections although this more complicated algorithm has not been implemented in this work.

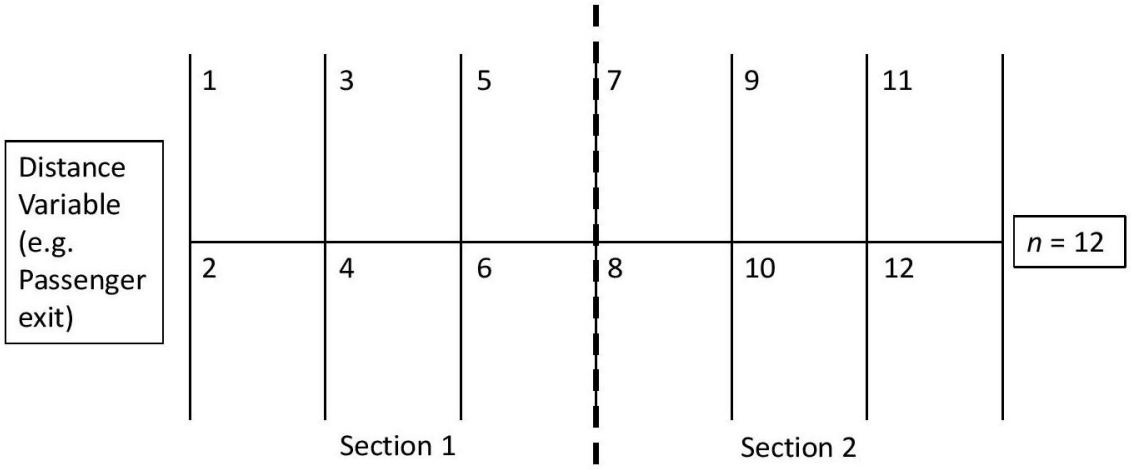

Figure 4-2: Generic car parking scenario for 12 spaces with tendency factor.

The work by [82] showed three sets of parking data at a specific parking building in the Netherlands with a specific duration of time. These parking data consist of 4 two-row parking and 3 single-row parking spaces as well as two distance variables; a railway station and a passenger exit to a shopping mall, but for this analysis only the two-row parking data were used to match with the simple model proposed in this work. By assuming that the railway station is the dominant distance variable it can be inferred that the weighting of a tendency factor at peak times is around 0.90 while at off-peak times it is around 0.70.

The parameters necessary for this component of the parking simulation model is the number of parking spaces, the number of vehicles, the number of iterations for the Monte Carlo simulations and the weighting for tendency factor. The input range for these variables are virtually unlimited, however, the limitations of Microsoft Excel restricts the input up to certain maximum values. The output from the Monte Carlo simulations is the result for each iteration presented in an Excel spreadsheet for further analysis.

4.2.2 Vehicle classification probability

Since this research particularly focuses on car parking buildings, the scope of the study is limited to private road passenger vehicles. Previous chapter shows that there are numerous

ways to categorise passenger vehicles and different jurisdictions have a variety of definitions for the purposes of classification. Some of the most common classifications are the vehicle engine size, the vehicle seating capacity, the vehicle dimensions (e.g. length, interior volume size), the vehicle curb weight, age, or wheelbase [46]. For this work, the American National Standards Institute (ANSI) [47] classification of road passenger vehicles based on curb weight of the vehicle is adopted (Table 3-1) as the mass is identified as a key parameter related to the potential fire load of vehicles.

Following on from the selection of an appropriate vehicle classification system, associated statistics for the proportion of the road passenger vehicle types are presented to the fire risk level calculation. The proportion statistics are used by the parking model to select the classification of a vehicle applied to a simulation. The statistics for composition of this classification is obtained from data from the USA [83] and from the European Union [49] and is shown in Table 4-1. Detailed statistics of the combined vehicle fleets can be found in Appendix B.1.

Table 4-1: Composition of vehicle classification.

Classification	Percentage composition
Passenger car: Mini	7%
Passenger car: Light	16%
Passenger car: Compact	20%
Passenger car: Medium	20%
Passenger car: Heavy	11%
Van / MPV	10%
SUV	16%

4.2.3 Vehicle fire involvement probability

This component uses statistics from past vehicle fire incidents in car parking buildings as input into the fire risk analysis. Incident statistics are typically obtained from organizations that provide emergency fire fighting and rescue services where the nature of the details available depends the particular individual organization. In New Zealand these statistics are extracted from the New Zealand Fire Services (NZFS) fire incident reporting system (FIRS). For vehicle-related fires FIRS contains records for the date and time of incident, the incident type, the number of vehicles involved, the vehicle types, the vehicle year of manufacture, general property use, specific property use, location of origin, heat source, objects ignited, and fire cause.

However, these statistics often do not provide a high level of detail regarding the incident. For example it can be difficult to determine at what stage of the fire NZFS intervention took place or whether an automatic sprinkler system activated to suppress the fire. The statistics also do not state the total number of vehicles in the car park at the time of the fire or the relative parking space locations of the fire-affected cars and those not affected. It can therefore be hard to know whether a vehicle fire in a parking building had the potential to spread to other vehicles had it been allowed to continue unchecked.

Earlier research by Li and Spearpoint [2] shows that the probability of a vehicle catching fire in car parking buildings in New Zealand from 1995 - 2003 was 4.74×10^{-6} per year. In this chapter the analysis was extended using the same approach used by Li and Spearpoint up until 2012 using data from 2004 - 2012 obtained from the NZFS [84]. The probability for 2004 - 2012 was 1.15×10^{-6} per year, which is lower than the previous research making the overall probability from 1995 - 2012 as 2.76×10^{-6} per year. This probability is coupled with the vehicle fire involvement statistics to produce a vehicle fire involvement probability. Further details on the probability for vehicle fires in car parking buildings in New Zealand can be found in Appendix B.2.

Vehicle fire involvement statistics have been obtained from the reported fire incidents in car park buildings acquired from the NZFS [84]. These statistics were strengthened by the collection of fire incident statistics in car park buildings compiled by Joyeux et al. [14] (discussed in 2.3.2) in 2002. The combined fire incident statistics is shown in Table 4-2. The table also shows the vehicle incidents probability and the annual vehicle fire involvement probability where the vehicle incidents probability is the number of incidents for a particular cluster divided by the total vehicle fire incidents and the vehicle involvement probability is the probability of a vehicle catching fire coupled with the vehicle incidents probability. Also from Table 4-2, there were a total of 401 incidents reported and the greatest number of vehicles involved were 7 with two incidents. The highest numbers of fire incidents are single vehicle cases with 344 incidents.

Table 4-2: Numbers of vehicles involved in fire and number of fire incidents.

Number of vehicles involved	Number of incidents	Probability of incidents	Vehicle fire involvement probability per year
1	344	0.858	2.37×10^{-10}
2	27	0.067	1.86×10^{-11}
3	21	0.052	1.45×10^{-11}
4	4	0.010	2.75×10^{-12}
5	3	0.007	2.06×10^{-12}
6	0	0.000	No data
7	2	0.005	1.38×10^{-12}

Since the fire risk analysis requires data for up to maximum occupancy number of vehicles and the number of incidents only involves a maximum of 7 vehicles, a correlation for vehicle fire involvements against number of vehicles has been made. This correlation is used to predict the probability of a fire scenario occurring for higher numbers of vehicles than can be determined from the statistics. For this purpose, a simple correlation is obtained and shown in Figure 4-3. A power law fit is used to correlate the known data because from the limited observation it is expected that the probability of incidents involving more vehicles will reduce. From this correlation an equation of $y = 0.66\times10^{-6}\ x^{-2.67}$ where x is the number of vehicles and y is the probability of incidents is obtained. Thus, this equation is used to predict the vehicle fire incident probability for more than 7 vehicles.

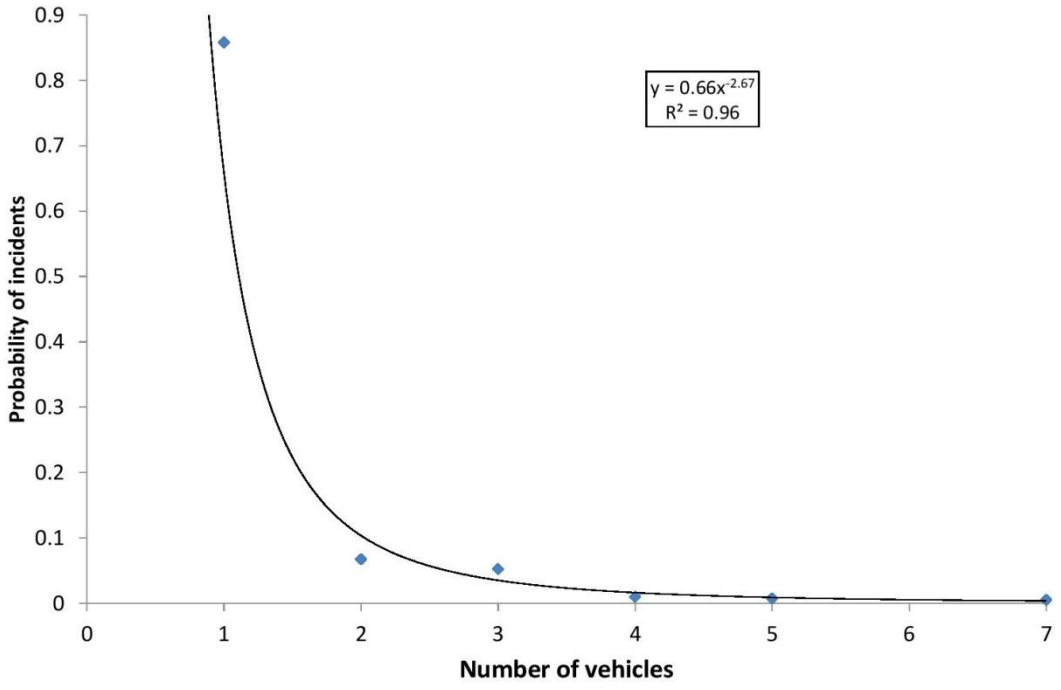

Figure 4-3: Correlation of probability of incidents over the number of vehicles involved.

4.2.4 Consequence

For the consequence component of the risk analysis the heat release rate of road passenger vehicles is taken to be the critical parameter in that a higher heat release rate contributes to a higher fire risk level. The previous chapter presents a distribution analysis for the fire severity characteristics of single passenger road vehicles using published heat release rate data. The work collates full-scale laboratory experiment data from 41 single passenger road vehicles in the form of the peak rate of heat release, the time to reach peak rate of heat release and total heat released. Even though in that work only four classes were analysed i.e. Passenger Car: Mini, Light, Compact and Medium; the remaining classes can be estimated through the frequency data plot of the vehicle peak heat release rate against the vehicle curb weight.

Figure 4-4 shows an example of the distribution plot of peak heat release for Passenger Car: Mini classification with the 5^{th} and 95^{th} percentile values indicated. A best-fit Weibull distribution has been determined for the data from 6 individual vehicle fire experiments. Average values for peak heat release rate are calculated for each classification that are then used for this study. The average values, 5^{th} and 95^{th} percentile distribution characteristics for each classification are shown in Table 4-3. However, due to limited data sets in the previous chapter, the distribution characteristics for Passenger Car: Heavy, Van/MPV and SUV vehicle classification are extrapolated from the lower curb weight classifications.

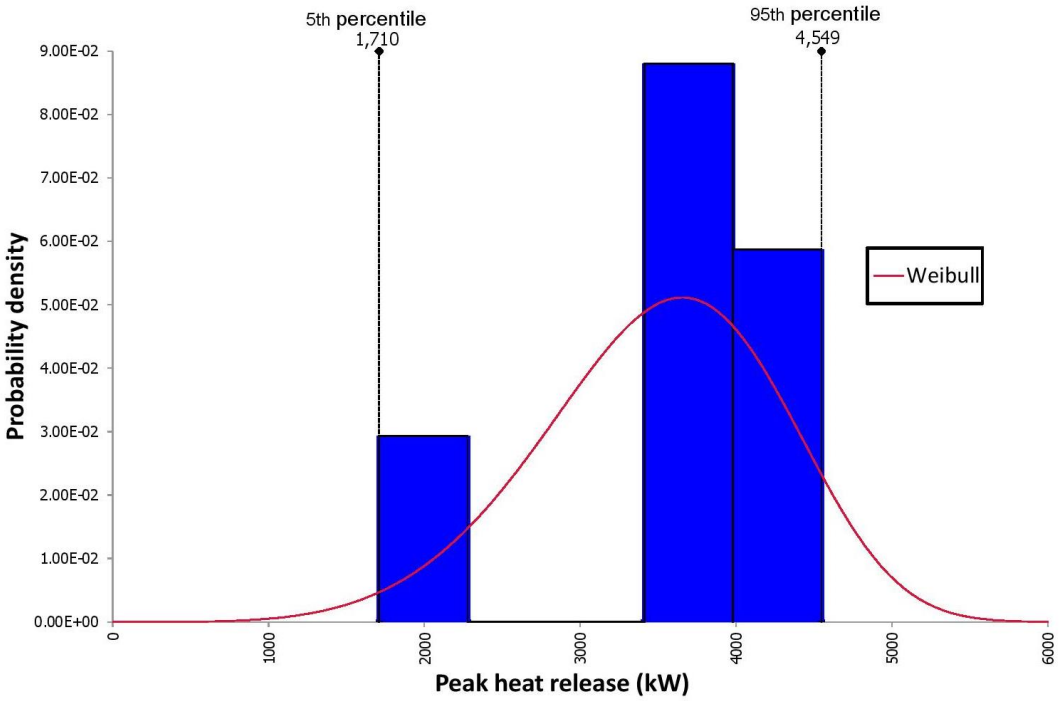

Figure 4-4: Distribution plot of the vehicle peak heat release rate for Passenger Car: Mini.

Table 4-3: Average estimated peak heat release rate values with its distribution characteristics for each classification.

Classification	Average, kW	5th percentile, kW	95th percentile, kW
Passenger car: Mini	3492	1710	4549
Passenger car: Light	4509	846	9802
Passenger car: Compact	4155	1352	7406
Passenger car: Medium	6843	3009	10850
Passenger car: Heavy	*8000	*1849	*13705
Van / MPV	*7000	*1604	*12016
SUV	*7000	*1604	*12016

*estimated values

It is noted that the procedures, standards and/or protocols varied between each experiment which likely lead to different effects on the fire spread, availability of air etc. and that the various heat release rate measurement techniques, namely mass loss rate, convective calorimetry and species-based calorimetry, could result in variability in the heat release rate measurements. However, due to limited data sets in each curb weight classification group meant it was not possible to create absolutely homogenous data sets that also provide sufficient items of data to be meaningful.

4.3 Application of the risk approach

4.3.1 Cluster size assessment

An example of the approach can be illustrated by presenting a simple parking problem. A single row of parking spaces is used for easier understanding of the process where the case of 5 parking spaces with 3 vehicles is illustrated. Figure 4-5 shows all of the possible parking distribution scenarios for this case.

Two methods to determine the number of possible fire scenarios are described. For both methods the assumptions made are:

- Only full vehicle fire involvement is considered; either a vehicle has caught fire or it has not, there is no partial vehicle fire.
- There is no time dimension in the fire risk analysis, i.e. fires occur instantaneously and simultaneously.
- For each vehicle on fire, a peak heat release rate is selected to maximise the risk.
- Fire spread does not occur across gaps formed by empty parking spaces.

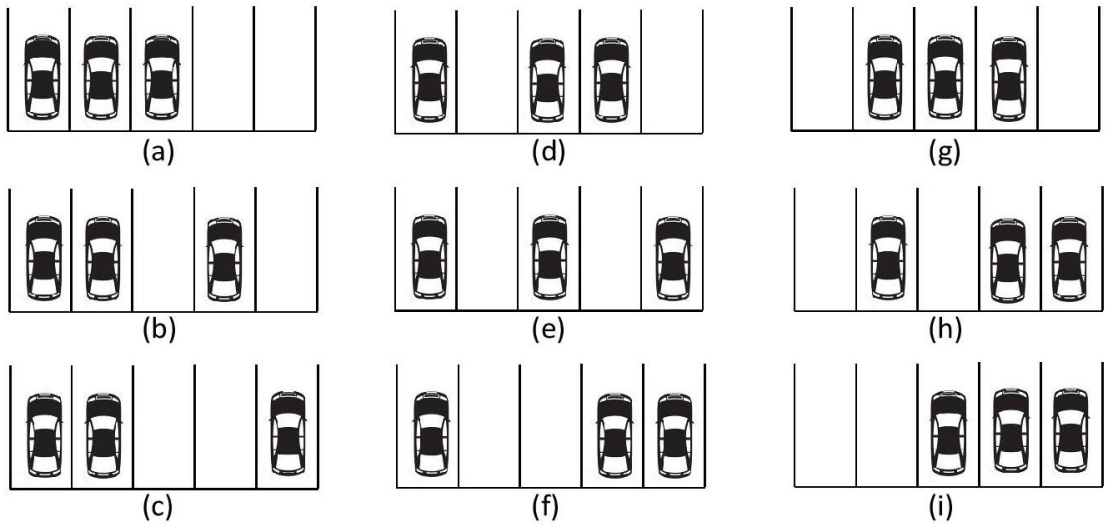

Figure 4-5: All distribution scenarios for 5 parking spaces with 3 vehicles.

The two methods are as follows:

i) Method 1 - In this method, vehicles located in contiguous parking spaces are considered to be a cluster such that they all catch fire simultaneously. Thus using Figure 4-5 distribution scenario (a), shows a cluster of three vehicles which means

only a single fire scenario is present. However Figure 4-5 distribution scenario (b), shows a cluster of two vehicles parked next to each other and a separate cluster which consists of a single vehicle. Thus in distribution scenario (b) there are two clusters and therefore two possible fire scenarios.

ii) Method 2 - This method is an expansion on Method 1 in which each cluster can have all of the conceivable fire scenarios available to represent the possibility that the fire does not spread to neighbouring vehicles regardless of the size of fire. For example, in Figure 4-5 distribution scenario (a), there is one case of 3 vehicles catching fire, two cases of 2 vehicles catching fire and three cases of 1 vehicle catching fire. Therefore in total there are six possible fire scenarios within the single distribution scenario. For Figure 4-5 distribution scenario (b), there are two separate clusters but in terms of probable fire scenarios, there is one case of 2 vehicles catching fire and three cases of a single vehicle fire.

The calculation of the total possible number of fire scenarios and the associated probabilities for the example using the two methods is shown in Table 4-4. It is evident that the probability of one vehicle on fire using Method 1 is 0.50 whereas for Method 2 it is 0.66 which is a 16% difference. For two vehicles there is a 4% difference and for 3 vehicles there is a 12% difference. These differences in probability show that using alternative assumptions for the possibility of fire occurring in multiple vehicles will result different outcomes in the fire risk level. For this research only Method 1 is adopted and further studied in detail although the possible implications of Method 2 are discussed.

Table 4-4: Total possible fire scenarios and probability for both methods.

Number of vehicles	Method 1		Method 2	
	Frequency	Probability	Frequency	Probability
1	8	0.50	27	0.66
2	5	0.31	11	0.27
3	3	0.19	3	0.07
Total	16	1.00	41	1.00

4.3.2 Maximum occupancy

The starting point to determine the vehicle parking probability is to obtain data for parking occupancy values at different times and for car parking buildings that exhibit different usage characteristics. These data will present the parking trends for specific parking buildings. For

this research, online data from several car parking buildings in San Francisco and Santa Monica, USA and two airport parking buildings in Switzerland and Italy have been obtained. Some of these parking trends data can be found in Appendix B.4.

An example of this data is taken from the Sutter-Stockton Garage in San Francisco. This 24 hour car park provides parking spaces for nearby shops and offices. The parking data for this particular building is taken for a typical week from 5th of May 2012 until 5th of May 2013. Figure 4-6 shows the normalized parking space occupancy as the number of vehicles parked over the total number of spaces available. Therefore the maximum occupancy is on Thursday where it almost reaches 75%. This maximum occupancy provides a measure of the maximum exposed fire risk and thus a value of 75% is taken as starting point for the parking simulation model.

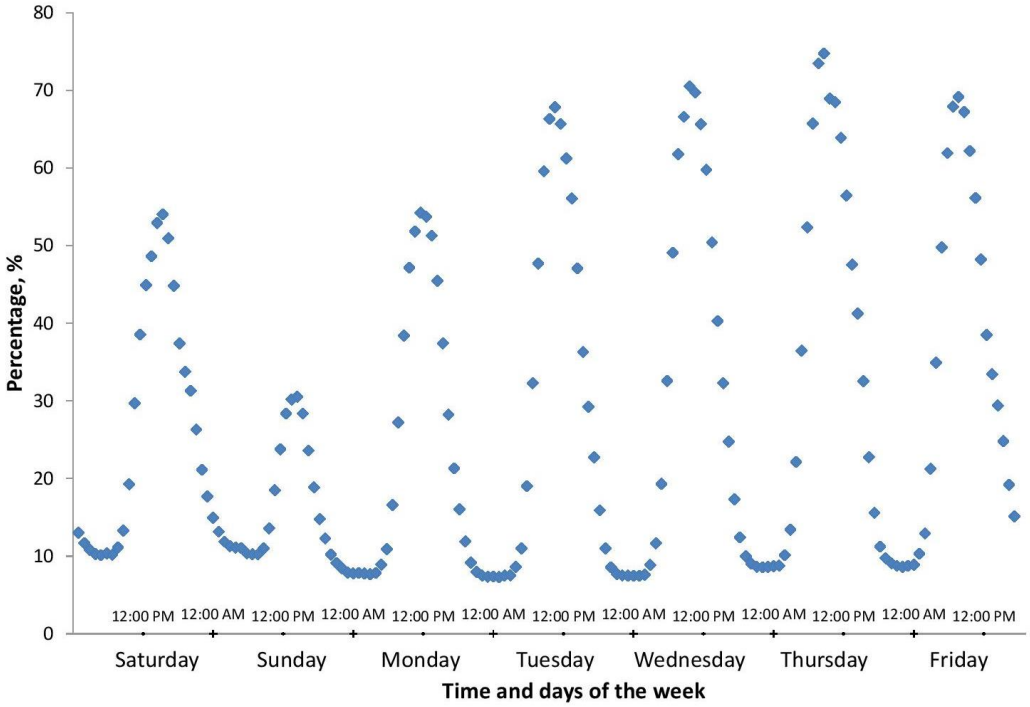

Figure 4-6: Sutter-Stockton parking garage distribution in different days of the week.

4.3.3 Accumulated peak rate of heat release

For each simulation run, the model specifies the location of each vehicle in the parking area and the class of the vehicle, from which the peak heat release rate of each vehicle can be identified. A single iteration of the simulation will select vehicle classes based on the vehicle classification probability distribution. Thus, every single iteration will produce a different accumulated peak heat release rate. By executing a sufficiently large number of iterations, a

range of possible scenarios is obtained. To simplify the analysis, these ranges of peak heat release rate for a given number of vehicles are averaged.

The accumulated peak heat release rate for vehicles are recorded from each simulation iteration. Trial runs of 10,000 iterations for single vehicle fire up to 11 simultaneous vehicle fires are recorded. This is shown in Figure 4-7, where it can be seen that the average peak heat release rate for a single vehicle to 11 vehicles shows a linear fit. In Figure 4-7 also shows the range of total accumulated peak heat release rate from the iterations. To verify the linearity assumption, 10,000 iterations is run for the peak heat release rate accumulation for 20 vehicles. Thus, the equation of the linear fit is used in the fire risk analysis to obtain the peak heat release rate for a specified number of vehicles.

It is also noted that the usage of probability distribution in the simulation will produces outlier(s) based on the extreme ends of the distribution shape. This explains why, for example for a single vehicle fire can reach over 40,000 kW.

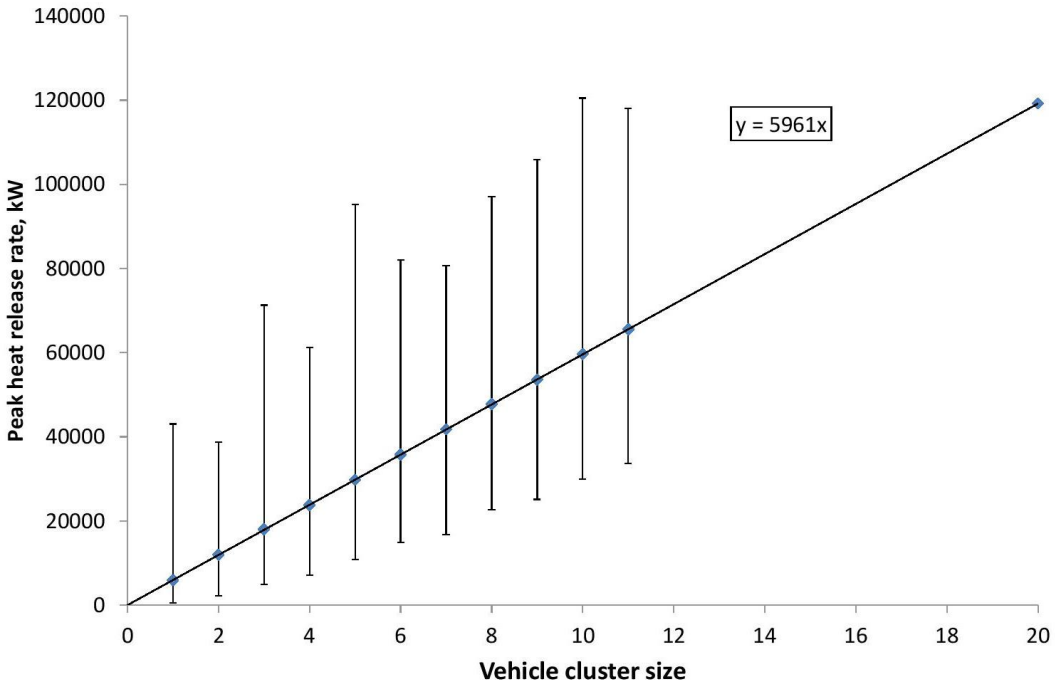

Figure 4-7: The total peak heat release rate for increasing vehicle cluster size.

4.4 Example analysis

An example of the application of the fire risk analysis approach is demonstrated with the inputs being 100 parking spaces, 75 vehicles (i.e. a 75% occupancy) and 10,000 iterations for

the parking simulation model. A two-row parking arrangement with a tendency factor weighting of 0.90 and Method 1 for determining fire scenarios is used in this example.

The outcome of the parking simulation model is in the form of the probability of having different cluster sizes, the vehicle involvement probabilities and total rates of heat release. The probability of having different cluster sizes is shown in the second column of Table 4-5. However, the results are not shown for all 75 vehicle clusters because not every one is obtained through the 10,000 iterations. Thus, only clusters of vehicles with probability results are shown where it can be seen that the highest occurs for the 51-vehicle cluster at 0.174. The second highest probability is the cluster with 52 vehicles at 0.135. This means that during the iterations, the simulation model tends to repeatedly form the 51 or 52 vehicle clusters in preference to other cluster sizes.

The third column in Table 4-5 is the vehicle involvement probability obtained using Figure 4-7 and the total rate of heat release for a given cluster size is obtained from Figure 4-7. The total heat release rate shows values that can exceed 380 MW which is a manifestation of the assumption that all cars ignite and burn simultaneously. However whether this value could be achieved would also depend on the ventilation available within a particular car park and any modelling would need to account for such conditions.

The fire risk level in Table 4-5 shows that the highest risk of vehicle fire is for a single vehicle at 4.90×10^{-4}. Even though, the total accumulated heat release rate for a single vehicle is low, the vehicle involvement probability governs the whole fire risk level. This is due to the large difference in the orders of magnitude since the vehicle involvement probability follows a power law.

Table 4-5: Simulation and fire risk analysis by using Method 1.

Number of vehicles	Cluster size probability	Vehicle involvement probability	Total rate of heat release (kW)	Fire risk level
1	0.041	2.00×10^{-6}	5952	4.90×10^{-4}
2	0.032	3.61×10^{-7}	11913	1.36×10^{-4}
3	0.042	1.32×10^{-7}	17874	9.94×10^{-5}
4	0.038	6.51×10^{-8}	23835	5.94×10^{-5}
5	0.033	3.75×10^{-8}	29796	3.65×10^{-5}
6	0.029	2.39×10^{-8}	35757	2.50×10^{-5}
7	0.020	1.63×10^{-8}	41718	1.36×10^{-5}

8	0.016	1.17×10^{-8}	47680	8.95×10^{-6}
9	0.013	8.77×10^{-9}	53641	6.21×10^{-6}
10	0.007	6.76×10^{-9}	59602	2.79×10^{-6}
11	0.006	5.34×10^{-9}	65563	2.26×10^{-6}
12	0.005	4.31×10^{-9}	71524	1.48×10^{-6}
13	0.003	3.54×10^{-9}	77485	7.60×10^{-7}
14	0.002	2.94×10^{-9}	83446	5.50×10^{-7}
15	0.001	2.48×10^{-9}	89407	1.78×10^{-7}
18	0.000	1.58×10^{-9}	107291	8.15×10^{-8}
20	0.001	1.22×10^{-9}	119213	7.75×10^{-8}
48	0.001	1.40×10^{-10}	286124	5.13×10^{-8}
49	0.004	1.33×10^{-10}	292085	1.53×10^{-7}
50	0.027	1.27×10^{-10}	298046	1.01×10^{-6}
51	0.174	1.21×10^{-10}	304007	6.39×10^{-6}
52	0.135	1.15×10^{-10}	309968	4.80×10^{-6}
53	0.099	1.10×10^{-10}	315929	3.43×10^{-6}
54	0.071	1.05×10^{-10}	321890	2.38×10^{-6}
55	0.059	1.00×10^{-10}	327851	1.93×10^{-6}
56	0.043	9.58×10^{-11}	333812	1.38×10^{-6}
57	0.029	9.17×10^{-11}	339773	9.00×10^{-7}
58	0.023	8.78×10^{-11}	345735	7.04×10^{-7}
59	0.016	8.42×10^{-11}	351696	4.66×10^{-7}
60	0.013	8.08×10^{-11}	357657	3.70×10^{-7}
61	0.007	7.75×10^{-11}	363618	1.83×10^{-7}
62	0.005	7.45×10^{-11}	369579	1.37×10^{-7}
63	0.005	7.16×10^{-11}	375540	1.36×10^{-7}
64	0.002	6.89×10^{-11}	381501	4.48×10^{-7}

A sensitivity analysis has been carried out by varying the weighting of the tendency factor in the example analysis. In this analysis, the same number of parking spaces and number of vehicles were used while the tendency factor weighting is differed from 0.70 to 0.90 based on the analysis of Waerden et al.'s [82] data.

Figure 4-8 shows how the parking tendency factor alters the average parking probability of each multiple vehicle cluster size. It is obvious that as the tendency factor weighting increases it will produce greater probabilities of large vehicle clusters. This sensitivity analysis also considers a random distribution i.e. a tendency factor weighting of 50% which is shown by the × symbols. The addition of the random distribution is presented for the purpose of comparison as people invariably have a range of parking behaviour tendencies [85] that would mean it is not a random process. However it is interesting to note that when the distribution is random it produces the highest probability of a single vehicle cases.

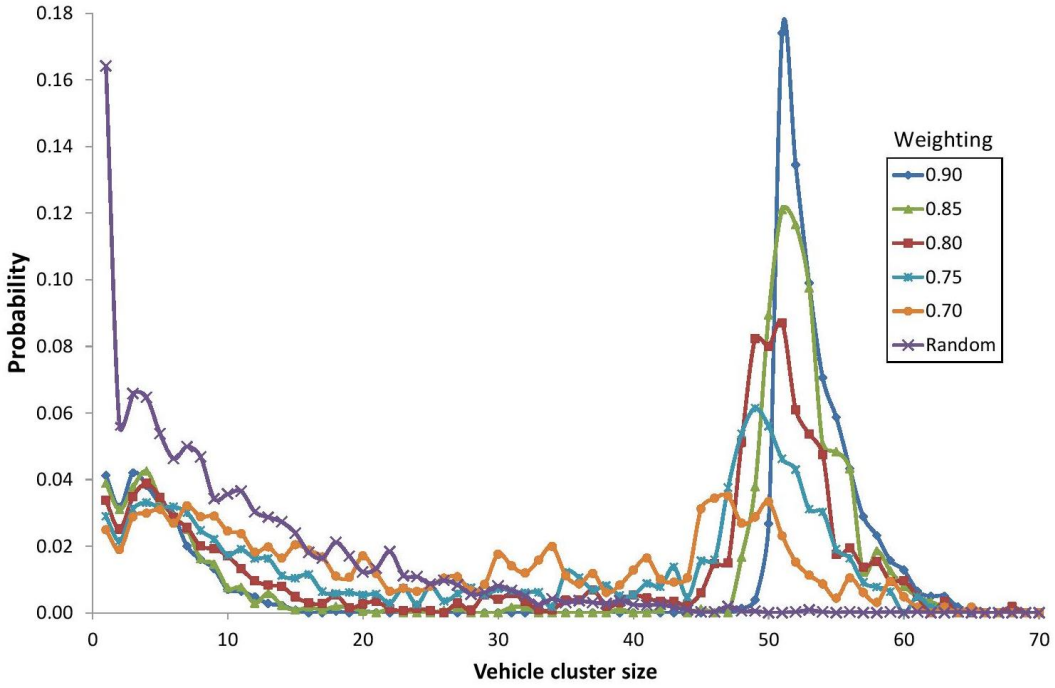

Figure 4-8: Cluster size probabilities for 75 vehicles in 100 parking spaces with different parking tendency factor weightings.

Figure 4-9 compares the fire risk level for different tendency factor weightings i.e. 0.70, 0.80 and 0.90, and the random distribution. The graph is shown using a semi-log scale to more clearly illustrate the wide range in the results as the cluster size increases. From Figure 4-9, varying the tendency factor weighting also affects the fire risk level even though it does not change the fact that a single vehicle fire has the highest fire risk level. This shows the importance of the vehicle involvement probability over the variations in the cluster size probability. The random distribution shows the highest fire risk level for a single vehicle due to the cluster size probability being directly related to the fire risk level.

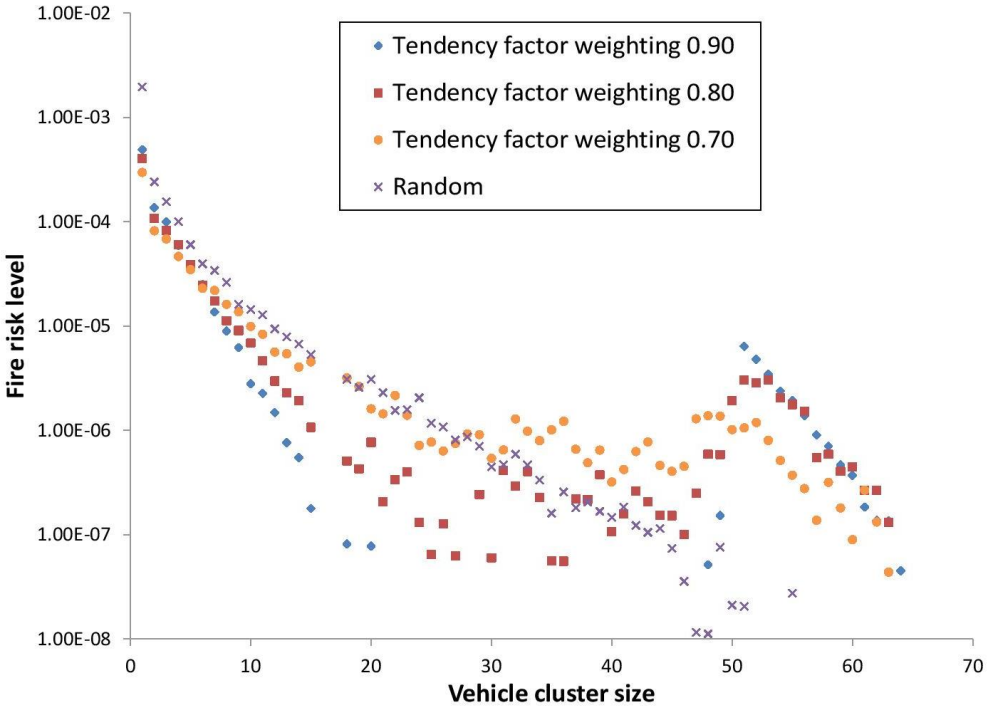

Figure 4-9: Fire risk level for 75 vehicles in 100 parking spaces with different parking tendency factor weightings.

4.5 Conclusion

There are several limitations upon the fire risk analysis method used in this work. Firstly the online data for parking probability are limited by the range of parking building data available and the distribution of the parked vehicles across the spaces is not included. This limitation could be addressed by making on-site observations in the required car parking building. Secondly the vehicle fire involvement probability used statistics that were a combination of data from different agencies and years. Finally the consequence part was limited due to inadequate rate of heat release data for vehicle experiments that cover Van/MPV, SUV and Passenger car: Heavy classifications.

By using Method 1 to find the fire scenarios, the highest fire risk is for a single vehicle at 4.90×10^{-4} for a 75% occupancy. More vehicles involved means higher consequences but the vehicle involvement probability governs the whole fire risk analysis since it shows significant difference in the order of magnitude of the probability. Thus, more attention to the collection of vehicle involvement probability is needed in future studies. The next steps in this research are to examine the fire growth characteristics of car fires rather than to only consider the peak rate of heat release and to model the spread of fire between cars using a tool such as B-RISK [18]

It is also noted that the current data for the vehicle involvement probability does not mention whether any suppression systems were operated or at what stage any fire fighters intervention occurred. Had the information regarding the suppression of the fire in the statistics been included, a more realistic analysis is likely to be produced. Furthermore the statistics do not indicate whether there were neighbouring vehicles present in the incident which could have got involved in the fire. These limitations in the statistics have an impact on the ability to provide appropriate data for a risk analysis model.

An initial assessment of Method 2 to find the fire scenarios suggests that it is likely to produce highest risk for a single vehicle due to a greater weight of probability of having a single vehicle fire. It could be argued that the formation of scenarios using Method 2 already incorporates the vehicle involvement probability. This sets grounds for more research to be carried out in the future.

The flexibility of the model allows for future analysis of car parking buildings with different number of spaces, different occupancy numbers and the effect of human vehicle parking behaviour. In trying to achieve the objective of this research it is acknowledged that there is a continued interest in the phenomenon of travelling fires in which a fire in a large space only burns over a limited area at any one time [86]. A car parking building is identified as one type of structure with the potential for travelling fires. However the fire risk analysis approach discussed here does not try to incorporate travelling fires as it requires more work to be done should it be desirable to include this phenomenon.

Chapter 5 PROBABILISTIC DESIGN FIRES FOR MULTIPLE PASSENGER VEHICLE SCENARIOS

5.1 Introduction

5.1.1 Background

The increased consideration of performance-based design has led to an expanded demand in engineering approaches to the assessment of fire safety in buildings. Performance-based design is being adopted as rational means of providing efficient and effective fire safety which gives flexibility to achieve the objectives so long as safety can be demonstrated. The typical tasks required for the design process i.e. defining the project scope; establishing objectives; developing performance criteria; identifying and selecting appropriate design scenarios etc. One of the critical components of the approach is the concept of the design fire which is typically is presented in terms of heat release rate as a function of time [45]. Therefore the identification and selection of one or more design fires is deemed as an integral part of the process to ensure that a performance-based design will satisfy its objectives. Further information on the design process can be obtained from guidelines, such as the International Fire Engineering Guidelines [87] and the SFPE Engineering Guide to Performance-Based Fire Protection Analysis and Design of Buildings [88].

Heat release rate is a key parameter which can be used as an input to a wide range of fire assessment tools, ranging from zone models to computational fluid dynamics models. The heat release rate is usually obtained from experimental data through the use of oxygen consumption calorimetry although other approaches such as measurement of temperature rise, mass loss, or species production can be evaluated. However the natural variability of fire means that even if the same item is burned using the same procedure for repeated experiments, the heat release rate curves obtained will not be exactly the same.

Characterising a design fire requires knowledge for the various phases of the heat release rate curve i.e. fire growth phase, peak heat release rate, decay phase, time to reach peak heat release and the total heat released or fuel load potential. A simplified characterisation method for the heat release rate curves of furniture items has been proposed by Babrauskas and Walton [89] where a triangular shape is seen to be a good representation for a large number of experiments. However, this triangular representation appears to be limited to heat release rate curves with simple characteristics. Alternatively Mowrer and Williamson [90] demonstrate two methods to characterise heat release rate curves. These methods are the

exponential and power law (i.e. a t-squared growth) representations of fire growth. Numajiri and Furukawa [91] have presented a single mathematical expression to characterise the whole fire development curve based on an exponential function. Ingason [92] found that a modified version of the exponential curve is a convenient way to describe the rate of heat release curves in tunnel scenarios which makes the process of characterising a design fire easier. The work by Ingason [93] postdates the earlier work where it introduces an optional constant heat release rate period to the exponential curve. This exponential curve method has proved to be good fit for characterising heat release rates of multiple objects in underground structures [94] and the heat release rate of train carriages [95]. However, this method has not been used for a risk-based probabilistic analysis perspective on multiple passenger vehicles as presented in this work.

This work is part of a larger research investigation into risk-based fire safety of passenger road vehicles in car parking buildings being undertaken at the University of Canterbury. Earlier research in Chapter 3 has compiled single passenger vehicle fire test data from available sources. These data were then analysed to produce sets of heat release rate distribution parameters for single passenger vehicles as a function of a vehicle classification system based on curb weight categories where curb weight is defined as which is defined as total weight of a vehicle with standard equipment while not loaded with passengers and cargo. The distribution parameters are for peak rate of heat release, total energy release and time to peak rate of heat release. Work in Chapter 4 has produced a method of generating vehicle parking scenarios using a risk analysis approach. The next step is to couple the vehicle parking scenarios with the single passenger vehicle fire heat release rate distribution parameters to create a risk-based assessment of the safety in parking buildings subject to multiple vehicle fire spread scenarios. In order to create the multiple vehicle fire spread scenarios it is necessary to be able to assess when subsequent vehicles will ignite as a result of the influence of the already burning vehicles. Some work has already been completed by Chapter 6 that examined seven multiple vehicle experiments. Thus, the main objective of this chapter is to establish a suitable method that can use input parameters obtained from the heat release rate distributions arrived from the earlier work in Chapter 3 to create design fires that can be used as input to a multiple vehicle fire analysis. The method needs to be able to describe the growth and decay components of the relevant design fire curves, where the

growth is the more important of the two, as well as giving an appropriate total energy release. This chapter also provides support to some of the assumptions put forward in Chapter 6.

5.1.2 Passenger vehicles

The definition of passenger vehicle used in this chapter is based on the New Zealand Transport Authority (NZTA) which states that it is a motor vehicle constructed primarily for the carriage of passengers, with not more than nine seating positions which include the driver's seating position, and either has at least four wheels or it has three wheels and a gross vehicle mass exceeding one tonne [6]. Design fires for passenger vehicles are important for fire safety in buildings that are associated with cars e.g. underground car parking or multi-level car parking structures; road tunnels; and vehicle showcase or exhibition centres. In these buildings, the primary fuel load are often the vehicles themselves which contain combustible materials including fluids such as engine fuels and oils, transmission oils, power steering fluids, brake fluids and lubricants; upholsteries; tyres; plastic materials such as in dashboards and bumpers; possibly the body work of the vehicle itself; and finally, any contents being carried in the vehicle. From Chapter 3, it is known that a single vehicle peak heat release rate could reach up to 9.8 MW and total heat released could reach up to 8000 MJ. Furthermore the total amount of energy available from a single vehicle is a function of the curb weight for which the American National Standards Institute [47] provides a convenient classification system.

There has been previous work that has been used to propose design fires for vehicles. One notable piece of work was by Joyeux [37] in which a series of vehicle fire experiments were carried out and from these experiments, as well as published results from previous experiments, a reference heat release rate curve representing a single vehicle fire in a closed car park was proposed (Figure 5-1). This reference curve is found to be widely used in vehicle fire related studies however it may not be representative for all types of vehicles since they vary in dimensions and masses. To that end Joyeux et al. [14] have reported information on different categories of 1990’s European cars. Vehicles are divided into five categories and for each category an average mass of the vehicle, mass of combustible materials and total energy released are given. In comparison to the Joyeux reference curve, the current New Zealand Verification Method: Framework for Fire Safety Design (C/VM2) [11] means of compliance to the New Zealand Building Code, requires that car parks with no stacking the

fire growth rate to be a medium t-squared fire, i.e. α_{peak} = 42.19 kW/min² (Figure 5-1) and a peak heat release rate of not more than 20 MW depending on ventilation conditions. Ingason [62, 96] has suggested that the design fire for a vehicle can be simplified by selecting linear growth and decay phases based on experiments involving vehicle fires. Ingason [51, 93] gives a linear function for two/three cars with a growth coefficient, $\alpha_{g,L}$ of 1600 kW/min, a peak heat release rate of 8 MW, a total time to peak of 5 min and the decay starting at 25 min with decay rate, $\alpha_{d,L}$ of -400 kW/min. Ingason [51, 93] also discusses the application of a quadratic function in which for a single car the growth coefficient, $\alpha_{g,q}$ is 36 kW/min² up to a peak heat release rate of 4 MW after which the decay coefficient, $\alpha_{D,q}$ is -0.06 min^{-1} for an exponential decay is suggested. Figure 5-1 shows the design fires for these linear and quadratic growth descriptions.

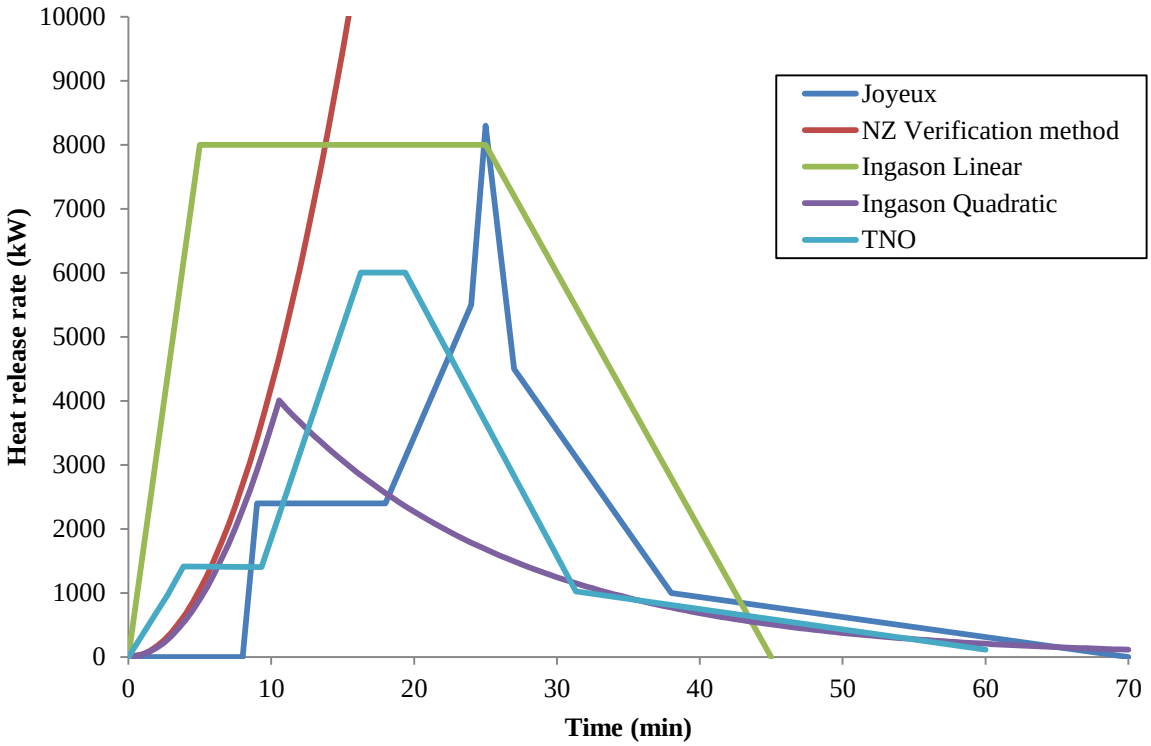

Figure 5-1: Design fire curves for a single/two/three vehicle from various literature sources.

The total energy released for the Joyeux and Ingason reference curves can be calculated by computing the area under the curve. The total energy released calculated for Joyeux and TNO reference design fire is 6700 MJ, and the Ingason quadratic design fire is 4700 MJ. The Ingason linear design fire calculation suggests that value of 7800 MJ or 5200 MJ for a single

vehicle is appropriate if the design fire is treated as two vehicles or three vehicles respectively.

5.1.3 Vehicle classification

Work in Chapter 3 collated data from 41 single vehicle fire experiments from various accessible sources dating back from the early 1990s up until the 2000s. However, recent data from Okamoto et al. [78] and Anonymous [77] adds four more vehicles to the total giving 45 vehicle fire experiments. All the experiments are categorised into seven vehicle classes according to the ANSI classification system i.e. Passenger Car: Mini, Light, Compact, Medium and Heavy; Minivan/MPV; and SUV. However, for this work, 12 experiments have been excluded due to incompleteness of data where the main cause was due to the fire being suppressed before it reached its potential peak rate of heat release. The exclusion of the 12 experiments leaves the Passenger Car: Heavy classification down to only one experiment and the SUV classification to be completely removed from the analysis. The definition of each classification is given by the range of curb weights and the total number of experiments for each classification is shown in Table 5-1. Each of the experiments has its own identifier for the purpose of the analysis.

Table 5-1: Single passenger vehicle classification by curb weight and number of experiments

ANSI classification	Number of experiments	Identifier (Number)
Passenger car: Mini	7	M(x)
Passenger car: Light	7	L(x)
Passenger car: Compact	7	C(x)
Passenger car: Medium	5	MED(x)
Passenger car: Heavy	1	H(x)
Minivan/MPV	6	MPV(x)

5.2 Assessment of the Ingason method

The Ingason exponential curve method [92] is firstly assessed here as a means to create the required design fire curves due to its relative simplicity and its successful application in previous work. It incorporates the growth and decay phases in one equation and is given as

$$\dot{Q}(t) = \dot{Q}_{max} n_{ing} r (1 - e^{-k_{ing} t})^{n_{ing}-1} e^{-k_{ing} t}$$

Equation 5-1

where

$$k_{ing} = \frac{\dot{Q}_{max}}{E_{tot}} r_{ing}$$

Equation 5-2

and

$$r_{ing} = (1 - \frac{1}{n_{ing}})^{1-n_{ing}}$$

Equation 5-3

where $\dot{Q}(t)$ is the heat release rate, $\dot{Q}_{max}$ is the peak heat release rate, n is the retard index which is an arbitrary chosen parameter, r_{ing} is the amplitude coefficient, k_{ing} is the time width coefficient, t is time, and E_{tot} is the total energy content. The time to reach peak heat release rate, t_{max} can be obtained by

$$t_{max} = \frac{\ln n_{ing}}{k_{ing}}$$

Equation 5-4

Equation 5-1 and Equation 5-4 are enough to characterise a design fire but iterative calculations are needed to determine a suitable value for n_{ing}. Alternatively Ingason [93] suggests n_{ing} can be estimated using

$$n \approx 0.74394 e^{\frac{2.9\dot{Q}_{max} t_{max}}{E_{tot}}}$$

Equation 5-5

However it has been noted by Li and Ingason [95] Equation 5-5 is only an approximation where for large values of n_{ing} or t_{max}, significant errors may be introduced.

For the Ingason method, the peak heat release rate, time to reach peak heat release rate, and total energy released is sufficient to construct the design fire. Using these three parameters for each of the 33 experiments of interest Equation 5-1 - Equation 5-5 are solved. Examples of applying the procedure are shown in Figure 5-2 - Figure 5-4 for experiments M1, C7 and MED5 which illustrate the variability in the shape of the heat release rate curves. In each example the solid line indicates the original heat release rate curve from the experiment, the dotted line is the Ingason's method, the long-dashed line is the Peak growth method, the short-dashed line is the Mowrer 20-80 growth method and the dashed-dot line is the Exponential growth method (the methods other than Ingason's are discussed later).

Figure 5-2 shows a "well-behaved" heat release rate curve in which the growth (and the decay) from the experiment follows an essentially monotonic function. Figure 5-3 shows a more complex growth curve than Figure 5-2 in which the heat release rate shows a local peak at round 10 min and a higher peak at around 25 min. Figure 5-4 shows one of the more multifaceted experimental heat release rate curves.

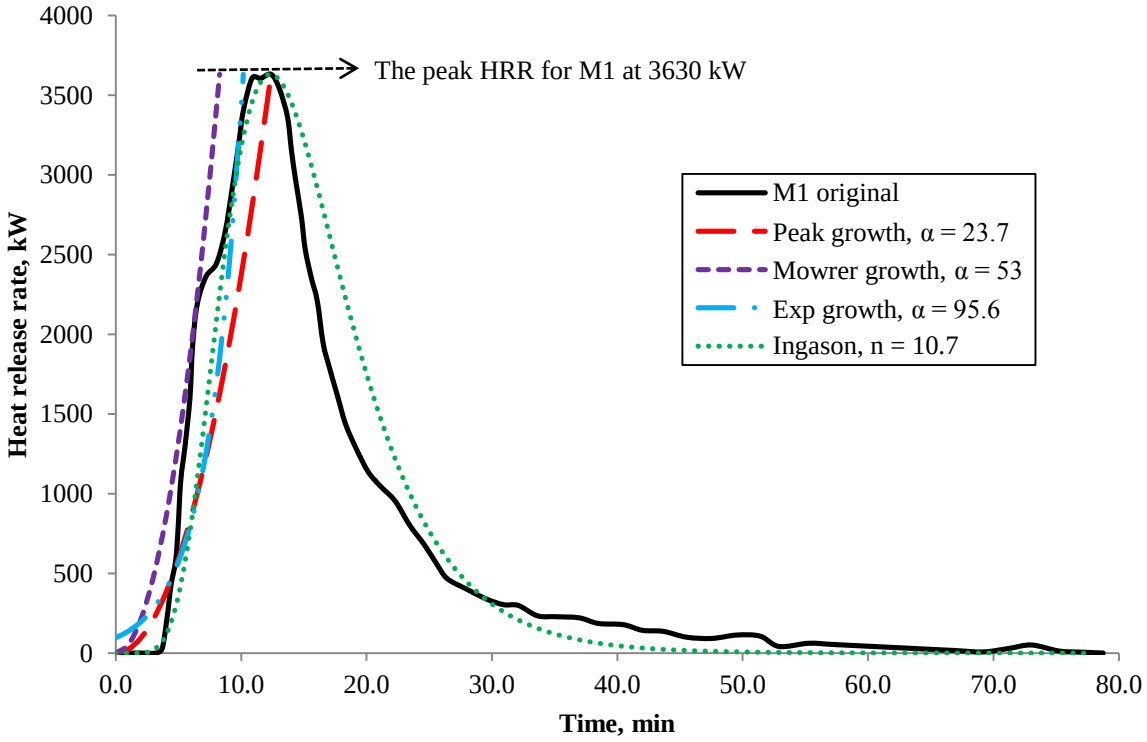

Figure 5-2: Experimental and design growth heat release rate curves for M1.

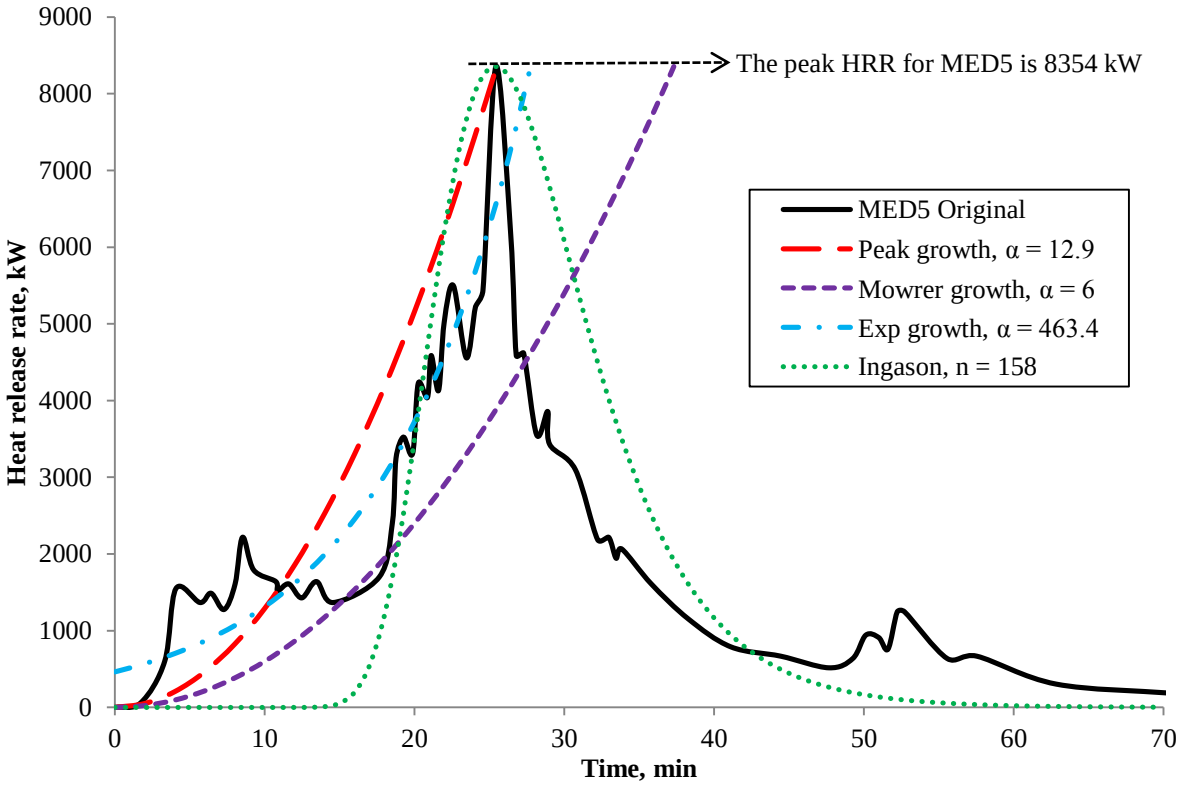

Figure 5-3: Experimental and design growth heat release rate curves for MED5

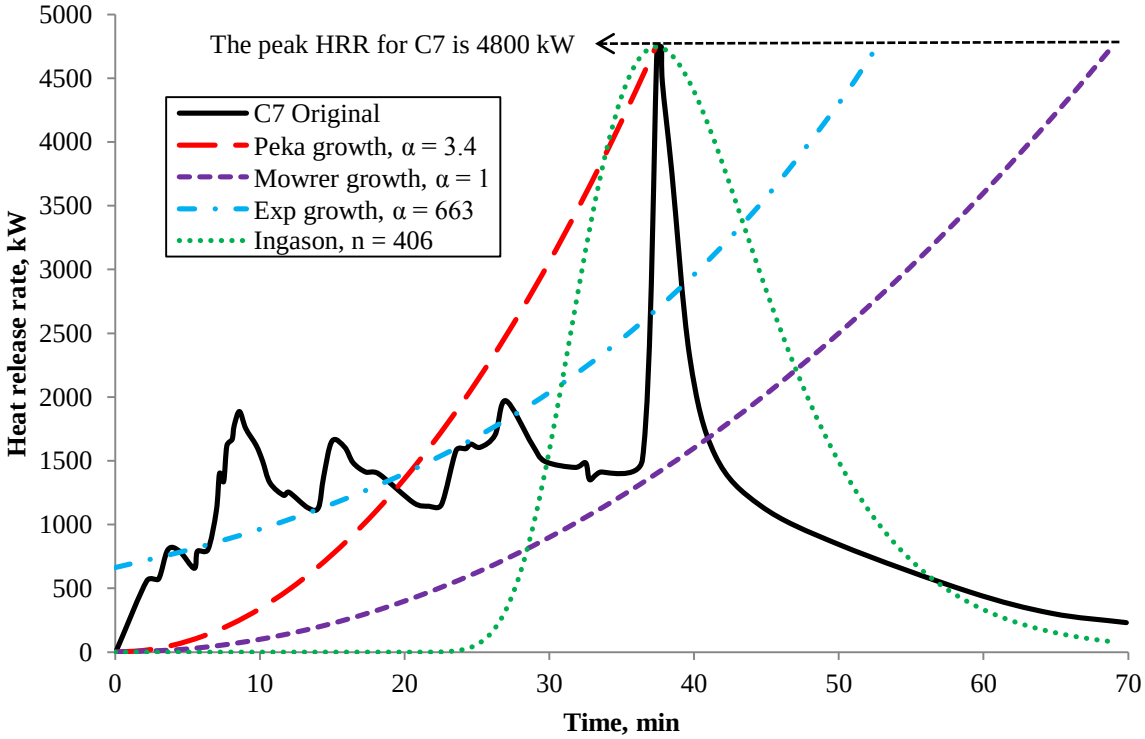

Figure 5-4: Experimental and design growth heat release rate curves for C7

Examining the comparison with the Ingason method shows an acceptable match with the experiment heat release rate curve for M1 however for C7 and MED5, it can be seen that both cases show longer incipient times as compared to the original data. The long incipient times are as a result of the high retard index, n_{ing}, calculated from Equation 5-5. The n_{ing} values obtained using the equation are 405 and 158, and these results in around ~20 min and ~12 min incipient phases for experiment C7 and MED5 respectively. Taking the n_{ing} values using Equation 5-5 for each of the 33 experiments and finding the average gives n_{ing} = 30 for Mini, n_{ing} = 73 for Light, n_{ing} = 143 for Compact, n_{ing} = 6450 for Medium and n_{ing} = 120 for MPV classifications. It is noted by Ingason that the n_{ing} value has no physical meaning but is used to vary the shape of the curve [92]. As such, there is no specific method to determine n, other than the estimation equation (Equation 5-5) given by Ingason [93] which had only been assessed for values of 1.5 to 45. Since the n_{ing} value in the Ingason method allows for an adjustment to be made to the curve Figure 5-5 shows a comparison between the MED5 experiment and various values for the n_{ing} value. The figure shows the Ingason curve calculated using Equation 5-5 (n_{ing} = 158), the upper and lower n values previously explored by Ingason [93] (n_{ing} = 45 and n_{ing} = 1.5 respectively) and finally an estimated n value to match the initial growth period (n_{ing} = 7.5).

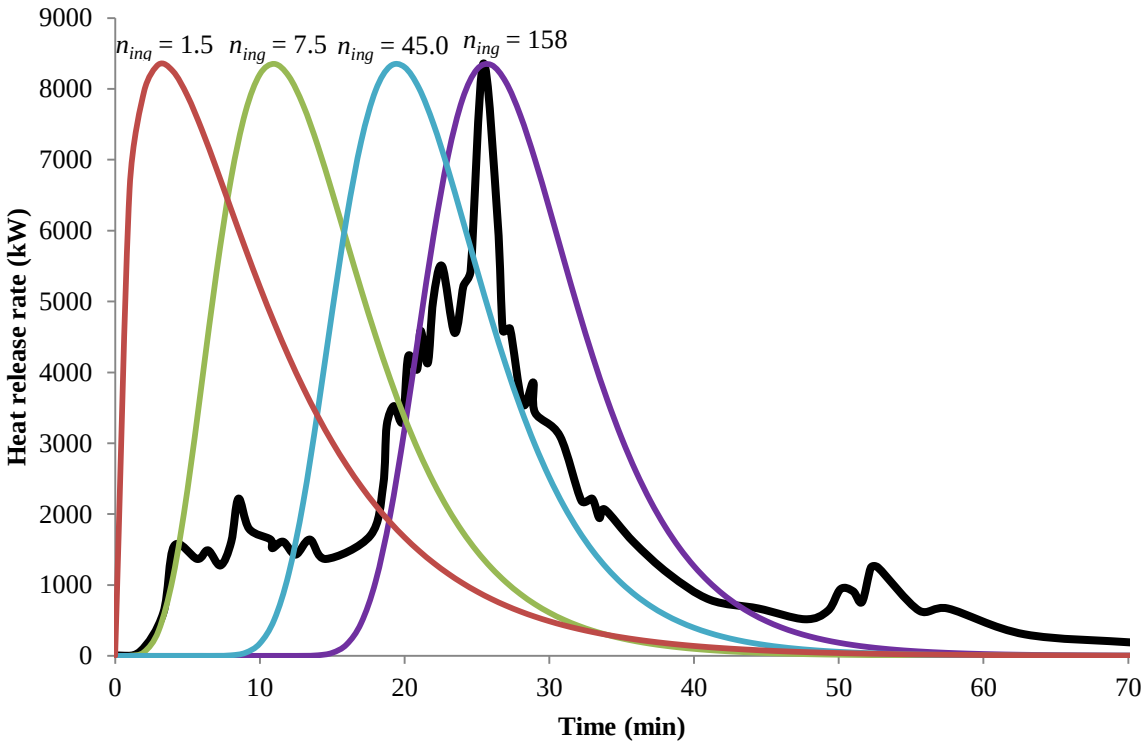

Figure 5-5: Comparison of n_{ing} for experiment MED5

For a risk-based probabilistic analysis values of n_{ing} for the Ingason method would need to be selected from some form of distribution. Notwithstanding the difficulty of getting an n_{ing} value that can adequately match certain experiments (already illustrated by MED5 and C7) the n_{ing} values can be determined by using Equation 5-5 or by human judgement, as illustrated in Figure 5-5. To that end the Ingason method is examined by constructing design fires using the probability distributions of peak heat release rate, time to reach peak heat release rate, and total energy released given in Table 3-24. For this purpose, after a curb weight classification of a vehicle is selected, a mean, standard deviation or 95th percentile value could be chosen, for example, to get the values for the three probability distributions. To be consistent with the work Chapter 6, the upper and lower standard deviations (i.e. the 66th and 34th percentile respectively) are chosen for the lowest curb weight class (Mini) and the highest curb weight class where distribution statistics are available (Medium). The 66th percentile values for peak rate of heat release for Mini and Medium are 3676 kW and 6365 kW respectively and the 34th percentile are 2881 kW and 4277 kW respectively. Figure 5-6 shows how the determination of the n_{ing} values affects the shape of the curve and that the design fires for Medium classification shows longer incipient times than the Mini classification.

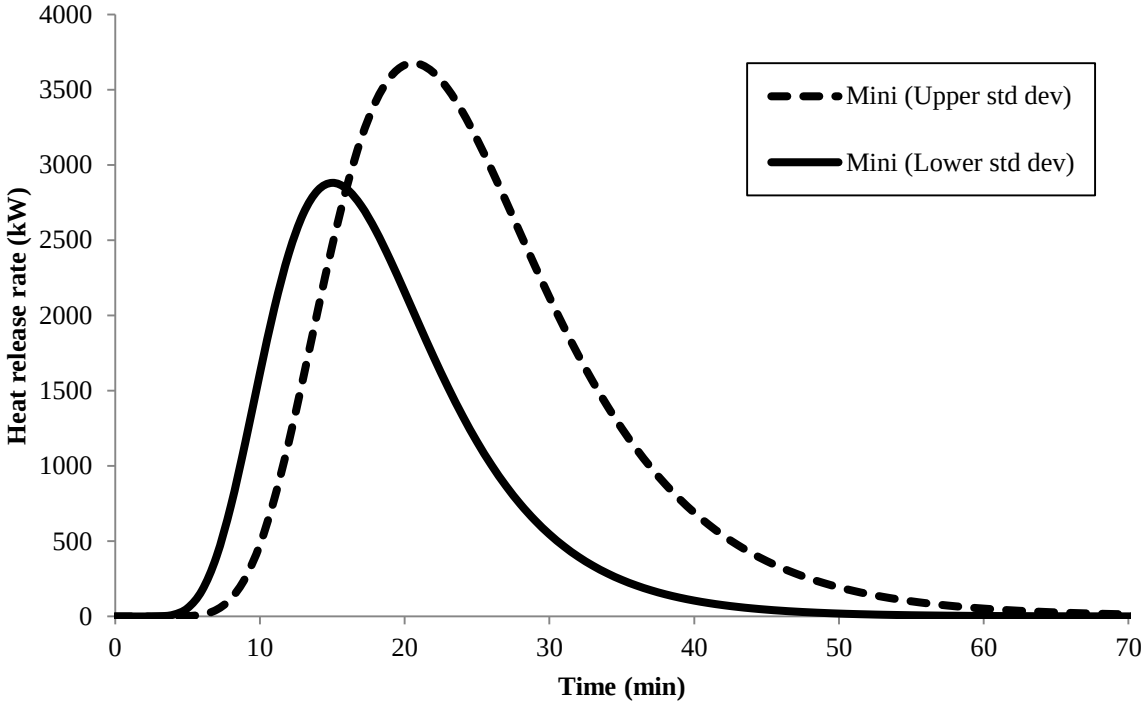

(a) Mini classification

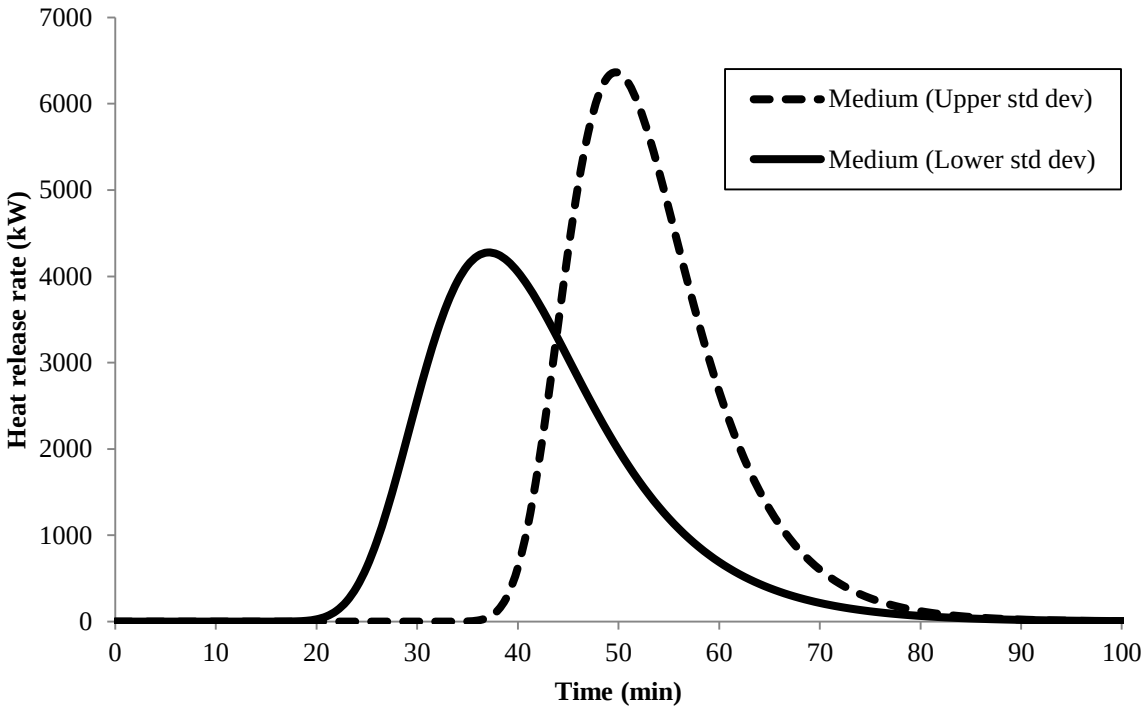

(b) Medium classification

Figure 5-6: Upper and lower standard deviation design fires using the Ingason method.

It is already clear that using Equation 5-5 will result in some large values of n_{ing} which in turn will mean any resultant distribution will be affected by them. Work in Chapter 3 note that heavier curb weight vehicles make up a significant proportion of vehicle fleets and more recent work by Anderson and Bell [97] shows a similar finding. As found above, the average n_{ing} values to match with the experiments increases with curb weight and as can be seen in Figure 5-6 where the values used for n_{ing} have a greater influence on these heavier curb weight vehicles both in terms of the offset in the growth of the fire from time zero as well as in the variability in the shapes of the rate of heat release curves.

5.3 Alternative growth methods

One of the main objectives of this work is to obtain design fire curves that can be used to predict the ignition and fire spread across multiple vehicles and, as already noted in Section 5.1.1, the Ingason method can result in long incipient times before the fire grows to the peak heat release rate. The duration of the incipient phase will likely have a significant impact on predicted times to ignition of target vehicles Therefore as an alternative to the

Ingason method three other methods are considered for the growth period, namely the Peak method, the 'Mowrer 20-80' method and the Exponential method described below.

5.3.1 The Peak method

This method uses a t-squared fire growth approach characterise the growth phase of the fire such that

$$\dot{Q}(t) = \alpha_{peak} t^2 \qquad (t \leq t_{max})$$

Equation 5-6

where $\dot{Q}(t)$ is the heat release rate, t is time and α_{peak} is the peak method fire growth coefficient. The term 'peak' heat release rate in this method means the single highest value of heat release rate in the curve history and so the method disregards any other distinct highpoints which have lower heat release rates. This approach of ignoring heat release rate curves which have two or more distinct peaks is a weakness of this method as illustrated later. The method assumes that the growth of the fire starts at time zero and by determining the peak heat release rate and time it occurs, the peak growth time coefficient is then calculated.

5.3.2 The Mowrer 20-80 method

This method is based on the work by Mowrer and Williamson [90]. This method also follows the t-squared fire growth approach given in Equation 5-6 but with different starting and peak data points. The growth curve is assumed to lie on a parabolic curve that includes two points that are at the times at which the rate of heat release are 20% and 80% of the peak value. The two pairs of data are defined as $(t_1, \dot{Q}_1)$ and $(t_2, \dot{Q}_2)$ where t_1 is found the first time the curve reaches 20% of peak heat release rate and t_2 is found the first time the curve reaches 80% of peak heat release rate. These two pairs of data with their corresponding equations which lie on the parabolic curve given as:

$$\dot{Q}_1 = \alpha_{mowrer}(t_1 - t_0)^2$$

Equation 5-7

$$\dot{Q}_2 = \alpha_{mowrer}(t_2 - t_0)^2$$

Equation 5-8

Equation 5-7 and Equation 5-8 are solved simultaneously to yield:

$$t_0 = \left[t_1 - \left(\frac{\dot{Q}_1}{\dot{Q}_2} \right)^{\frac{1}{2}} t_2 \right] / \left[1 - \left(\frac{\dot{Q}_1}{\dot{Q}_2} \right)^{\frac{1}{2}} \right]$$

Equation 5-9

$$\alpha_{mowrer} = \dot{Q}_1 / (t_1 - t_0)^2$$

Equation 5-10

The fire growth coefficient α_{mowrer} is then applied to the t-squared fire growth equation to produce the characterised fire growth phase.

5.3.3 The Exponential method

This method is adopted from the work by Mowrer and Williamson [90]. This method uses an exponential approach to characterise the growth phase of the heat release rate curve such that,

$$\dot{Q}(t) = \dot{Q}_0 \exp(\alpha_{exp} t) \qquad (t \leq t_{max})$$

Equation 5-11

where $\dot{Q}(t)$ is heat release rate, $\dot{Q}_0$ is heat release rate at time = 0, α_{exp} is fire growth coefficient and t is time. For this method, the exponential growth variables $\dot{Q}_0$ and α_{exp} are obtained by fitting the experiment heat release rate history data to Equation 5-11. The starting point for the heat release rate is not necessarily at 0 kW as it depends on the $\dot{Q}_0$ value obtained from the fitting. The mathematical formulation of the exponential function can lead to inappropriate values for the heat release at the start of the design fire as illustrated later.

5.3.4 Growth stage comparison

The coefficients for the corresponding growth methods are obtained from the experimental heat release rate curve data then the calculated time to the recorded peak rate of heat release is found. Thus the growth phase starts from time zero until it reaches the recorded peak heat release rate at the calculated time.

An assessment of the three growth methods indicates that the exponential growth is not suitable for this work. This is because when the growth part is characterised using this method the initial heat release rate value at 0 min always exceeds 1 kW due to the mathematical formulation of the exponential function. If the initial heat release rate value is less than 50 kW we can assume this could be the representation of an ignition source but in this work most of the initial values are greater than 50 kW. For example, Figure 5-4 shows the characterisation of experiment C7 in which the exponential growth method has an initial heat release rate value of 663 kW which is the highest value found across all of the experiments assessed. The Exponential method has been found to be relevant for the examples given elsewhere in Mowrer and Williamson [90] as the initial heat release rate value obtained were less than 50 kW but it is not the case for the experiments used in this work. Thus, the Exponential growth has been excluded from further assessment here.

Figure 5-2 - Figure 5-4 also show the corresponding difference in the time to reach the peak heat release when using the different growth methods. The Power law exhibits a better match with the experiments than the Mowrer and Williamson [90] approach and so the Power law growth is considered to be the more appropriate for this work. To illustrate the difference between the Ingason and Power methods the 66^{th} percentile values for the probability distributions of a Medium curb weight vehicle are plotted in Figure 5-7. The seven multiple vehicle fire experiments examined in Chapter 6 are used to assess the possible impact on the determination of time to ignition of a second vehicle of the two methods. It is found that the measured rate of heat release values from the first vehicle at the time the second vehicle ignites are of the order of 3030 ± 1255 kW. Applying these values to the Ingason curve the equivalent times to ignition form a narrow range of times in the order of 43 ± 1 min whereas the Peak growth suggests earlier times that in the order of 35 ± 7 min.

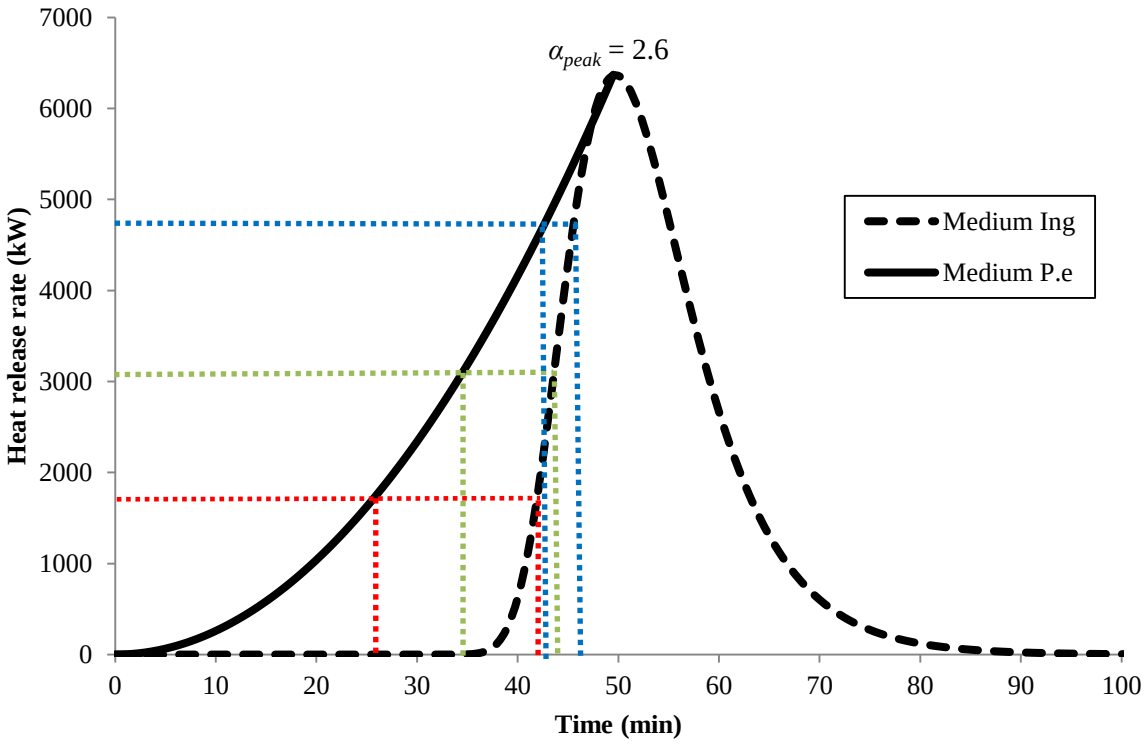

Figure 5-7: The comparison of using different characterisation methods for Medium classification vehicle (dotted lines show estimated times to ignition: red at 1900 kW, green at 3030 kW, and blue at 4900 kW).

Clearly assessing the likely time to ignition of a target vehicle using the rate of heat release from a source vehicle can only give an indication of what might be expected. Further work is currently ongoing to apply a point source model and the flux-time product method to the prediction of the time to ignition in vehicle fires based on the previous work by Baker et al. [98]. However what is important in a risk-based approach to this issue is that times to ignition are sufficiently representative to allow for conservatism in design where earlier ignition times will likely result in more rapid fire spread and potentially higher peak total rates of heat release from the combined effects of multiple burning vehicles.

5.4 Selection of decay method

5.4.1 Methodology

To complete the design fire curve a suitable decay method needs to be identified. One objective of this work is to ensure when the risk-based calculations are carried out that the total energy release is appropriate when the fire statistics are selected from the distributions. Thus the decay method is determined by comparing the total energy released obtained from the characterised design fire curve with the total energy released given from the literature for

the 33 experiments. Where available the total energy released cited in the original source material is noted and it is also calculated by integrating the area under the heat release rate curve. The trapezoidal method is used in this chapter to calculate the area under the heat release rate curve using a time interval of one minute.

Once the peak heat release rate is reached, the decay phase begins and continues until it reaches the time at which the experimental data stops being recorded. In some cases the experimental data drops to effectively 0 kW but in other instances the published data terminates at some higher value. To create a consistent general characterisation for the heat release rate of a single passenger vehicle it has been decided in this work that the decay need only be continued until it reaches 50 kW. This value is suggested by Mowrer and Williamson [90] as a heat release value that by itself does not normally represent a significant threat, but does indicate an established fire of a size similar to a small wastebasket fire.

The next step is the calculation of the total energy released of the characterised heat release rate curve and to compare it against the recorded total energy released obtained from literature. A ranking system is introduced as a measure to determine which method shows the most appropriate representation of the original heat release rate curve where a percentage difference between the total energy released of characterised and original heat release rate curve is applied using a similar approach to that adopted by Babrauskas and Walton [89]. For this work, there are five classifications of single passenger vehicles that contain 5 – 7 experiments and thus the ranking system is applied to each of the classifications. The ranking system is based on two independent mathematical methods to compare the percentage difference. The two mathematical methods are:

1. Average method – the average value of the percentage difference of a growth/decay sample combination for all of the experiments in each classification. The lowest average value ranks the highest.
2. Standard deviation method – the standard deviation value using the sample standard deviation given by Equation 5-12.

$$\boldsymbol{\sigma} = \sqrt{\frac{\sum(\boldsymbol{X} - \bar{\boldsymbol{X}})^2}{\boldsymbol{n_{samples} - 1}}}$$

Equation 5-12

For this particular work, the sample, σ, is the standard deviation of a growth/decay combination and X, is the coefficient in each classification, $\bar{X}$, is the average of the coefficients in the data set and $n_{samples}$, is the number of samples (i.e. experiments). The outcome that has the lower value ranks the highest as it represents the closest approximation to the original heat release rate curve.

Three methods are considered for the decay phase, namely the t-squared decay method, the Power Law decay method and Exponential decay method. The individual methods are discussed below.

5.4.2 Decay phase methods

The t-squared decay method uses a similar approach to the t-squared fire growth to characterise the decay phase of the heat release rate curve. The fire decay coefficient, β_{peak} is obtained from the correlation of experimental data from the peak heat release rate, $\dot{Q}_{max}$ until the curve terminates. Thus the equation is given as

$$\dot{Q}(t) = \beta_{peak} t^{-2} \qquad (t \geq t_{max})$$

Equation 5-13

The decay phase starts once the heat release reaches the peak, $\dot{Q}_{max}$ at time t_{max} and effectively finishes when all of the energy available from the burning item has been consumed. The definitions of the beginning and end times apply to all the other decay methods used for this work.

The Power Law decay method uses a power law to characterise the decay phase of the heat release rate curve from experiment data such that

$$\dot{Q}(t) = \dot{Q}_{max}(t - t_{max})^{\beta_{power}} \qquad (t \geq t_{max})$$

Equation 5-14

where $\dot{Q}(t)$ is the heat release rate, $\dot{Q}_{max}$ is the peak heat release rate, t is time, t_{max} is the time to reach peak heat release rate and β_{power} is the fire decay coefficient for power law.

Finally the Exponential method uses the same exponential approach already discussed to characterise the decay phase of the heat release rate curve. The exponential decay equation is such that

$$\dot{Q}(t) = \dot{Q}_{max} e^{\beta_{exp}(t-t_{max})} \qquad (t \geq t_{max})$$

Equation 5-15

where $\dot{Q}(t)$ is the heat release rate, $\dot{Q}_{max}$ is the peak heat release rate, t is time, t_{max} is the time to reach peak heat release rate and β_{exp} is the fire decay coefficient.

5.4.3 Ranking analysis

The results for the percentage difference in the total energy released for the six curb weight classifications are shown in Table 5-2. The column labelled 'SRC' is the total energy released value given in the literature for the particular experiment while the column labelled 'CALC' is the calculated value. In this chapter the calculated values for the total energy released are used for the comparative analysis as there are some experiments in which the total energy released is not given in the literature. Overall it is obvious from the comparison that the Ingason method has performed the best for all classifications. This is as expected as the Ingason method uses the total energy as an input so as to provide a matching result when the heat release rate curve is generated. When examining the three decay methods, Table 5-2 give percentage differences from as low as 0% and up to as high as 1153% (i.e. experiment MED4 using the power decay).

Table 5-2: Total energy released for 33 experiments

	Ing		t-squared		Power law		Exponential		SRC		CALC
	MJ	%	MJ	%	MJ	%	MJ	%	MJ	%	MJ
M1	2940	0	3206	9	2087	29	3388	15	3100	5	2940
M2	2081	1	2466	19	1342	35	1722	17	2100	1	2070
M3	4053	0	7125	76	4887	20	5401	33	4090	1	4059
M4	1056	1	3108	64	15585	82	12545	47	8500	1	8544
M5	3065	1	3217	5	2391	22	2621	14	3200	5	3050
M6	3480	0	4800	38	3310	4	3431	1	3466	0	3466
M7	7677	10	3257	206	1222	15	1245	17	1500	41	1063
L1	3110	0	3164	2	2821	9	4051	30	3000	4	3110
L2	3400	0	3487	3	2446	28	2996	12	3300	3	3391
L3	6653	0	5669	15	4078	39	5616	16	8000	20	6662

L4	3979	2	1753	57	3040	25	5172	28	3900	4	4051
L5	3948	1	9967	149	4030	1	4186	5	4008	0	3999
L6	4987	0	4739	5	3443	31	4215	15	4957	0	4977
L7	4072	2	10740	160	5855	42	7254	75	4134	0	4134
C1	5651	0	6654	18	4369	23	5802	3	5280	7	5651
C2	6585	1	15558	134	9624	45	11118	67	6670	0	6659
C3	4850	1	5798	20	5130	6	6150	27	4950	3	4825
C4	4694	0	4641	1	7112	52	6692	43	4860	4	4682
C5	4367	2	8182	84	3722	16	3788	15	4930	11	4438
C6	4795	2	11960	145	5071	4	5264	8	5040	3	4878
C7	4814	2	13271	171	6533	33	6983	43	*N/A*	*N/A*	4900
MED1	6037	0	11309	87	5748	5	6094	1	6144	2	6038
MED2	6810	3	22911	228	8931	28	9326	34	7000	0	6984
MED3	5713	4	27441	363	10397	76	10117	71	6806	15	5924
MED4	7390	0	12253	65	92867	1153	22657	206	5280	29	7412
MED5	6811	1	16123	134	11065	61	11916	73	6700	3	6885
H7	6051	0	8419	39	4501	26	5286	13	7648	26	6054
MPV4	4937	2	2208	56	2562	49	3642	28	5028	0	5027
MPV5	5426	1	11123	104	4615	16	4751	13	*N/A*	*N/A*	5465
MPV6	6471	1	2325	64	10369	59	9257	42	7000	8	6502
MPV7	5363	2	14475	165	6662	22	7157	31	5200	5	5466
MPV8	5319	1	11935	122	5755	7	6449	20	5070	6	5386
MPV9	5694	1	6108	8	5280	7	7045	24	5160	9	5667

Where feasible, Table 5-2 also shows the percentage difference between the total energy released given in the literature and that calculated from the area under the curve. It can be seen that in some cases the difference has a percentage difference of more than 10% and up to 41%. The reasons for these variations are not clear since the information was scarce on how the quoted total energy released was obtained in some of the literature sources. It is interesting to compare the calculated total energy released in Table 5-2 with the reference design fire curves previously identified from the literature. The Ingason linear design fire value of 7800 MJ for a single vehicle (if the curve is treated as two vehicles) and Joyeux and TNO design fire curves of 6700 MJ are considered at the top end of the results. While the Ingason linear design fire value of 5200 MJ for a single vehicle (if the curve is treated as three vehicles are considered) and Ingason quadratic design fire curve of 4700 MJ are close to the average of the calculated total heat released value for all 33 experiments at 4900 MJ.

Table 5-3 shows the results for the average and standard deviation methods where the values in the brackets are the calculated percentage difference between the total energy released calculated area under curve of the original design fire and the calculated area under curve of

the design fire using the different combination methods introduced. From the two mathematical methods results, the final ranking is formed and shown in Table 5-3. The exponential (E) method never ranks lower than the second position in every curb weight classification. Where it is ranked second the percentage difference with the higher ranked method is comparatively small.

Table 5-3: Final ranking of decay methods for curb weight classifications.

	Mini		Light		Compact		Medium		Minivan/MPV	
Ranking	**Avg.**	**S.D**	**Avg.**	**S.D**	**Avg.**	**S.D**	**Avg.**	**S.D**	**Avg.**	**S.D**
1	E (21)	E (15)	P (25)	P (15)	P (26)	P (18)	E (77)	E (78)	E (26)	E (10)
2	P (30)	P (25)	E (26)	E (24)	E (29)	E (23)	T (176)	T (122)	P (27)	P (22)
3	T (60)	T (70)	T (56)	T (70)	T (82)	T (70)	P (264)	P (498)	T (86)	T (55)

Method: E = exponential; P = power; T = t-squared

5.4.4 Final design fire curve formation

Figure 5-8 illustrates the combination of the peak fire growth method and the exponential fire decay method that forms a single vehicle design fire curve. Given the variables α_{peak}, t_{max}, β_{exp}, and $\dot{Q}_{max}$ a design fire can be formed. It can be seen that the design fire is constructed by the combination of the growth line, which grows up until $\dot{Q}_{max}$ at t_{max} and at this peak point, the exponential decay starts taking over for the decay part.

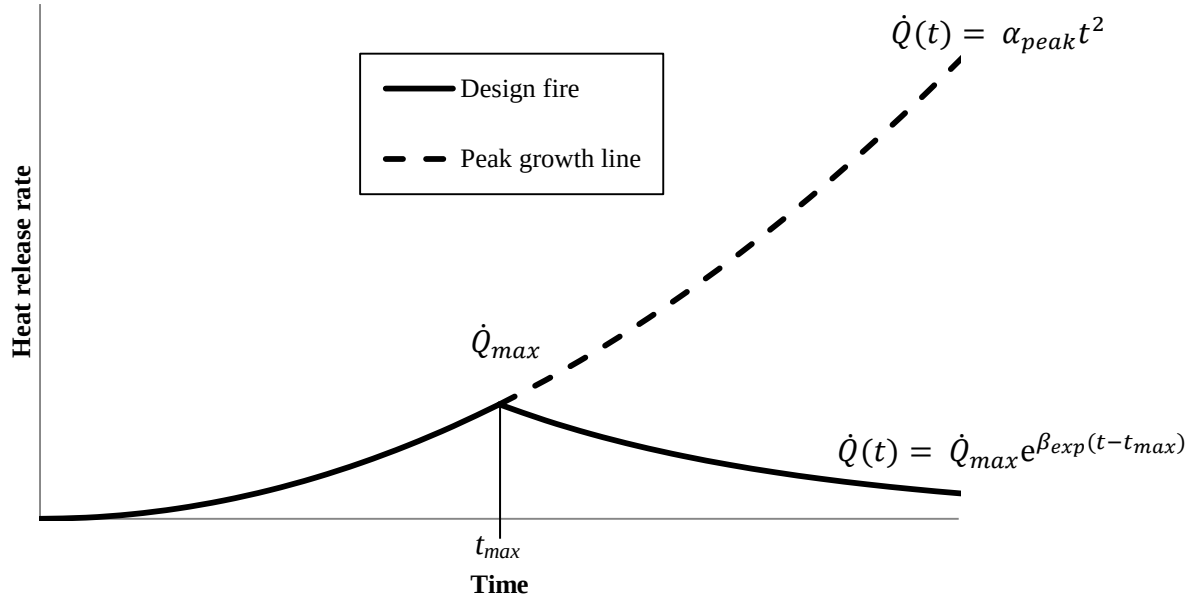

Figure 5-8: Characterisation of design fire using peak growth and exponential decay methods.

For a probabilistic application of the design fire curve $\dot{Q}_{max}$ can be found in Table 3-24 in which Weibull distributions was recommended. Subsequently work in Chapter 6 fitted various common distributions to the α_{peak} growth and β_{exp} decay coefficients corresponding to the experimental data. A ranking analysis identified the best fit distribution such that the gamma distribution is recommended for the growth coefficient and the Weibull distribution for the decay coefficient with the statistics shown in Table 5-4 for each curb weight classification. These statistics were applied to a comparison of the seven multiple vehicle experiments investigated in Chapter 6.

Table 5-4: Summary of the design fire distribution statistics for curb weight classes.

		Peak heat release rate, $\dot{Q}_{max}$ (kW)		**Fire growth coefficient, α_{peak} (kW/min²)**		**Fire decay coefficient, β_{exp} (min^{-1})**	
	Distribution shape	Weibull		Gamma		Weibull	
	Distribution parameters	**κ**	**θ**	**κ**	**θ**	**κ**	**θ**
Class	**Mini**	5.19	3809	1.39	11.86	0.93	0.17
	Light	1.66	5078	1.23	14.78	1.21	0.11
	Compact	2.40	4691	1.18	5.14	3.93	0.08
	Medium	3.18	7688	2.24	2.75	1.38	0.11
	Minivan/MPV	4.25	4588	0.36	159.18	2.51	0.08

Since the Ingason method needs to have the total energy release to obtain its curve parameters then one advantage of spitting the design fire curve into two distinct curves is that growth curves can still be determined from incomplete data. Thus the 12 experiments that were originally excluded from the work could be revisited to find appropriate α_{peak} values.

5.5 Conclusion

This chapter has used previously published experimental data from 33 experiments to determine a method to generate design fire curves that best characterise the rate of heat release curves for single passenger vehicles. The curves are to be used in risk-based probabilistic calculation approach for car parking buildings that applies distributions to create design fire curves and these curves need to be able to generate representative predicted times to ignition of multiple vehicles.

The Ingason method provides an elegant approach to create a design fire curve using a single equation but when examining it in the context of multiple vehicle fires this work suggests that it is likely to have limitations in its ability to allow reasonable predictions for the time to ignition of subsequent vehicles in the risk-based probabilistic analysis. Instead the analysis suggests separate growth and decay curves be used. For the growth phase the Peak method such that $\dot{Q}(t) = \alpha_{peak} t^2$ up until the peak heat release rate $\dot{Q}_{max}$ at time t_{max} is recommended. For the decay phase the Exponential method such that $\dot{Q}(t) = \dot{Q}_{max} e^{\beta_{exp}(t-t_{max})}$ until the heat release rate reaches 50 kW is recommend. Distribution statistics have been identified for the growth and decay coefficients as a function of the vehicle curb weight classification. An alternative method to specify growth and decay coefficients is presented in Appendix C.2

Chapter 6 PREDICTION OF HEAT RELEASE RATE CURVES FOR MULTIPLE VEHICLE FIRES USING SIMPLIFIED APPROACH

Published as Tohir, M.Z.M., and Spearpoint, M. "Simplified approach to predict heat release rate curves from multiple vehicle fires in car parking buildings" in 3rd International Conference on Fires in Vehicles, 2014. [99]

Abstract

A risk-based study of passenger vehicle fires in car parking buildings is on-going at the University of Canterbury. This chapter discusses a simplified approach to obtaining heat release rate curves for multiple passenger vehicle fires. The approach employs the superposition of two or more probabilistic single vehicle design fire curves where vehicles are categorized by their curb weight and statistical distributions are used to characterise the growth rate, decay rate and peak heat release rate. These single vehicle design fire curves are then used to define regions of likely design fire curves for multiple vehicle fires. In order to assess the robustness of the simplified method, experimental data from a total of seven two-vehicle fires have been compared using the approach. The comparisons show that the simplified approach gives reasonable predictions for the accumulated heat release rate for multiple vehicle fires.

6.1 Introduction

Vehicle fires in car parking buildings can impact on the life safety of the vehicle occupants as well as the building occupants who are the vicinity of the fire. Vehicle fires in car parking buildings can also result in material losses in terms of the vehicles, to the building structure and contents as well as to neighbouring property. Recently there have been several significant fires in car parking buildings involving multiple vehicles and in some cases these have led to fatalities. One of the most serious incidents reported was in 2006 in Gretchenbach, Switzerland where seven fire fighters were killed in an underground car park due to structural failure caused by fire [1]. Again in the same year there was a car park fire incident in Bristol, United Kingdom where 22 vehicles were destroyed and one person died in the occupancy above the car park [1]. Therefore it is prudent to understand the risks of vehicle fires and the need to potentially reduce the probability of a fire starting and/or mitigate the severity if a fire does occur.

This work is part of a larger research investigation into risk-based fire safety of passenger road vehicles in car parking buildings being undertaken at the University of Canterbury. The definition of passenger vehicle used throughout the research is based on the New Zealand Transport Authority (NZTA) which states that it is a motor vehicle constructed primarily for the carriage of passengers, with not more than nine seating positions which include the driver's seating position, and either has at least four wheels or it has three wheels and a gross vehicle mass exceeding one tonne [6]. The research has developed a method of generating multiple vehicle parking scenarios using a risk analysis approach (Chapter 4). The research has also compiled data from 41 single passenger vehicle fire experiments from various available sources dating back from the early 1990s up until the 2000s (Chapter 3). Recent data from Okamoto et al. [78] and Anonymous [77] adds four more vehicles to the total giving 45 single vehicle fire experiments. The experiments have been categorized into seven vehicle classes by their curb weight according to the ANSI classification system [47] i.e. Passenger Car: Mini, Light, Compact, Medium and Heavy; Minivan/MPV; and SUV and these data have been analysed to produce distributions of peak heat release rate.

6.1.1 Passenger vehicle design fires

The design fire is an important concept which can be described as the characterisation of the fire typically presented in terms of heat release rate as a function of time [45]. Design fires may also include other information such as an estimate of the area of burning and/or smoke and gaseous species production rates which are also typically expressed as a function of time. A design fire is a key component of performance based design which is an approach adopted as rational means of providing efficient and effective fire safety. The design process gives flexibility to achieve defined objectives provided that safety can be demonstrated. There are guidelines, such as the International Fire Engineering Guidelines [87] and the SFPE Engineering Guide [88] which specify the tasks required for the design process i.e. defining the project scope; establishing objectives; developing performance criteria; identifying and selecting appropriate design scenarios etc. Therefore, the identification and selection of one or more design fires is deemed as an integral part of the process to ensure that a performance-based design will satisfy its objectives.

Design fires for passenger vehicles are important for fire safety design in car parking buildings and any other related structures which contain vehicles. In Chapter 3, a detailed analysis was completed in an attempt to determine a reliable approach to characterise a passenger vehicle design fire. Out of the 45 single vehicle fire experiments identified, only 33 experiments have been analysed in detail. The other 12 experiments have been excluded due to incompleteness of the data where the cause was mostly due to the fire being suppressed before it reached its full potential. Table 5-1 shows the single passenger vehicle classification by curb weight and number of experiments available in each category.

6.1.2 Characterisation of design fire curves

For this work the focus is on the heat release rate as this is often a key driver for a design analysis and could be sufficient for the determination of fire hazard in car parking buildings. Previous chapter has discussed about the method which best characterise the rate of heat release curves for single passenger vehicles. It was found from the analysis that combination of Peak method for growth and Exponential method for decay was the best method, therefore is used in this chapter.

The general features of a single vehicle design fire typically exhibit an incipient phase, growth phase, fully developed phase and decay phase. In this chapter, design fires are

represented by the combination of a growth and a decay curve. The growth i.e. Peak growth is be defined as a t-squared function as shown in Equation 5-6. The decay i.e. Exponential decay is shown in Equation 5-15.

Figure 5-8 illustrates the combination of two equations i.e. Equation 5-6 and Equation 5-15 to form a single vehicle design fire curve. This approach gives fixed values for the coefficients for each individual experiment but it does not provide any distributions to the coefficient values across the curb weight classifications.

The question is then, how well do these single vehicle design fires produce reliable results for further use? The main objective of this work is to establish a simplified, reliable approach to represent multiple vehicle fire spread scenarios which could be used for the design of car parking buildings. To achieve this objective, comparisons of the simplified approach and seven two-vehicle fire spread experiments found in the literature are undertaken to demonstrate the capability of the approach. The outcome from the comparisons can then be used to produce a reasonable approximation of the heat release rate curve for multiple vehicle fire spread scenarios in an enclosure such as a parking building.

6.1.3 Simplified Approach

Although previous work in Chapter 4 has shown that most fire incidents in car parking buildings around the world involved only a single vehicle, there have also been cases which involved two or more vehicles. Thus, it is useful to establish an approach to creating design fires which is not limited to only single vehicle fire scenarios.

Given the single vehicle design fires, how can they be combined to create multiple vehicle scenarios? There are a number of challenges that need consideration for combining multiple item design fires. Firstly, the ignition time for each item has to be obtained and this can be determined by calculation or obtained from experimental results. Secondly, there are numerous factors which can affect the heat release rate development in an enclosed space such as the burning enhancement due to the incident radiation flux from the hot gas layer and boundary surfaces.

A simplified approach is used here that employs the superposition of two or more single item heat release rate curves. This approach has been previously introduced by Mowrer and Williamson (1990) which the concept is given as;

$$\dot{Q}(t)_{tot} = \sum \dot{Q}\, t_i$$

Equation 6-1

where $\dot{Q}(t)_{tot}$ is the combined total heat release rate of all of the burning items and $\sum \dot{Q}\, t_i$ is the summation of the heat release rate of each individual item. Mowrer and Williamson noted that the approach was limited by the lack of a methodology to characterise the challenges of multiple item fires which cannot be clearly isolated.

This simplified approach has been chosen here because the creation of a risk-based approach to the design of car parking buildings is already a complex problem and so it is important to keep the level of detail consistent for each part throughout the whole research project. The approach uses a combination of several key probabilistic components of a single passenger vehicle design fire as explained in the methodology section.

6.1.4 Multiple Vehicle Fire Spread Experiments

There are several notable experiments involving multiple vehicle fire spread in which the complete heat release rate curves are reported. The work by Steinert [57] in 1998 and 1999 presents 10 experiments in a study of burning and fire spread to vehicles parked next to each other. There were three experiments with only a single vehicle involved, six experiments in which two vehicles were parked next to each other and a single experiment with three vehicles parked next to each other. In 1997, Joyeux [37] compiled a report of a series of vehicle fire experiments performed in 1995 and 1996. The main objective of this work was to study the heat release rate of vehicles where 10 experiments were conducted for this purpose. The experiments were conducted under a hooded calorimeter to simulate a car park fire. Out of the 10 experiments, four experiments involved a single vehicle and the other six involved a pair of vehicles parked next to each other. There is also a report published by the Building Research Establishment (BRE) [1] which compiles the results of series of vehicle fire experiments. There were 10 experiments altogether in which four of the experiments involved a single vehicle fire scenario, two experiments involved a two vehicle fire scenario and four experiments involved a three vehicle fire scenario.

At this stage, only scenarios with two vehicles involved are considered for this work. This decision is to ensure that the simplified approach works for simpler scenarios before going to the more complex scenarios that involved three vehicles. The BRE experiments which involved the two vehicles have not been included in this work due to lack of information on the heat release rate curves. Only two of the six two-vehicle experiments presented by Joyeux have been considered due to the completeness of the heat release rate information against time. The selected experiments given by Steinert and Joyeux are compiled where the main parameters which are important for the comparisons are the heat release rate curve and the timeline of the experiment, i.e. the time of each vehicle ignition where in some instances the first vehicle is ignited by an external source at some time after the start of the experiment.

For each experiment the make, model and the year of manufacture have been used to determine the appropriate curb weight classification for each vehicle. In some cases it has not been possible to directly identify the exact appropriate classification since the year of manufacture was not reported even though the make and model are known. The year of manufacture is necessary as the curb weights of some makes and models vary throughout the vehicle production run. Thus, where the year was not available, a decision has been made to select the appropriate classification by estimating the year of manufacture based on the date of published report or when the experiment was conducted. The details of the seven experiments considered are shown in Table 6-1.

Table 6-1: Details of the experiments for the comparison with the simplified approach.

Experiment number	Manufacturer & model of vehicle (ANSI classification)	Second vehicle ignition time relative to first vehicle (min)	Reference
A	Peugeot 309 (Light*) and Limousine Trabant (Mini)	20.0	[57]
B	Limousine Trabant (Mini) and Volkswagen Polo (Light*)	7.5	[57]
C	Limousine Trabant (Mini) and Citroen BX (Light)	12.0	[57]
D	Fiat Ascona (Light*) and Volkswagen Jetta (Light*)	10.0	[57]
E	Limousine Trabant (Mini) and Citroen BX (Light)	14.5	[57]
F	Renault Twingo (Mini) and Renault Laguna (Compact)	8.0	[37]
G	Renault Laguna (Compact) and Renault Twingo (Mini)	14.0	[37]

* Classification based on year of report / experiment

6.2 Methodology

This section is divided into two main parts where the first part is to establish the distribution curves for the key components of a single passenger vehicle design fire and the second part is to use the simplified approach to compare these curves with the two-vehicle fire experiments.

6.2.1 Fire Growth and Decay Distribution Curves

The fire growth and decay coefficients for each of the 33 single vehicle experiments have been obtained by fitting appropriate curves to the experimental heat release rate data. Figure 6-1 shows the analysis in terms of fire growth coefficient against log-scaled fire decay coefficient for each classification. It can be seen that the Mini and Light classifications generally show the highest growth coefficients although there is a considerable overlap with the other heavier classifications. The results also suggest that vehicles with higher growth rates also exhibit faster decay rates.

The values shown in Figure 6-1 are used to establish distribution curves for fire growth and decay for each classification. To process the data sets, the BestFit capability in the @RISK software [53] is used. The outcome of the distribution fitting process is a ranked order of fitting statistics for each potential distribution shape where a smaller value indicates a better fit. For this particular analysis, the selections of distribution shapes are not only based on the ranking of the fitting statistics but also based on the distribution shapes that are commonly used and likely to be available in other software tools for further analysis, and also on selecting consistent distribution shapes for the growth and decay coefficients.

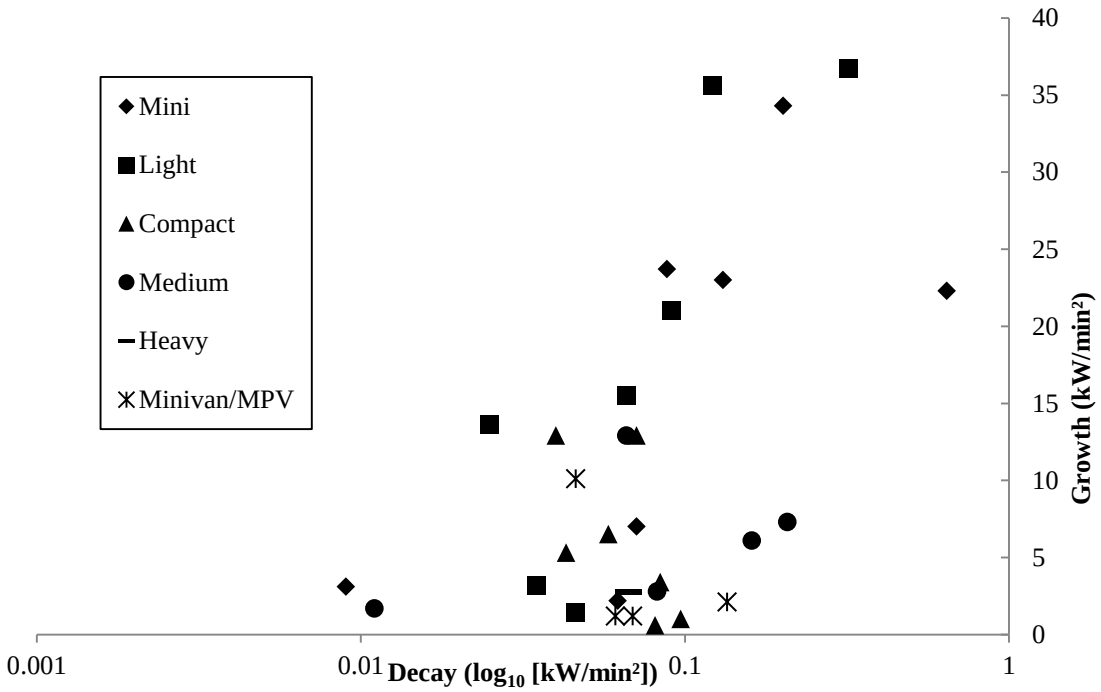

Figure 6-1: The growth and decay data for the different vehicle classifications.

6.2.2 Explanation of the Simplified Approach

With the distribution shapes for the fire growth coefficient, the peak heat release rate (found previously in Section 3.4.3) and fire decay coefficient for each of curb weight classification in place, a probabilistic design fire can then be formed. To form the design fire probabilistically, a suitable range of limits from the distribution shapes needs to be used. One option is to consider the 5th and 95th percentile values as the border for each distribution meaning most of the possible design values lie in this range. Having limits lower than 5th and larger than 95th percentile would mean that the design curves would encompass almost any possible value in the range and would mean there would be no distinct differentiation between the classification groups. Another range of limits for the distribution shapes is to consider the standard deviation in which is the lower limit gives the 33rd percentile and the higher limit gives 66th percentile. This range of value is smaller than using the 5th and 95th percentiles but is sufficient to cover 66% of the range of possibilities. The upper and lower distribution limit values taken from the three distributions are sufficient to form an envelope of possible design fires for a given curb weight classification where the design fire is formed by the combination of the peak method equation for the growth (Equation 5-6), the exponential method for the decay (Equation 5-15) and a maximum heat release rate.

With the design fire region available for every classification, the comparison with the two-vehicle fire spread experiments results is then performed. However, the comparison requires some further information from the original literature source such as the time of ignition of the first and second vehicle. With the curb weight classification for each experiment known, the design fire region can be superpositioned from the single vehicle design fire curves offset by the ignition times measured in the experiments.

Peacock et al. [100] has introduced a technique to quantify the differences between experimental measurements and model predictions. However, the technique is only applicable for comparison between two distinct single datasets whereas for this work, the comparison is made with the probabilistic region against the single dataset from an experiment. The quantification of the comparison of the design fire region with the experimental data is introduced here as a normalized indicator. Thus, the quantification of the fit is calculated as the percentage of points in the experimental heat release rate that intersect with the design fire region.

6.3 Results

6.3.1 Fire Growth and Decay Distributions

Table 6-2 and Table 6-3 shows the ranked order distribution shapes for the t^2 fire growth coefficient and exponential fire decay coefficient for each classification with the exception of Heavy since data is only available from a single experiment.

Table 6-2: Ranked order distribution for the peak method fire growth coefficient.

Rank	Mini		Light		Compact		Medium		Minivan/MPV	
	Shape	**Val.**	**Shape**	**Val.**	**Shape**	**Val.**	**Shape**	**Val.**	**Shape**	**Val.**
1	BG	0.30	W	0.19	*G*	*0.17*	T	0.17	LL	0.23
2	LL	0.30	T	0.21	E	0.17	*G*	*0.19*	LN	0.26
3	*G*	*0.31*	*G*	*0.22*	W	0.18	W	0.19	*G*	*0.27*
4	W	0.31	LL	0.22	LL	0.18	LL	0.21	E	0.51
5	E	0.31	E	0.24	LN	0.19	LN	0.22	T	0.60

BG = Beta General; LL = Log Logistic; G = Gamma; W = Weibull; T = Triangular; E = Exponential; LN = Log Normal

For the growth coefficient (Table 6-2), the fitting statistics show a range of results in which Compact has a relatively low and narrow range of 0.17 to 0.19 for the top five rankings whereas Minivan/MPV has a top ranked distribution that has a fitting statistic that is greater than the 5th ranked Compact distribution as well as a greater spread in the fitting statistics

between the top and bottom ranked distributions. From the analysis of the five classifications, the Gamma (G) distribution has been chosen as the single distribution shape for the fire growth coefficient due to its high ranking i.e. top three ranking for each classification and low statistical value throughout.

Table 6-3: Ranked order distribution for the exponential method fire decay coefficient.

	Mini		**Light**		**Compact**		**Medium**		**Minivan/MPV**	
Rank	**Shape**	**Val.**	**Shape**	**Val.**	**Shape**	**Val.**	**Shape**	**Val.**	**Shape**	**Val.**
1	E	0.18	LL	0.12	T	0.17	*W*	*0.20*	LL	0.16
2	*W*	*0.19*	LN	0.14	*W*	*0.18*	LL	0.20	G	0.17
3	LL	0.19	G	0.16	G	0.19	G	0.20	LN	0.17
4	LN	0.23	*W*	*0.17*	LN	0.19	T	0.22	T	0.19
5	T	0.40	E	0.22	BG	0.29	LN	0.26	*W*	*0.19*

BG = Beta General; LL = Log Logistic; G = Gamma; W = Weibull; T = Triangular; E = Exponential; LN = Log Normal

In Table 6-3 it can be seen that even though Weibull (W) is ranked 5th for the Minivan/MPV classification for the decay coefficient fitting statistic it is still similar to the other classifications. Therefore the Weibull distribution is chosen due to its reasonably low statistical fitting value compared to other distribution shapes.

A summary of the distribution analyses for peak heat release rate, fire growth coefficient and decay coefficient is shown in Table 6-4 where it contains the parameters to characterise the Gamma and Weibull distribution shapes for each classification. There is no obvious pattern for the fire growth coefficient and fire decay coefficient statistics as a function of classification, so it is difficult to form a more general design fire curve. However for the peak heat release rate, there is an increasing trend as the function of classification apart for Minivan/MPV. This is partly due to Minivan/MPV classification having an unspecified curb weight range which means that the experimental results may contain Minivan/MPV vehicles with wide range of curb weights. The distribution using these parameters gives suitable values for peak heat release rate, fire growth and decay coefficients that are used for the characterisation of the single vehicle design fires. For specific distribution plots for fire growth and decay coefficients for Mini, Light, Compact, and Medium classification can be found in Appendix D.1.

Table 6-4: Summary of the single vehicle distribution analyses for peak heat release rate, fire growth coefficient and decay coefficient.

		Peak heat release rate, $\dot{Q}_{max}$ (kW)		Fire growth coefficient, α_{peak} (kW/min^2)		Fire decay coefficient, β_{exp} (min^{-1})	
	Distribution shape	Weibull		Gamma		Weibull	
	Distribution parameters	**κ**	**θ**	**κ**	**θ**	**κ**	**θ**
Class	**Mini**	5.19	3809	1.39	11.86	0.93	0.17
	Light	1.66	5078	1.23	14.78	1.21	0.11
	Compact	2.40	4691	1.18	5.14	3.93	0.08
	Medium	3.18	7688	2.24	2.75	1.38	0.11
	Minivan/MPV	4.25	4588	0.36	159.18	2.51	0.08

6.3.2 Application of Simplified Approach

Figure 6-2 shows an example of an envelope of the possible range of design fires for Passenger Car: Mini classification. The dashed line is the range of possible design fires region within the 5th and 95th percentile of the distributions. The bold line is the range of possible design fires region for higher and lower standard deviation of the distribution. In each case the upper and lower limits for the growth have been selected and allowed to reach the upper and lower range of the peak heat release rate values respectively. For the upper limit, the peak heat release rate is maintained constant until it reaches the time where the slowest possible growth is able to reach the peak while for the lower limit, the slowest possible growth crosses the earliest possible decay from the peak thus creating the earliest possible duration of the item to finish burning. By forming this region, one can expect that for corresponding vehicle classification to burn within the possible region.

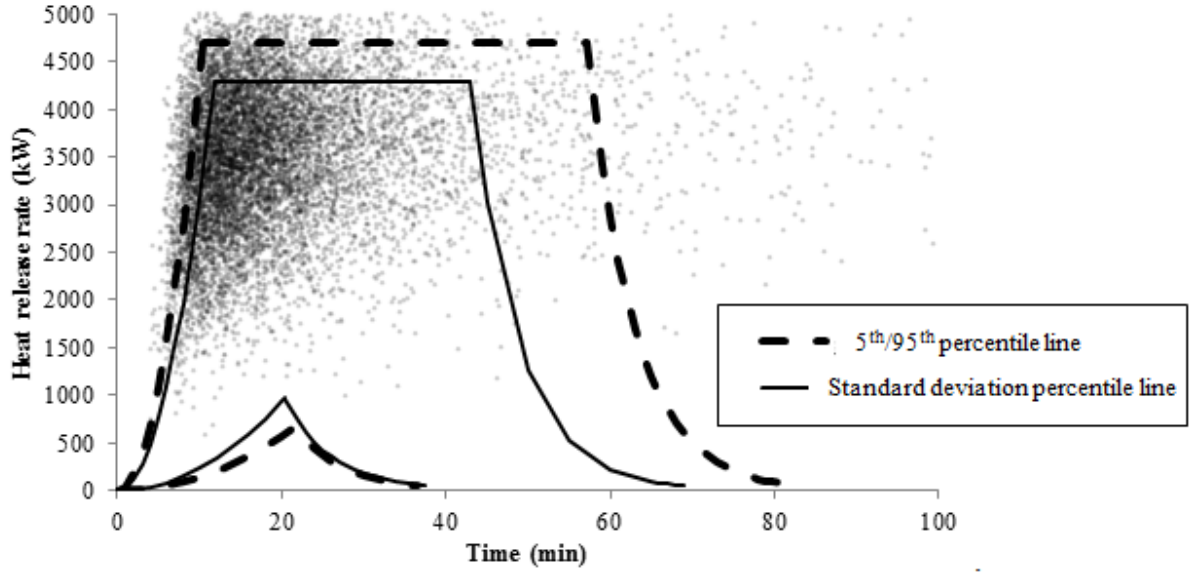

Figure 6-2: Range of possible design fires for Passenger Car: Mini classification.

Also shown in Figure 6-2 are scatter of dots which represent the possible peak heat release rate at certain time to peak generated by using a Monte Carlo simulation. Ten thousand random values from the fire growth and peak heat release rate distributions have been generated to compare with the two ranges of possible design fires. It is found that 90% of scatter dots fall inside the $95^{th}/5^{th}$ probabilistic design fire region and 68% of the scatter dots are inside the standard deviation probabilistic design fire region, as might be expected. Similar envelopes can be obtained for the other vehicle classifications and for this current work, it is decided that only the standard deviation design fire region will be used for comparison with the experiments.

The application of the superposition method has been completed for the seven two-vehicle fire spread experiments. Three comparisons of the superpositioned design fire region with experiments heat release rate history data are selected for detailed explanation. The selected experiments for comparison are Experiment A, Experiment D and Experiment F. These experiments are selected due to their unique combinations of two different vehicle curb weight classifications. In each comparison the dotted line indicates the combination of the probabilistic design fire region and the bold line indicates the heat release rate history data from the original experiment. The ignition times of the vehicles are indicated where a vertical line indicates the time of ignition of the second vehicle.

Figure 6-3 shows the comparison of superpositioned probabilistic design fire region with the Experiment A heat release rate data. In this experiment the first vehicle was not ignited directly but was exposed to an external flame. Thus, the time of ignition for the first vehicle; a Passenger Car: Light class was recorded at 15 minutes and the ignition of the second vehicle; a Passenger Car: Mini was recorded at 35 minutes. The probabilistic design fire region starts after the first vehicle was ignited and it can be seen that the measured heat release rate values mostly lie inside the probabilistic design fire region. The peak heat release rate for the experiment reached around 6200 kW and starts to decay afterwards. The calculation of the quantification of the fit gives 90% of the experiment data points intersecting with the standard deviation probabilistic design fire region.

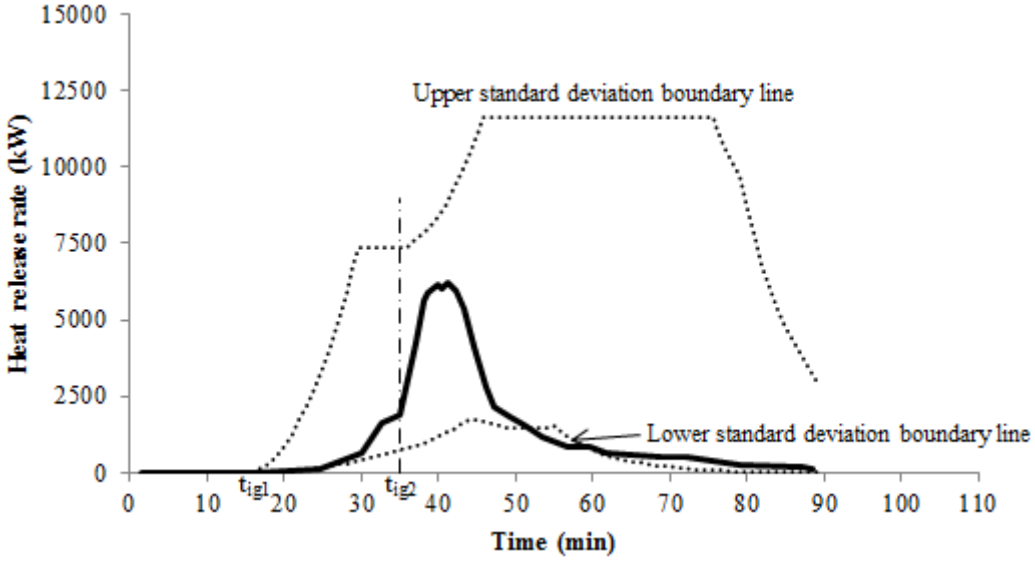

Figure 6-3: Comparison of superpositioned design fire region with Experiment A heat release rate data.

Figure 6-4 shows the comparison of the superpositioned probabilistic design fire region with Experiment D heat release rate data but this time as an example of the combination of two Passenger Car: Light vehicles. From the information given by the literature source, the time of ignition for the first vehicle is after 42 minutes and the ignition of the second vehicle ignites 10 minutes later at 52 minutes. It can be seen that the experimental heat release rate grows quicker than the design fire region up until it reaches peak and then begins to decay. The experimental data points only start to intersect with the probabilistic design fire region during its decay phase at is around 57 minutes. Since both of the vehicles were of the same classification, the ignition of the second vehicle does not significantly alter the growth combination, hence keeping the experimental growth outside of the design fire region until it

just passes the peak. For this comparison the calculation of the quantification of the fit gives 28%.

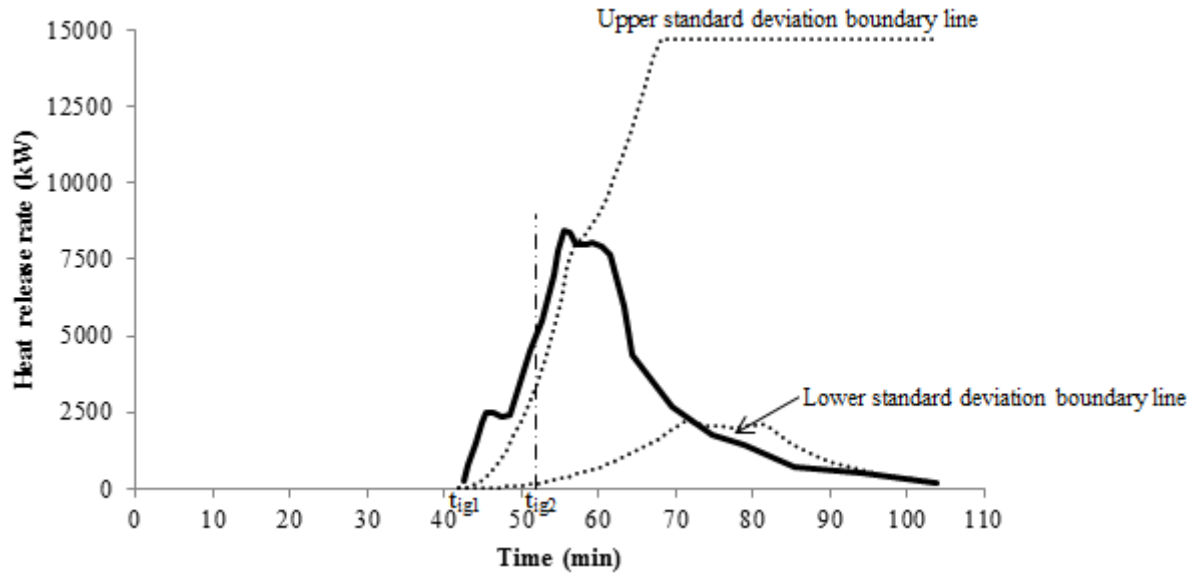

Figure 6-4: Comparison of superpositioned design fire region with Experiment D heat release rate data.

Figure 6-5 shows the comparison of superpositioned probabilistic design fire region with Experiment F heat release rate data for Passenger Car: Mini and Compact class vehicles. From the information given in the literature source, the first vehicle ignites just after the data recording was started and the ignition of the second vehicle was at 10 minutes. The beginning of the experiment shows the heat release rate growth rise to within the range of the probabilistic design fire up until around 9 minutes where rapid growth occurred to reach peak at around 7500 kW. Then the experimental heat release rate starts to decay up until 19 minutes where it starts to lie within the probabilistic design fire range. Interestingly, there was a second peak which reaches around 6600 kW and lies within the probabilistic design fire range. The calculation of the quantification of the fit gives 70% of the experiment data points intersecting with the standard deviation probabilistic design fire region. Comparisons for other experiments can be found in Appendix D.2.1. Comparisons of all seven experiments with $95^{th}/5^{th}$ percentile boundary lines can be found in D.2.2.

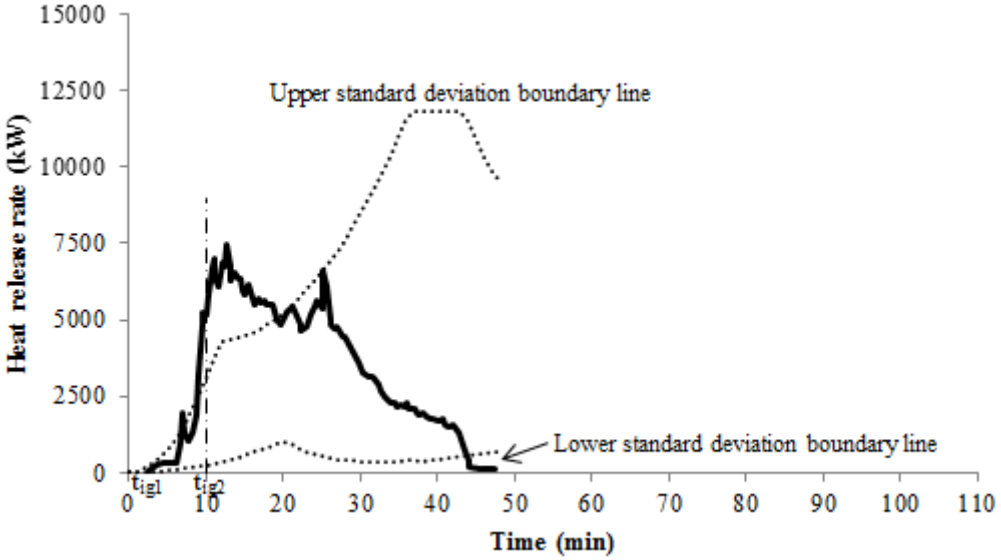

Figure 6-5: Comparison of superpositioned design fire region with Experiment F heat release rate data.

Table 6-5 shows the percentage of fit between the experiment data and the corresponding probabilistic design fire region. Five of the scenarios have minimum percentage of at least 62% and two have exceeded 90% however Experiment B and Experiment D both exhibit a low percentage fit of 28%. Examination of the comparison shows a relatively small difference between the experimental data and design region (e.g. as can be seen in Figure 5 during the initial growth) and by having a broader region i.e. $5^{th}/95^{th}$ percentiles, would increase the fit percentage. This analysis shows that the simplified approach can be considered to be a reasonable method to predict heat release rate for a two vehicle fire scenario.

Table 6-5: The percentage of experiment data within the probabilistic design fire region.

Experiment number	Percentage of experimental data within the standard deviation probabilistic design fire region
A	90
B	28
C	85
D	28
E	91
F	70
G	62

6.4 Discussion and conclusion

This chapter has presented a simplified approach of using single vehicle design fire distributions to represent multiple vehicle fire spread scenarios. The probabilistic design fire

region shows the possible range of heat release rate curves of multiple vehicles without considering a limit on the total energy that can be released by each single vehicle. The total energy could be included as part of forming a probabilistic design fire in which the shape of heat release rate curve is modified by the maximum total energy that could be released. For example, an analysis of the total energy released in single vehicle experiments can be obtained from Section Chapter 3. However such an approach would need to consider whether the cumulative energy release is tracked for each individual vehicle or whether only the total energy release is assessed. It is also possible that should a combination of lower growth and decay coefficients be selected from the distributions then the total energy release from the subsequent design fire will be less than the expected range obtained in experiments. These factors add more complexity to the proposed risk-based approach particularly where greater numbers of vehicles are involved in the analysis.

The current comparison of the proposed design fire curves with the two-vehicle experiments has used the measured ignition time of the second vehicle rather than attempting to calculate it. In order to extend the methodology to include a probabilistic assessment of multiple vehicle ignition times it may be possible to use experimental data to create distributions in terms of measured times or by using heat release rate values at the time a new vehicle ignites. Alternatively it might be necessary to try to calculate ignition times from material properties and incident radiation similar to the approach taken by Baker et al. [101] in which is done in the next chapter.

In conclusion, the simplified method of using the superposition of single vehicle design fire curves is considered to be a reasonable approach to assess the heat release rate of two-vehicle fire scenarios as shown by the comparisons with the seven experiments illustrated. The results suggest that there is value in continuing with the on-going research to determine suitable design fires for multiple vehicles scenarios. The next step is to expand the number of vehicles involved in the fire spread scenarios beyond two and to couple the fire spread with the multiple vehicle parking scenarios described in Chapter 4.

Chapter 7 PREDICTION OF TIME TO IGNITION IN MULTIPLE VEHICLE FIRE SPREAD EXPERIMENTS

Submitted as Tohir, M.Z.M., and Spearpoint, M. "Prediction of time of ignition in a multiple vehicle fire spread experiment" to *Fire and Materials*.

Abstract

This chapter describes the application of the flux-time product ignition criterion and the point source flame radiation model to predict the time to ignition in multiple vehicle spread scenarios. Ten experiments from the literature have been selected due to sufficiency of information required to apply the methods. The outcome of this work is to be applied to a risk-based model for the design of car parking buildings to determine when and if a fire spreads between vehicles therefore the analysis suggests properties of a representative material that can reasonably account for those external vehicle components that are most likely to ignite first. The application of both methods to the complex problem of multiple vehicle ignition requires several assumptions and simplifications which are discussed in the chapter.

7.1 Introduction

7.1.1 Background

One of the fire development scenarios in car parking buildings is the possibility of fire to spread from a burning vehicle to a neighbouring vehicle. The spread of fire will cause the potential energy released to increase as there will be more fuel burning. A single passenger vehicle can release up to 8000 MJ of energy and reach a peak heat release rate of up to 9.8 MW based on the collation of tests results of a single passenger vehicle fire (Chapter 3). The magnitude of a multiple vehicle fire could increase the threat to the life safety of occupants of the car parking buildings and any connected buildings; as well as damage to the structure of the building itself.

In Chapter 4, work on the fire risk analysis of car parking buildings conservatively assumed that all of the vehicles catch fire simultaneously. As a result, the combined heat release rates of the vehicles involved will be at a maximum at a given time. However, a travelling fire phenomenon should be taken into account as part of an analysis since it is unlikely that all of the vehicles will catch fire simultaneously. If a vehicle is ignited, it takes time for the fire to develop within the vehicle before it can spread to a neighbouring vehicle. Thus, by the time the fire in the neighbouring vehicle starts to grow, there is a possibility that the preceding vehicle is burning out. It is therefore necessary to be able to assess if and when neighbouring vehicles will ignite.

The ignition of a target vehicle due to its exposure to a neighbouring burning vehicle (or vehicles) is clearly a complex problem. For example, the fire could be located in the passenger compartment, in the vehicle engine etc., the availability of air to the fire will be affected by the status of the vehicle windows etc., the energy release will depend on the type, amount, distribution and ignition of combustible materials. The fire in the burning vehicle will grow and spread such that the radiant energy from the flames will change accordingly but also the radiant energy to the target will also be potentially blocked by parts of the vehicles. In addition if the vehicles are burning in an enclosed space such as a car parking building then there may be radiation feedback from the wall and ceilings, ventilation effects due to constrictions or external wind, etc. A number of these challenges were similarly identified by Noordijk and Lemaire [40] and thus any method that tries to predict the time to

ignition will not be able to account for all of these factors but can only be expected to achieve results that are approximate.

The Building Research Association New Zealand (BRANZ) and the University of Canterbury have been collaborating on the development of a probabilistic zone modelling software, B-RISK [18]. One of the components of the development of B-RISK software is to develop suitable radiative fire spread sub-model in which an ignition criterion methodology and flame radiation model is required [101]. Based on number of criteria including their suitability as engineering approximations, the flux-time product (FTP) has been selected as the ignition criterion and the point source model (PSM) as the flame radiation model [102]. For the radiative fire spread to work, the PSM estimates the heat flux from the burning item and using the heat flux, the FTP will then able to estimate the time to ignition of the target. This work is similar to other related research that has used the point source flame radiation model and the FTP ignition criterion to compare item-to-item fire spread predictions against a series of furniture calorimeter and room-size experiments [98].

7.1.2 Objective

The overall objective of this work is to determine a suitable method to apply the PSM to a vehicle fire and FTP properties for a representative material that can reasonably account for those external vehicle components that are most likely to ignite first which can then be used in the fire risk tool discussed in Chapter 4. To achieve this the chapter examines the ability of FTP ignition criterion method and PSM flame radiation model to predict the time to ignition of a subsequent vehicle when exposed to a fire in a preceding burning vehicle in a multiple vehicle fire scenario. However, due to complexity, this chapter is not dealing with the challenges mentioned in Section 7.1.1. Nevertheless, challenges such as heat radiation effect from the ceiling and compartment will be dealt in the next chapter. The assessment compares the measured times to ignition of vehicles from published fire spread experiments with predicted values using the combined PSM and FTP methods. The analysis requires the selection of representative materials for the target vehicle in terms of their likelihood to be commonly found externally on vehicles and those that were seen to ignite in the published fire spread experiments. Appropriate cone calorimeter data available in the literature is used to determine suitable ignition properties of those selected materials.

7.2 Previous experimental work

7.2.1 Multiple vehicle fire experiments

To perform the time to ignition comparison there is a minimum amount of information required from published multiple vehicle fire experiments. Firstly, the experiment must have two or more vehicles involved with known distances apart. Details regarding the vehicle manufacturer and model are useful additional information. Secondly, a timeline of ignition observations is critical for comparison purposes i.e. when and which vehicle was initially ignited, and when and which vehicle/s subsequently ignited. Information regarding where and what material ignited first on a vehicle is also valuable. Thirdly, a complete heat release rate history is required and a corresponding set of heat flux measurements to one or more target locations are useful. Any other additional information which can improve the comparison is highly valued. Three series of experiments are briefly described below which meet the criteria listed here.

7.2.1.1 Joyeux 1997 [37]

Centre Technique Industriel de la Construction Metallique (CTICM), France conducted vehicle fire experiments with the objective of gaining more understanding of vehicle fire scenarios. A total of 10 experiments were conducted between 1995 and 1996 under a hood arrangement which simulated a car park fire. The floor area under the hood was 25 m² corresponding to two parking bays and the hood was 2.30 – 2.60 m above floor level depending on the specific experiment. Heat release rates were determined by using the oxygen consumption method. For this study, only Experiment 9 and Experiment 10 achieved the minimum requirements for the time to ignition comparison where both experiments were conducted in open-sided conditions. In both experiments a pair of vehicles with the same manufacturer and model was used i.e. a Renault Twingo and a Renault Laguna, and the two vehicles were positioned 0.7 m apart. In Experiment 9, the Renault Twingo was first ignited using a litre of petrol under the car at the gearbox level. In Experiment 10, the Renault Laguna was ignited first using the same procedure as for Experiment 9.

7.2.1.2 Steinert 2000 [57]

Between 1998 and 1999 the Leipzig Institute for Materials Research and Testing (MFPA) conducted 10 separate experiments involving a total of 17 vehicles. The main objective of the experiments was to study the burning and fire spread behaviour vehicles parked next to each

other. Out of the 10 experiments, three were single vehicle scenarios, six involved a pair of vehicles and one experiment had three vehicles parked next to each other. The experiments collected the mass loss rate, heat release rate (using the oxygen consumption method), the mass and volume production of smoke, temperatures and gas concentrations. The tests were undertaken in a partially open-sided rig with a floor area of 35 m² and with a height of 4.5 m. A 10 m high duct was installed in the rig which had an opening cross-sectional area of 6 m².

For this work, six experiments altogether have been selected based on the minimum requirements. Out of the six experiments, five involved two vehicles (Experiments 5, 6, 7, 8 and 9b) and one experiment involved three vehicles (Experiment 4). For all of the experiments, the first vehicle was ignited by the aid of 250 ml isopropanol on the front seat. For Experiments 6, 7, 8 and 9b, the distance between the first vehicle and the second vehicle was 0.8 m and for Experiment 5 the distance was 0.4 m. For Experiment 4, the vehicle parked between the other two vehicles was first ignited and each vehicle was 0.8 m apart for its neighbour.

7.2.1.3 BRE 2010 [1]

In 2006, the Communities and Local Government (CLG) Sustainable Buildings Division commissioned the Building Research Establishment (BRE) to carry out a project on fire spread in car parks. The main objective of the project was to gather information on the nature of fires involving the then current design of vehicles and to use this new knowledge as a basis for future work. To achieve the objective several key studies were completed that included data collection, computational modelling, materials testing and several full-scale vehicle fire experiments.

The full-scale vehicle fire experiments were conducted in a test rig (Figure 7-1) which had a floor area of 72 m² with a height of 2.9 m from the floor. The structure comprised of a steel frame with breeze block infill and the roof was of hollow-core concrete slabs. One end of the rig was open but with a 0.5 m downstand. Window openings which allowed ventilation were provided along one side and the back wall. At one end of the roof, a 1.6 m wide window channelled smoke via a deflector into a 9 m high calorimeter hood.

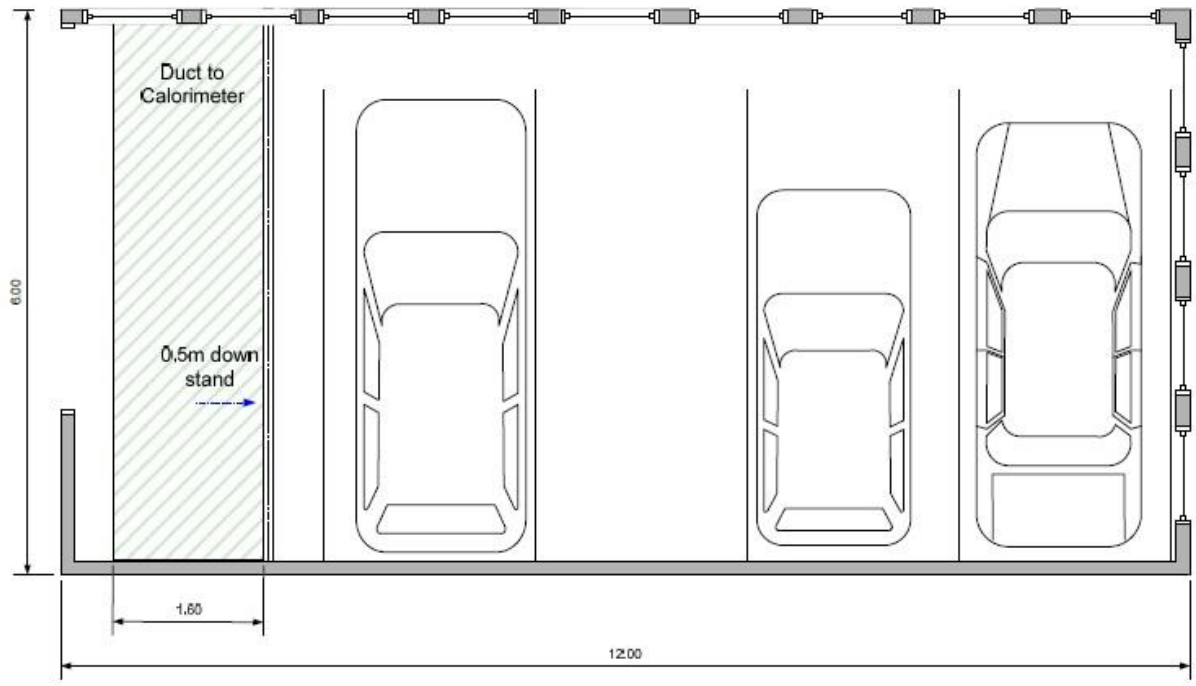

Figure 7-1: Plan of the experiment rig and vehicle arrangement for BRE Experiment 1 [1].

The experiments involved 22 vehicles of which 16 were recent working vehicles (aged less than five years old from the test date). The only modification made to all of the vehicles was that the air conditioning gas removed. The 22 vehicles were divided into 12 separate experiments which consisted of a single experiment involving four vehicles, three experiments involving three vehicles, a single experiment involving two vehicles in a car stacker and seven experiments involving a single vehicle. Only Experiment 1 and Experiment 3 have been selected based on the minimum requirements for this work.

In the experiments involving multiple vehicles the intervening distances were not stated so an estimation has been made from available information given in the report. For Experiments 1 and 3, the distances from the first vehicle ignited i.e. the one on the right hand side of in Figure 7-1 to the second vehicle are estimated as 0.7 m and the third vehicle estimated to be 2.5 m from the second vehicle.

For both experiments, there were two heat flux measurement probes of particular interest to this work; HFM3 and HFM4 were installed at the side of the third vehicle. However for Experiment 1, only the measurements from HFM3 are available to be used in this analysis.

7.2.2 Summary of selected experiments

In this chapter the experiments identified previously have been compiled and assigned a unique experiment ID (Table 7-1). The first vehicle listed in Table 7-1 indicates the first vehicle that was ignited in the experiment. Also shown are the manufacturer and the model of the vehicles and the original source reference.

Table 7-1: Multiple vehicle experiments with minimum required information.

Expt. ID	Vehicles involved	Manufacturer and model of vehicles	Reference
A	2	Peugeot 309 and Limousine Trabant	Experiment 5, [57]
B	2	Limousine Trabant and Volswagen Polo	Experiment 6, [57]
C	2	Limousine Trabant and Citroen BX	Experiment 7, [57]
D	2	Fiat Ascona and Volswagen Jetta	Experiment 8, [57]
E	2	Limousine Trabant and Citroen BX	Experiment 9b, [57]
F	2	Renault Twingo and Renault Laguna	Experiment 9, [37]
G	2	Renault Laguna and Renault Twingo	Experiment 10, [37]
H	3	Renault Laguna, Renault Clio and Ford Mondeo	Experiment 1, [1]
I	3	Renault Espace, Peugeot 307 and Land Rover Freelander	Experiment 3, [1]
J	3	Volkswagen Golf, Limousine Trabant and Ford Fiesta	Experiment 4, [57]

Table 7-2 shows the ignition time for the first and second vehicle observed in the experiments, where the reported values were obtained from the respective references, along with corresponding time difference. Also reported in Table 7-2 is the probable first component/material to ignite and burn for the second vehicle based on the observations given in the respective references. The table does not include the times to ignition and first component ignited on the third vehicle in Experiments H, I and J but these are discussed later.

Table 7-2: Multiple vehicle experiments observed results

Expt. ID	Distance between first and second vehicle (m)	First vehicle ignition (min)	Second vehicle ignition (min)	Time difference (min)	First component to ignite on the second vehicle
A	0.4	15.0	35.0	20.0	Window rubber/rubberized trim
B	0.8	15.0	22.5	7.5	Window rubber/rubberized trim
C	0.8	0.0	12.0	12.0	Window rubber/rubberized trim
D	0.8	42.0	52.0	10.0	Window rubber/rubberized trim
E	0.8	14.0	28.5	14.5	Window rubber/rubberized trim
F	0.7	0.0	8.0	8.0	Rubber
G	0.7	0.0	14.0	14.0	Rubber
H	0.7	3.5	20.0	16.5	Trim/paint
I	0.7	0.0	5.0	5.0	Unknown
J	0.8	1.4	30.0	28.6	Window rubber/rubberized trim

7.2.3 Cone calorimeter data

Two sources in the literature have reported the results of cone calorimeter tests conducted on component materials found on the exterior of vehicles and these are briefly presented here.

BRE [1] conducted cone calorimeter tests on potential exterior components of vehicles which are likely to ignite first during fire spread between vehicles. The main objective of tests was to investigate the burning characteristics of exterior vehicle components and determine the likely contribution to fire spread in vehicle fire scenarios. The burning characteristics were identified by determining the critical heat flux for ignition with a pilot source and their heat

release rate in accordance with ISO 5660:2002. Eleven samples from list of potential components which are likely to burn were chosen for the tests based on their location on a vehicle, the percentage area covered and perceived potential for ignition. The eleven components tested were hubcap, mudflap, rubber tyre, bumper trim, bumper, bumper grill, wheel arch, fuel tank, roof box, mohair soft top, and PVC soft top.

The Motor Vehicle Fire Research Institute (MVFRI) conducted cone calorimeter tests on selected automotive parts used in vehicles [103]. The main objective of this work was to assess possible means for determining the individual flammability characteristics of automotive components, obtain data on the range of flammability behaviour of each component and obtain insights into the fire behaviour observed in related full-scale vehicle fire experiments. However, most of the cone calorimeter test results reported were for the interior components of a vehicle and the only exterior component which is considered appropriate for this analysis is the 'windshield' which was made of polyvinyl butyral (PVB).

7.3 Theory

7.3.1 Flux-time product (FTP) ignition criterion method

Originally defined by Smith and Satija [104], FTP is a concept which predicts the time to piloted ignition of a combustible material exposed to incident radiation. The concept was then extended by Smith and Green [105], Toal et al. [106], and Shields et al. [107]. The method was then further improved by Shields et al. [108] and Silcock et al. [109] to include materials (plastics and timber) of different thermal thicknesses.

The FTP equation is expressed by:

$$FTP = t_{ig}(\dot{q}^{"} - \dot{q}^{"}_{cr})^{n}$$

Equation 7-1

where t_{ig} is the time for the combustible material to ignite, $\dot{q}^{"}$ is the incident radiation flux, $\dot{q}^{"}_{cr}$ is the critical heat flux (kW/m²) of the combustible material, n is the power law index (typically $1 \leq n \leq 2$) and the units for the FTP are $\frac{kW \cdot s^{n}}{m^{2}}$.

Equation 7-1can be rearranged to give a linear relationship which is shown by:

$$\dot{q}^{"} = \frac{FTP^{\frac{1}{n}}}{t_{ig}^{\frac{1}{n}}} + \dot{q}_{cr}^{"}$$

Equation 7-2

From this linear relationship, the FTP and the critical heat flux values can be obtained for a material using the experimentally measured times to ignition at different irradiance levels.

The concept is that when a combustible material is exposed to an external radiation flux, the FTP accumulates until it exceeds a critical value and the material ignites, thus giving the time to ignition. In terms of mathematical formulation, the accumulation of FTP is calculated at every time step such that:

$$FTP = \sum_{i=1}^{m} (\dot{q}_i^{"} - \dot{q}_{cr}^{"})^n \cdot \Delta t_i$$

Equation 7-3

where Δt_i is the i^{th} time increment and $\dot{q}_i^{"}$ is the heat flux at i^{th} time increment. Thus for this study, the FTP method is used to obtain the ignition time of a subsequent vehicle with respect to the ignition and burning of a preceding vehicle.

The FTP analysis is identical to the classical thermal solutions of Mikkola and Wichman [110], i.e., thermally thin, thermally thick, and thermally intermediate. In the FTP method when n = 1 the material is regarded as thermally thin, if n = 2 the material is regarded as thermally thick and when n = 1.5 the material is considered thermally intermediate. The FTP method has the advantage of allowing ignition predictions to be more general than the classical thermal solutions by allowing the power law index to be chosen to provide the best fit to the experimental ignition data rather than forcing a solution based on the physical thickness of the sample. Both Janssens [111] and Silcock, et. al. [109] have shown that often timber and some plastic materials are better characterized using power law indexes other than 1, 1.5, or 2.

7.3.2 Point source model (PSM) flame radiation

Fleury et al. [102] carried out an evaluation of thermal radiation models as part of the development of a radiative fire spread model for the B-RISK software. The performance of six thermal radiation models was investigated where the predictions made by the models

were compared with experiments. As a conclusion, the point source model was recommended for the software.

The point source model assumes the thermal radiation originates isotropically from a single point located at the centre of the burning item and the radiation heat flux received by the target $\dot{q}''_{fl}$ can be expressed by the following equation:

$$\dot{q}''_{fl} = \frac{\dot{Q}\lambda_r}{4\pi R^2}$$

Equation 7-4

where $\dot{Q}$ is the energy released from the burning item in kW, λ_r is the radiative fraction, and R is the radial distance from the centre of the burning item to the nearest point of the target item. The radiative fraction is dependent on the fuel type, flame size and flame configuration.

In this chapter the heat release rate data from the multiple vehicle fire experiments are used to determine the heat flux estimation using Equation 7-4. Since the PSM method considers the source of heat is fixed at the centre of burning item then as a fire spreads within a vehicle the centre of the fire moves and thus the effective radial distance to a neighbouring vehicle does not remain constant. In this work a sensitivity analysis on different positions for the heat source is investigated such that it is assumed to be located in the centre of the vehicle, the nearest and the farthest edge of the burning vehicle to the target vehicle. However, to keep the analysis simple, these points are kept along a perpendicular line to the vehicles' lengths. The application for the prediction of the time to ignition of the second vehicle is illustrated in Figure 7-2(a) where Vehicle 1 is the burning item which has three different heat source positions. The positions are defined as "2-Near" which is located at the exposed edge of Vehicle 1 to the target vehicle, "2-Centre" which is at the centre of Vehicle 1, and "2-Far" which is at the farthest edge of Vehicle 1 to the target vehicle. For the third vehicle scenario, illustrated in Figure 7-2(b), the burning item is a combination of Vehicle 1 and 2. In this case, the three heat source positions are located at the edge of the second vehicle exposed to the third vehicle which is named as "3-Near", the centre of the second vehicle which is named as "3-Centre", and at the other edge of second vehicle which is named as "3-Far". Finally a baseline value of 0.3 is chosen for the radiative fraction in accordance with Heskestad [112] for cases without specific knowledge.

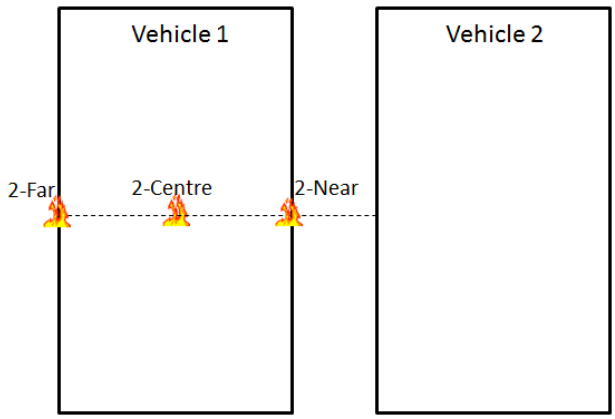

(a) Two-vehicle scenario.

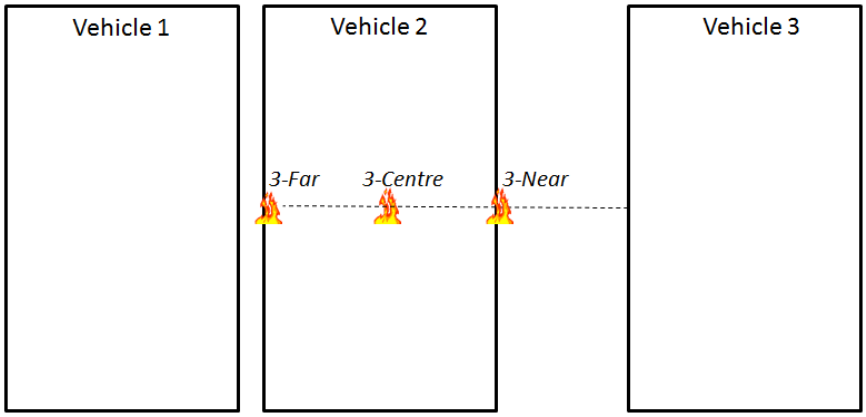

(b) Three-vehicle scenario.

Figure 7-2: Heat source positions of the burning item to the target item.

7.4 Material properties

7.4.1 Selection of components/materials

As the objective of this work is to examine how well the fire spread can be predicted using FTP and PSM methods, a decision on what would be the first component to ignite and burn has to be made. From Table 7-2, window rubber, rubberized trim, rubber, trim, and paint are listed as the first component observed to be ignited on the second vehicle. From these observations it is hypothesised that components which are made from rubber as well as components which serve as trim are likely to be ignited first as compared to other components and materials. Based on this hypothesis, further investigation is carried out on the eleven components tested in the BRE cone calorimeter tests and the one component in the MVFRI cone calorimeter test with the purpose of selecting a single material representative of that which is likely to be first ignited.

According to Lush [113], hubcaps are usually mostly made of acrylonitrile butadiene styrene (ABS) plastic due to its lightness and durability. Since mudflaps are required to be flexible and durable, materials such as natural rubber or synthetic rubber are predominately used in their manufacture. According to Miller et al. [114] passenger vehicle fuel tanks are usually made of polyethylene while roof boxes are typically made of ABS. Bajus and Olahova [115] note that rubber tyres for passenger vehicles and trucks contain around 80% - 85% rubber while the remaining material content consists of metal, textiles, zinc oxide, sulphur and additives. Sullivan [116] notes that the rubber content for passenger vehicles usually comprises of 45% natural rubber and 55% synthetic rubber. While the main function of a bumper is to absorb impact should a collision occur, bumper trim and bumper grill function as protector for the bumper if there is minor frictional contact as well as also contributing to the styling of the vehicle. According to Helps [117] modern bumpers are likely to be made of plastics due to cosmetic design freedom they offer and similarly for bumper grills. Bumper trim usually is made from PVC as are also wheel arches. Finally convertible cars often have a cover to protect the passenger compartment from the weather and provide security. Covers can be made of rigid materials (hard tops) or alternatively flexible textile or textile like materials (soft tops). In the BRE component tests mohair and PVC soft top materials were tested.

7.4.2 FTP and critical heat flux analysis

Using the time to ignition versus external heat flux results from the BRE cone calorimeter tests, Equation 7-2 is used to obtain the associated FTP, *n*, and critical heat flux values. An example of the application of Equation 7-2 is illustrated in Figure 7-3 for the mudflap component. The gradient of the fitting is the FTP while the y-intercept is the critical heat flux of the component. The figure shows the results of the fitting for three different power law index i.e. $n = 1$, $n = 1.5$ and $n = 2$. The form of the FTP analysis allows for optimising the *n*-value to minimise the R^2 value of the best fit line and thus provide an optimised fit the ignition data. However, the inherent uncertainties associated with the fundamental assumption that ignition occurs at a single material dependent temperature does not warrant such optimisation of the *n*-value beyond the discrete values of 1, 1.5, or 2. Baker et al. [101] point out that if the y-intercept gives a negative value then in the context of implementing the FTP data set the critical heat flux would equate to a value of 0 kW/m^2.

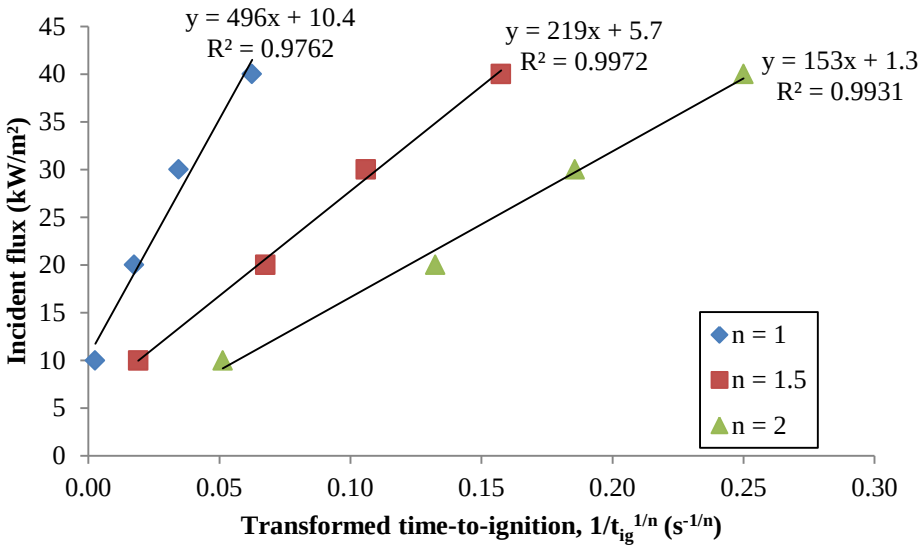

Figure 7-3: FTP analysis for mudflap component using the BRE cone calorimeter test results.

The critical heat flux of the eleven components were analysed by BRE [1] and it was found that mohair and PVC soft tops exhibited two of the lowest values which were 8.2 kW/m² and 9.8 kW/m² respectively. Due to the nature of the materials and their behaviour when exposed to a heat source, PVC and mohair soft tops do not take long in a fire for them to burn away [1]. According to the New Zealand motor vehicle registration statistics [118], the number of convertible cars registered each year is less than 0.01% which means that it is a very small chance that a vehicle on the road in New Zealand is a convertible. It is decided to eliminate both soft tops components from further analysis due to the low likelihood of a vehicle being a convertible. It is also decided to eliminate the roof box and bumper grill components from further consideration due to both components being accessories that might not feature on a standard vehicle.

The tests on the other components resulted in critical heat fluxes ranging from 10 to 19 kW/m² which appear to indicate that there is a likelihood of fire spread between vehicles if parked near to each other. From the components tested, it is found that four components; mudflap, rubber tyre, bumper trim and wheel arch have the most similar properties with what are reported in Table 7-2 and are likely to be found on most vehicles. These four components also display among the lowest critical heat flux values which increases their likelihood of being ignited first in a multiple vehicle fire scenario.

As a result of the FTP analysis Table 7-3 summarises the attributes for the components which are likely to be ignited first on a vehicle and these are used for the further evaluation of time to ignition. A corresponding two letter abbreviation for each component is used in the remainder of this chapter. Alternative method of estimating power law index can be found in Appendix E.1.

Table 7-3: Power law index, FTP and critical heat flux values for selected components.

Component and abbreviation	Power law index	FTP ($\frac{kW \cdot s^n}{m^2}$)	$\dot{q}''_{cr}$ (kW/m²)
Mudflap (MF)	1.5	3258	5.7
Rubber tyre (RT)	1.5	9828	8.0
Bumper trim (BT)	2.0	21862	3.1
Wheel arch (WA)	2.0	50234	0.0

7.5 Heat flux and ignition analysis

7.5.1 Methodology

The ability of the FTP and PSM method is examined through the prediction of ignition of second and third target vehicles from the experiments mentioned previously. The heat release rate histories from the experiments are used as the input to the FTP and PSM calculations. Using these heat release rate histories, the PSM predicts how much energy is radiated from the beginning of the experiment and then the FTP predicts when the target vehicle ignites. Radiation feedback from the enclosure is not considered in the FTP calculations as all of the experiments were conducted in rigs that were not fully enclosed. Radiation feedback from a smoke layer was unlikely in the experiments by Joyeux and by Steinert since these had a hood/duct arrangement above the burning vehicles. In the two BRE experiments there was an accumulation of smoke due to the presence of the 0.5 m deep downstand. In this work a contribution due to the radiation feedback from the smoke layer has been neglected to give results consistent with the simple approach currently used in the fire risk tool discussed in Chapter 4.

The results from the calculations are compared with the observed results from the experiments. An error of ±30 s is taken into consideration for the observed time based on a greatest possible error calculation which is equal to one-half of the precision of the measurement [119]. In this case, the order of precision of the observations is up to a single

minute. However any over-predicted times to ignition need to be treated with care because after the target vehicle has ignited the measured heat release rates will include the burning of that target vehicle which would in turn affect the PSM calculation.

7.5.2 Predictions using measured heat flux

7.5.2.1 Predicted heat flux by PSM

Since Experiments H and I included the measurement of heat flux to the third vehicle ignited these data can be used to examine how well the PSM performs. To perform the comparison between the measured and predicted heat fluxes the main challenge is to decide the position of the central point of the heat source since PSM assumes the heat source to be the middle of the burning item. In Experiments H and I there are two burning items present when the third vehicle ignites i.e. the first and second vehicle where the point heat source is likely to be moving due to a combination of the spreading fires in each vehicle and the ignition of the second vehicle. Applying the methodology previously discussed in Section 7.3.2 for the three point source positions, it is assumed that both burning vehicles can be treated as a single burning body.

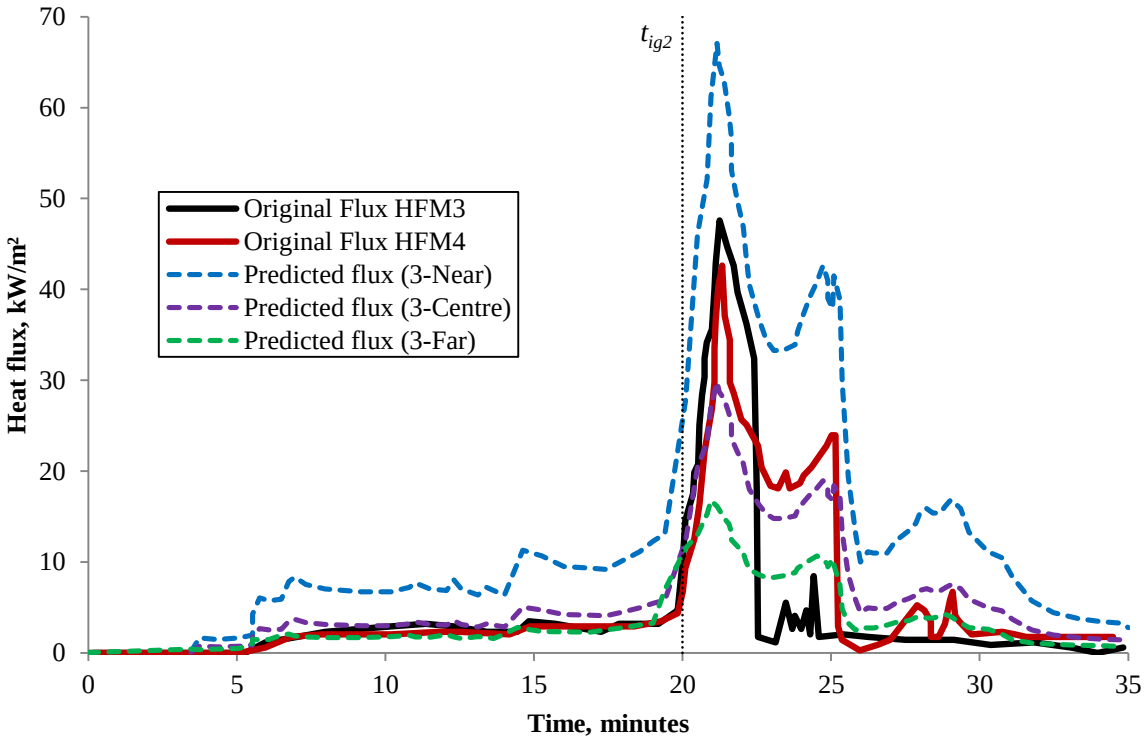

Figure 7-4: Predicted heat flux comparison with the heat flux data from Experiment H.

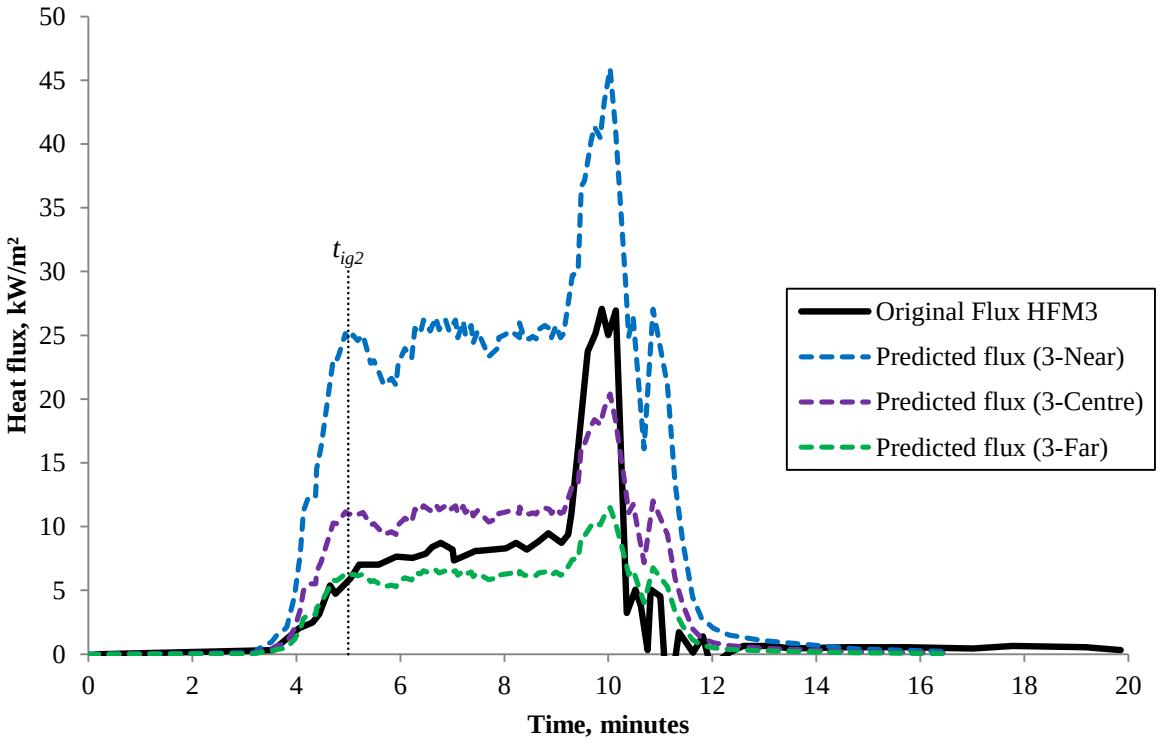

Figure 7-5: Predicted heat flux comparison with the heat flux data from Experiment I.

In Figure 7-4, the heat flux data for Experiment H from probe HFM3 and HFM4 are compared with predicted heat fluxes at the '3-Near', '3-Centre' and '3-Far' positions. It can be seen that the predictions at the '3-Centre' and '3-Far' positions closely match the results from both probes apart from not reaching the same intensity in the peak heat flux. Similar results are also obtained for Experiment I (Figure 7-5) where again the prediction of heat fluxes at the '3-Centre' and '3-Far' positions produce comparable results although not reaching the same intensity as the peak heat flux data from the experiment. In both figures, the time of ignition of the target vehicle, t_{ig2} is indicated by the dotted lines. However, in the context of this work, it is only important to compare the heat flux data and the predicted heat flux up until the ignition time of the target vehicle so the fact that the maximum intensities do not compare so well is not critical.

Overall, it can be concluded that PSM method, although not perfect, does reasonably well to predict heat flux using the heat release rate data given the limitations and assumptions that have been made. Also, the selection of the position of heat source is important as shown in Figure 7-4 and Figure 7-5 where the variation in position changes the calculated heat flux to the target by up to around 116%. While it is shown that the '3-Centre' and '3-Far' position is

an appropriate selection for the position of heat source for the three vehicle ignition scenario, it is possible that other situations may require a different selection for the heat source position.

7.5.2.2 Application of FTP

Using the measured heat flux data, the time to ignition in both experiments is predicted using the FTP method independent of the PSM. For Experiment H the recorded time of ignition for the third vehicle is unclear, the literature source only mentions that the third vehicle ignited few minutes later after the ignition of second vehicle which was reported at 20 min. Thus, it is estimated that the range of possible ignition times of third vehicle was somewhere around 22 – 25 min. For Experiment I, it was also was unclear about the ignition time for vehicle three. However it is observed from a video recorded for this experiment that the time of ignition for the third vehicle was close to 10 min. Considering there was no reported information on which component or material ignited first for the third vehicle this analysis examines all four possible components which have been recommended in Section 7.4.2.

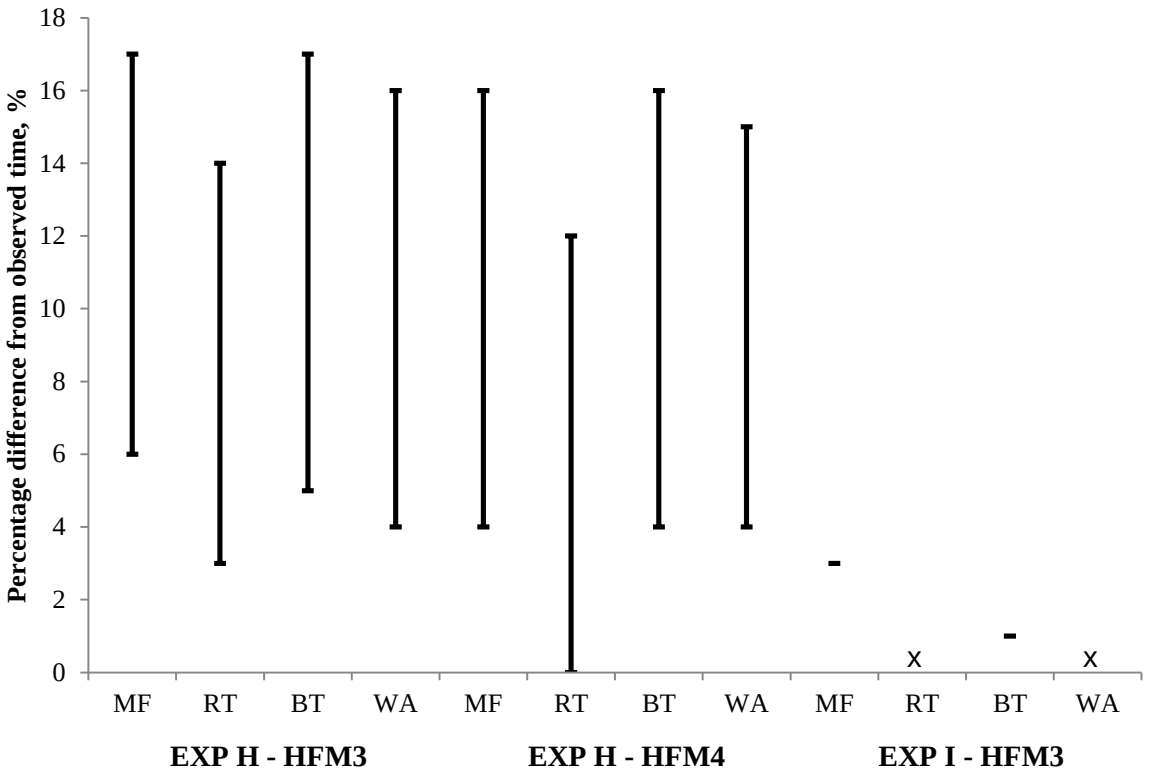

Figure 7-6: Prediction of time to ignition using heat flux data from Experiments H and I ("MF" is mudflap, "RT" is rubber tyre, "BT" is bumper trim, "WA" is wheel arch and "x" means no ignition).

Figure 7-6 shows the predicted time to ignition using heat flux data from probes HFM3 and HFM4 taken from Experiment H and a probe HFM3 from Experiment I. The results are

shown in terms of percentage difference from the time to ignition observed in the report. The error bars for both probes in Experiment H indicate the range of possible percentage difference from the observed time and the single dash indicates the percentage difference for Experiment I. The "x" symbol in Figure 7-6 means that there was no ignition of the selected component.

Results from Experiment H show that for every component examined for both probes, the predicted times to ignition were 0 - 6% faster than the lowest range of the observed ignition time at 22 min. The highest percentage difference at the top end of the range of the observed ignition time of 25 min is 17% for the bumper trim. Experiment I also shows a good prediction for the time to ignition compared to the observed values where the mudflap and bumper trim components result in a 1 – 3% faster prediction time than the observed time of 10 min. Overall, the results give an indication that FTP method is able to reasonably predict the time to ignition based on the heat flux data collected from the two experiments. Therefore, this gives confidence on using FTP method to reasonably predict the time to ignition of a vehicle given an appropriate material component is chosen.

7.5.3 Prediction of time to ignition

7.5.3.1 Second vehicle

This section presents the predictions for the time to ignition for the second vehicle for all of the experiments being considered, as shown in Table 7-2. The primary input into the analysis is the heat release rate which is then used to find the heat flux to the target from the PSM which in turn is then used by FTP to predict the time to ignition of the second vehicle. Table 7-4 shows the radial distance in terms of the three fixed heat source positions; '2-Near', '2-Centre' and '2-Far'. The ignition properties of the four components recommended in Section 7.4.2 are used to represent the target material so as to examine the sensitivity of the predictions.

Table 7-4: Radial distance from the burning item in terms of the fixed heat source positions.

Experiment ID	2-Near (m)	2-Centre (m)	2-Far (m)
A	0.40	1.22	2.03
B	0.80	1.56	2.33
C	0.80	1.56	2.33
D	0.80	1.63	2.47
E	0.80	1.56	2.33
F	0.70	1.52	2.33
G	0.70	1.58	2.48
H	0.70	1.58	2.48
I	0.70	1.60	2.50
J	0.80	1.65	2.50

Figure 7-7 shows the results for the time to ignition prediction of the second vehicle in terms of percentage difference from the observed time of ignition using the three heat source positions. A positive percentage means that the ignition time is under-predicted (i.e. faster than in the experiment) while a negative percentage means that the ignition time is over-predicted. The "x" symbol in Figure 7-7 means that there was no ignition of the selected component. For the '2-Near' heat source position the results generally show a higher average percentage difference from the observed time of ignition when compared with the other two positions. Figure 7-7(c) shows the results for '2-Far' heat source position, where two components i.e. mudflap and bumper trim component properties produce the best results where both are able to predict eight experiments out of ten with the average percentage difference of 9% and 8% respectively. Even though both of the components over-predict the time to ignition in five experiments, the results obtained using bumper trim component is within the ±30 s uncertainty range except for Experiment F and G as opposed to the mudflap which exceeds the uncertainty range in all five experiments. Using these findings it is concluded that the best position for the time to ignition prediction of a second vehicle is the '2-Far' heat source position while the component which performs reasonably well using PSM and FTP method is the bumper trim.

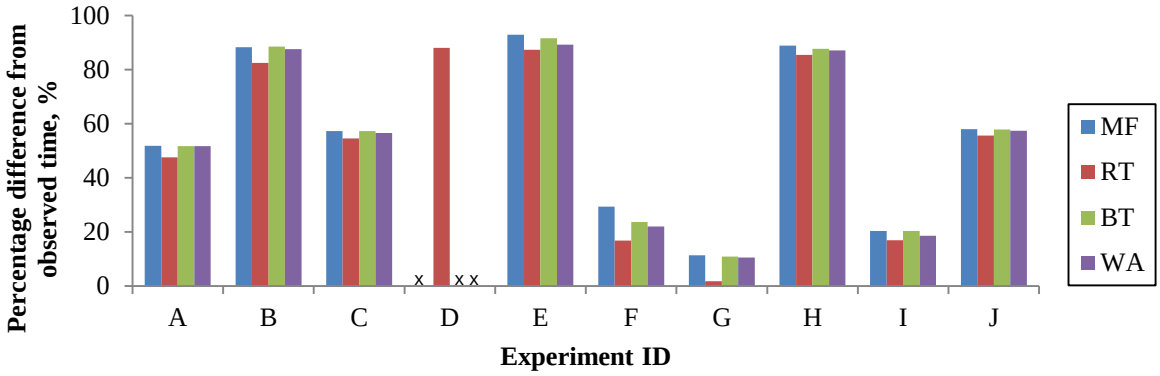

(a)

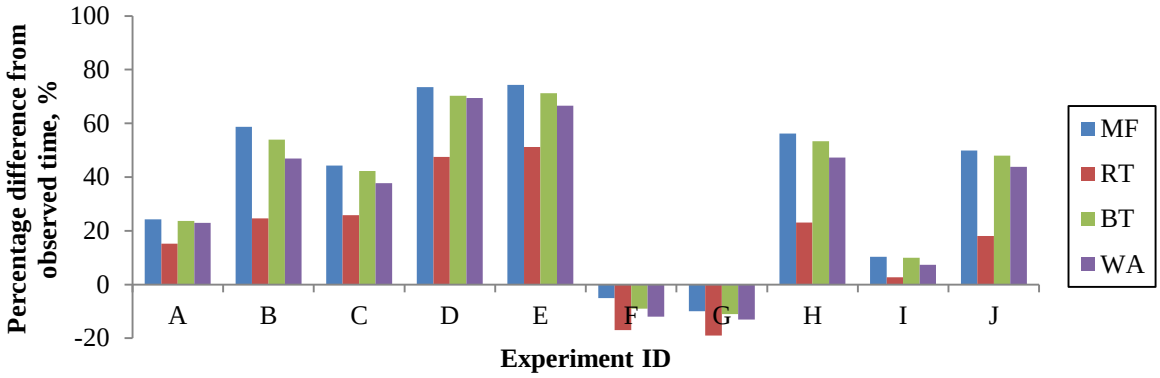

(b)

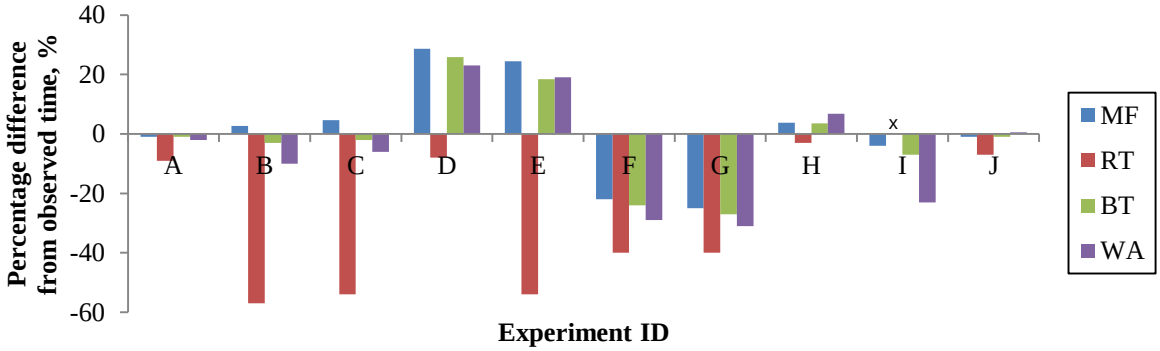

(c)

Figure 7-7: Prediction of time to ignition at (a) '2-Near'; (b) '2-Centre' and (c) '2-Far' heat source positions.

7.5.3.2 Third vehicle

Experiments H, I, and J are initially considered for the prediction of the time to ignition of the third vehicle. However, Experiment J is not included in the analysis due to the first vehicle ignited being in the middle of the group of three and there being an equal distance between the vehicles then the predicted times to ignition for the two neighbouring vehicles are the same and equivalent to that shown in Section 7.5.2.2. In the experiment the second vehicle

ignited at 30 min and the third at 32 min suggesting that it might be reasonable to consider both as 'second vehicle' targets.

Applying the similar principle explained in Section 7.5.2.1 in which assuming two vehicles as a single burning body, the time to ignition of the third vehicle in Experiments H and I is now determined using the same approach as used for the second vehicle. Table 7-5 shows the radial distance in terms of the three fixed heat source positions; '3-Near', '3-Centre' and '3-Far'.

Table 7-5: Radial distance from the burning item in terms of the fixed heat source positions.

Experiment ID	3-Near (m)	3-Centre (m)	3-Far (m)
H	2.50	3.38	4.26
I	2.50	3.40	4.30

Figure 7-8 shows the results for the time to ignition prediction of the third vehicle in terms of percentage difference from the observed time of ignition using the three heat source positions. In the figure, similar to what has been presented in Section 7.5.3.1, a positive percentage means that the ignition time is under-predicted while a negative percentage means that the ignition time is over-predicted and "x" indicates no ignition.

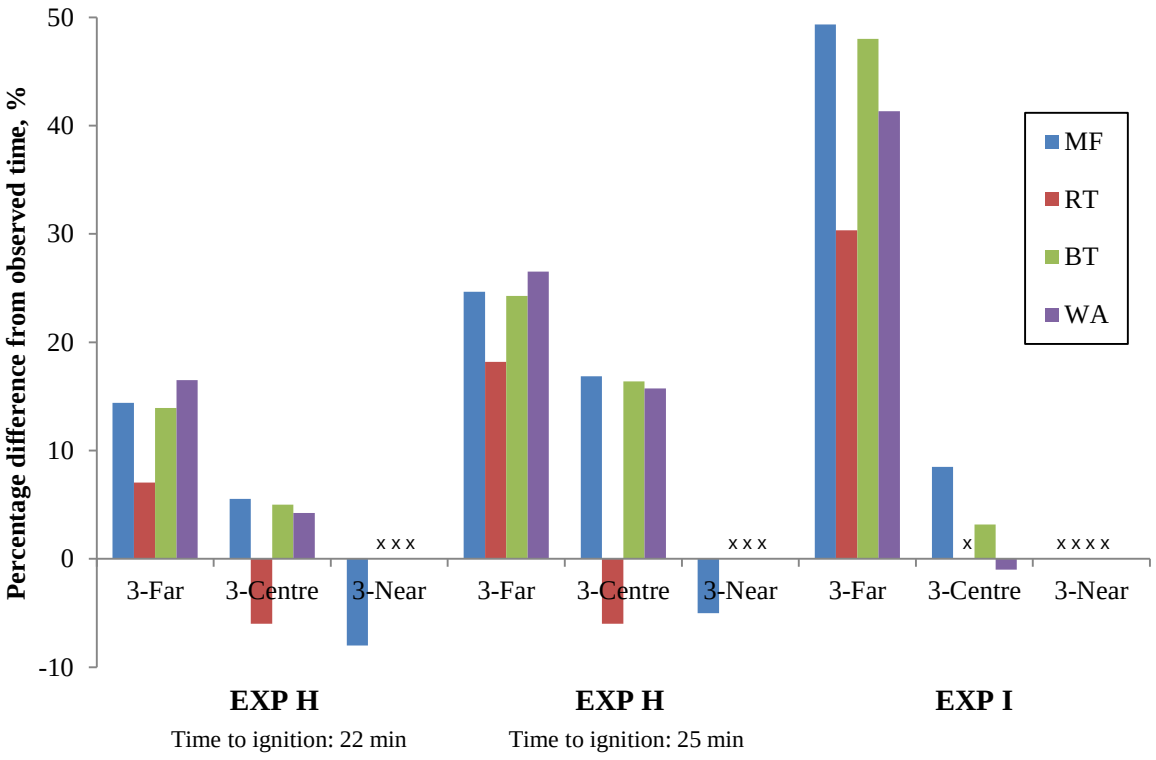

Figure 7-8: Predicted time to ignition using predicted heat flux at different positions for Experiments H and I.

For Experiment H, the predicted time at the '3-Centre' position gives the best result with average percentage difference of around 5 – 14% for all components. For Experiment I, the '3-Centre' position also gives the best result with the average percentage difference of 4% for all components except the rubber tyre which did not ignite. For both experiments, the results obtained using '3-Centre' position when compared with the results using the measured heat flux in Section 7.5.2.2 gives similar predictions for the time to ignition. These results demonstrate that despite having to predict heat flux and time to ignition with the accompanying assumptions and limitations, a combination of the PSM and FTP method is able to perform reasonably well as compared to the observed times to ignition.

7.5.4 Discussion and sensitivity analysis

7.5.4.1 Radiative fraction

A sensitivity analysis on radiative fraction is conducted to examine the difference in the predictions in the time to ignition of the second vehicle. For this purpose, Experiments A-J are taken as sample with the '2-Far' distance of the burning item and the bumper trim component. The baseline radiative fraction of 0.3 used in the previous analysis is used as comparison point. A study by Davis [120] estimated that an uncertainty for radiative fraction is of the order of ±20% hence values of 0.24 and 0.36 are used as the ±20% radiative fractions from the baseline 0.3 value.

Table 7-6: Results of sensitivity analysis on the radiative fraction.

Experiment no.	Percentage difference from observed time, %		
	λ_r = 0.24	λ_r = 0.30	λ_r = 0.36
A	-4	1	3
B	-27	3	13
C	-27	2	13
D	12	26	33
E	-27	18	40
F	-30	-24	-20
G	-33	-27	-24
H	0	4	21
I	-24	-7	1
J	-4	1	4

The results in terms of percentage difference from observed time are shown in Table 7-6. As might be expected, the results generally show that the time taken to ignite will be shorter when the radiative fraction is increased. However, no clear trends are seen since the

percentage difference range varies for each experiment. For example in Experiment A, the +20% change in radiative fraction gives an increase of 2% while in Experiment B, the same change results in a 10% increase. In the end, the selection of an appropriate radiative fraction is important since a change of ±20% could lead to a possible 45% difference in the time to ignition from the baseline radiative fraction.

7.5.4.2 Sensitivity of power index of material

The selection of *n* (the power law index) in the FTP methodology for a material is important to retain the practicality of the analysis so a sensitivity analysis of *n* = 1, 1.5, or 2 is carried out to examine the degree of differences in the predicted time to ignition. For this purpose, Experiment A was used with the heat source position at the centre of the burning item i.e. 1.22 m, the baseline radiative fraction of 0.3, and with four different components chosen for comparison. The selection of the centre heat source position is to prevent over-predictions in the time to ignition calculations for the three power law indices. The results of the sensitivity analysis are shown in Table 7-7 in terms of time to ignition and the percentage difference from the observed ignition time.

Table 7-7: Sensitivity analysis of the FTP power law index of Experiment A.

Exposed material	*n* = 1		*n* = 1.5		*n* = 2	
	Time (min)	% difference	Time (min)	% difference	Time (min)	% difference
Mudflap	15.6	22	15.2	24	14.8	26
Rubber tyre	17.2	14	17.0	15	16.8	16
Bumper trim	15.6	22	15.4	23	15.3	24
Wheel arch	15.9	21	15.2	24	15.4	23

Table 7-7 generally shows that the increment in the power law index results a reduced time to ignition apart for the change from *n* = 1.5 to *n* = 2 for the wheel arch component which produces slower time to ignition due to the *n* = 2 case using a critical heat flux value of 0 kW/m² from the FTP analysis procedure. It can also be seen that the mudflap component possesses biggest percentage difference range with a difference of up to 4% with 22% using power law index of 1.0 and 26% using power law index of 2. The percentage difference range of rubber tyre and bumper trim shows only 2% difference while wheel arch shows a 3% difference. Since, bumper trim is the recommended component it can be concluded that the selection of power law index will only give a deviation of ±2% from the observed values.

7.5.4.3 Variable distance analysis

Another assumption to examine is the use of a fixed heat source positions from the burning item to the target item. In the experiments the heat source is not fixed to a position and this is evident from the video recorded for Experiment I where the fire in the first vehicle was ignited on the driver's seat and then the fire spreads to the front passenger seat window in a matter of minutes. This phenomenon is illustrated in Figure 7-9 where the picture on the left shows the experiment at 4 s after a wood crib was ignited, the middle picture at 4 min and 3 s shows that the fire begun to come out of the roof of the first car, and the picture on the right shows at 4 min 42 s that the fire already broken out of the passenger seat window.

Figure 7-9: Timeline of fire from the video of Experiment I [1].

Thus a variable distance for the heat source position is proposed to determine whether it changes the result when compared to using an assumed fixed position. This analysis requires a much more detailed and specific timeline of the growth of the fire within the first vehicle in which this can be only be found in Experiment I with the aid of the video footage. For this analysis, heat source is first assumed to be located at driver's seat which is around 2.3 m from the target vehicle, the fire is then assumed to steadily spread at a constant rate up to the point it comes out of the passenger seat window i.e. 0.7 m away from the target vehicle at around 4 min and 30 s. The results of the predicted time to ignition using this variable distance compared to the fixed heat source at '3-Centre' is shown in Table 7-8.

Table 7-8: Variable heat source positions comparison for Experiment I.

Exposed material	Heat source: 3-Centre		Heat source: Variable	
	Time (min)	% difference	Time (min)	% difference
Mudflap	4.5	10	4.2	16
Rubber tyre	4.8	4	4.4	12
Bumper trim	4.5	10	4.2	16
Wheel arch	4.6	8	4.3	15

The results show that for this experiment, the '3-Centre' fixed heat source position actually gives a better set of results than the variable heat source position. The results for the variable position are quicker by 5 - 8% compared to the fixed distance and this was due to the target vehicle being exposed to higher radiation heat fluxes when the radial distance becomes closer over time. Given there is only one experiment available for the comparison, the results shown do not present a strong case for or against the use of a variable distance. However, at this stage, a fixed heat source position appears to be a sufficiently rational choice for the purposes of relatively simple vehicle ignition calculation.

7.6 Conclusion

The PSM and FTP methods have been applied in this chapter to the prediction of the time to ignition of vehicles using the using the heat release rate from already burning vehicles. In order to get a single set of conditions that can reasonably predict the time to ignition for a two-vehicle scenario the analysis suggests that radiative fraction of 0.3 and the '2-Far' heat source position for the burning item can be applied to the PSM for the prediction of the heat flux to the target vehicle. The analysis also suggests that a power law index, n = 2 corresponding to a thermally thick material component that is equivalent to bumper trim with a FTP value of 21862 $\frac{kW \cdot s^n}{m^2}$, and critical heat flux of 3.1 kW/m² can be selected as the first component to ignite on a vehicle. The analysis shows that the predicted percentage difference from observed time to ignition of a second vehicle in experiments using these suggested conditions is on average 8%.

It is found that the selection of radiative fraction has a greater influence on the time to ignition predictions than the choice of the FTP power law index or the application of a variable heat source position although only one experiment allowed for an analysis of the variable heat source position. The effect of radiation from the enclosure and/or a smoke layer has not been included in this work however using the B-RISK model to carry out similar ignition predictions would enable these factors to be accounted for and this is the subject of future work.

Given the complexity of the vehicle ignition problem it is remarkable that the application of the PSM and FTP methods have done as well as they have. The

results from this study will be used in subsequent research on the prediction of ignition time of vehicles in a risk-based car parking simulation tool as part of its fire spread assessment calculations.

Chapter 8 PREDICTION OF TIME OF IGNITION USING B-RISK

Contents of this chapter were given as an oral presentation at the *Society of Fire Protection Engineers' 2014 Engineering Technology Conference*, Long Beach, California.

8.1 Introduction

In the previous chapter, it was concluded that the combination of flux-time product (FTP) and point source model (PSM) to predict ignition the time of ignition of a subsequent vehicle gives a reasonable set of results when compared to results obtained from the multiple vehicle experiments given the complexity of the problem. This is subject to the selection of an appropriate target burning component/material, which it has been identified in the previous chapter. The next step is to use B-RISK zone modelling software to predict time of ignition using selected experiments.

The B-RISK zone modelling software uses the FTP as the ignition criterion and PSM for its flame radiation model, but has several other features which made it different from the hand calculation especially the effect of radiation from the enclosure. Thus, the main objective of this work is to examine the capability of the B-RISK software program regarding its ability to reproduce the time of ignition obtained from the real experiments as a comparison with the results obtained using hand calculation in Chapter 7. This work aims to answer whether the hand calculation is sufficiently robust for ignition analysis given the exclusion of various elements.

Consequently, to achieve the main objective, this work will attempt to recreate selected Building Research Establishment [1] full-scale experiments using B-RISK. Although B-RISK is capable of producing outputs such as layer temperature, smoke layer height, and gas yields, in this work the main focus of the output will be the time of ignition of the subsequent vehicle after the previous vehicle has ignited. However, as opposed to using hand calculation, B-RISK requires additional information on the test rig characteristics and dimensions, and several other input parameters such as heat of combustion, latent heat of gasification, soot yield, CO_2 yield, etc. Sensitivity analyses are performed to see the effects of changing certain parameters of combustible materials.

8.2 Background

8.2.1 B-RISK zone modelling software

The B-RISK zone modelling software is a part of a larger project that was funded by the Ministry of Science of Innovation (MSI) of New Zealand, Building Research Levy and Department of Building and Housing (DBH) of New Zealand involving Building Research

Association of New Zealand (BRANZ) and the University of Canterbury. The main goal of the project was to produce a tool to support future risk-based building fire safety regulations and designing with B-RISK as one of the outcomes.

B-RISK is developed based on an existing deterministic fire zone modelling software named, BRANZFIRE. The development of B-RISK incorporates three primary areas of enhanced functionality as compared to BRANZFIRE [31, 98]. The three primary areas are:

1. The ability to conduct probabilistic simulations rather than deterministic simulations. For this purpose, B-RISK uses Monte-Carlo sampling for certain input parameters where the users can provide probability distributions. The probabilistic sampling will select a set of values for the input calculation parameters for each calculation iteration run, hence producing a set of different output values. These sets of results will be collated and can be produced as probabilistic outputs such as cumulative density functions (CDF). [98]

2. The software is also capable of incorporating fire safety systems reliability and efficacy into the B-RISK modelling predictions. The user has the ability to quantify effectiveness of the fire safety systems in the software's calculation algorithm. [98]

3. The software is also capable of automatically generating unique designs of fire input for every loop iterations processes. The software introduces the design fire generator (DFG) submodel based on the concept of a fire compartment being populated with combustible items and a fire growing and developing as it ignites and spreads to secondary objects. The user will be able to either select items for their modelling from the existing items database or create new items into the database.

   After getting all the necessary input, the DFG can be either be randomly populated across the room or the user can enter the exact position of the items in the room. Once these item placements are done, the user can determine which item is to be ignited first. The DFG predicts the time of ignition of the second item to be ignited using ignition criterion and radiation models programmed in the software. [98]

As noted above, B-RISK has one feature which is relevant to this work, which is the capability of the software to predict the ignition of items. Therefore, at this stage the simulation results obtained from this work will only focus on the time of ignition of vehicles.

8.2.1.1 Ignition criterion and radiation model in B-RISK

The software has an option where the user is able to activate the secondary item ignition module in which the ignition of the secondary items is based on the radiation that is received by the secondary item [18].

There are two methods of the target item receiving the radiation. The first method is by point source model (PSM) which is a flame radiation model and the second method is by the radiation from the underside of the hot upper layer [18]. The former has been explained in Section 7.3.2. The latter assumes the underside of the hot upper layer to be a planar, uniform, and isothermal "surface". The surface is also assumed to emit radiation uniformly across directions and independent of wavelength. The ability to receive radiation from the underside of the hot upper layer is one feature which makes it different from the hand calculation explained in Chapter 7.

The software checks the two radiation/ignition mechanisms concurrently. The PSM is more important where secondary objects are relatively close to burning items, and the radiation is assumed to be received by the closest vertical surface of a secondary object. While for the other method, it is more important for remote items, where radiation from the underside of the hot upper layer is received by the top surface of the secondary object. The user has to define the target material ignition properties for both of the methods.

During the simulation, the software uses the flux-time product (FTP) to predict the ignition of the secondary item. For every item in the database, an FTP dataset for both piloted and auto-ignition modes are available. However, the user can define their own material with its FTP dataset which consists of an FTP value, a critical incident flux and thermal thickness of the material. The radiation used in the FTP method comes from either the PSM or hot upper layer of the underside, whichever ignites the secondary item first will be recorded as the time of ignition.

8.2.1.2 Burning rate enhancement

An additional function is available in the software that allows the option of enhancing the burning rate of the fire based on the level of incident radiant heat flux received at the floor due to heat transfer from the gas layers and the room surfaces [18]. The user has the option to either enable or disable it in the settings. This is another feature which could not be performed using hand calculation.

The additional heat release from the fuel, which is defined as ΔQ, is added to the free burning heat release rate for use in the energy balance calculations. This calculation is done for each burning item and the total summed to determine the total unconstrained rate of heat release for the fire. The additional heat release is given as such,

$$\Delta Q = \frac{\Delta H_c A \dot{q}_e^{"}}{L_g}$$

Equation 8-1

where $\dot{q}_e^{"}$ is the radiant heat from the gas layers and the room surfaces, ΔH_c is the heat of combustion, L_g is the heat of gasification of the fuel (averaged over all fuel items), and A is the estimate of the surface area.

The surface area can be calculated in two ways. The first way, if the heat release rate per unit area (HRRPUA in kW/m²) parameter for the item/object is non-zero then the equation is,

$$A = \frac{\dot{Q}_f}{HRRPUA}$$

Equation 8-2

where $\dot{Q}_f$ is the heat release rate of the free burning fuel item. The other way of calculating the surface area is when the HRRPUA parameter for the item/object is zero then the equation is,

$$A = \frac{\dot{Q}_f}{\Delta H_c \dot{m}^{"}}$$

Equation 8-3

A characteristic burning rate per unit area is represented by $\dot{m}''$ and this can optionally be defined for an individual item as a linear function of the incident heat flux in the form,

$$\dot{m}'' = B\dot{q}_e'' + C$$

Equation 8-4

where B (in g/kJ) and C (in g/s/m²) are constants defined as item properties.

8.2.2 Full-scale multiple vehicle fire experiment

Two full-scale multiple vehicle fire experiments identified as suitable for the purpose of simulation using B-RISK. Experiment H and Experiment I i.e., the identification number introduced in previous chapter or 'Test 1' and 'Test 3' respectively from the original report which is by BRE [1]. The experiments were considered suitable due to the completeness of information as an input to perform simulation using B-RISK.

The experiments were conducted in a test rig that has a floor area of 72 m² with a height of 2.9 m from the floor. The structure of the rig comprised of a steel frame with breeze block infill and the roof was made of hollow-core concrete slabs. One end of the rig was open, but with a down stand of 0.5 m. Windows which allow ventilation were provided along one side and the back wall. At one end of the roof, a 1.6 m wide window channels the smoke via a deflector into the 9 m high calorimeter hood.

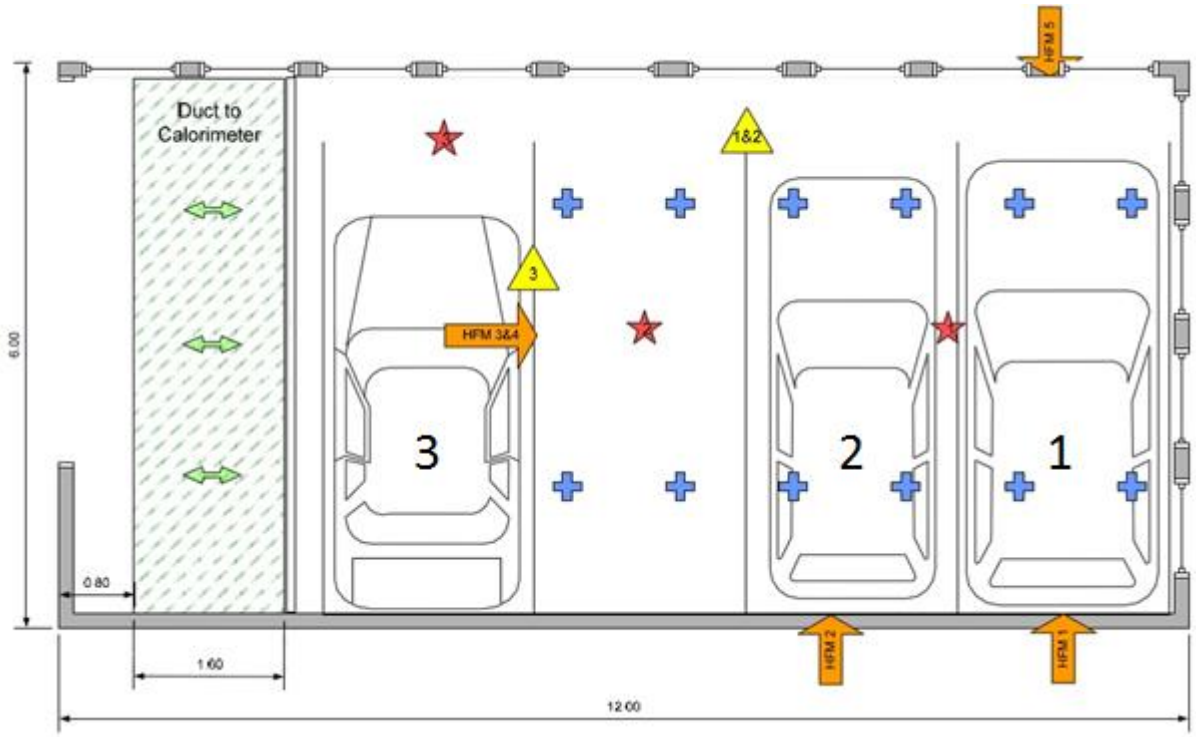

Figure 8-1: The diagram and instrument schematic for Experiment I (Reproduced from BRE [1])

An example of the diagram and the instrument schematic of Experiment I is shown in Figure 8-1. From the diagram, there were several instruments installed in the test rig for the purpose of results collection. The orange arrows in the diagram were the heat flux measurement gauges, the blue crosses were the slab temperature gauges, the yellow triangles were the gas samples collectors, the red stars were the thermocouple trees, and the green arrows refer to flow measurement and temperature gauges.

The specific vehicles used in the experiments were also mentioned in the literature source whereas this piece of information is important for the simulation as input in recreating the experiment in the software. The vehicles for both experiments were:

Table 8-1: Vehicle details for Experiment H

No.	Make	Model	Year of manufacture	Variant
1	Renault	Laguna	2002	V6 24v Privilege
2	Renault	Clio	1998	RXE
3	Ford	Mondeo	2003	LX TDCI

Table 8-2: Vehicle details for Experiment I

No.	Make	Model	Year of manufacture	Variant
1	Renault	Espace	1998	RT Auto
2	Peugeot	307	2004	SW Hdi
3	Land Rover	Freelander	2002	1.8i

'No.' indicated in both tables corresponds with the the number shown in Figure 8-1. The vehicles used in the experiments were in full working order where all components such as gas struts, air bags, pressurised or pyrotechnic components were left in place except for the air condition gas which was removed. The fuel tanks for each of the vehicles were left with 20 litres of fuel.

8.3 Procedure

This section provides information in order to recreate of the experiments using the B-RISK software. The inputs, simplifications and assumptions in using the software are explained in detail.

8.3.1 Input – ROOM DESIGN AND VENTILATION

In B-RISK, the user has to manually enter the information of the room and its ventilation in the room design tab. The test rig for the experiment is represented by a single room with certain dimensions. Also required by the software for the room is the surface material for wall, floor and ceiling. The inputs are:

Table 8-3: Input for room design and ventilation

Attribute	Description
Room name	Test rig
Length	12 m
Width	6 m
Minimum height	2.9 m
Maximum height	2.9 m
Elevation	0 m

Table 8-4: Room surface materials

Attribute	Description
Wall material	Concrete
Wall thickness	100 mm
Ceiling material	Concrete
Ceiling thickness	100 mm
Floor material	Concrete
Floor thickness	50 mm

For the ventilation in the test rig, there are 13 windows, a main door and a ceiling vent on the test rig served as ventilation ports which are shown in Figure 8-2 and Figure 8-3. This information was entered as the inputs where:

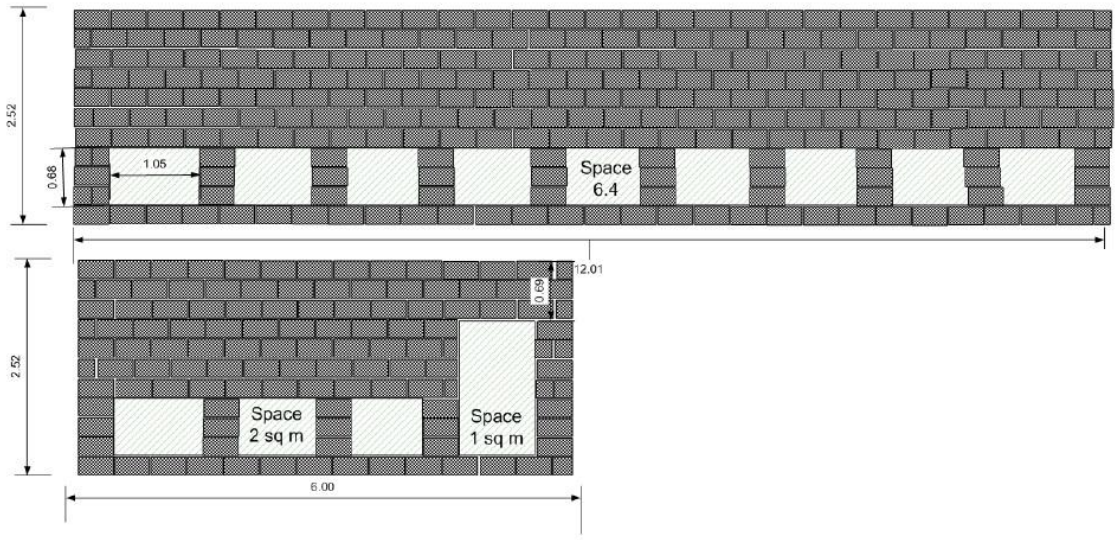

Figure 8-2: Windows in the test rig (Reproduced from BRE[1])

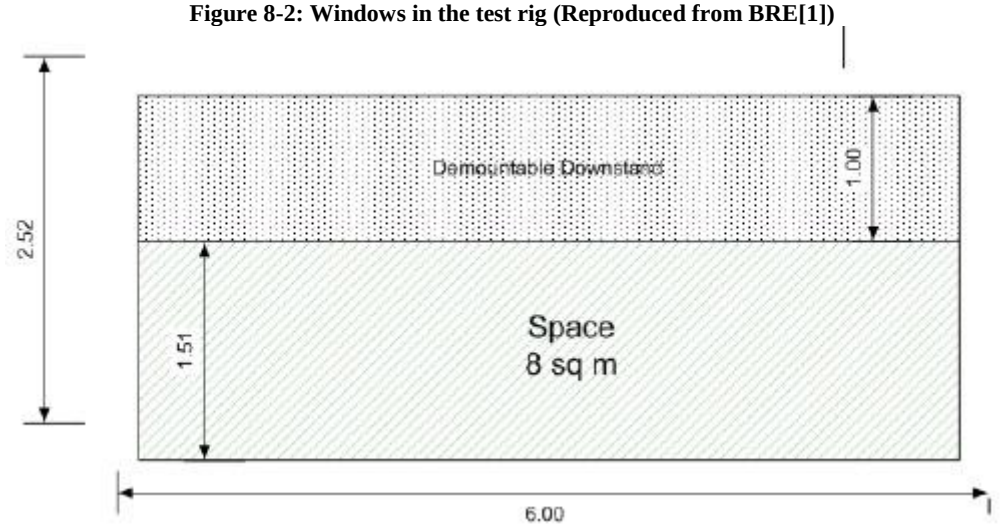

Figure 8-3: The main door of the test rig (Reproduced from BRE[1])

Table 8-5: Wall vents

Attribute	Description
Vent 1 – 9	Side vents
Vent 1 – 9: Width	1.05 m
Vent 1 – 9: Height	0.65 m
Vent 10 – 12	Rear vents
Vent 10 – 12: Width	1.05 m
Vent 10 – 12: Height	0.65 m
Vent 13	Rear vent
Vent 13: Width	1.05 m
Vent 13: Height	1.47 m
Door 1	Front vent
Door 1: Width	4.2 m
Door 1: Height	2.5 m

Table 8-6: Ceiling vent

Attribute	Description
Ceiling 1: Area	9.6 m²

8.3.2 Input – PROPERTIES FOR THE BURNING ITEMS

In the fire specification tab, the user is able to enter the details about the experiments. This includes the number of items in the room, the dimensions of the items, the position of the items, the material geometry and chemical properties, the FTP properties and the heat release rate curves.

In the simulation, the vehicles, which are the main burning items, were considered a simple geometrical rectangle shape in which the heat source is fixed at the centre of the rectangle. The vehicles are treated as a single type of material, which represented the first component possibly to be exposed to the radiant heat flux. The dimensions and the position of the vehicles were obtained from the report [1]. However, the chemical properties of the vehicles have to be assumed due to being unreported in the literature. The best way to assume the chemical properties such as heat of combustion and latent heat of gasification is by estimation since there are no specific studies on mentioned properties of a vehicle.

A review by Taub [121] shows that in the 2000s, a typical vehicle usually consists of around ~70% metals and ~30% polymers, glass, rubbers, and ceramics. A study by Swift [50] shows that combustible materials in vehicles such as polymers take around 8.0% - 9.7% as the percent of the total weight of a vehicle from the 2000s while rubber ranges from 4.3% - 6.2% of the total weight of a vehicle. Large parts of the polymers are polypropylene, polyurethanes, and nylon.

The work by Harper compiles heat of combustions for selected polymers and states that the heat of combustions of polymers ranges from 6.4 MJ/kg to 44.0 MJ/kg. Polypropylene is listed at 42.6 or 44.0 MJ/kg, polyurethane at 24.7 MJ/kg, and nylon at 27.9 MJ/kg. Thus, for the simulation a minimum value of 24.7 and maximum value of 44.0 will be selected for the heat of combustion of a vehicle.

Mark [122] listed the latent heats of gasification of polymers where the latent heat of gasification for polypropylene is 2.0 MJ/kg and for nylon is 2.4 MJ/kg. There was no latent

heat of gasification for polyurethane was found. Thus, for the simulation a range of values between 2.0 and 2.4 is estimated since there were only two available data on latent heat of gasification.

Finally, the averaged heat release rate per unit area (HRRPUA) for each of the vehicles are estimated using the probability distributions of design fire for different classifications introduced in Table 6-4. The HRRPUA could not be obtained from the full-scale experiment heat release rate curves results due to complication of the curves which were a combination of three vehicles rather than one. This are further explained in Section 8.3.3.

For the soot yield and the CO_2 yield, default values for a generic vehicle pre-programmed in the fire object database of the software are used. It was decided to use the generic values for the two parameters since at this stage, the focus on the results are on the prediction of time of ignition. The radiative fraction for all the vehicles are set at 0.3 following assumptions made in previous chapter. With the dimensions known and the chemical properties have to be assumed for each vehicle in the simulation, the burning items properties for both experiments can be filled with attributes as follows:

Table 8-7: Information for the 3 vehicles for Experiment H

Attribute	**Vehicle 1**	**Vehicle 2**	**Vehicle 3**
Detail description	Renault Laguna	Renault Clio	Ford Mondeo
Length	1.8 m	1.6 m	1.8 m
Width	4.6 m	3.8 m	4.8 m
Height	1.4 m	1.4 m	1.5 m
Elevation	0 m	0 m	0 m
x-axis coordination	9.5 m	7.2 m	3.5 m
y-axis coordination	0.5 m	0.5 m	0.5 m
Combustible mass	1455 kg	975 kg	1357 kg
Heat of combustion	24.7 or 44 kJ/g	24.7 or 44 kJ/g	24.7 or 44 kJ/g
Soot yield	0.03 g/g	0.03 g/g	0.03 g/g
CO_2 yield	1.27 g/g	1.27 g/g	1.27 g/g
Latent heat of gasification	2.0 or 2.4 kJ/g	2.0 or 2.4 kJ/g	2.0 or 2.4 kJ/g
Radiative fraction	0.3	0.3	0.3
HRRPUA	248 kW/m²	137 kW/m²	168 kW/m²

Table 8-8: Information for the 3 vehicles for Experiment I

Attribute	Vehicle 1	Vehicle 2	Vehicle 3
Detail description	Renault Espace	Peugeot 307	Land Rover Freelander
Length	1.8 m	1.7 m	1.9 m
Width	4.4 m	4.4 m	4.5 m
Height	1.7 m	1.6 m	1.7 m
Elevation	0 m	0 m	0 m
x-axis coordination	9.5 m	7.1 m	3.5 m
y-axis coordination	0.5 m	0.5 m	0.5 m
Combustible mass	1660 kg	1070 kg	1425 kg
Heat of combustion	24.7 or 44 kJ/g	24.7 or 44 kJ/g	24.7 or 44 kJ/g
Soot yield	0.03 g/g	0.03 g/g	0.03 g/g
CO_2 yield	1.27 g/g	1.27 g/g	1.27 g/g
Latent heat of gasification	2.0 or 2.4 kJ/g	2.0 or 2.4 kJ/g	2.0 or 2.4 kJ/g
Radiative fraction	0.3	0.3	0.3
HRRPUA	258 kW/m²	157 kW/m²	248 kW/m²

In previous chapter, it was suggested that bumper trim to be used as the component to be ignited first in a multiple vehicle fires simulation. The FTP properties of bumper trim are given as:

Table 8-9: FTP properties for bumper trim

Component	Power law index	FTP ($\frac{kW \cdot s^n}{m^2}$)	$\dot{q}''_{cr}$ (kW/m²)
Bumper trim	2.0	21862	3.1

8.3.3 Input – HEAT RELEASE RATE

In B-RISK, the user can choose the heat release rate from a generic item from the fire object database, or they can manually provide own heat release rate. The heat release rates from the experiments are used to predict the time of ignition of the secondary vehicle, thus manually entered in the fire specification section. The heat release rate curves from Experiment H and I exhibit the collective heat release rates for the whole three vehicles' fire. Therefore, for both experiments, only heat release rates for the first vehicle up until the second vehicle ignites are possible to be identified in isolation.

In both experiments, the heat release rates for the first vehicle are assumed to be the curve from the beginning of the experiment up until the observed time the secondary vehicle ignited. This is because that from the beginning of the experiment up until second vehicle ignites, during that time it was only one vehicle that was on fire and the recorded results should show the heat release rate for only a single vehicle. After the ignition of the second vehicle, it is assumed that the heat release rate is a combination of the first vehicle and the

second vehicle. Finally, after the ignition of the third vehicle, it is assumed that the heat release rate is a combination of first, second and third vehicle.

However, it has to be considered that there will be uncertainty in the observed time of ignition due to human observational error. Thus, following the same assumption in previous chapter, an error of ±30 s is taken into consideration for the observed time based on greatest possible error (GPE) calculation which is equal to one-half of the precision of the measure [119].

The input for the heat release rates of the vehicles in Experiment H are shown in Figure 8-4 where the blue line represents the heat release rate of Vehicle 1 up until the observed time of ignition of second vehicle at 20 minutes, the red line is the combined heat release rates for Vehicle 1 and 2 up until observed time of ignition of the third vehicle at 22 - 25 minutes, and the green line represents the combined heat release rates for Vehicle 1, 2 and 3. The green line with black dash indicate the possible range of time of ignition which is from 22 – 25 minutes. Since the time of ignition of the second and third vehicle were uncertain, ±30 s time of ignition were added and indicated as error bars in Figure 8-4.

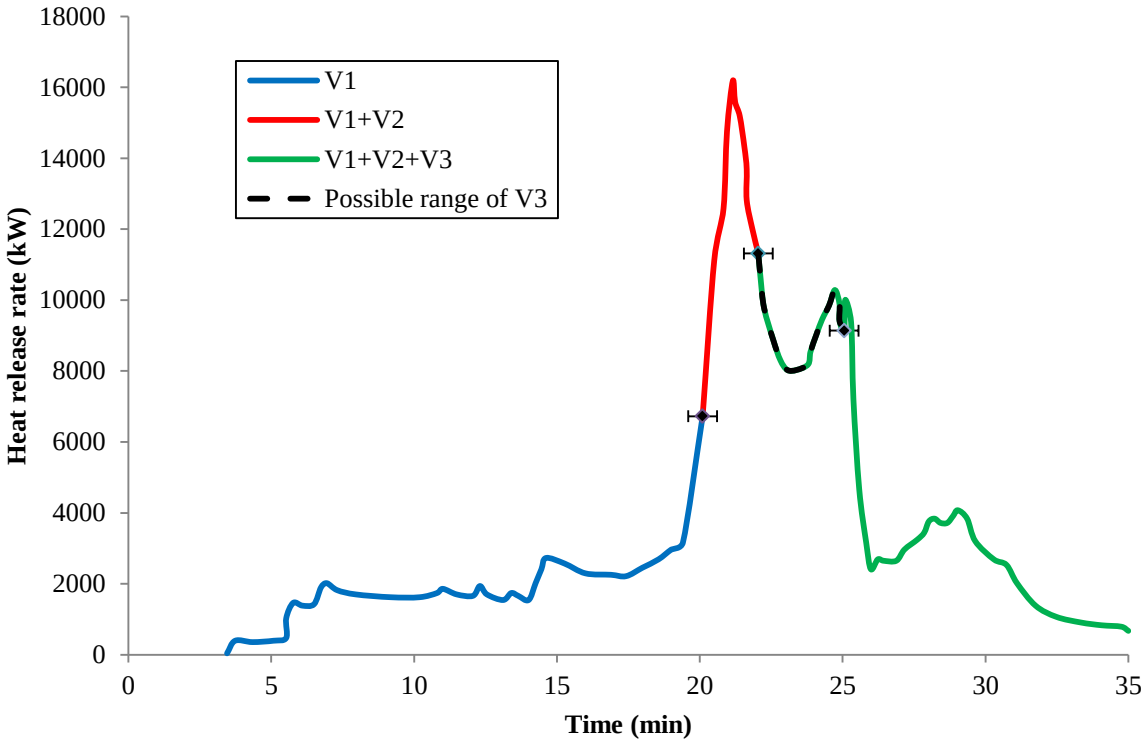

Figure 8-4: Heat release rate for Experiment H B-RISK input.

The input for the heat release rates of the vehicles in Experiment I are shown in Figure 8-5 where the blue line represents the heat release rate of Vehicle 1 up until the observed time of ignition of second vehicle at 5 minutes, the red line is the combined heat release rates for Vehicle 1 and 2 up until observed time of ignition of the third vehicle at 10 minutes, and the green line represents the combined heat release rates for Vehicle 1, 2 and 3. Since the time of ignition of the second and third vehicle were uncertain, ±30 s time of ignition were added and indicated as error bars in Figure 8-5.

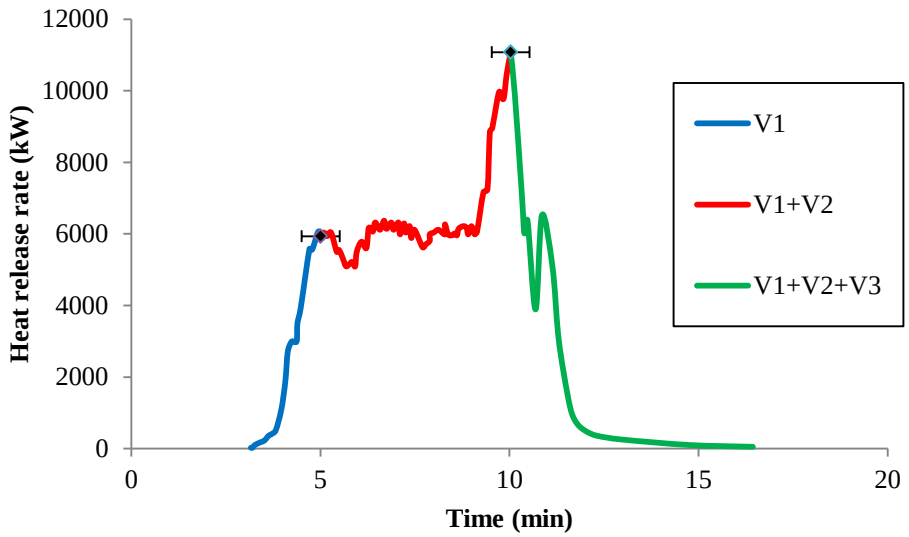

Figure 8-5: Heat release rate for Experiment I B-RISK input.

8.3.4 Input – OTHER INPUTS FOR THE SIMULATION

Other inputs which are needed for the simulation run are mainly in B-RISK CONSOLE where the information about how many iterations, how long is duration of the simulation, output intervals, and other options are asked to the user. The suggested inputs are:

Table 8-10: Other inputs for the simulation in B-RISK

Attribute	Description
Max. no of iteration	1
Maximum simulation time (second)	1000
MC Output interval (second)	30
EXCEL Output interval (second)	10
Display/Print interval (second)	10
Ignite secondary items	Check
Terminate iterations at flashover	Uncheck
Sent vent data in log file	Uncheck
Burning rate enhancement	On

8.4 Results and analysis

This section presents the results obtained from the simulation of the experiments using B-RISK software with the inputs mentioned in previous section. The results from the simulations were compared with the full-scale experiments results as well as with the ones obtained using hand calculation using the PSM and FTP methods in Chapter 7.

8.4.1 Experiment H and Experiment I

8.4.1.1 Variation of heat of combustion and latent heat of gasification input

Table 8-11 and Table 8-12 shows the results of the simulation of Experiment H and Experiment I where four different simulations with a variation of combination of heat of combustion and latent heat of gasification. The brackets in the table imply what the minimum and maximum values of the possible range for heat of combustion and latent heat of gasification explained in Section 8.3.2.

From the results, it was shown from both of the simulations that increasing the heat of combustion (using both latent heat of gasification minimum and maximum range value) shortens the time it took to ignite the second and third vehicles. Though for most cases the time of ignition did not change by much, the prediction of time ignition could lead to a possible 23% change by varying the heat of combustion.

Also from the results, it was demonstrated from the simulation for both experiments that the increase of latent heat of gasification by 0.2 did not change the time of ignition. This signifies that the selection of latent heat of gasification from the available range does not give any changes.

Table 8-11: Simulation results of Experiment H

Simulation	1	2	3	4
Heat of combustion, ΔH_c (kJ/g)	24.7 (MIN)	44.0 (MAX)	24.7 (MIN)	44.0 (MAX)
Latent heat of gasification, L_g (kJ/g)	2.0 (MIN)	2.0 (MIN)	2.4 (MIN)	2.4 (MIN)
Time of ignition for second vehicle (min)	6.8	5.8	6.8	5.8
Time of ignition for third vehicle (min)	16.7	15.0	16.7	15.0

Table 8-12: Simulation results of Experiment I

Simulation	1	2	3	4
Heat of combustion, ΔH_c (kJ/g)	24.7 (MIN)	44.0 (MAX)	24.7 (MIN)	44.0 (MAX)
Latent heat of gasification, L_g (kJ/g)	2.0 (MIN)	2.0 (MIN)	2.4 (MIN)	2.4 (MIN)
Time of ignition for second vehicle (min)	5.0	4.5	5.0	4.5
Time of ignition for third vehicle (min)	8.6	6.8	8.6	6.8

8.4.1.2 Comparison of B-RISK and hand calculation results

Figure 8-6 and Figure 8-7 shows the comparison for the time of ignition between the observed time of ignition, the predicted time of ignition from B-RISK simulation, and predicted time of ignition performed using hand calculation for Experiment H and I respectively. In the figures, the bar with black diagonal pattern indicates the observed time of ignition from the experiment. In Figure 8-6, the error bar for the third vehicle observed time of ignition indicates the possible range of ignition times.

For the predicted time of ignition from B-RISK simulation, the ranges of possible time of ignition using the variation of heat combustion and latent heat of gasification in Table 8-11 and Table 8-12 were used, therefore the range is shown in the error bars in the figures. It has to be noted that in B-RISK, the heat source position is assumes to be at the centre of the burning object, hence, the result for heat source position '2-Centre' from the hand calculation is used for comparison. This is decided as to being consistent with the radial distance used in both methods, even though it was suggested that '2-Far' gave the best results for the hand calculation. For the third vehicle prediction, the result from '3-Centre' heat source position.

In Figure 8-6, it can be seen that comparing the time of ignition predicted by using B-RISK for both second and third vehicle ignition are 0.9 and 4.2 min faster respectively than using hand calculation. The slight difference of results from the simulation and hand calculation could be due to the radiation effects from the underside of hot upper layer and burning rate enhancement feature in the simulation which provides additional heat flux to the targeted item. The analysis also shows that the predicted time using B-RISK gives bigger difference to the observed time as compared to the results from hand calculation. Figure 8-7 shows some consistency with the prediction of the results where the prediction of results using hand

calculation is within the range predicted by using B-RISK. The third vehicle prediction again shows that the ranges of results calculated by B-RISK are faster than both observed time and the hand calculation time.

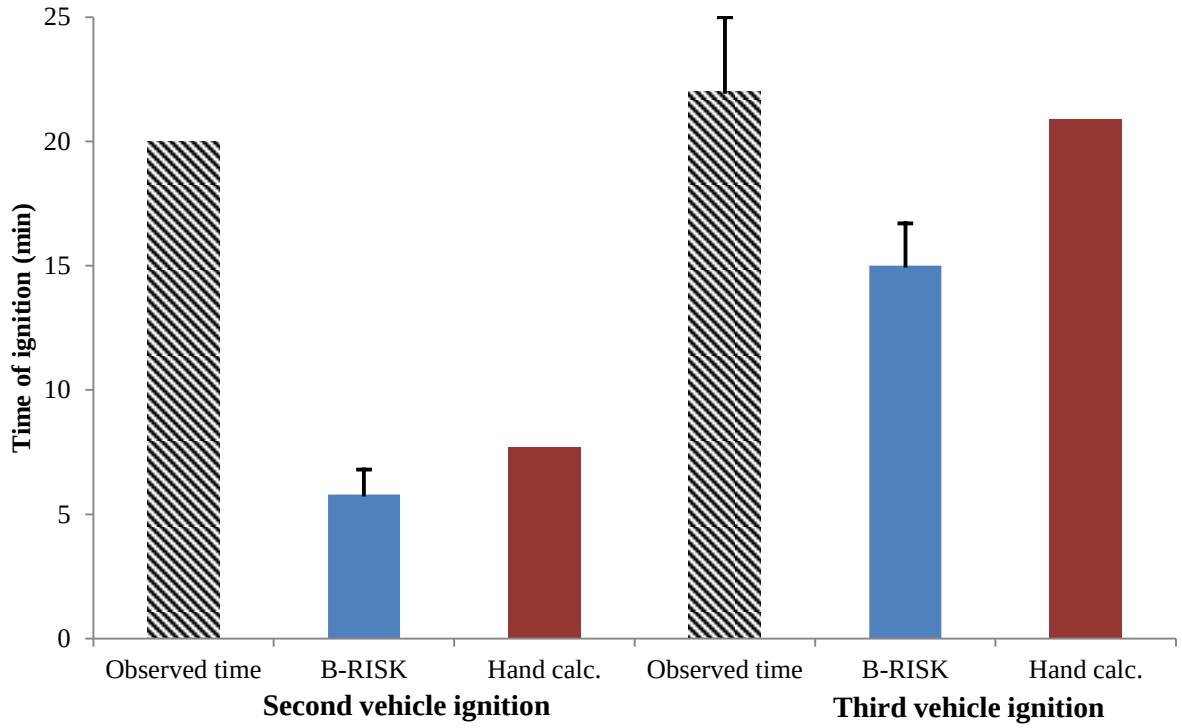

Figure 8-6: Comparison of time of ignition for Experiment H

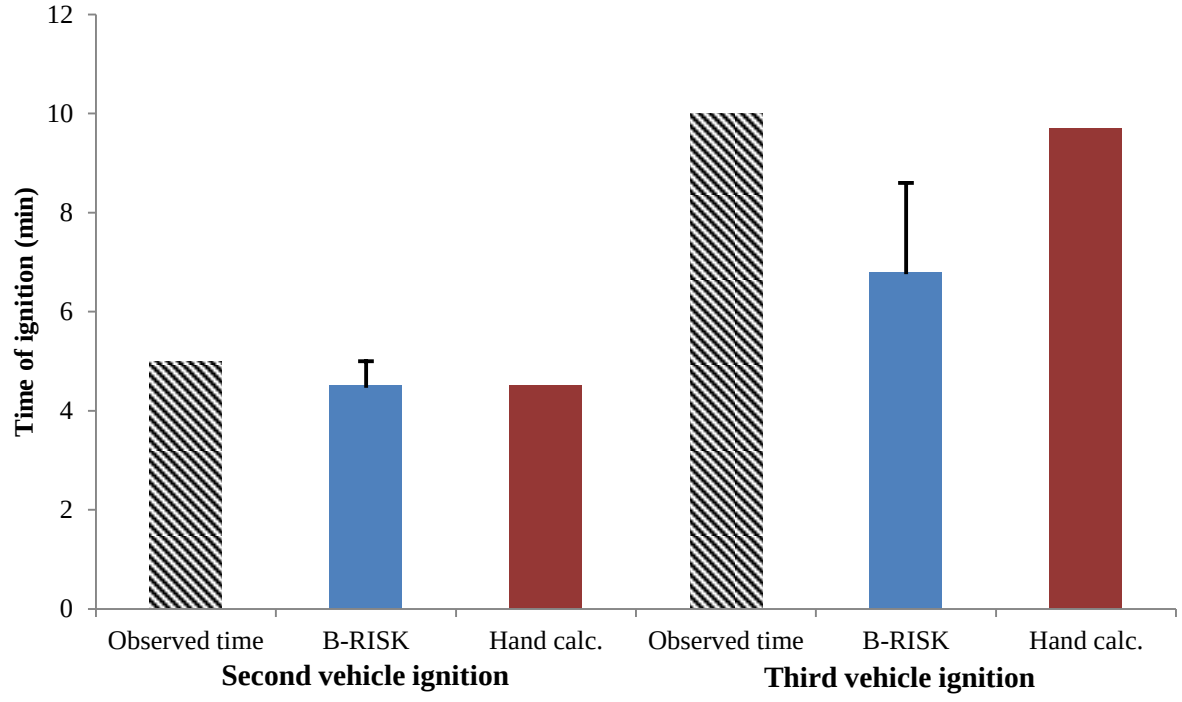

Figure 8-7: Comparison of time of ignition for Experiment I

The analysis shows that the predicted time of ignition using B-RISK in both experiments gives quicker time of ignition for the second and the third vehicle. This could be due to B-RISK includes the radiation effect from the underside of the hot upper layer. This shows that hand calculation gives better match for the comparison on the observed time for these two experiments.

8.4.2 Sensitivity analysis

Three sensitivity analyses have been carried out to assess the effects of changing parameters in the software.

8.4.2.1 Burning rate enhancement

As a sensitivity analysis, simulations for both experiments with the burning rate enhancement function being disabled were conducted. For the comparison with the predicted results with burning rate enhancement function turned on, heat of combustion at 44.0 kJ/g and latent heat of gasification of 2 kJ/g were selected. Table 8-13 shows the results of sensitivity analysis on burning rate enhancement function. It can be seen that in both simulations, disabling the burning rate enhancement function could delayed the time of ignition from 4.9% and up to 15%.

Although disabling the burning rate enhancement function could delay the time of ignition up to 15%, it has to be reminded that the heat of combustion and latent heat of gasification have to be known or at least made a justified assumption for the function to be working. In the case of the heat of combustion and latent heat of gasification are unknown and impossible to be assumed, then it would be better to disable the function.

Table 8-13: Results of sensitivity analysis on burning rate enhancement function.

Experiment	Experiment H		Experiment I	
Burning rate enhancement	ON	OFF	ON	OFF
Time of ignition for second vehicle (min)	5.8	6.1	4.5	5.3
Time of ignition for third vehicle (min)	15.0	15.6	6.8	7.5

8.4.2.2 Distance change between vehicles

The distances between the first and second vehicle for both experiments taken from the literature were 0.7 m. In this sensitivity analysis, the consequences of varying the distances by ±0.1 m were assessed. This value was selected using the greatest possible error (GPE) method. Therefore for this purpose, the distance was increased by 0.1 m as well as being decreased by 0.1 m to be 0.8 m and 0.6 m respectively. In this sensitivity analysis, other input parameters were fixed.

Table 8-14 and Table 8-15 show the predicted time of ignition results from the simulations with different distances between the first and second vehicles and the percentage difference from the initial distance of 0.7 m. It is evident from both simulations that an increase of 0.1 m in the distance delays the time of ignition of the second vehicle to at least 4.2% and possibly up to 6.6%. Likewise, the decrease of 0.1 m in the distance speeds up the time ignition to at least 4.4% and possibly up to 5.1%. This sensitivity analysis concludes that it is important to have the exact position of the vehicles (if known) as an input for the simulation since a slight change on the distance will possibly affect the end results.

Table 8-14: Varied distance sensitivity analysis for Experiment H

Distance between first and second vehicle	d = 0.6 m	d = 0.7 m	d = 0.8 m
Time of ignition of second vehicle (min)	5.5	5.8	6.3
Percentage difference from 0.7 m	-5.1%	-	+6.6%

Table 8-15: Varied distance sensitivity analysis for Experiment I

Distance between first and second vehicle	d = 0.6 m	d = 0.7 m	d = 0.8 m
Time of ignition of second vehicle (min)	4.3	4.5	4.7
Percentage difference from 0.7 m	-4.4%	-	+4.2%

8.4.2.3 Variation of radiative fraction

Another sensitivity analysis conducted was on the variation of the radiative fraction as an input parameter for B-RISK. In this analysis, the consequences of varying the radiative fraction from the initial value of 0.3 by ±20% based on a study by Davis [120] was conducted. Therefore, for this analysis, the radiative fraction used in the simulation were 0.24, 0.30 and 0.36. For the simulations in this sensitivity analysis, other input parameters were fixed.

Table 8-16 and Table 8-17 show the time of ignition of the second vehicle and the percentage difference from the initial radiative fraction of 0.3 for both experiment simulations. For both simulations, the decrease of 20% of the radiative fraction delayed the time of ignition by 7.9% for Experiment H and 10% for Experiment I. While increasing 20% of the radiative fraction sped up the time of ignition by 10.3% for Experiment H and 8.9% for Experiment I. In the end, the selection of sensible radiative fraction is important since a change of ±20% could lead to a possible 10.3% difference in the time of ignition.

Table 8-16: Varied radiative fraction sensitivity analysis for Experiment H

Radiative fraction	**λ_r = 0.24**	**λ_r = 0.30**	**λ_r = 0.36**
Time of ignition of second vehicle (min)	6.3	5.8	5.2
Percentage difference from λ_r = 0.30	-7.9%	-	+10.3%

Table 8-17: Varied Radiative fraction sensitivity analysis for Experiment I

Radiative fraction	**λ_r = 0.24**	**λ_r = 0.30**	**λ_r = 0.36**
Time of ignition of second vehicle (min)	5.0	4.5	4.1
Percentage difference from λ_r = 0.30	-10%	-	+8.9%

8.5 Conclusion

The main objective of this work is to examine the capabilities of B-RISK software in regards to whether it will be able to reproduce the time of ignition in the real experiments. The analysis in Section 8.4.1 shows that the predicted results from the B-RISK simulations give slightly faster time of ignition to the ones obtained using hand calculation. This could be due to B-RISK includes the radiation effect from the underside of the hot upper layer. As a conclusion, the analysis shows that using the B-RISK simulation software with additional radiation effects does not improve the result as compared to using the hand calculation considering the level of uncertainties which required to be assumed on some input parameters e.g. HRRPUA, heat of combustion, and/or latent heat of gasification. Another aspect that currently lacks on B-RISK is the ability to have probabilistic design fire as input hinders the usage of the software at this stage as the following chapters are focusing on probabilistic analysis on multiple vehicle fires. Therefore, to keep the consistent level with the simple approach used in the fire risk tool in Chapter 4, it is suggested that the application using hand calculation to predict time of ignition of subsequent vehicle is adequate at this stage.

From the sensitivity analyses, it was found that enabling the burning rate enhancement will speed up the time of ignition of the subsequent vehicle. However, assumptions and justifications have to be made for the heat of combustion and latent heat of gasification in order to enable the function. Also from the sensitivity analysis, it was found that it is better to have the exact position of the vehicles (if known) as an input for the simulation since a slight change i.e. 0.1 m on the distance will possibly affect the end results by up to 6.6%. Finally, from another sensitivity analysis, it was found that the selection of sensible radiative fraction is important since a change of ±20% could lead to a possible 10.3% difference in the time of ignition. It can be concluded that the analyses are able to give an indication that in a risk based research, wide range of inputs will possibly resulting in large range of answers.

Chapter 9 FIRE LOAD ENERGY DENSITIES FOR RISK-BASED DESIGN

Accepted for publication as Spearpoint, M, Tohir, M.Z.M., Abu, A.K., and Xie, P. “Fire load energy densities for risk-based design of car parking buildings” in *Case Studies in Fire Safety*. [123]

Abstract

The time-equivalence method is one way to determine the appropriate fire severity in buildings. One of the input parameters required is the fire load energy density (FLED) and in a deterministic design this is taken to be a fixed value. This chapter illustrates the use of a simple Monte Carlo tool that accounts for statistical variations in car energy content as a function of vehicle size to determine probabilistic FLED values for a risk-based calculation approach to the design of car parking buildings. The chapter briefly discusses FLED values for car parking buildings that can be found in the literature and results from the Monte Carlo tool suggest that 260 MJ/m² could be used as an appropriate design value in lieu of using a probabilistic approach.

9.1 Introduction

9.1.1 Background

Currently there is debate in New Zealand regarding the design of steel structure car parks and the use of the time-equivalence calculations to determine appropriate severity for these buildings. Equations for calculating time-equivalence can be found in the New Zealand verification method C/VM2 [11]. These are based on equations from the Eurocode [124], but with an expanded set of factors to allow for adequate consideration of the contributions of different room lining materials [125].

In order to calculate fire severity using a time-equivalence method one of the parameters needed is the fire load energy density (FLED) which is the sum of all the energy available for release when the combustible materials are burned, divided by the total floor area of the compartment. The available energy content can be distinguished into permanent, variable, protected and unprotected loads [126]. Typically an 80^{th} percentile variable fire load is used as a design value when using data from fire load surveys [126, 127]. For a car parking building the variable load is essentially the vehicles and the calculation of FLED incorporates any floor areas used for vehicle lanes and ramps, pedestrian walkways etc.

Typically time-equivalence calculations are carried out deterministically with fixed values assigned for FLED, compartment geometry, ventilation conditions, lining materials and the structural material being used for the design. The process considers that the compartment is uniformly heated throughout the fire exposure and for a car park fire scenario this effectively assumes the building is densely populated with vehicles and that they are on fire simultaneously. However in a densely populated car park it is possible that the fire will travel from vehicle to vehicle rather than assuming all are burning simultaneously. Recent work on travelling fires by Stern-Gottfried et al. [128] has introduced a new methodology using travelling fires to produce more realistic fire scenarios in large, open-plan compartments for structural fire design. Stern-Gottfried et al. examined the impact of FLED on their estimation of the peak structural member temperature. Their results show that local concentrations of dense fuel loads produce long-duration fires and have a significant effect on structural resistance. Alternatively in a sparsely populated car park fires could be localised, may involve only a small number of cars and, depending on the location of the fire, they could be detrimental to the structure. Thus advanced calculation methods for the design of car parking

buildings investigate localised fires of different sizes at different locations in the building and their resulting building structural response [129].

In order to provide adequate fire resistance there needs to be a realistic assessment of the response of the structure as a whole as deformations in one part of the building need to be resisted by other parts. As discussed by Moss et al. [130] a statistical approach to fire behaviour could be used in fire safety and structural engineering applications instead of using a deterministic methodology. As part of a statistical approach to find appropriate fire resistance ratings for car parking buildings the structural fire severity assessment needs to incorporate the variable fire load. This requires an investigation on how the FLED can vary depending on the energy content of cars, the occupancy of car parks, the area of parking spaces etc. and this chapter illustrates an approach to this subject.

9.1.2 Static efficiency of car parks

As well as the space for each vehicle, a car parking area will also include lanes, ramps, pedestrian walkways etc. Every parking layout has its own advantages and disadvantages depending on the functional design of the parking building. The spaces within a parking layout can be angled with 90°, 60°, 45° or 30° being typical. Large capacity parking areas give a better efficiency than smaller capacity areas since there has to be proportionally less room for ramps and accessways.

Chrest et al. [131] has a set of recommended values for designing a parking area. The recommendation considers the classification of the vehicles and the level of service (LOS). LOS is method developed by traffic engineers to classify the degree of congestion of traffic where the higher the degree of congestion, the lower the LOS. The highest LOS is Category A, which is considered as free flow and no delay, while the lowest LOS is Category F which is popularly called ‘gridlock’. From the set of recommendations, the static efficiency of a parking area could be as low as 16 m²/space for a LOS D category while it could be as high as 40 m²/space for a LOS A category. Chrest et al. note that efficiencies as low as 16 m²/space are car park designs for 100% ‘small’ cars.

Hill [132] suggests that a ‘good’ parking efficiency ranges from 20 m^2/space for 300 parking spaces at 90° up to 35 m^2/space for 30 spaces at 45° while Butcher et al. [20] cited parking areas per vehicle in the range of 18.5 m^2 to 26.8 m^2. A survey of open top floors of 41 New

Zealand multi-storey car parking buildings using Google Earth found typical static efficiencies are 28.9 ± 5.1 m^2/space. Assuming the top floor is representative, then a lower 80th percentile design value for calculating FLED of 25 m^2/space appears to be reasonable for New Zealand car parking buildings. If anything it is possible that there could be slightly more spaces on an open top floor than lower floors since there are no columns etc. to take up some of the footprint and so the static efficiency might be slightly higher on lower floors.

9.1.3 Available FLED values

Research as far back as the late 1960s by Butcher et al. [20] found that the wood equivalent fire load density for a car park could be taken to be 17 kg/m^2 using an area per vehicle of 18.5 m^2. Using a heat of combustion for wood as 17-20 MJ/kg [126] gives a FLED of 290 to 340 MJ/m^2. Alternatively Gewain [21] suggested that the wood equivalent fire load density for a car park would generally be below 9.75 kg/m^2, equivalent to 166 to 195 MJ/m^2.

A survey of fire loads cited by Thomas [126] suggests an average variable fire load density ($\overline{F}$) of 190 MJ/m^2 with a standard deviation of 105 MJ/m^2 for 'Garaging, maintenance and exploitation of vehicles'. The survey gave 80%, 90% and 95% fractile values of 270, 340 and 420 MJ/m^2 respectively for this category. Thomas [126] also quotes Swiss data which gives an average FLED of 200 MJ/m^2 for 'Parking buildings'. Thomas suggests that 80%-fracticle and 90%-fractile values for well-defined occupancies can be found from (1.45 – 1.75) × $\overline{F}$ and (1.65 – 2.0) × $\overline{F}$ respectively, giving 250-300 MJ/m^2 and 270-330 MJ/m^2. A more recent study on the design of a car parking building as part of the rebuild of L'Aquila, Italy [129] used a FLED value of 268 MJ/m^2.

Clearly there are a range of suggested values for the FLED of a car park that start around 166 MJ/m^2 and reach an upper value of 420 MJ/m^2. Many of the results are based on data that is now several decades old and it might be argued does not account for any changes in the energy content of modern vehicles and the layout of modern car parks.

In terms of design guidance Eurocode 1 [124] contains a table of recommended FLED values but not for car parking occupancies. C/VM2 on the other hand gives a value of 400 MJ/m^2 for regular car parking buildings and a value of 400 MJ/m^2 per tier of car storage for car stacking systems. The C/VM2 FLED value of 400 MJ/m^2 is comparable to the work by Collier [30]

which suggested that a FLED of 400 MJ/m^2 was reasonable. Collier's value was obtained by using an upper value of 12,000 MJ for the energy content of a car from the range of values cited by Schleich et al. [23] and using a typical parking space area of 29 m^2/space as used by Li & Spearpoint [133] to give 414 MJ/m^2, comparable to the CIB 95% fractile value. Prior to the introduction of C/VM2 the earlier New Zealand compliance document for fire design (C/AS1 [127]) specified that the FLED for car parks are considered to be in the range 0 - 500 MJ/m^2 and consequently had a design value of 0.8 × 500 = 400 MJ/m^2.

9.2 Analysis

9.2.1 Monte Carlo modelling

Work in Chapter 4 has investigated a probabilistic approach to examine how spaces in a car park might be populated. A relatively simple model has been developed that allows a specified number of parking spaces configured into a continuous double row be populated by a specified number of vehicles. The model allows for the possibility that vehicles might be preferentially parked at one end of the row. The model also allows the probability of each vehicle to correspond to a set of statistics such as size and energy content. By using the Monte Carlo capabilities of the model it is possible to generate distributions of FLED based on the input distributions.

9.2.2 Total energy content

Chapter 3 completed a comprehensive survey of full-scale car fire experiments. This work uses the curb weight classification system given by ANSI [47] to categorise the vehicles and obtain values for the total energy released (Table 9-1). The ANSI classification system separately considers vans / MPVs and SUVs. However in this work these vehicles are integrated into the corresponding Passenger car classes by using the specified vehicle weight.

Where sufficient data was available a Weibull distribution with parameters as shown in Table 9-1 have been assigned to the total energy content values to each classification. However, since the work in Chapter 3 only found a single applicable dataset for Passenger car: Heavy, the distribution parameters for this classification are extrapolated from the distribution parameters for the lighter weight classes. The extrapolation uses the increasing trend in the mean of the total energy released as the curb weight class increases.

Table 9-1: Mean and standard deviation fire severity characteristics by curb weight classification, adapted from Chapter 3

Vehicle classification	Curb weight	Total energy released (MJ)				Distribution parameters	
		Mean	Standard deviation	Max value	Min value	κ	θ
Passenger car: Mini	1500 – 1999 lbs (680 – 906 kg)	2909	945	4090	1500	4.02	3222
Passenger car: Light	2000 – 2499 lbs (907 – 1134 kg)	4471	1677	8000	3000	2.93	5009
Passenger car: Compact	2500 – 2999 lbs (1135 – 1360 kg)	5288	692	6670	4860	7.49	5591
Passenger car: Medium	3000 – 3499 lbs (1361 – 1587 kg)	6386	695	7000	5960	14.53	6648
Passenger car: Heavy	≥ 3500 lbs (≥ 1588 kg)	7648	N/A	N/A	N/A	16.27*	7830*

n/a – insufficient data; *assumed values from the extrapolation of lighter weight classes.

The previous work by Schleich et al. [23] proposed values for the total energy release for five different European car classifications and these were incorporated into the work by Joyeux et al. [14]. Other work by Shintani et al. [48] gives a trend line based on their experiments. Work in Chapter 3 showed a close agreement with Shintani et al. whereas this is not the case with Schleich et al. (Figure 9-1). It is clear that heavier vehicles have a greater total energy content than lighter vehicles.

Anderson & Bell [97] note that specific models of cars have increased in curb weight with one example of a 26% increase in weight between the equivalent 1985 and 2012 models. Work in Chapter 3 also investigated whether the energy content of vehicles has increased in newer vehicles however the analysis was inconclusive based on the available experimental data.

9.2.3 Vehicle fleet characteristics

Given that the total energy content can be related to vehicle curb weight it is then appropriate to investigate the proportion of curb weights within a vehicle fleet. Using data from the European Union and USA (Section 4.2.2/ Appendix B.1) obtained a distribution of vehicle population curb weights shown in Figure 9-2 in which form hereon is indicated by Tohir & Spearpoint.

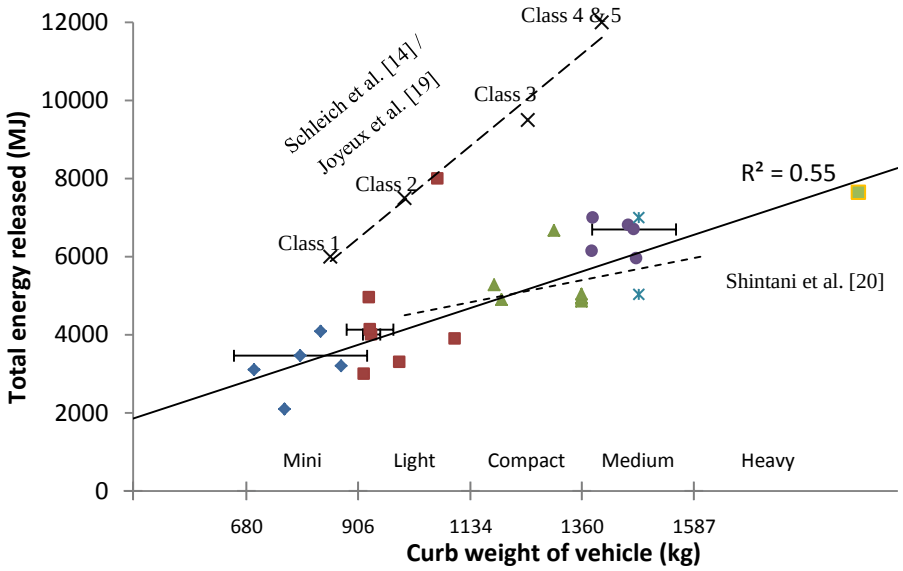

Figure 9-1: The total energy released against curb weight of vehicles and associated classifications. (Solid symbols correspond to ANSI vehicle curb weight classifications; ✳ symbol for ANSI MPV classification; and × symbol for Joyeux's European car classification, 1 – 5, adapted from Chapter 3).

In addition a survey of almost 5000 vehicles in New Zealand by Anderson & Bell [97] is also shown in Figure 9-2. Similar to the total energy content analysis, vans / MPVs and SUVs are included in the appropriate vehicle classification by using their known weight rather than by identifying them as separate categories.

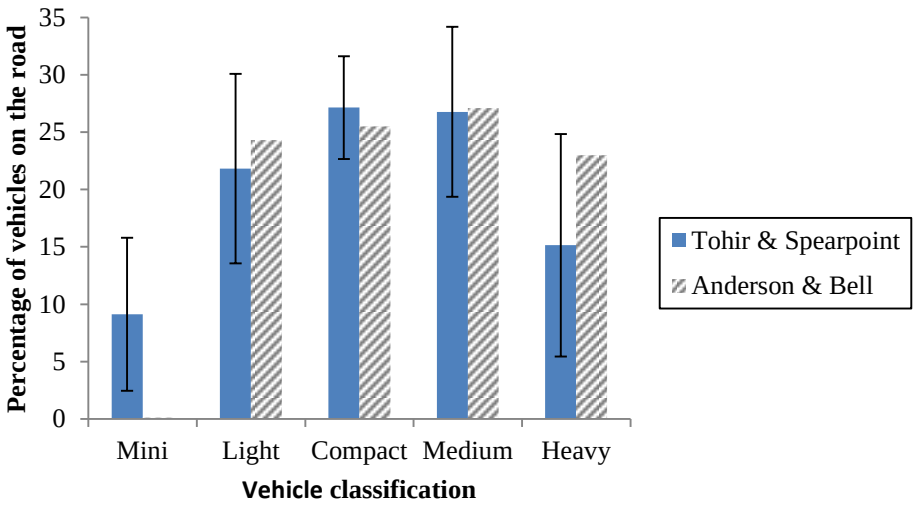

Figure 9-2: Distribution of vehicle population curb weights, standard deviation indicated for Tohir & Spearpoint values.

As well as assessing the distribution of curb weights, it is useful to examine likely occupancy proportion of a car parking building. Anderson & Bell [97] carried out a survey of parking space occupancy in a New Zealand shopping mall covered car park over a two week period including weekdays and weekends. They found that the highest occupancy level was around 99% during the middle of the day and then values reduced during the morning and afternoon (Figure 9-3). Their results found that on average the parking building was 90% occupied during the peak period although their study did not distinguish between weekdays and weekends which may have shown different trends.

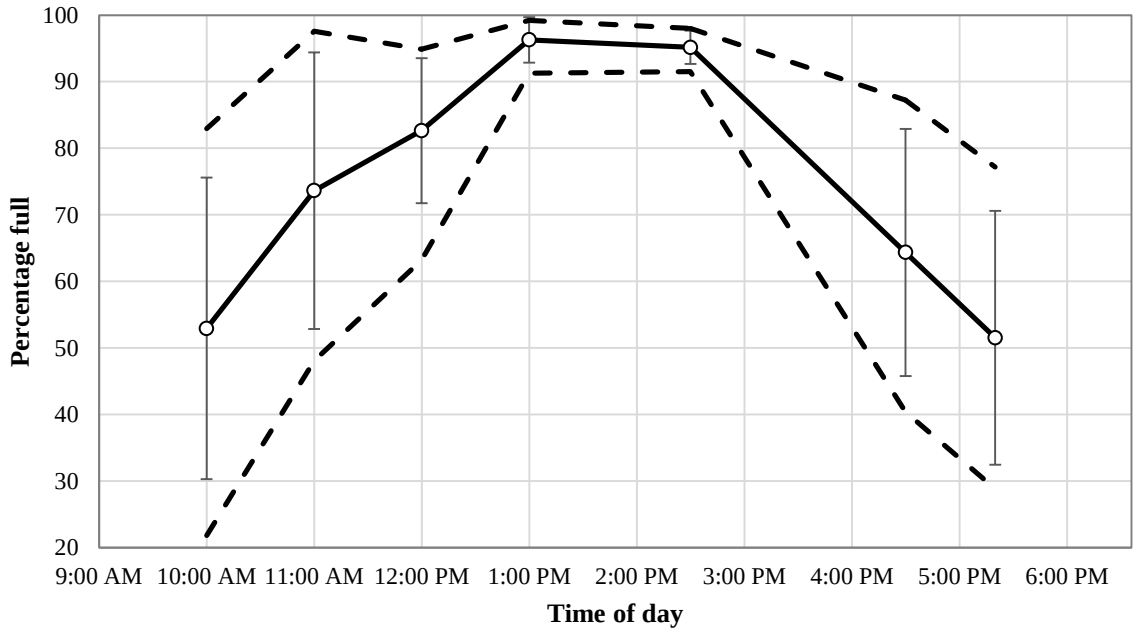

Figure 9-3: Occupancy of car parking spaces, adapted from Anderson & Bell [97]. (Mean values with standard deviation shown; maximum and minimum recorded values shown by dashed lines)

A separate analysis of a 24 hr car parking building in San Francisco that services nearby shops and offices (Chapter 4) found a maximum occupancy value of 75% at around midday on a weekday, 55% at around 3 PM on the weekend and again the occupancy reduced other times. The results from the two surveys suggest that the expectation that a car park would be 100% full throughout its daily operation is unlikely and this variable could be included in a probabilistic analysis particularly if the time of day at which ignition occurs was being assessed. However from a general design perspective assuming a car park is 100% full is likely to be reasonable and for example this was the approach taken by Nigro et al. [129].

9.2.4 Probabilistic analysis of FLED

By assuming that all parking spaces are full, that each space contains a vehicle with the highest expected total energy content, where in Table 9-1 this value is 8000 MJ, and using the LOS range A to D then FLED values from 200 to 500 MJ/m^2 are obtained. This range of FLED values brackets the 400 MJ/m^2 given by Collier and C/VM2 even though the total energy content used here is less than 12000 MJ used in Collier's previous work and also covers many of the values previously identified in the literature.

However from a risk-based perspective it is unlikely that every available parking space would be populated by a car that would give the highest expected energy content. Therefore in this study distributions of FLED values are generated by using the measured energy content distribution of cars for each curb weight classification paired with vehicle curb weight population data, and specified values for the occupancy and number of parking spaces. For each analysis, using the Tohir & Spearpoint data for the distribution of vehicle population curb weights, 1000 iterations are applied for the distribution sample size and the results are shown in Figure 9-4. An analysis using different static efficiencies is carried out to examine the resultant change in FLED values using the maximum limits for the static efficiency quoted by Chrest et al. [131]. From the analysis, at 16 m^2/space the FLED is 392 MJ/m² with a standard deviation of ±13.0 MJ/m². As the static efficiency is increased then the FLED decreases approximately linearly, as expected, so that at 29 m^2/space the FLED is 216 MJ/m^2 similar to Thomas [126] and at 40 m^2/space the FLED is 157 MJ/m^2 with standard deviations of ±6.8 MJ/m² and ±5.0 MJ/m² respectively. Thus the median FLED ($\tilde{F}$) can be estimated for a given static efficiency (SE) as $\tilde{F} = -9.9 \times SE + 536$ (MJ/m^2).

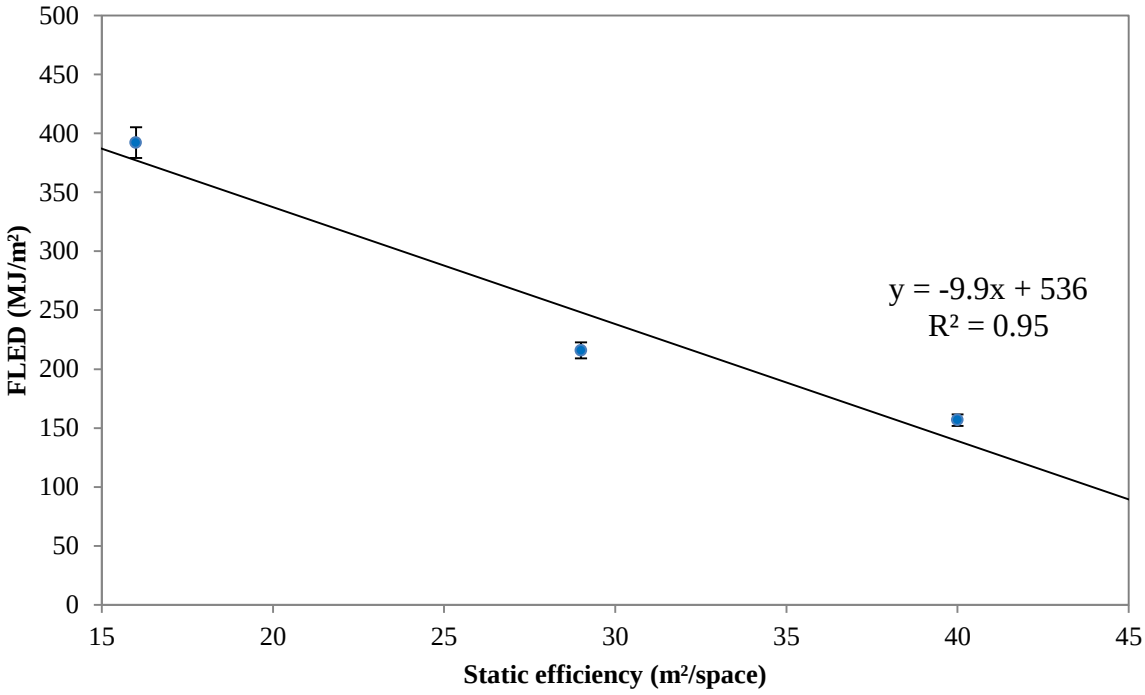

Figure 9-4: Probabilistic model variation of FLED with static efficiency.

It is useful to investigate how the FLED varies with the distribution of vehicle population curb weights obtained by Anderson & Bell [97] using the suggested static efficiency for New Zealand parking buildings of 25 m^2/space. Figure 9-5 shows that the median FLED increases from 251 MJ/m^2 with the Tohir & Spearpoint data to 252 MJ/m^2 when the Anderson & Bell data is applied. At a 100% occupancy for the Anderson & Bell data, the 80%, 90% and 95% fractile FLED values are 258, 261 and 263 MJ/m^2 respectively.

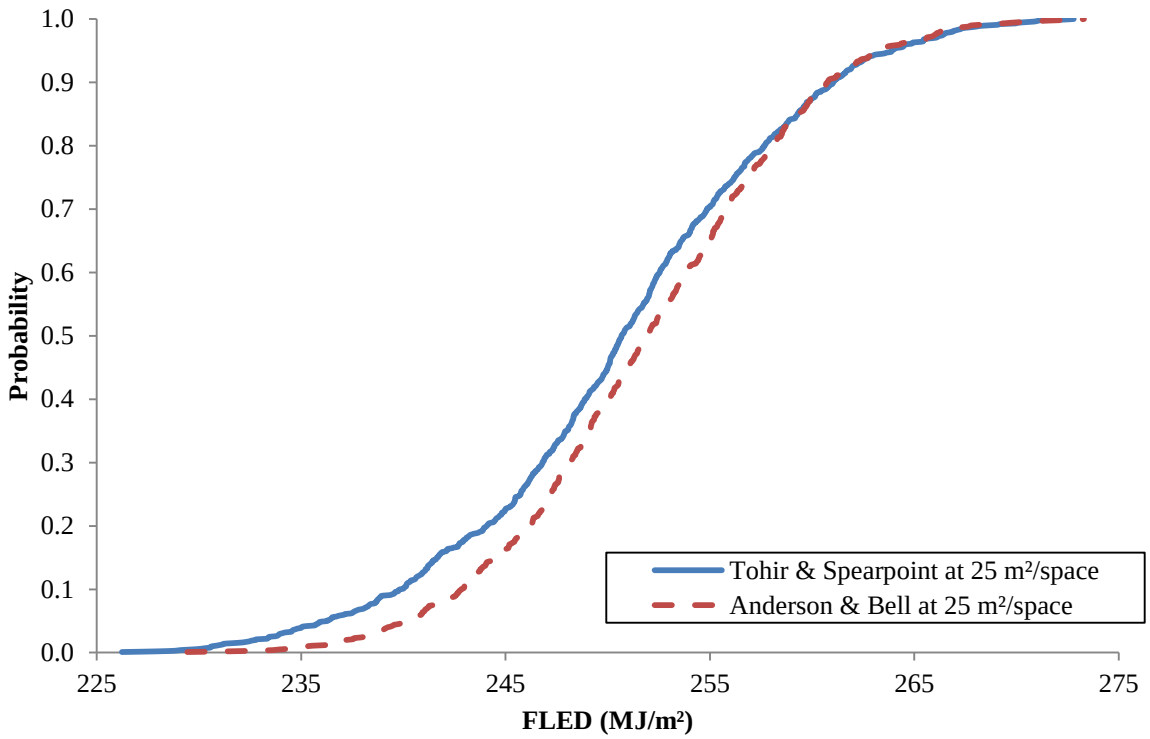

Figure 9-5: FLED cumulative probability density curves for the Tohir & Spearpoint and Anderson & Bell (2014) vehicle curb weight distributions.

The fractile bands that result from the probabilistic model are less than those given by Thomas [126] even though the median values are similar. As such this study suggests that the ratio of the median FLED to the 80%, 90% and 95% fractile values are 1.024, 1.036 and 1.047 respectively. Thus to determine a specified percentile FLED (F_p) for a given static efficiency (p) then $F_p = f \times \tilde{F}$ (MJ/m^2) where f is the appropriate fractile value given above.

Finally Figure 9-6 shows the effect of reducing the parking occupancy from 100% to 90% for the Anderson & Bell distribution of vehicle population curb weights at 25 m²/space static efficiency. As expected the median value proportionally reduces from 252 MJ/m^2 at 100% occupancy down to 227 MJ/m^2 at 90% occupancy. Similarly at a 90% occupancy the 80%, 90% and 95% fractile FLED values are 233, 236 and 238 MJ/m^2.

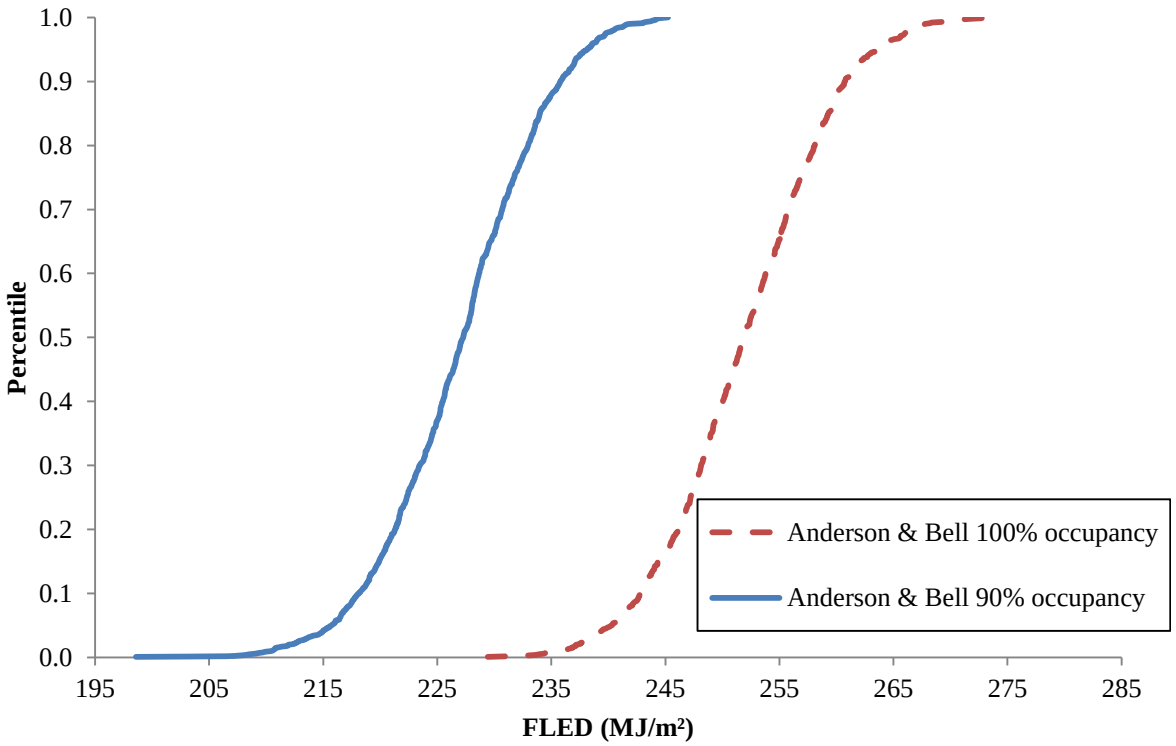

Figure 9-6: FLED cumulative probability density curves for 100% and 90% occupancy and the Anderson & Bell (2014) vehicle curb weight distributions.

9.3 Conclusions

The chapter demonstrates how a probabilistic approach to obtaining FLED values can be applied by bringing together a number of recent studies related to car parking buildings. The application of the Monte Carlo model allows for a future reassessment of FLED values for car parking buildings should there be new energy content measurements for cars or changes in the composition of a vehicle fleet. The approach could also be modified to account for the occupancy of car parking spaces as a function of the time of day.

Since the change in FLED from the Monte Carlo tool is directly related to the static efficiency then deciding what is an appropriate value becomes important. However the linear relationship from the probabilistic model means results can be easily applied to any static efficiency that is deemed suitable. In addition the ratio of the median FLED to the 80%, 90% and 95% fractile values allows fractile values to be estimated for a given static efficiency. Therefore a simple calculation method is presented in the chapter to estimate the median FLED and associated percentile values for a given static efficiency in lieu of performing a Monte Carlo analysis. Using a static efficiency of 25 m^2/space, a 100% parking space occupancy, the distribution of curb weights obtained by Anderson & Bell [97] and the vehicle

energy content distributions from Chapter 3, the 80% fractile FLED is 260 MJ/m^2 (rounded up to the nearest 10 MJ/m^2).

It is interesting to compare the FLED values from the Monte Carlo model to values quoted in the literature given this work has used energy content values from vehicles subsequent to the 1980s and also adjusts for the apparent higher percentage of heavier vehicles in modern fleets. Thomas [126] gives an average FLED value for 'Garaging, maintenance and exploitation of vehicles' as 190 MJ/m^2 and 200 MJ/m^2 for 'Parking buildings' which are of the order of 20% less than median values obtained in this study. However the method proposed by Thomas to obtain 80% fractile values means values of 270 MJ/m^2 for 'Garaging, maintenance and exploitation of vehicles' and 250-300 MJ/m^2 for 'Parking buildings' are comparable with the 260 MJ/m^2 value suggested in this study.

Using a time-equivalence calculation for the structural fire design of car parking vehicles may not always be the only approach that should be considered and the effects of travelling fires and/or severe localised fire in the vicinity of structural elements may also need to be investigated.

Chapter 10 MULTIPLE VEHICLE FIRE SPREAD SIMULATION TOOL

10.1 Introduction

Chapter 5 and Chapter 6 discusses the characteristics of single passenger vehicle design fires based on experimental results from the literature. The current i.e. in literature design fires for single passenger vehicles are either represented by the specified rate of heat release history, or as mathematical functions with fixed coefficients irrespective of the size (curb weight) of the vehicle, hence, the motivation for this chapter. The outcome of both chapters provides the user to use probability distributions of the parameters to construct design fire.

An approach to predict the time of ignition of a subsequent vehicle, given it is already burning, is discussed in Chapter 7. This approach uses the point source model (PSM), which is a flame radiation submodel for predicting heat flux from a burning vehicle, and uses the flux-time product (FTP) as the ignition criterion for the prediction of the time of ignition of the targeted vehicle.

The other fire simulation software, B-RISK which was used to predict time of ignition of vehicles currently does not have the ability to use probabilistic design fire as the input. Moreover, the work in Chapter 8 has demonstrated that additional radiation effects do not show significant difference on the results considering additional assumptions have to be made for running the simulations. Therefore, a simple tool combining the probabilistic design fire as input with the approach of predicting time of ignition of vehicle is developed.

As a result, a Microsoft Excel and Visual Basic Application (VBA) tool was written to ease the combination of both approaches. This tool is then coupled with @RISK software for generating random numbers from different sets of probability distributions. This chapter discusses this tool in detail, since it is used in the subsequent chapters as a means of application of what has been investigated throughout this research.

10.2 Multiple vehicle fire spread simulation (UCVFire) tool

This section discusses the features, limitations, assumptions and the algorithm of the multiple vehicle fire simulation tool *UCVFire* (University of Canterbury Vehicle Fire).

10.2.1 Features

The main feature of the tool is the ability to conduct probabilistic analysis of multiple vehicle fire spread experiments on a single row arrangement. The tool is able to predict the time of

ignition of the subsequent vehicle, given a vehicle is already burning, using the design fire curve for a single passenger vehicle generated from the appropriate probability distribution. For the probabilistic input, the classification of the vehicles involved in the tool can either be randomly selected using the distribution of vehicle fleets, or manually set by the user. Also, another probabilistic input is the design fire of each of the vehicles involved in the experiments as a function of vehicle classification. The tool is able to run for multiple iterations, hence producing a family of results.

As the fixed input parameter in the tool, the user can decide on how many vehicles are involved in the simulation, specify the distance between vehicles, and specify number of total iterations to be run. The user can also choose the first vehicle that is ignited, in which the duration of the fire of the whole experiment will only be started after the first vehicle is ignited. The tool is written with the capability to be flexible in terms of application, and expandable in terms of content.

For each iteration, the tool is able to pick values randomly from the probability distributions for the selection of the classification of vehicles, and the construction of design fires for each vehicle. This is explained in more detail in the algorithm section.

The main output of the tool is presented in the form of a plot of family of heat release rate curves for a desired number of iterations. Outputs such as time and order of ignition of each vehicle involved are also recorded. Other outputs such as heat release rate of each vehicle and total energy released for each can also be obtained, depending on the requirements of the user.

The tool being programmed using Microsoft Excel and VBA is flexible enough for further developments and improvements of the features in the future. For example, instead of having of probabilistic vehicle parking distribution, the tool can be set for pre-determined vehicle parking distribution for the study of the cases such as such as offices, or apartments where individual spaces are already designated. The tool is currently developed for in-house use, particularly for this research project. Thus, at this stage, there is no commercial release to the public.

10.2.2 Limitations

The tool provides valuable outputs for probabilistic multiple vehicle fire analysis, however, it does have several limitations. The limitations of the tool are as follows:

- The tool is only able to record the heat release rate curves, predicted heat flux and time of ignition of the experiments. No other outputs, i.e., temperature measurements, gas concentrations, and smoke productions are produced.

- The tool is only able to run the simulation in a single row configuration. However, there is a possible way to represent a two row configuration by igniting a vehicle in the middle of a single row. Thus, the fire from the middle vehicle spreads in both directions to the vehicle on the left and right, which virtually represents fire spread in double rows.

- At this stage, the maximum number of iterations is based on the limitation of Microsoft Excel. However, only 100 iteration results are allowed for a plot due to a limitation in the Microsoft Excel plotting system.

- There is a maximum number of 30 vehicles that can be simulated at once, due to programming limitations.

10.2.3 Assumptions

There are several assumptions that were made in developing the tool. The following are some of the main assumptions of the model:

- For vehicle-to-vehicle fire spread, the ignition of the subsequent vehicle only relies on the radiated heat flux from another burning vehicle. This tool does not consider any other effects such as radiation from the underside of the hot upper layer during the fire and other compartment effects.

- It is assumed that there is no intervention to the fire from any fire suppression systems or manual fire-fighting by the fire brigade.

- It is assumed that the no wind effects on the spread of fire.

- It is assumed that, after the supposed component on the subsequent vehicle ignites, a design fire is assigned, and starts to grow for that vehicle at the time of ignition.

- It is assumed that all the vehicles potentially receive heat flux from any burning vehicle, which disregards the possibility of a blocking body in between

10.3 The input of the tool

This section explains in detail the fixed and probabilistic input parameters used in the tool.

10.3.1 Vehicle fleet distribution

Vehicle fleet distribution is an input for the simulation tool as a process of selecting the vehicle classification. One of the vehicle fleet distributions available is based on the data from the European Union and USA, obtained from Chapter 4. The distribution of vehicle fleet in its corresponding curb weight classification is shown in Figure 9-2. The figure also depicts the standard deviation values for each classification of the data from Tohir & Spearpoint. In addition, a survey of almost 5,000 vehicles in New Zealand, by Anderson and Bell [97], is also shown in Figure 9-2. These two sets of distributions give options for further work, and can be used for sensitivity analysis purposes.

10.3.2 Characterisation of design fire curves

The design fire, presented in terms of heat release rate as a function of time, requires knowledge on all phases of the curve. Therefore, in constructing the design fire, knowledge of the peak heat release rate, fire growth coefficient and fire decay coefficient must be known. For the tool, the growth i.e. Peak growth is be defined as a t-squared function as shown in Equation 5-6. The decay i.e. Exponential decay method is shown in Equation 5-15.

Figure 5-8 illustrates the combination of two equations i.e. Equation 5-6 and Equation 5-15 to form a single vehicle design fire curve. This approach gives fixed values for the coefficients for each individual experiment but it does not provide any distributions to the coefficient values across the curb weight classifications.

The information for the peak heat release rate, fire growth coefficient and fire decay coefficient for different classifications come from sets of probability distributions introduced

earlier in Chapter 6 (Table 6-4). Table 10-1 outlines the distribution analyses for peak heat release rate, fire growth coefficient and decay coefficient for every classification. The parameter α is the shape parameter, which determines the shape of a distribution function; and parameter θ is the scale parameter, which determines the position of the data distribution along the *x*-axis.

Vans/MPVs and SUVs classifications are included in the appropriate vehicle classification by using their known curb weights, rather than by identifying them as separate categories, due to lack of data. Also, due to lack of data, the distribution parameters value for heavy classification has to be extrapolated from the distribution parameters of the lighter weight classes. The extrapolation uses the average value of the lighter weight classes for the shape parameter (κ). It is decided that an average value is taken for extrapolation because there is no clear trend from the lighter weight class values.

However, for the scale parameter (ϑ), different approaches were taken for different distributions. For peak heat release rate distribution, an increasing linear trend was used for the extrapolation as the curb weight class increases. For the fire growth coefficient, a decreasing exponential trend was used for the extrapolation, since it was the best fit as the curb weight class increases. For fire decay, it was evident from the analysis that there is no obvious trend, thus, it was assumed a value of 0.11 for the heavy class fire decay coefficient using the average values of the lighter weight classes (The value is also consistent with the work in C.1).

Table 10-1: Summary of the single vehicle distribution analyses for peak heat release rate, fire growth coefficient and decay coefficient.

		Peak heat release rate, $\dot{Q}_{max}$ (kW)		**Fire growth coefficient, α_{peak} (kW/min²)**		**Fire decay coefficient, β_{exp} (min^{-1})**	
Distribution shape		Weibull		Gamma		Weibull	
Distribution parameters		**κ**	**θ**	**κ**	**θ**	**κ**	**θ**
Class	**Mini**	5.19	3809	1.39	11.86	0.93	0.17
	Light	1.66	5078	1.23	14.78	1.21	0.11
	Compact	2.40	4691	1.18	5.14	3.93	0.08
	Medium	3.18	7688	2.24	2.75	1.38	0.11
	Heavy	3.11*	8723*	1.51*	1.82*	1.86*	0.11*

*extrapolated values

10.3.3 Ignition prediction characteristics

The work in Chapter 7 suggests that the attributes for the usage of PSM for the prediction of heat flux is 0.3 for radiative fraction, and "2-Far" position as the heat source to the targeted item. The analysis also suggests that the bumper trim has a power law index of 2 (thermally thick), an FTP value of 21862 $\frac{kW \cdot s^n}{m^2}$, and a critical heat flux of 3.1 kW/m² is selected as the first component to ignite the vehicle. These attributes are used as the default values in this tool.

10.3.4 Effective distance

The effective distance is the radial distance from the heat source to the nearest point of the targeted vehicle. Based on the ignition prediction characteristics, "2-Far" (refer to Figure 7-2 (a)) is suggested as the heat source position. This principally positions the heat source at the far end of the burning vehicle, away from the targeted vehicle. The effective distance is best explained in Figure 10-1 where *a* is the width of the burning vehicle where the "2-Far" heat source position is at the left side of the burning vehicle and *2b* is the is the distance from the burning vehicle to the targeted vehicle. It is noted that *b* is the distance from both vehicles to the parking line. For simplification, it is assumed that each vehicle is parked in the middle of the parking space, which makes the distance to both sides of the parking line symmetrical. The effective distance is simply:

$$EFFECTIVE\ DISTANCE = a + 2b$$

Equation 10-1

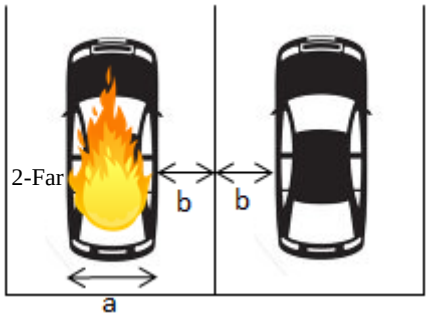

Figure 10-1: Illustration of the effective distance

10.4 Algorithm of the tool

This section explains in detail the algorithm of the tool for the purpose of understanding the mechanism on how the outputs are obtained. The algorithm of the tool is explained the flow diagram shown in Figure 10-2.

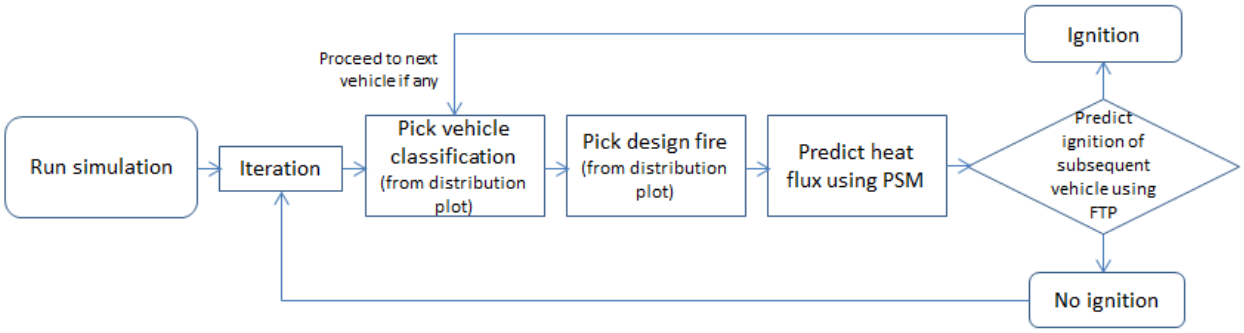

Figure 10-2: The algorithm of the tool

Prior to running the simulation tool, the user can enter the attributes desired, i.e., number of iterations, classification of vehicles, the effective distance, and the classification of the vehicles at the 'Input' tab. The user has the option to set the classification of vehicles manually, or to randomly selects the probability distribution of vehicle fleets.

For a single iteration, after starting the simulation, the tool selects vehicle classification for the first vehicle from the vehicle fleet probability distribution if no manual selection of classification was assigned. Then, the tool constructs a design fire of the first vehicle based on a random sampling of three probability distributions, i.e., fire growth coefficient, peak heat release rate and fire decay coefficient. The tool uses @RISK software feature i.e. the Monte Carlo simulation to select random samples from the probability distributions. The design fire of the first vehicle, which is essentially the heat release rate curve, is used as an input to predict the heat flux received by the exposed component of the second vehicle using the PSM. If the exposed component of the second vehicle receives enough heat from the first vehicle (i.e., when the accumulated FTP exceeds the FTP threshold value), the second vehicle is ignited. If the second vehicle does not receive enough heat, it does not ignite, and the simulation is stopped and proceeds to the next iteration.

Based on how the algorithm was developed, the tool initially predicts the time of ignition of the second vehicle without selecting its classification. However, under the condition that the second vehicle ignites, the algorithm proceeds to select the classification for the second vehicle, and consequently, chooses the design fire.

It is assumed that all the vehicles potentially receive heat flux from any burning vehicle, which disregards the possibility of a blocking body in between. This assumption follows Baker et al.'s [98] assumption in the creation of the B-RISK software. For example, as shown

in Figure 10-3, vehicles two and three receive heat flux from vehicle one, although vehicle two is supposedly blocking the radiation from vehicle one. After vehicle two ignites, vehicle three receives heat flux from vehicles one and two until either one of the heat sources burns out. This also occurs for the next vehicle, and so on. The same algorithm proceeds continuously up until there are no other vehicles left to be ignited. After that, the tool performs a continuous loop of the algorithm, based on the number of iterations set.

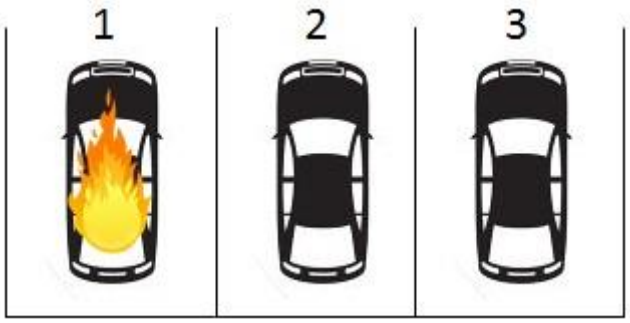

Figure 10-3: Example of three vehicles fire spread

10.5 The interface and code of the tool

The screenshot of the interface and the coding of the tool are shown in Appendix F.

Chapter 11 UCVFire APPLICATION: PROBABILITY OF FIRE SPREAD BETWEEN VEHICLES

11.1 Introduction

On 27th of February 2015, a van caught fire in a shopping mall's car park in Auckland, New Zealand, depicted in Figure 11-1. Questions arise: "Should there be a vehicle parked next to or a space away from the van, will the fire be able to spread? If so, what is the probability of the fire to spread?" Up until now, no specific studies on the probability of fire spread between vehicles has been done. Previously in Chapter 4, a similar study has been attempted to be solved using limited statistics of vehicle fires from several sources. However, later in the research, an enhanced analytical approach on solving the problem was found, hence, the motivation for this work.

Therefore, the main objective of is to quantitatively assess the probability of fire spread from a burning vehicle to another vehicle within its vicinity, given no interruption to the fire by fire fighters and/or fire suppression systems. The probability of fire spread is formulated using the knowledge of design fire of a single passenger vehicle, and the prediction of time of ignition approach, which has been combined into the UCVFire simulation tool. Prior to achieving the main objective, there are several points that must be discussed.

Figure 11-1: Burnt van inside a shopping mall parking in Auckland, New Zealand (Retrieved from stuff.co.nz [4])

11.1.1 Parking space dimensions

When considering the probability of fire spreading between vehicles, one important parameter to analyse is the distance between vehicles. Based on the PSM flame radiation model, the shorter the distance, the higher the heat flux received by the target item, thus, increasing the possibility for the fire to spread between vehicles. In a car park, the common closest distance would be that of vehicles parked in parking spaces next to each other.

Therefore, a study on parking space dimensions is conducted based on the literature. Chrest et al. [131] describes that dimensions of a parking space vary depending on the level of service (LOS) and classification of vehicles. Further discussion on LOS is discussed in Section 9.1.2. While, Hill [132] mentioned that parking dimensions depend on the timing of a single vehicle parked in a space. This shows that different sources have different approaches of considering the dimensions of a parking space. Hence, a summary of parking dimensions are collected for comparison purpose. Table 11-1 shows the summary of parking dimensions from accessible resources.

Table 11-1: Summary of parking dimensions from different resources

Source	Parking space dimensions		Reference
	Width (m)	Length (m)	
Parking structures: planning, design, construction, maintenance and repair	2.2 – 2.7	N/A	[131]
Car park designers' handbook	2.3 – 2.5	4.8	[132]
County of San Diego Parking Design Manual	2.7	5.5	[134]
Asphalt paving design guide	2.7 – 2.8	5.6	[135]
Information bulletin / Public-zoning code: Parking design	2.3 – 2.6	4.5 – 5.4	[136]
USAF Landscape Design Guide	2.75	6	[137]
Parking Design Standards	2.5 – 3.2	N/A	[138]
Parking Standards Design and Good Practice Supplementary Planning Document	2.5 – 2.9	5.0 – 5.5	[139]
Parking Structures: Recommended Practice for Design and Construction	2.3 – 2.7	N/A	[140]

Based on the summary, it appears that the parking space width is in the range of 2.2 – 3.2 m, and the parking space length is in the range of 4.8 – 6 m.

11.1.2 Probability of fire spread method

For the formulation of the probability of fire spread, considering a scenario of two vehicles parked in a space next to each other, this study performs a prediction of ignition for the second vehicle after the first vehicle already burning using the UCVFire simulation tool. The explanation of the tool has been previously discussed in Chapter 10. It is assumed that there are no fire suppression systems installed in the car park, thus, no there will be no intervention on the fire once it grows.

The design fire of a vehicle is dependent on the classification, where each classification has its own distribution of design fires. In addition, each classification is also dependent on the vehicle fleet distribution on the road. Thus, by performing the prediction model over a certain number of iterations with various distribution inputs, the results are able to show how many times the second vehicle ignited or not ignited. Therefore, the probability of fire spread from the first vehicle to the second vehicle can be calculated.

11.2 Approach

Two scenarios are examined: (1) vehicles parked next to each other, and (2) vehicles parked one parking space away from each other. These scenarios are simulated using the UCVFire simulation tool. Further explanation on the inputs for each scenario and the simulations are discussed in this section.

11.2.1 Simulation input

All input parameters such as numbers of iterations, the first component to be ignited and number of vehicles involved, are fixed, except for the main variable for this work, which is the effective distance. The width of the vehicle is unimportant, since the effective distance has already incorporated the width of the vehicle and the distance between one vehicle and another. The simulation model allows the user to vary the effective distance before running the simulation.

The probability of the fire spread from one vehicle to another is able to be calculated from a certain number of iteration runs, therefore 10,000 iteration runs is selected per simulation. This iteration number is deemed to be enough after series of 10,000 iterations were carried out for the same effective distance, and the results were similar due to the convergence of the iteration sequence. Also, the first component to be ignited is fixed to the bumper trim, as

suggested in Chapter 7. The work also suggests a power law index of 2 (thermally thick), an FTP value of 21,862 $\frac{kW \cdot s^n}{m^2}$, and a critical heat flux of 3.1 kW/m² is selected as the first component to ignite on a vehicle.

The algorithm for UCVFire is adjusted for the purpose of this work. The simulation process flowchart per iteration run is shown in Figure 11-2, where at the end of the iteration, the user is informed if the second vehicle is ignited or not. The selection of vehicle classification and design fire is performed using the Monte Carlo algorithm, where it randomly selects a value from each distribution plot (fire growth coefficient, peak heat release rate, and fire decay coefficient), as previously mentioned in Section 10.3.2.

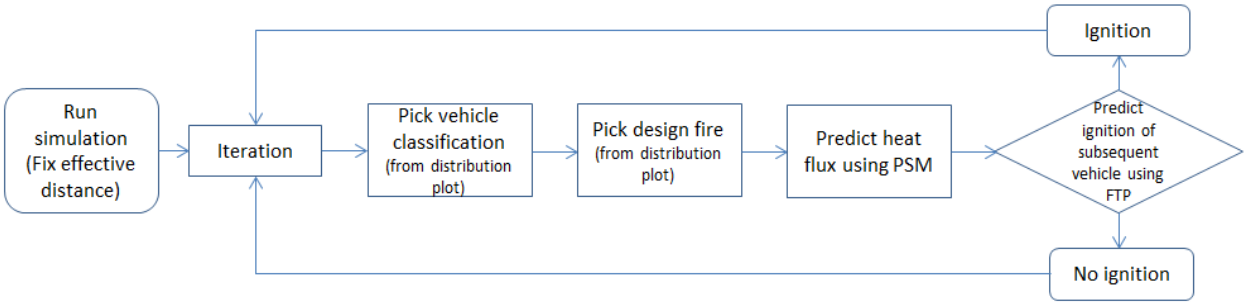

Figure 11-2: Simulation process flowchart

11.2.1.1 Scenario 1: Vehicle parked next to each other

This scenario represents the common closest distance in a car park, where two vehicles are parked next to each other. It is assumed that each vehicle is parked in the middle of the parking space, which makes the distance to both sides of the parking line symmetrical. In this scenario, the effective distance is the vehicle width of the burning vehicle, i.e., the heat source plus the distance between the edge of one vehicle to another, which is represented by *a* and *2b* respectively (Figure 11-3). Since different works in the literature consider different widths of parking spaces, a range with a minimum parking space width of 2.2 m, and a maximum of 3.2 m, are used. Thus, this will be the range of effective distances used in the simulation.

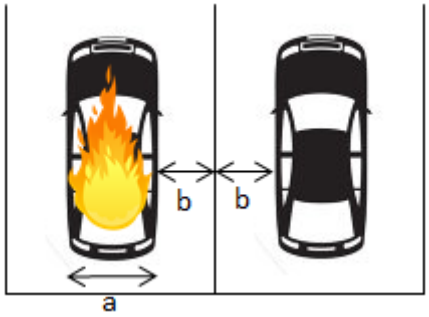

Figure 11-3: Vehicle parked next to each other

11.2.1.2 Scenario 2: Vehicle parked one space away

This scenario is chosen to study the effect of having an empty space in between a burning vehicle and another vehicle. Consistent to the assumption for Scenario 1, each vehicle also assumed to be parked in the middle of their parking space. In this scenario, the effective distance is the vehicle width of the burning vehicle, i.e., the heat source plus an empty parking space plus the distance between the tip of one vehicle to another vehicle, which is represented by *a*, *c* and *2b* respectively (Figure 11-4). Using the same range of parking space width 2.2 – 3.2 m, and adding another parking space width, this makes the range of effective distance for this scenario 4.4 – 6.4 m.

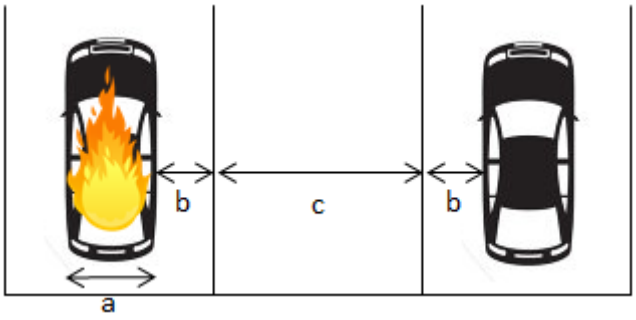

Figure 11-4: Vehicle parked a space away from each other

11.3 Results and discussion

11.3.1 Scenario 1: Vehicle parked next to each other

Figure 11-5 shows the plot of results of probability of fire spread for Scenario 1. According to the results, the shortest effective distance of 2.2 m yields the highest probability of fire spread, with 0.90, and the longest effective distance of 3.2 m yields the lowest probability, with 0.63. The results shows that, if a vehicle is parked next to a burning vehicle, there is a chance of 0.63 – 0.90 for the fire to spread to another vehicle.

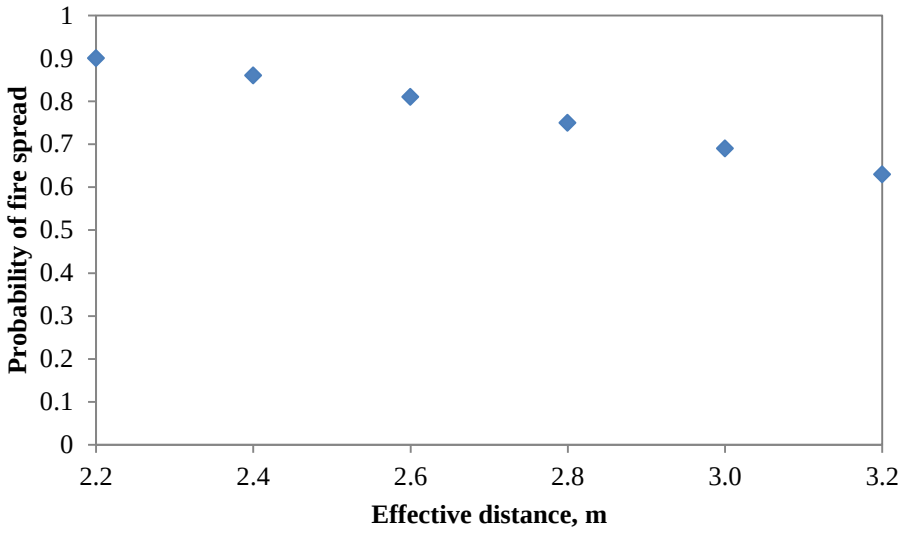

Figure 11-5: Plot of results of probability of fire spread for Scenario 1

11.3.2 Scenario 2: Vehicle parked one space away

Figure 11-6 shows the plot of results of probability of fire spread for Scenario 2. The results for this scenario show a lower probability than that of Scenario 1. The results show that the shortest effective distance of 4.4 m yields a 0.23 probability of fire spread, and the longest effective distance of 6.4 m results in no possibility of the fire spreading. The analysis suggests that having an empty parking space in between two vehicles lowers the probability of at least 0.40 in comparison to Scenario 1.

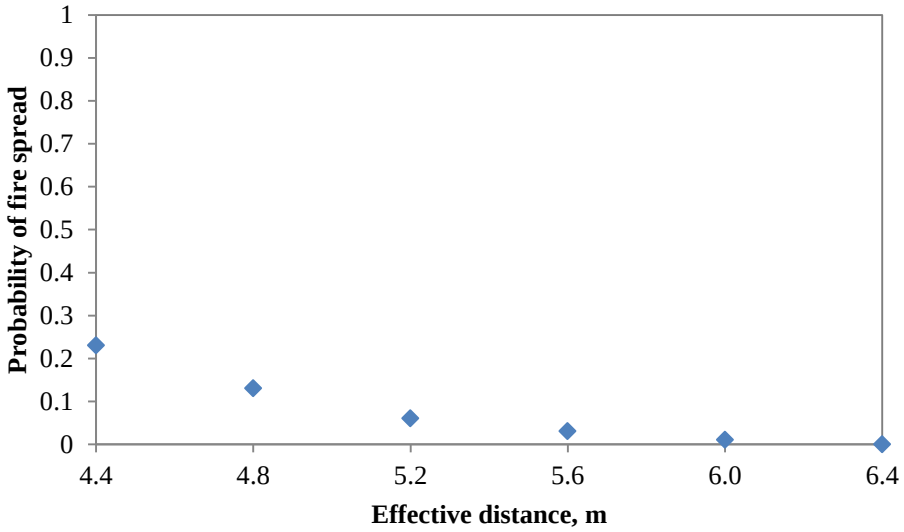

Figure 11-6: Plot of results of probability of fire spread for Scenario 2

11.3.3 Estimation of probability of fire spread for other distances

Essentially, the difference between Scenario 1 and Scenario 2 was only the distance between vehicles, which is the input for the simulation. Therefore, this section presents the combination of probability of fire spread results for Scenario 1 and 2 in a plot in order to fit a trendline which one can use to estimate the probability of fire spread for any distance. This combination is shown in Figure 11-7 where a polynomial trendline with the order of two was fitted to the results. An equation of

$$y = 0.045x^2 - 0.62x + 2.11$$

Equation 11-1

with the R^2 value of 0.99 is obtained. This equation can be used to estimate the probability of fire spread at different effective distances in between 2.2 – 6.4 m.

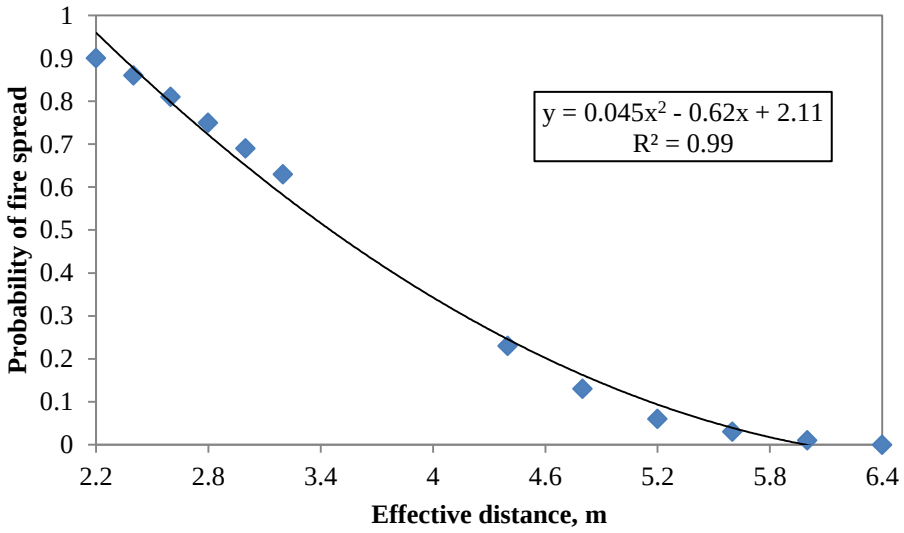

Figure 11-7: Combination of probability of fire spread results for Scenario 1 and 2

11.3.4 Sensitivity analysis – Varying vehicle fleet distribution datasets

A sensitivity analysis on varying the vehicle fleet distribution datasets in the simulation was performed, and the results are shown in Figure 11-8. Two different datasets; Tohir and Spearpoint, and Anderson and Bell were used in the analysis. The results show that Anderson and Bell's dataset produces a higher overall probability of fire spread as compared to Tohir and Spearpoint's dataset. This is because Anderson and Bell's data has a higher portion of heavier vehicles compared to Tohir and Spearpoint's. One notable example is Anderson and Bell's portion for Passenger Car: Mini class is 0.1%, while for Tohir and Spearpoint it is 9.0%. A higher portion of heavier vehicles means a higher possibility of getting higher peak

of heat release rate, thus, a higher possibility of igniting the neighbouring vehicle. Thus, the sensitivity analysis study shows that different vehicle distributions affect the probability of fire spread between vehicles.

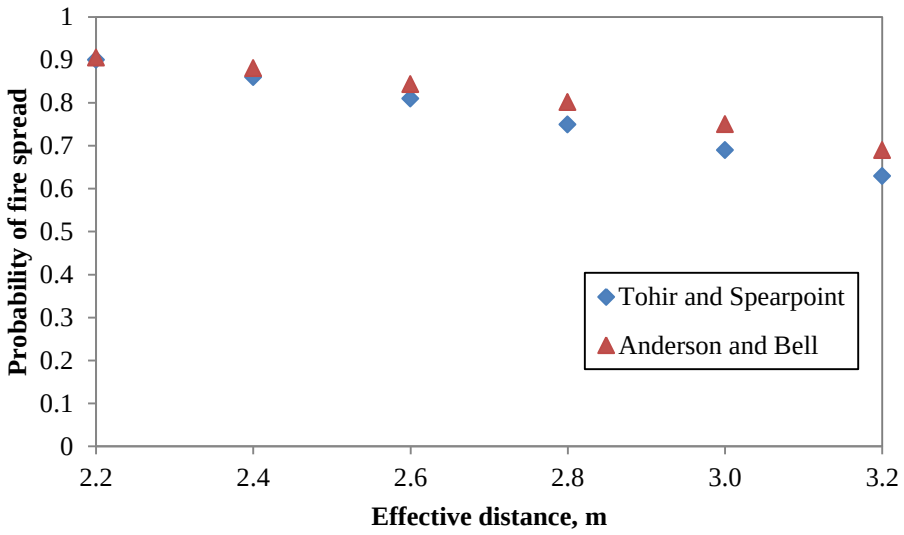

Figure 11-8: Sensitivity analysis of using different vehicle fleet distributions

11.4 Conclusion

This study was undertaken to quantitatively assess the probability of fire spread from a burning vehicle to another vehicle within its vicinity, given no interruption of the fire by fire fighters and/or fire suppression systems. Using the specified inputs, this study has shown that, for Scenario 1, the probability of fire spreading to the neighbouring vehicle is 0.63 – 0.90, depending on the effective distance.

For Scenario 2, the highest probability of fire spreading for the shortest effective distance is 0.23, and probability for the longest effective distance (6.4 m) is 0. It is also found that the empty space between two vehicles is able to reduce the probability by at least 0.40.

Using the combination of results for Scenario 1 and 2, an equation of $y = 0.045x^2 - 0.62x + 2.11$ is obtained to estimate the probability of fire spread for different effective distance between 2.2 – 6.4 m.

Using different vehicle fleet distributions datasets affect the selection of design fire, thus, produces different sets of results. For more specific investigation, a different dataset of vehicle distribution fleet can be adopted in future analysis. However, this study is limited to

only one vehicle initially burning. The effect of having two vehicles burning could have been different due to the higher intensity of energy released from the two vehicles.

It is to note that the work in this chapter excludes the intervention of fire fighters and fire suppression systems to the fire. The intervention to the fire could have given a different effect to the probability of the fire spread to other vehicles. This is subject to future work where potential research such as the introduction of fire sprinkler systems into the model can be made. Further discussions on future work are discussed in Chapter 14.3.4.

Chapter 12 UCVFire APPLICATION: CASE STUDY

12.1 Introduction

Multiple vehicle fire scenarios can now be performed with the combination of probabilistic design fire for a single passenger vehicle, and prediction of time ignition using the point source method (PSM) and the flux-time product (FTP) approach. Chapter 10 discusses the simulation tool developed to combine both approaches, called UCVFire. An important question to ask is: how well does this simulation tool perform in comparison to real fire incidents? Is UCVFire able to recreate a real fire incident which occurred, given enough information? It is almost impossible to compare directly to real fire incidents, since there are rarely any detailed observations or any measurements recorded.

Therefore, the main objective of this chapter is to assess the ability of UCVFire to recreate a real fire incident and compare it with the results from other researcher's attempts in recreating it. The selection of a case study is based on the richness of the information for the incident, and information on its attempted recreation by other researchers

12.1.1 Selection of case study

The criteria required to perform the case study are;

a. Layout of the vehicles involved in the fire. This enables recreation of the scenario.
b. Make and model of each vehicle involved in the fire. This is for the purpose of assigning the classification of the vehicle and for getting the information of the dimensions of the vehicle.
c. Distance between vehicles. This is for the purpose of assigning the effective distance between vehicles.
d. Observed timeline of the incident. This is for the comparison with the simulated fire scenario results and in particular the ignition sequence of vehicles.
e. Attempted simulation/fire development estimation by other researchers. This is for comparison with the simulated fire scenario results using UCVFire.

There are several literatures which reported an attempt to recreate real car park fire incidents. However, not all of the literatures satisfy the criteria required to perform the case study. Table 12-1 shows the list of available literatures against the listed required criteria (mentioned previously). In the table, 'Y' indicates that the literature satisfy that particular criteria while 'N' means the literature did not satisfy that particular criteria. Also in the table,

on top of the name of the author(s) listed (as to identify the literature), the name of the incident is also mentioned in the bracket.

Table 12-1: List of required criteria for each literature

	de Feijter and Breunese (Harbour Edge) [43]	BRE (Monica Wills House) [1]	Ponziani et al. (Rome car park fire) [141]	Annerel et al. (Gretchenbach) [39]
Layout (a)	Y	N	Y	Y
Make and model (b)	Y	N	N	N
Distance (c)	Y	N	Y	Y
Timeline (d)	Y	N	Y	Y
Attempt (e)	Y	Y	Y	Y

From the comparison, only one work satisfy all the criteria required i.e. the work by de Feijter and Breunese [43], and therefore this is selected to be the case study.

12.1.2 Lloydstraat car park fire [43]

A research team assigned by Efectis Nederland BV conducted a detailed investigation of the fire in a car park building in Lloydstraat, Rotterdam, the Netherlands. The car park had seven half levels, with a total area of 2100 m², and could accommodate 60 vehicles. It is under a residential building called Harbour Edge, which experienced a fire incident on the 1st of October 2007. At 4.16 AM, the occupants of the residential building reported a fire in the car park under the building.

On arrival of the fire brigade, it was reported that external flaming was visible out of the two openings in the façade of the floor where the fire had occurred. At the time the fire brigade arrived, it was considered (by the fire brigade) that two or three vehicles were on fire. After the fire, it was found out that five cars were completely burned, one car was partially burned, and another underwent charring and melting. The building structure was severely damaged, and there were some parts of the floor that collapsed during the fire. It was unclear if there were other cars in the car park from the report.

The layout of vehicle positions and details of the seven vehicles involved in the fire are shown in Figure 12-1 and Table 12-2. It was reported that the distance from Vehicle 3 to Vehicle 4 was 0.5 m, while the distance for every other vehicle was 0.7 m, except for vehicle one, which was parked a space away from Vehicle 2. In Table 12-2, the classification based on curb weight for each of the vehicle is obtained from several car specification database

websites [55, 56], since this was not mentioned in the report. The dimensions of each of the vehicles were also obtained from the websites. From the damage patterns of the wall and ceilings of the car park, it was suspected that the fire either began from Vehicle 3 or Vehicle 4.

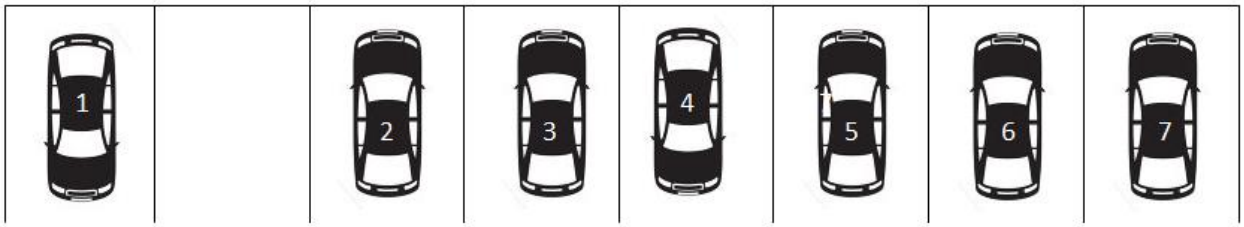

Figure 12-1: Layout of the vehicles involved in the fire

Table 12-2: Details of the vehicles involved in the fire

Vehicle no.	Make & Model	Year of manufacture	Classification	Note
1	Renault 5	1989	Mini	Underwent charring
2	Volkswagen Golf	2006	Compact	Completely burned
3	Kia Sportage	2005	Medium	Completely burned
4	Ford Mondeo	2002	Medium	Completely burned
5	Renault Megane	2003	Compact	Completely burned
6	Volvo V50	2005	Medium	Completely burned
7	Volkswagen Fox	2005	Light	Partially burned

A detailed timeline of the fire can be found in Table 12-3. The intensity of the fire reported in the table; 'Middle fire' and 'Large fire' seems to be qualitative based on the observation of the fire fighters.

Table 12-3: Timeline of the fire (Reproduced from de Feijter and Breunese [43])

Time of incident	Fire brigade action	Evacuation
4.16 AM	First notification by the residents of Harbour Edge	First internal alarm of building
4.17 AM	Alarm for TS23-1 (Fire engine)	
4.22 AM	TS23-1 arrived on scene	
4.24 AM	Middle fire	
4.25 AM	Large fire	
4.32 AM	Start using dry main	
4.48 AM	Fire extinguishing boat started to extinguish car number 7 (the which is partially burned) which has been burning for 10 minutes (The building stands on a wharf)	Evacuation completed

5.01 AM	Start damping down	

12.1.3 Fire recreation attempt by Efectis Nederland BV

The main driver of the fire recreation attempt of the incident was when the fire brigade questioned whether a fire of this magnitude is a phenomenon that should be considered in the future. If so, what was the rate of fire development? What was the maximum heat release rate? What was the fire load? These were the questions which were attempted to be answered by Efectis Nederland BV research team during the investigation of the fire. Thus, these questions led the team to recreate the possible fire development of the incident.

It was suggested from de Feijter and Breunese [43] that the average fire load of a single vehicle is 6,650 MJ, which is based on a car sales figure in the Netherlands. This value is derived from the total heat released in Category 3 (from Joyeux classification system explained in 2.3.1), which is 9500 MJ [37]. This value was then multiplied by an efficiency factor of 0.7, as an assumption that not all material burns completely. Thus, the fire loads for seven vehicles involved in the fire was estimated to be about 46,550 MJ in total.

One of the earlier decisions prior to attempting to recreate the fire development of the real fire was to decide on the heat release rate to be used for the simulation. The research team decided to adopt the reference heat release rate curve suggested by Joyeux [37] for all seven vehicles, as a global view on how the fire developed. Since, it was uncertain of which vehicle was ignited first, the research team decided to create two possible scenarios of how the fire could have occured.

Another decision was that the time of fire spread from the first vehicle to the second vehicle has to be within 15 minutes. In both of the scenarios, the research team decided to use a time of 10 minutes for the fire to spread from the first vehicle to the second. However, the decision for ignition of each of the subsequent vehicles was unclear. The two possible scenarios i.e. Scenario 1 and 2 with proposed heat release rate for each vehicle at suggested time of ignition are shown in Figure 12-2 and Figure 12-3. The orders of vehicle ignition were shown in both figures where it was unclear how the order of the vehicle ignition was decided in both scenarios.

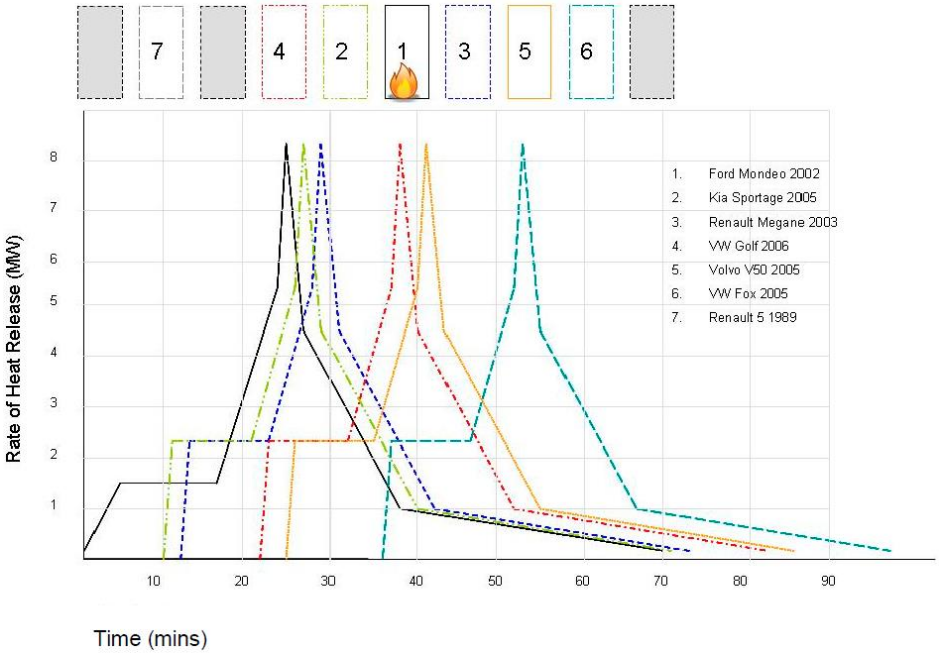

Figure 12-2: Scenario 1 (Reproduced from de Feijter and Breunese [43])

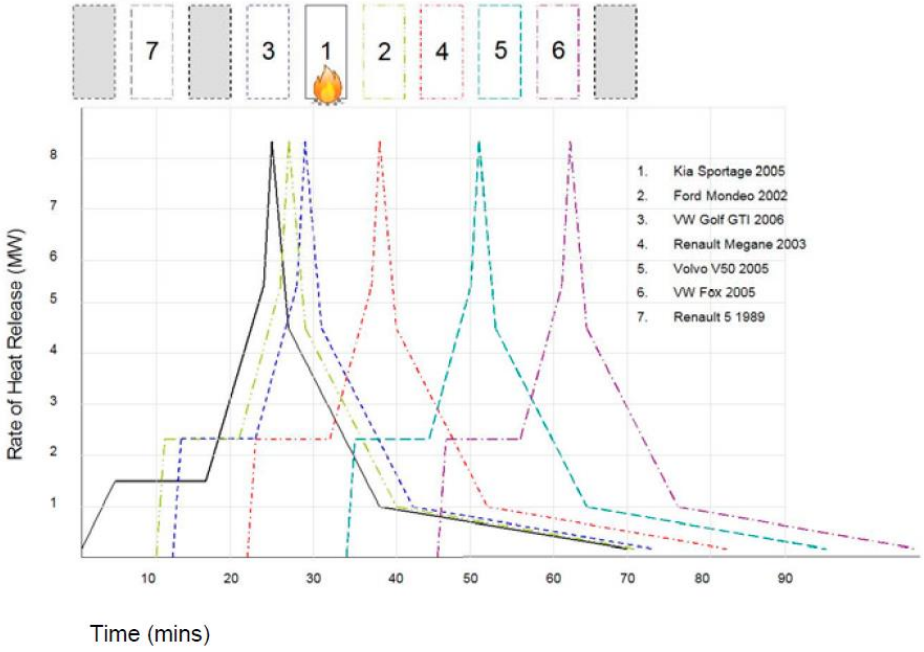

Figure 12-3: Scenario 2 (Reproduced from de Feijter and Breunese [43])

The results of the combination of the proposed heat release rate of a single vehicle for both scenarios are shown in Figure 12-4 and Figure 12-5. For Scenario 1, the peak heat release rate reaches up to 22,000 kW, and the time taken for the fire to burn out for all six vehicles was 95 minutes. For Scenario 2, the time taken for the fire to burn out for all six vehicles was longer, at 107 minutes, while the peak heat release rate was just little over 20,000 kW.

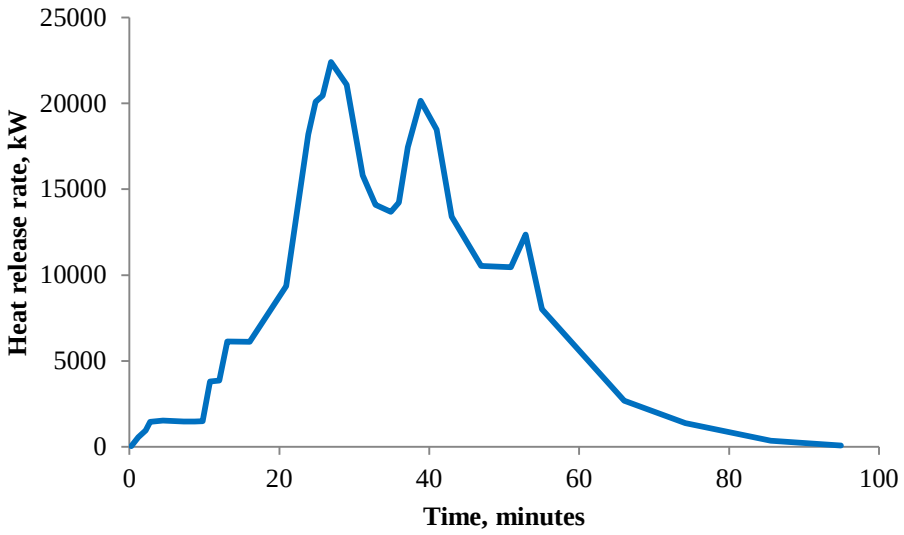

Figure 12-4: Heat release rate curve for Scenario 1 (Reproduced from de Feijter and Breunese [43])

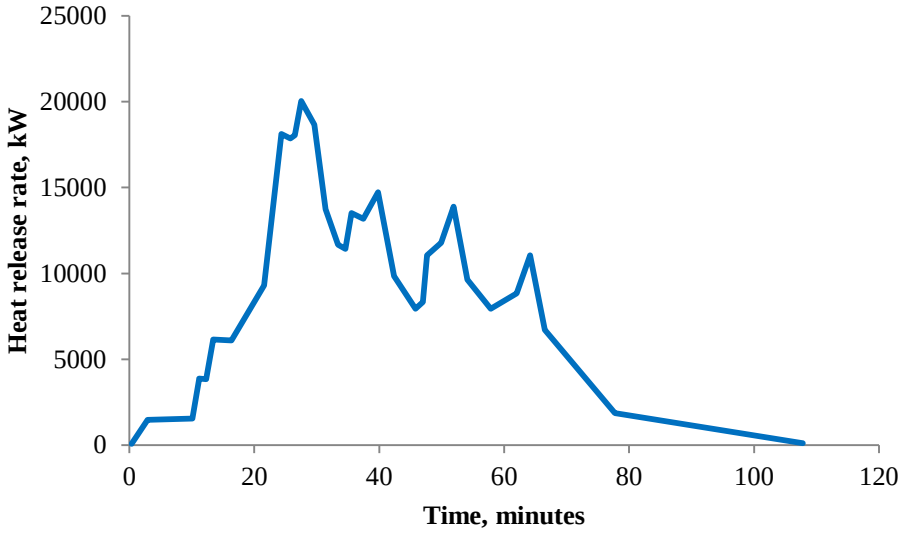

Figure 12-5: Heat release rate curve for Scenario 2 (Reproduced from de Feijter and Breunese [43])

12.2 Fire development using UCVFire

Using the UCVFire simulation tool, the development for Lloydstraat Car Park fire is now able to be recreated. The tool is able to produce probabilistic results of the time of ignition of each of the vehicles given the first vehicle is ignited, the order of ignition of the vehicles, and the heat release rate curves of the entire fire in comparison to what has been attempted by the researchers from Efectis Nederland BV.

Since it was uncertain which vehicle was ignited first, the simulation using UCVFire is performed in two scenarios, similar to the work done by Efectis Nederland BV. In the

simulation, Scenario 1 assumes that Vehicle 4 was the first vehicle to be ignited, and Scenario 2 assumes that Vehicle 3 was to be the first vehicle to be ignited. The order of the vehicle ignition is determined from the simulation as part of the outcome.

Each of the vehicles had been assigned a classification based on its curb weight (Table 12-2). This is the input for the design fire, where each vehicle classification has its own probabilistic distributions (fire growth coefficient, peak heat release rate, and fire decay coefficient).

12.2.1 Fire load analysis

A fire load analysis on the seven vehicles is conducted using the probabilistic distributions of the total energy released, introduced in Chapter 3 (Section 3.4.3). This is because it was suggested that the fire load for a single vehicle is 6,650 MJ in the report by de Feijter and Breunese (2007). The outcome is presented in the form of the average fire load for a single vehicle for the purpose of comparison with the values suggested in the report.

The analysis consists of running 10,000 iterations, where a single iteration selects a value of total heat released for each of the seven vehicles. Finally, the average total heat released is calculated out of the 10,000 iterations. The number of iterations is deemed to be enough for the analysis due to convergence of the average fire load value simulated.

12.2.2 The input for the simulation

Based on the available information in the report, Table 12-4 shows the vehicle input parameters for the simulation. In the table, the distance between Vehicle 1 and 2 is based on the assumption of a parking space with a width of 2.2 m, since it was not clear in the report. This width size is taken from the range of parking width explained in Section Chapter 11, where it is the lowest width from the range of parking spaces available in the literature. This value is selected as part of the worst case, and for the lowest width, if the fire is not able to spread across the empty space, then this is also true for larger widths.

Table 12-4: Vehicle input parameters for the simulation

Vehicle number	Classification	Vehicle width (m)	Distance between vehicles (m)	
1	Mini	1.6	Vehicle 1 to 2	2.9*
2	Compact	1.7	Vehicle 2 to 3	0.7
3	Medium	1.8	Vehicle 3 to 4	0.5
4	Medium	1.8	Vehicle 4 to 5	0.7
5	Compact	1.7	Vehicle 5 to 6	0.7
6	Medium	1.8	Vehicle 6 to 7	0.7
7	Light	1.6	-	-

*denotes an assumption of a parking space with width of 2.2 m

The other inputs of the simulation are shown in Table 12-5. These inputs followed what has been suggested in Chapter 7. The number of iterations per simulation is currently set at 100, due to the limitation of the plot function in Microsoft Excel, which only permits 100 different datasets in a plot.

Table 12-5: Other input parameters for the simulation

Radiative fraction for PSM	0.3
First component ignited for all vehicles	Bumper trim
Power law index, *n*	2
FTP value	21862
Critical heat flux, (kW/m²)	3.1
Number of iterations	100

12.3 Results and discussion

This section discusses the fire load analysis, simulation results summary and comparison of the simulation results with the real fire, and the fire development attempt by the Efectis Nederland BV research team.

12.3.1 Fire load analysis

The fire load analysis obtained an average fire load of 5,500 ± 1016 MJ per single vehicle, where the advised value by the Efectis Nederland BV research team was 6,650 MJ. In total, from the analysis, the fire loads for seven vehicles involved in the fire was estimated to be 38,500 ± 7112 MJ in total while from the Efectis Nederland BV was 46,550 MJ.

It seems that the value suggested by the Efectis Nederland BV research team is just over the standard deviation region from the simulated values for both single (difference of 134 MJ from the higher standard deviation region) and the total of seven vehicles (difference of 938 MJ from the higher standard deviation region).

12.3.2 Simulation results summary

12.3.2.1 Scenario 1

Table 12-6 shows the results summary of 100 iterations for Scenario 1. Out of the 100 iterations, it was found that, in 40 different scenarios, all seven vehicles were involved even though in the real fire, only six vehicles were ignited, and the other vehicle only underwent charring. This shows that there is a possibility of all seven vehicles to be ignited if the fire is not interrupted. This also shows that, with the lowest parking width gap, only 40% of the iterations were able to spread the fire across to Vehicle 1, and it is expected that the percentage is lower if the gap widens. Furthermore, the number of times six vehicles ignited was 86, which is a high possibility of occurrence. This means that the number of vehicles which were involved in the real fire was of high possibility of occurrence. The average peak heat release rate from the simulation was 17,577 ± 5300 kW, in comparison to 22,000 kW obtained from the results by the Efectis Nederland BV research team. The value by Efectis Nederland BV seems to be within the range standard deviation of the simulated ones. The minimum number of 786 kW was recorded when only the first car was ignited for the whole iteration.

Table 12-6: Results summary for Scenario 1

Percentage of fire spread from first to second vehicle	98%
Percentage of all seven vehicles ignited	40%
Percentage of six vehicles ignited	86%
Average peak heat release rate ± standard deviation	17,577 ± 5300 kW
Minimum peak heat release rate	786 kW
Maximum peak heat release rate	32,978 kW

From 100 simulations, there were two patterns of vehicle ignition order, which are shown in Table 12-7. Out of 100 iterations, it was 60 times Pattern 1 occurred and 38 times Pattern 2 occurred. The average time of ignition and the standard deviation for each of the ignition of the vehicles was also recorded for comparison with the timeline reported.

Table 12-7: Patterns of vehicle ignition order for Scenario 1

Pattern 1	Avg. Pattern 1 time of ignition (min)	Pattern 2	Avg. Pattern 2 time of ignition (min)
Vehicle 4 to Vehicle 3	27.7 ± 13.0	Vehicle 4 to Vehicle 3	25.8 ± 10.0
Vehicle 4 to Vehicle 5	29.8 ± 12.7	Vehicle 4 to Vehicle 5	27.9 ± 10.7
Vehicle 3 to Vehicle 2	43.5 ± 12.9	Vehicle 3 to Vehicle 2	45.2 ± 16.1
Vehicle 5 to Vehicle 6	56.3 ± 17.5	Vehicle 5 to Vehicle 6	41.8 ± 18.8
Vehicle 6 to Vehicle 7	71.6 ± 26.3	Vehicle 6 to Vehicle 7	59.0 ± 25.8
Vehicle 2 to Vehicle 1	91.3 ± 37.1	Vehicle 2 to Vehicle 1	91.2 ± 37.3

12.3.2.2 Scenario 2

Table 12-8 shows the results summary of 100 iterations for Scenario 2. This scenario also shows that there is a possibility of all seven vehicles to be ignited if the fire is not interrupted. This has been shown in 35 out of the 100 iterations. Almost similar to Scenario 1, the number of times six vehicles were ignited was 87, which is a high possibility of occurrence. The average peak heat release rate from the iterations was 16,594 ± 4773 kW as compared with the peak heat release rate obtained by Efectis Nederland BV also seems to be within the range of standard deviation of the 100 iterations.

Table 12-8: Results summary for Scenario 2

Percentage of fire spread from first to second vehicle	94%
Percentage of all seven vehicles ignited	35%
Percentage of six vehicles ignited	87%
Average peak heat release rate ± standard deviation	16,594 ± 4773 kW
Minimum peak heat release rate	1971 kW
Maximum peak heat release rate	29,408 kW

For this scenario, from 100 iterations, only one pattern of vehicle ignition order was attained which is shown in Table 12-9. The average time of ignition and the standard deviation for each of the ignition of the vehicles was also recorded for comparison with the timeline reported.

Table 12-9: Patterns of vehicle ignition order for Scenario 1

Pattern 1	Avg. time of ignition (minutes)
Vehicle 3 to Vehicle 4	23.8 ± 7.7
Vehicle 3 to Vehicle 2	25.6 ± 8.3
Vehicle 4 to Vehicle 5	41.2 ± 13.5
Vehicle 5 to Vehicle 6	59.3 ± 19.1
Vehicle 6 to Vehicle 7	73.3 ± 27.2
Vehicle 2 to Vehicle 1	95.0 ± 36.9

Figure 12-6 and Figure 12-7 illustrate the family of curves from the run of iterations for Scenario 1 and 2 respectively. The red bold line on top of the family of curves represents the maximum boundary of heat release rate possibilities from the 100 iterations. This maximum boundary can be used as the worst possible outcome that could occur in the fire.

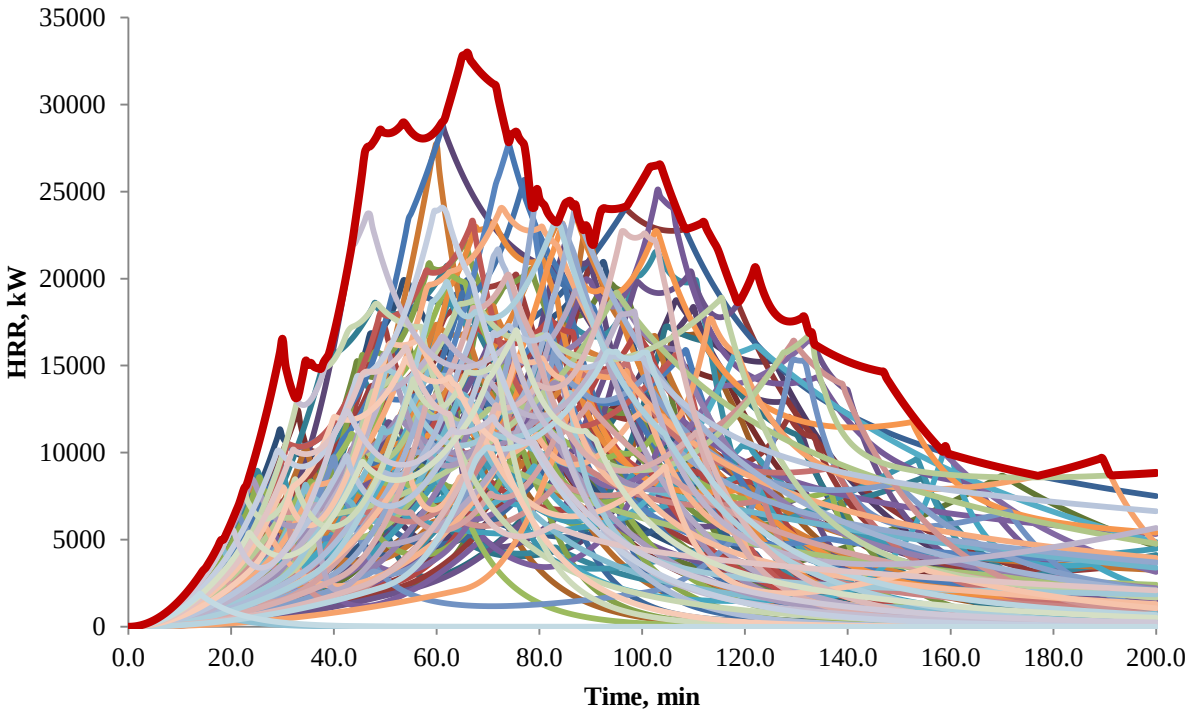

Figure 12-6: Family of predicted heat release rate curves for Scenario 1

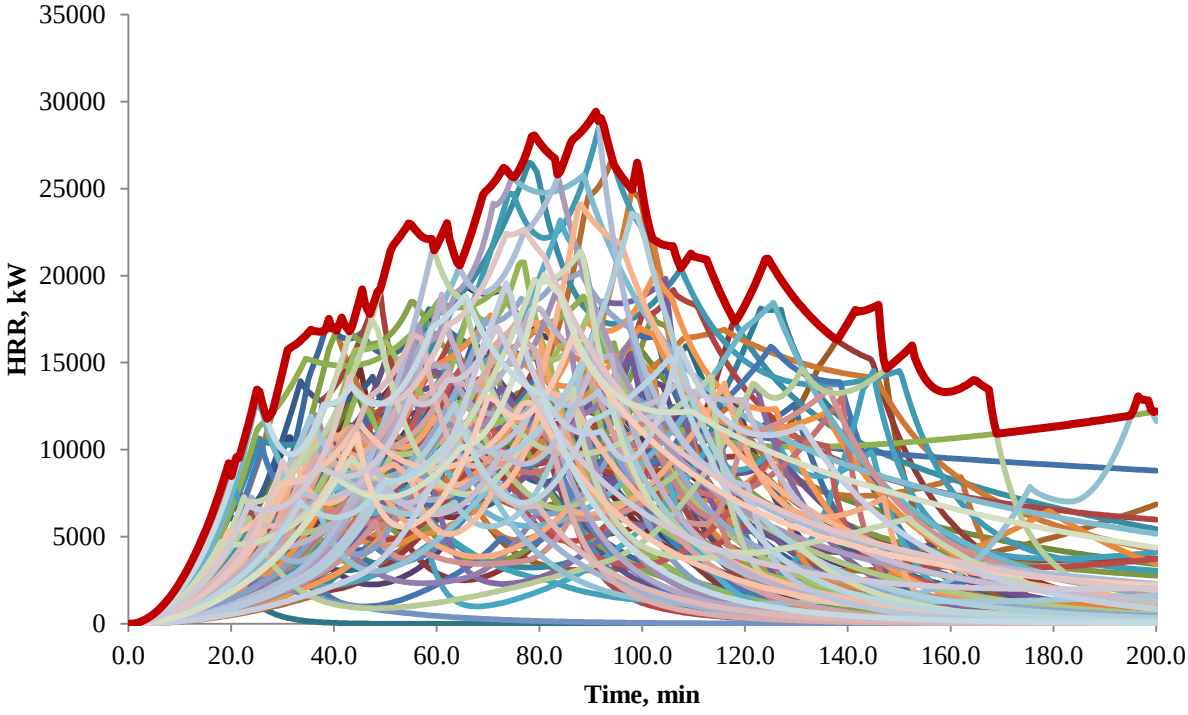

Figure 12-7: Family of predicted heat release rate curves for Scenario 2

12.3.2.3 Comparison with Efectis Nederland BV time of ignition

Table 12-10 and Table 12-11 shows the results of time of ignition developed by Efectis Nederland BV, and the average predicted time of ignition and the standard deviation obtained from UCVFire simulations. Overall, it can be seen that the average values for all predicted time of ignition from the simulation are behind by at least more than double the time of ignition developed by Efectis Nederland BV. Comparing the time of ignition by Efectis with the lower standard deviation for both scenarios show a closer match where for Scenario 1 Pattern 2 the developed time of ignition by Efectis even match within the standard deviation range for order of ignition of Vehicle 6 and 7.

Table 12-10: Comparison of time of ignition of Efectis Nederland BV with UCVFire Scenario 1

Order of ignition	Efectis' predicted time of ignition (min)	Scenario 1	
		Pattern 1	Pattern 2
		Avg. time of ignition (min)	Avg. time of ignition (min)
Vehicle 4	0.0	0.0	0.0
Vehicle 3	10.0	27.7 ± 13.0	25.8 ± 10.0
Vehicle 5	12.0	29.8 ± 12.7	27.9 ± 10.7
Vehicle 2	22.0	43.5 ± 12.9	45.2 ± 16.1
Vehicle 6	24.0	56.3 ± 17.5	41.8 ± 18.8
Vehicle 7	36.0	71.6 ± 26.3	59.0 ± 25.8

Table 12-11: Comparison of time of ignition of Efectis Nederland BV with UCVFire Scenario 2

Order of ignition	Efectis' predicted time of ignition (min)	Scenario 2
		Pattern 1
		Avg. time of ignition (min)
Vehicle 3	0.0	0.0
Vehicle 4	10.0	23.8 ± 7.7
Vehicle 2	12.0	25.6 ± 8.3
Vehicle 5	22.0	41.2 ± 13.5
Vehicle 6	24.0	59.3 ± 19.1
Vehicle 7	36.0	73.3 ± 27.2

Figure 12-8 and Figure 12-9 shows the comparison between the heat release rate curve developed by Efectis Nederland BV, the average heat release rate from the 100 iterations at each time step, and the maximum boundary of heat release rate possibilities from the 100 iterations for Scenario 1 and 2 respectively. It seems that for both Scenarios, the growth part of the curves by Efectis Nederland BV seem to be almost similar to the maximum boundary i.e. the worst case out of the 100 iterations. This is expected due to the fact that Efectis

Nederland BV predicted the time of ignition of the second vehicle up until the sixth vehicle to be much quicker than the predicted times from the simulation.

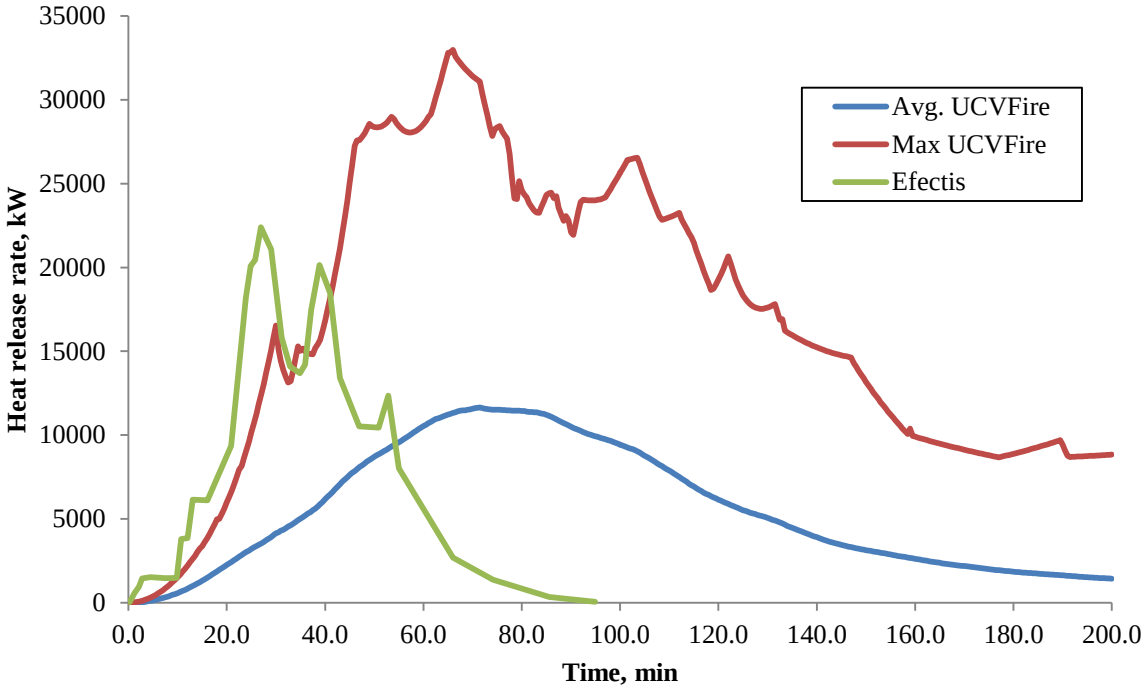

Figure 12-8: Comparison of heat release rate curve between Efectis and UCVFire for Scenario 1

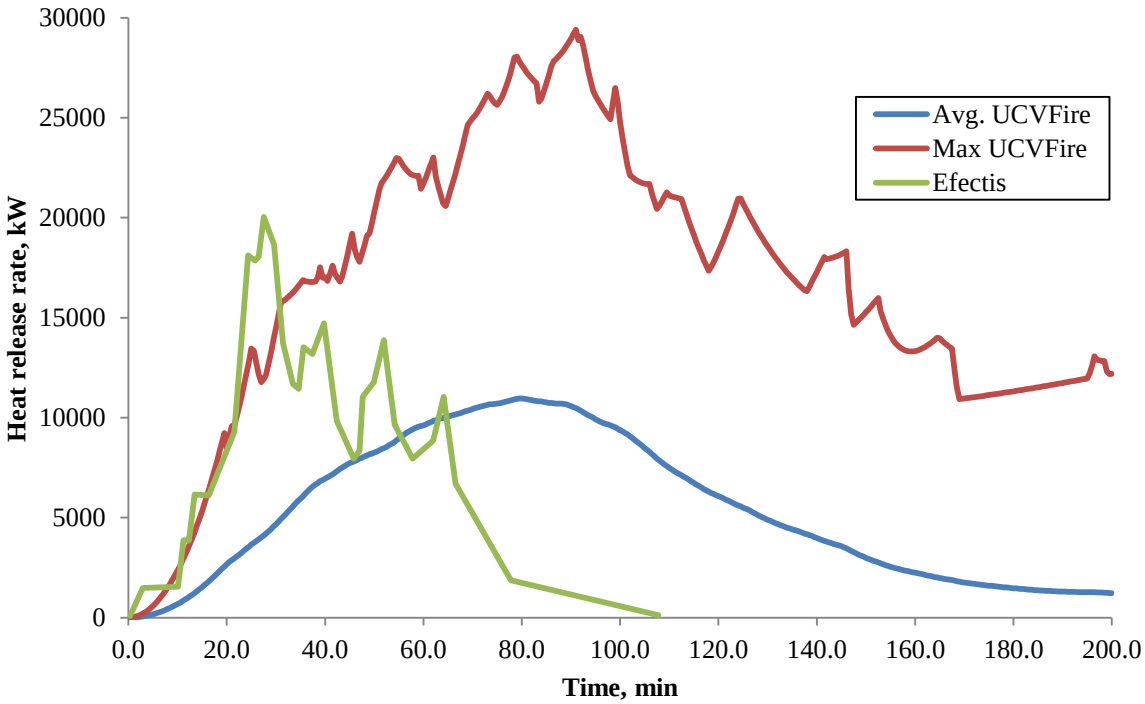

Figure 12-9: : Comparison of heat release rate curve between Efectis and UCVFire for Scenario 2

12.3.3 Comparison with the incident timeline

The results from the simulation for Scenario 1 and 2 can now be compared with the reported observation of the fire, in order to obtain the possible timeline of the fire. The comparisons were performed such that the time of incidents were tallied with the average simulated time. The comparisons for both scenarios are shown in Table 12-12 and Table 12-13.

Table 12-12: Comparison for average simulated time for Scenario 1 and the reported observation of the fire

Avg. simulated time / Possible time range (min)	Time of incident	Simulated fire development	Observation
0.0		Origin fire vehicle 4	
27.0		Origin fire vehicle 3	
29.1		Origin fire vehicle 5	
23.2 - 38.1	4.16 AM		Resident called fire brigade
29.2 - 44.1	4.22 AM		Fire engine arrives
44.2		Origin fire vehicle 2	
51.2		Origin fire vehicle 6	
55.2 - 70.1	4.48 AM		Fire boat start extinguishing the sixth vehicle (i.e. vehicle 7)
67.0		Origin fire vehicle 7	
68.2 - 83.1	5.01 AM		Start damping down

Table 12-13: Comparison for average simulated time for Scenario 2 and the reported observation of the fire

Avg. simulated time / Possible time range (min)	Time of incident	Simulated fire development	Observation
0.0		Origin fire vehicle 3	
23.8		Origin fire vehicle 4	
25.6		Origin fire vehicle 2	
19.7 - 35.1	4.16 AM		Resident called fire brigade
25.7 - 41.1	4.22 AM		Fire engine arrives
41.2		Origin fire vehicle 5	
51.7 - 67.2	4.48 AM		Fire boat start extinguishing the sixth vehicle (i.e. vehicle 7)
59.3		Origin fire vehicle 6	
64.7 - 80.2	5.01 AM		Start damping down
73.3		Origin fire vehicle 7	

The first incident which was possible to be tallied was when the fire engine arrived to the scene at 4.22 AM, where at the time of arrival of the fire brigade, there were two or three vehicles that were already on fire. Thus, referring to Scenarios 1 and 2, the arrival of the fire engine could mean that the fire had already started for at least 29.2 minutes and 25.7 minutes

respectively. The range of possibilities of the arrival of the fire engine is within the time range prior to the ignition of the fourth vehicle, hence, the time range in both tables. Also, since it was unknown from the incident how many vehicles were actually on fire when the resident notified the fire brigade, the comparisons were able to indicate that there is a possibility that the resident may have noticed the fire after the first vehicle was burning. This was possible, since for both scenarios, the average times of spread from the first to the second and third vehicles were less than six minutes. Therefore explains the range of the time where the resident called the fire brigade for Scenario 1 and 2 which were 23.2 – 38.1 minutes and 19.7 – 35.1 minutes respectively.

The other incident which is possible to be tallied is when the fire boat started to extinguish the sixth vehicle (Vehicle 7) after it was ignited for approximately ten minutes, at 4.48 AM. This is approximately 26 minutes after the fire brigade arrived. Based on comparisons for this incident, Scenario 1 gives a fitter range of possible times when tallied with reported observations of the fire, since in Scenario 2 it takes a longer time for the fire to spread up until the sixth vehicle (Vehicle 7).

The comparison with the individual results of each iteration suggests that, for Scenario 1, there were 11 times during the simulation during which the timing between the arrival of the fire brigade and the timing the fire boat extinguishes the sixth vehicle (Vehicle 7) was 26 ± 1 min. While for Scenario 2, the earliest time of ignition of the sixth vehicle (Vehicle 7) was 22 min, and adding approximately ten minutes gives the difference time of 32 min, which is inconsistent with what was reported. The individual results can be found in Appendix G.

The findings from the analysis suggest that Scenario 1 gives a better representation of the real fire scenario based on the tallied information, as compared to Scenario 2. This is in agreement with what has been concluded by Efectis Nederland BV in their report. Therefore, it can be concluded that the first possible ignited vehicle from the real fire was Vehicle 4, which was a Ford Mondeo.

12.4 Conclusion

The aim was to assess the ability of UCVFire to be able to recreate a real fire incident and compare it to the results given by other researchers in their attempt to recreate the real fire. The probabilistic fire load analysis gives a value of 5,500 ± 1016 MJ per single vehicle, or 38,500 ± 7112 MJ in total, of the seven vehicles involved; as compared to 6,650 MJ per single vehicle or 46,550 MJ in total, of the seven vehicles involved. It seems that the value suggested by the Efectis Nederland BV research team is just over the standard deviation region from the simulated values for both single (difference of 134 MJ from the higher standard deviation region) and the total of seven vehicles (difference of 938 MJ from the higher standard deviation region).

It was also found that the average values for all predicted time of ignition from the simulation are behind by at least more than double the time of ignition developed by Efectis Nederland BV. However, Comparing the time of ignition by Efectis with the lower standard deviation for both scenarios show a closer match where for Scenario 1 Pattern 2 the developed time of ignition by Efectis even match within the standard deviation range for order of ignition of Vehicle 6 and 7.

The analysis from the work has shown that UCVFire was able to recreate the Lloydstraat Car Park fire scenario, which was in agreement with the reported timeline of the fire, as well as to identify possible fire loads for each of the vehicles using probabilistic distribution. The analysis indicates that Scenario 1 is the most possible scenario to occur during the real fire incident, based on the tallied information of the fire by the simulation results. By indicating Scenario 1 as the most possible scenario, this means that the first vehicle to possibly be ignited in the real fire incident was Vehicle 4, i.e., Ford Mondeo.

One of the advantages of using UCVFire is its capability to predict ignition times based on the design fire of vehicles, eliminating the uncertainty of selecting ignition times manually. Another advantage of the approach is that it is based on probabilistic rather than deterministic approaches, such that the results can be shown as the range of possibilities for the fire to occur.

Based on this analysis, the probabilistic approach seems to work well for forensic fire investigation purposes. It does give an alternative from the deterministic approach to conduct such research. In the future, researchers can adopt the approach for the use in fire investigations, to find out the desired information regarding multiple vehicle car park fires using this probabilistic approach. However, it has to be noted that the attempt was based on only one incident, hence, in the future, further analyses using the approach has to be conducted in order to better assess the robustness of the approach.

Chapter 13 FIRE RISK ANALYSIS USING ENHANCED ANALYTICAL DATA

13.1 Introduction

Chapter 4 discusses using probabilistic quantitative risk analysis model to determine appropriate fire scenarios for car parking buildings. The model i.e. fire risk analysis model which is a dimensionless measurement of comparison, defined as fire risk level depends on number of components. However in the conclusion, due to the limitation of supported data for several components to be used in the model there is the need to get enhanced analytical data to gain the confidence of the results from the model.

Therefore, in order to obtain the enhanced analytical data, several separate works have been conducted up until this chapter. The main objective of this chapter is to combine the enhanced analytical inputs into the probabilistic quantitative risk analysis model and produce similar analysis to that carried out in Chapter 4.

This chapter provides enhanced analytical analysis and data for two components of the model i.e. the fire severity component and vehicle fire involvement probability component. Then, using these data, analysis on fire risk level and sensitivity analyses are conducted. In the end, conclusions are drawn out from the analysis.

13.2 Fire severity component

The fire severity component of the model is represented by the vehicle peak heat release rate which means that the higher peak heat release rate contribute to a higher fire risk level. In Chapter 4, it was assumed that all vehicles in a cluster catch fire simultaneously. For example, if there are three vehicles in a cluster, it was assumed that all three vehicle will catch fire simultaneously, thus tripling the peak heat release rate due to combination of every single vehicle heat release rate curve at the same ignition time. This assumption seems to be highly unlikely based on the statistics mentioned in Section 4.2.3 where most of the reported case of vehicle fire involved only one vehicle. Even if there were cases of more than a vehicle involved, it was unlikely to have of the vehicles to catch fire simultaneously under normal circumstances.

This chapter will seek to improve on the previous assumption by examining the fire growth characteristics of vehicle fires rather than only considering combination of the peak heat release rate of single vehicle. It is expected from multiple vehicle fires that after fire grows in

the first vehicle, it will spread to second vehicle and by the time the fire spreads to the third vehicle, it is possible that the fire of the first vehicle is declining. In other words, this is a phenomenon which is known as travelling fires [86] in which a fire in a large space burns over limited area at any one time.

To analyse the fire growth characteristics, UCVFire simulation tool explained in Chapter 10 is used. For this analysis, the fire risk level is still accounted on the basis of peak heat release rate. This means that, for a particular fire scenario simulated, the highest peak from the design fire curve is considered as the highest fire risk level. Since UCVFire uses probabilistic approach, the analysis is performed in series of iterations and the average peak heat release rate obtained from the iterations is used.

In using the tool, some assumptions on the input parameters for running the simulation have to be made. For each of the simulation there are fixed parameters and for this analysis there is only one variable parameter i.e. number of vehicles in a cluster. Thus, for the fixed parameters in the simulation, the list of assumptions is listed in Table 13-1.

Table 13-1: The fixed parameters for fire growth characteristics simulation

Parameter	Value
Vehicle width	1.6 m
Distance between vehicles	0.7 m
Effective distance	2.3 m
Parking width	2.3 m
No. of iterations	10,000 times
Distribution of vehicle fleet	European & USA

For the vehicle width, an assumed initial value of 1.6 m is going to be used where it is based on the average width of several vehicles in the Passenger Car: Mini classification. This assumed width is chosen as to produce the lowest reasonable effective distance. The distance between vehicles is taken as 0.7 m as what mentioned by de Feijter and Breunese [43] for a generic distance. The addition of the vehicle width and the distance between vehicles equates to 2.3 m which is the effective distance. The effective distance is essentially the parking width, and from Table 11-1 in Chapter 11, the range of parking width from literature ranges from 2.2 – 3.2 m. Thus, it can be said that the 2.3 m effective distance being at the lower end of the range could represent worst case scenario.

The other parameters such as the radiative fraction for the PSM and first component to burn and its attributes will follow what has been decided in Chapter 7. Another important assumption for this fire characteristic analysis is the arrangement of the vehicle during the fire. This is better illustrated in Figure 13-1 which is an example of five vehicle cluster scenario. To maximize the consequence, it is assumed that for each simulation iteration, the first vehicle ignited would be the vehicle in the middle of a single row. Apart from maximizing the consequence, the other reason why the first vehicle ignited is in the middle, is somewhat representing a two row fire since the simulation tool does not allow for a two row simulation at the moment.

For the variable parameter, all the numbers are decided to be odd numbers considering the vehicle in the middle to be ignited and spread to even number of vehicles to its left and right. For this chapter, the number of vehicles to be involved in a scenario is varied from 1 to 29 which is the maximum odd number of vehicles permitted in the tool.

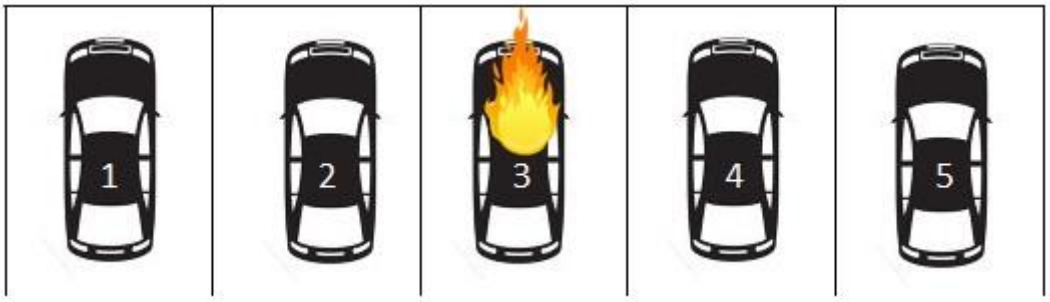

Figure 13-1: Example of five vehicle cluster scenario

13.2.1 Fire growth characteristics analysis results

The results of the simulations are presented in the form of a plot of average peak heat release rate against vehicle cluster which is shown in Figure 13-2. From the plot, it is evident that as the number of vehicles in a cluster increases the average peak heat release rate also increases in logarithmic trend. The logarithmic trend shows that it agrees with the hypothesis of a travelling fire that by the time fire spreads to the subsequent vehicle, the fire in the previous vehicle is already declining. A logarithmic trendline fitted through the points gives an R^2 value of 0.99 which indicates a good fit of the points and the equation of the logarithmic trendline is given as;

$$y = 6197 \ln(x) + 6158$$

Equation 13-1

This equation can be used to extrapolate the peak heat release rate, y for xth number of vehicles in further analysis. Also displayed in the plot are the maximum and minimum peak heat release rate value obtained from the 10,000 iterations.

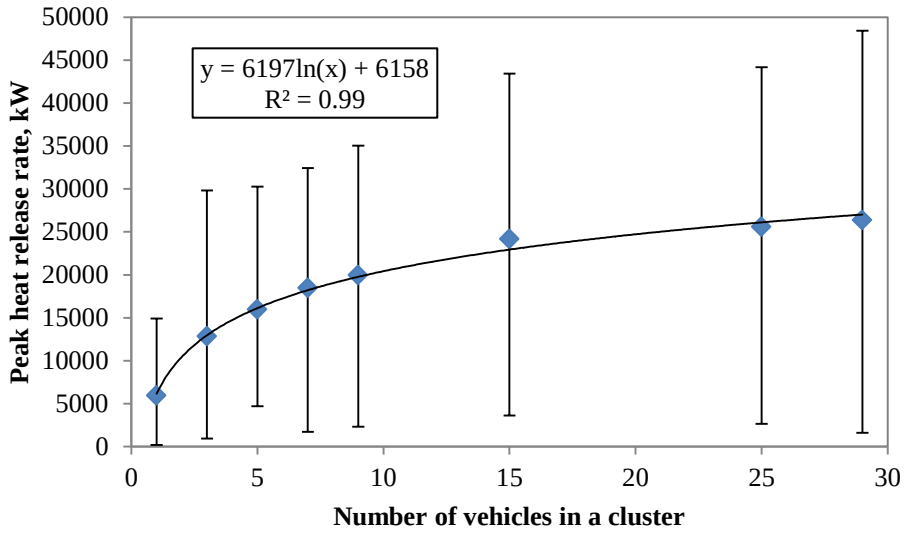

Figure 13-2: Results from series of simulations for fire characteristics analysis

Using Equation 13-1, the expected average peak heat release rate for 1 to 30 vehicles in a cluster can be compared with a plot of assumed all vehicles in the cluster catch fire simultaneously (which the values is taken from Figure 4-7 in Chapter 4). The comparison of the plots is shown in Figure 13-3. The red squares in the figure are the peak heat release rate for all vehicles in the cluster catches fire simultaneously where it follows linear trend while the blue diamonds in the figure are the peak heat release rate using Equation 13-1. It is obvious from the comparison that the difference between both heat release rates will be increasing as the number of vehicles in a cluster increases. This means that the usage of the fire growth characteristics as a consequence component in the probabilistic quantitative risk analysis model will significantly change the fire risk level. The incorporation into the risk model is addressed later in Section 13.4.

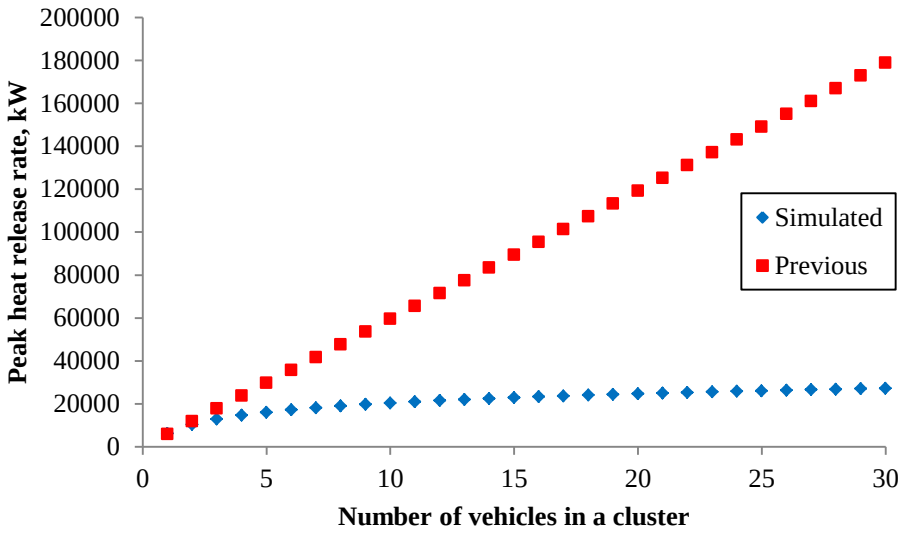

Figure 13-3: Comparison of plot resulted from the simulation and the plot from Figure 4-7 in Chapter 4

13.3 Vehicle fire involvement probability

This component is the probability of how likely a vehicle is going to be ignited and then spread to the neighbouring vehicle. In Chapter 4, this component entirely uses statistics from past vehicle fire incidents in car parking buildings as input to the probabilistic quantitative risk analysis model. In Chapter 11, an analytical approach to determine whether fire will spread to consequent vehicle(s) was developed. The approach is able to generate the probability of fire to spread to consequent vehicle(s), hence is applied into this chapter. However, the approach only able to generate the probability of the consequent vehicle given the first vehicle is already burning. Therefore, the approach is coupled with the probability of the first vehicle to ignite from the statistics in Section 4.2.3 to give what is called as the vehicle involvement probability.

Work in Chapter 4 uses combined statistics collected from several resources to form the vehicle involvement probability due to too little information on vehicle fire in car park reports. Therefore, the combination of data can only be made up until 7 vehicles because it was the most vehicles involved in a fire reported. In the previous work, from the trend line fitting of the points of probability of incidents against number of vehicles, a power law trend line was fitted and an equation is obtained. The equation was given as;

$$P(x) = 2 \times 10^{-6} x^{-2.7}$$

Equation 13-2

where $P(x)$ is the probability of multiple vehicle fires and x is the number of vehicles involved in the fire. This equation was used to extrapolate the probability of multiple vehicle fires for more than 7 to get the vehicle involvement probability.

Using the UCVFire simulation tool to get the probability of fire spread from a vehicle to another vehicle in car parks, a simulation over certain number of iterations is performed for a chosen number of vehicles in a cluster. The outcomes of the simulations are presented in the form of how many times the fire spreads to all vehicles involved for that chosen number of vehicles in a cluster. For example, consider three vehicles in a cluster, if the fire involved all three vehicles it will be counted as one occurrence. This number of occurrences divided over the number of iterations will be the probability of fire spread for the chosen number of vehicles.

In the simulation, fixed parameters for the input are listed in Table 13-1 and the variable parameter is the number of vehicles involved in a cluster. To be consistent, parameters such as vehicle width, distance between vehicles, effective distance, number of iterations, and distribution of vehicle fleet followed on what have been decided in Section 13.2.1. Other parameters such as the radiative fraction for the PSM and first component to burn and its attributes also follow what has been decided in earlier in Section 13.2.

13.3.1 Fire spread probability analysis results

The results of the simulations are presented in the form of a plot of probability if fire to spread to all vehicles in a cluster against vehicle cluster which is shown in Figure 13-4. From the plot, it is obvious that the probability decreases as the number of vehicles in a cluster increases. As number of vehicles in a cluster increases, the number of probability distributions involved in the simulation increases, thus decreasing the probability of fire to spread to all vehicles. A linear trend line was fitted to the series of probability and Equation 13-3 with an R^2 of 0.93 was obtained.

$$y = -0.0099x + 0.88$$

Equation 13-3

Since there is no negative probability, the equation is only true to up until 88 of vehicles in a cluster. In other words, there is zero probability of fire to spread to all vehicles if there are 89 or more vehicles in a cluster. This in itself is an important finding where it is impossible to have 89 vehicles to be involved in a fire according to this model, thus this becomes the maximum limit of the number of vehicles for design fire scenario in a car park.

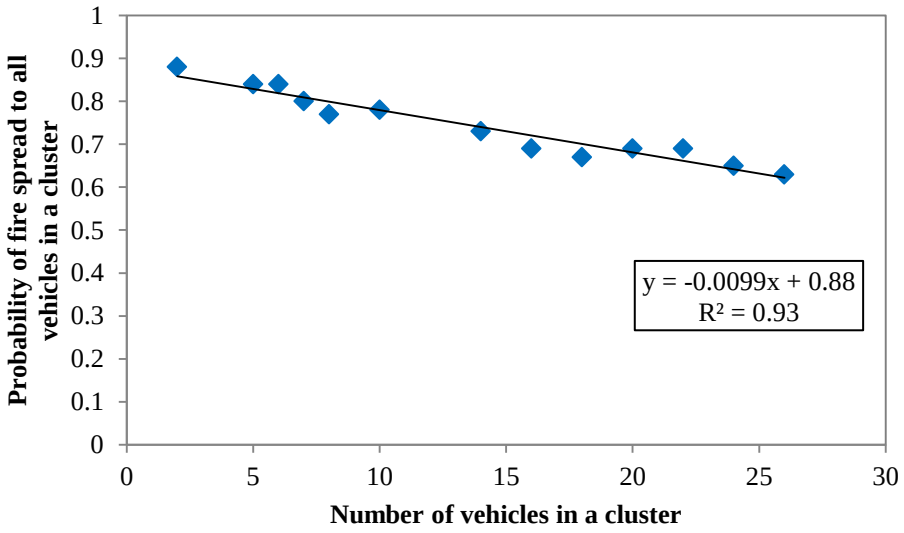

Figure 13-4: Results from series of simulations for fire spread probability analysis

From the analysis in Section 4.2.3, the probability of a single vehicle to catch fire is 2.76×10^{-6} per year. This value is used as the probability of the first vehicle to ignite thus coupled with Equation 13-3. This coupled probability becomes the probability of fire to ignite the first vehicle and spreads to all vehicles in a cluster which is defined as the vehicle involvement probability.

For comparison purposes, the predicted probabilities of fire spread using Equation 13-2 were also coupled with the probability of a single vehicle to catch fire. Figure 13-5 shows the comparison between the vehicle fire involvement from this chapter and previous work from Chapter 4. The red squares displayed are the vehicle involvement probability obtained from this chapter while the blue diamonds are the vehicle involvement probability using Equation 13-2 which effectively the values from Section 4.2.3. From the plot, it is obvious that the differences between both sets of probabilities are around ten times larger, thus will significantly change the fire risk level if incorporated into the probabilistic quantitative risk analysis model. The incorporation into the risk model is addressed later in the next section i.e. Section 13.4.

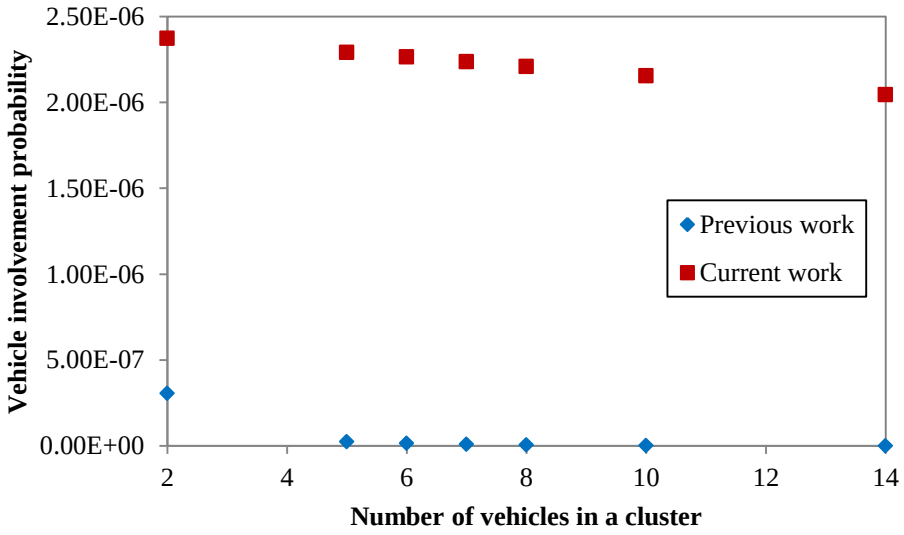

Figure 13-5: Comparison between the vehicle fire involvement from this chapter and previous work

13.4 Fire risk analysis using the enhanced analytical data

Previously in Section 4.4, an example of application of the fire risk analysis approach was demonstrated using the input of 100 parking spaces car park, with 75% parking occupancy i.e. 75 vehicles, 10,000 iterations for the parking simulation model, two-row parking arrangement, and tendency weightage of 0.9. The definitions of tendency weightage and parking occupancy are described in Section 4.2.1 and 4.3.2 respectively.

For comparison reasons, the same identical parameters are used on the enhanced analytical data. Thus, using the same cluster size probability obtained in Table 4-5 in Chapter 4 and enhanced data of vehicle involvement probability and fire severity component, the modified fire risk analysis is shown in Table 13-2. For this purpose, the fire spread probability from Equation 13-3 was used and coupled with the probability of a single vehicle to catch fire which is 2.76×10^{-6} per year to get the vehicle involvement probability for the respective number of vehicles. For the fire severity component, Equation 13-1 was used to get the average peak heat release rate for the respective number of vehicles.

Table 13-2: Modified fire risk analysis for 100 parking spaces car park with 75% occupancy

Number of vehicles	Cluster size probability	Vehicle involvement probability	Fire severity (kW)	Fire risk level
1	0.041	2.76×10^{-6}	6158	7.00×10^{-4}
2	0.032	2.37×10^{-6}	10453	7.85×10^{-4}
3	0.042	2.35×10^{-6}	12966	1.28×10^{-3}
4	0.038	2.32×10^{-6}	14749	1.31×10^{-3}
5	0.033	2.29×10^{-6}	16132	1.21×10^{-3}
6	0.029	2.26×10^{-6}	17262	1.14×10^{-3}
7	0.020	2.24×10^{-6}	18217	8.14×10^{-4}
8	0.016	2.21×10^{-6}	19044	6.73×10^{-4}
9	0.013	2.18×10^{-6}	19774	5.70×10^{-4}
10	0.007	2.16×10^{-6}	20427	3.05×10^{-4}
11	0.006	2.13×10^{-6}	21018	2.89×10^{-4}
12	0.005	2.10×10^{-6}	21557	2.17×10^{-4}
13	0.003	2.07×10^{-6}	22053	1.27×10^{-4}
14	0.002	2.05×10^{-6}	22512	1.03×10^{-4}
15	0.001	2.02×10^{-6}	22940	3.71×10^{-5}
18	0.000	1.94×10^{-6}	24070	2.24×10^{-5}
20	0.001	1.88×10^{-6}	24723	2.48×10^{-5}
48	0.001	1.12×10^{-6}	30148	4.31×10^{-5}
49	0.004	1.09×10^{-6}	30276	1.29×10^{-4}
50	0.027	1.06×10^{-6}	30401	8.61×10^{-4}
51	0.174	1.04×10^{-6}	30524	5.50×10^{-3}
52	0.135	1.01×10^{-6}	30644	4.15×10^{-3}
53	0.099	9.81×10^{-7}	30762	2.98×10^{-3}
54	0.071	9.53×10^{-7}	30878	2.08×10^{-3}
55	0.059	9.26×10^{-7}	30991	1.68×10^{-3}
56	0.043	8.99×10^{-7}	31103	1.21×10^{-3}
57	0.029	8.71×10^{-7}	31213	7.85×10^{-4}
58	0.023	8.44×10^{-7}	31321	6.13×10^{-4}
59	0.016	8.17×10^{-7}	31426	4.04×10^{-4}
60	0.013	7.89×10^{-7}	31531	3.19×10^{-4}
61	0.007	7.62×10^{-7}	31633	1.57×10^{-4}
62	0.005	7.35×10^{-7}	31734	1.16×10^{-4}
63	0.005	7.07×10^{-7}	31833	1.13×10^{-4}
64	0.002	6.80×10^{-7}	31931	3.71×10^{-5}

The comparison of the fire risk level from the modified fire risk analysis and from previous work (Figure 4-9) is shown in Figure 13-6. The highest fire risk level from the previous work is 4.90×10^{-4} which is for a single vehicle. This was due to the fire risk analysis is highly governed by the vehicle involvement probability which decreases significantly as the number of vehicles in a cluster increases. The highest fire risk level obtained from this chapter is 5.50×10^{-3} which is for 51 vehicles. It seems that from the current analysis, the cluster size probability becomes a substantial parameter in determining the fire risk level.

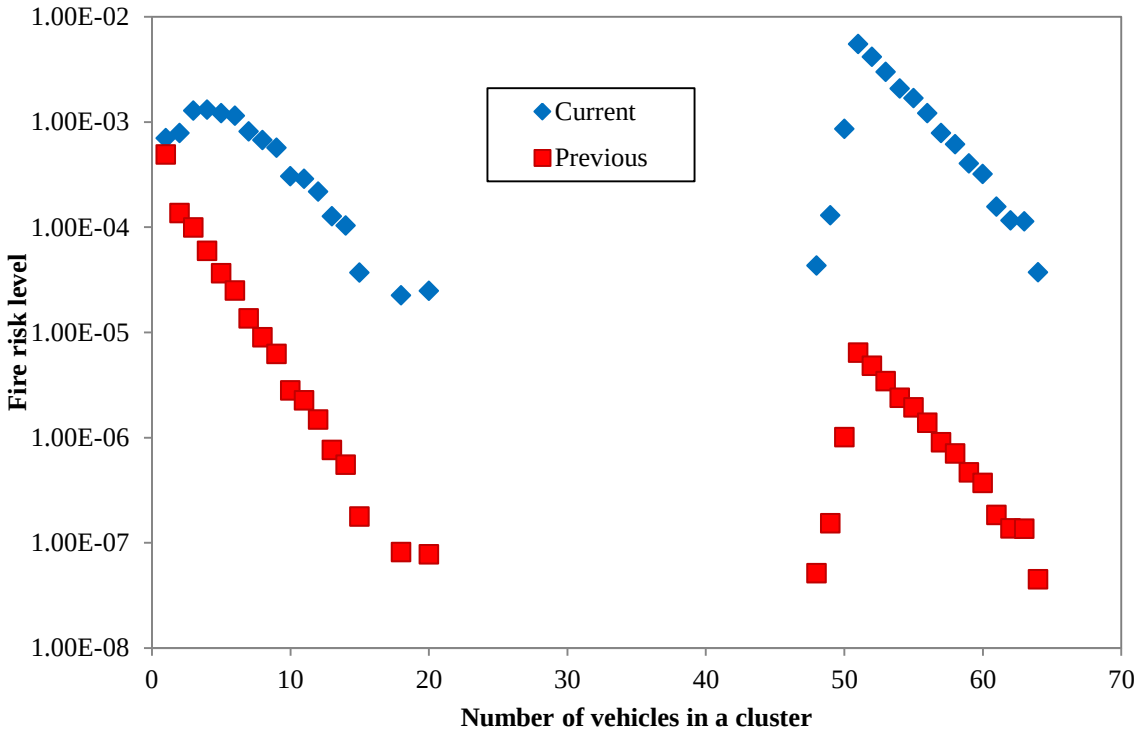

Figure 13-6: Comparison of the fire risk level from previous work and current analysis

13.4.1 Sensitivity analyses of input parameters

Sensitivity analyses on varying the parking occupancy and tendency factor weightage were conducted to assess the effect on the outcomes of the fire risk analysis. For the sensitivity analyses, the fixed parameters for the analysis were 100 parking spaces car park and 10,000 iterations for each simulation.

13.4.1.1 Variation of the parking occupancy

Figure 13-7 shows the plot of fire risk level for parking occupancy variation of 50%, 60%, 70%, 80%, and 90% where the tendency factor is fixed at 0.7. As for comparison purpose in this analysis, a plot of cluster size probability for parking occupancy variation of 50%, 60%, 70%, 80%, and 90% is shown in Figure 13-8.

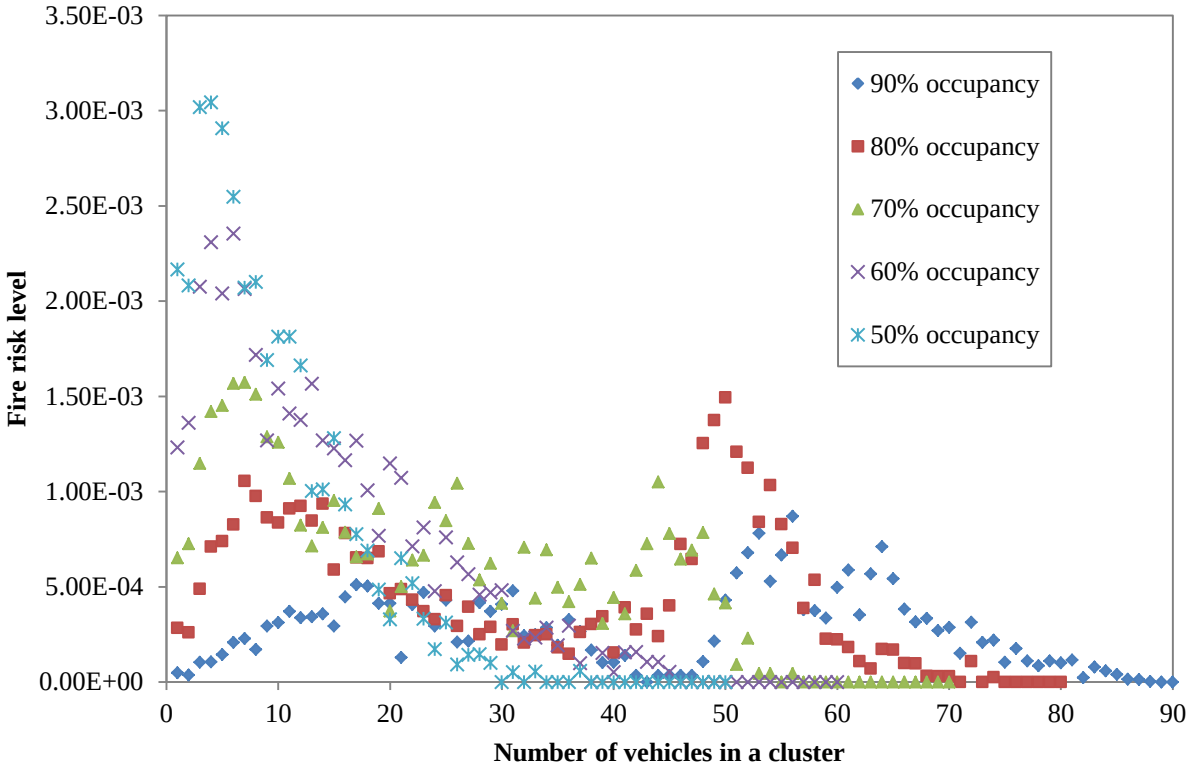

Figure 13-7: Sensitivity analysis on different parking occupancy

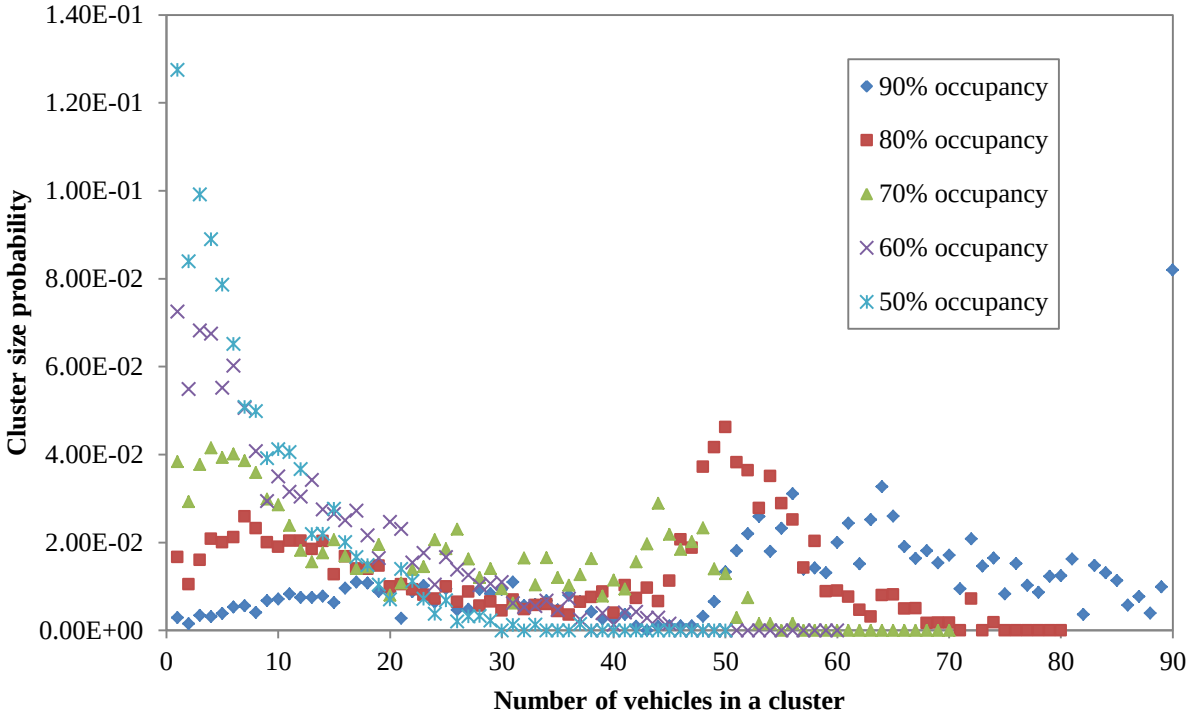

Figure 13-8: Cluster size probability for different parking occupancies

From Figure 13-7, it can be seen that the highest fire risk level for 90% parking occupancy is 8.70×10^{-4} for 56 vehicles in a cluster even though the largest cluster size probability is for 90

vehicles in a cluster. This is because the vehicle involvement probability for 89 or more vehicles in a cluster is zero, hence brings down the fire risk level to zero. At 80% parking occupancy, the highest fire risk level is 1.49×10^{-3} for 50 vehicles in a cluster due to largest cluster size probability of 50 vehicles in a cluster.

For 70% parking occupancy, the highest fire risk level is 1.57×10^{-3} for seven vehicles in a cluster. For this parking occupancy, the largest cluster size probability is the highest for four vehicles. However, due to high fire severity for seven vehicles in a cluster, thus gives the highest fire risk level for this occupancy is for seven vehicles in a cluster. Likewise for 60% parking occupancy, the highest fire risk level is for six vehicles in a cluster even though the cluster size probability for one vehicle was the largest. This occurred because the fire severity for six vehicles in a cluster was substantially higher than of for one vehicle. For 50%, 60%, and 70% occupancy, the fire risk level obtained is irrespective of cluster size probability since it is more dependent to the fire severity component.

Thus, an extra analysis was conducted to see the effect at which occupancy the vehicle cluster size probability is important to influence the fire risk level. For this purpose, using the same tendency factor of 0.7, fire risk level for smaller parking occupancy variation of 75%, 76%, and 77% were compared in Figure 13-9. From the figure, it can be seen that for 76% parking occupancy, the highest fire risk level is 1.45×10^{-3} for 48 vehicles in a cluster which is indeed the highest cluster size probability. However, for 75% parking occupancy, the highest fire risk level is 1.35×10^{-3} for seven vehicles in a cluster even though the cluster size probability for 51 vehicles in a cluster was the largest. This occurred because as the parking occupancy decreases, there is higher chance of vehicles to be grouped in smaller clusters as there are more empty spaces for vehicles to be distributed, hence increasing the cluster size probability for smaller clusters.

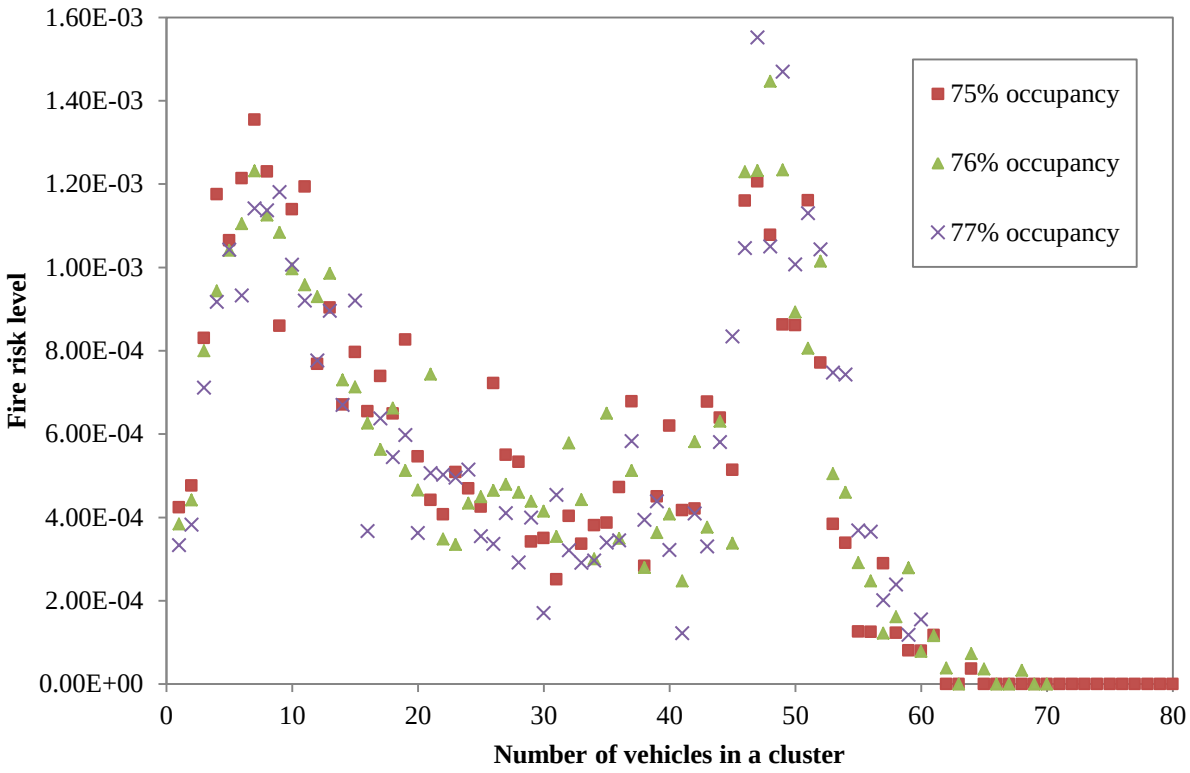

Figure 13-9: Extra analysis for variation of parking occupancy

As a conclusion for this analysis, for parking occupancy bigger than 75%, the fire risk level depends heavily on vehicles cluster size probability, where larger parking occupancy will more likely to produce higher probability of bigger cluster size. However, for parking occupancy of less or equal to 75%, the tendency of vehicles to be grouped in smaller clusters increases, thus the fire risk level is much more reliant on the fire severity component. However, this conclusion is only true, for which the tendency factor is fixed at 0.7.

13.4.1.2 Variation of tendency factor weightage

Another sensitivity analysis conducted was the variation of tendency factor weightage. In the analysis, the parking occupancy was fixed at 75% and the tendency factors weightage varied were 0.7, 0.8 and 0.9. The results from the analysis are shown in Figure 13-10. It can be seen from the figure the highest fire risk level is 5.29×10^{-3} for 51 vehicles in a cluster at 0.9 tendency factor weightage. At 0.8 weightage, the highest fire risk level is 2.84×10^{-3} for 51 vehicles in a cluster and at 0.7 weightage, the highest fire risk level is 1.35×10^{-3} which is for 7 vehicles in a cluster.

This shows that the higher the tendency weightage, the higher then tendency of more vehicles to be grouped in a cluster, hence increasing the fire risk level as expected. This was due to the higher the weightage, the likelihood of vehicles to be parked in a cluster to be high because vehicles tend to be distributed at one end of the parking. Therefore, it can be concluded that the higher the weightage, the higher the probability of having cluster size for larger number of vehicles in a cluster, hence the high fire risk level.

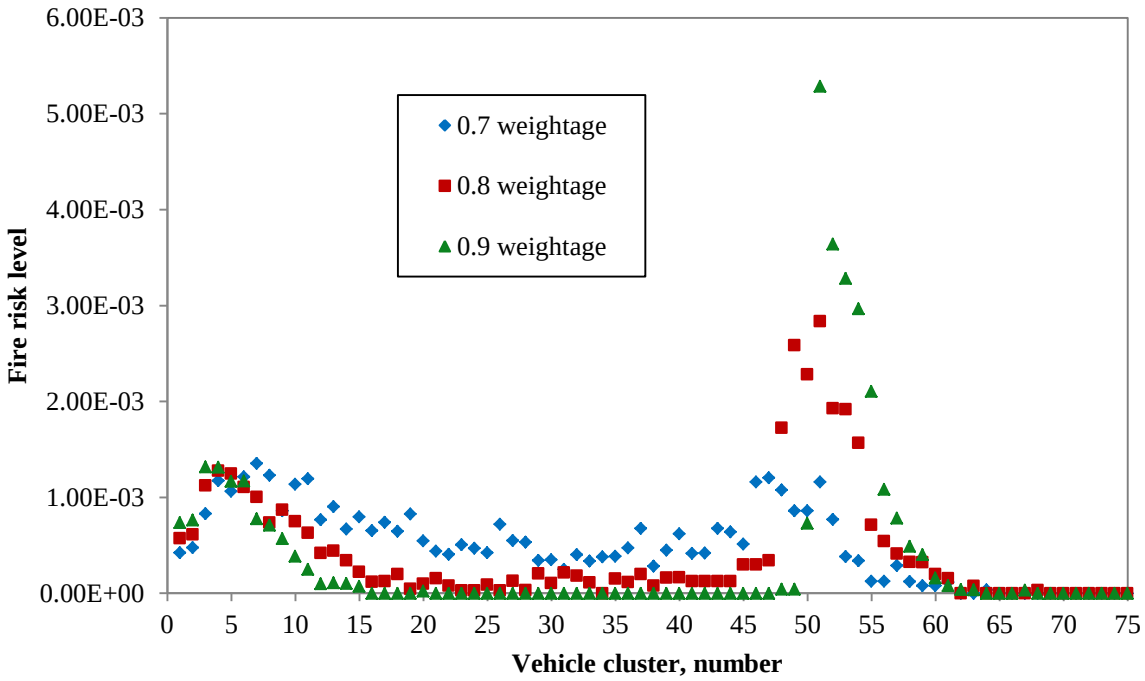

Figure 13-10: Sensitivity analysis on tendency factor

13.5 Conclusion and discussion

The aim of this chapter was to assess the effect of using enhanced analytical analysis and data for two components i.e. the fire severity component and vehicle fire involvement probability component to the fire risk analysis.

It was found from the fire growth characteristics analysis that as the number of vehicles in a cluster increases, the average peak heat release rate also increases in logarithmic trend (Figure 13-2). The logarithmic trend shows that it agrees with the hypothesis of a travelling fire that by the time fire spreads to the subsequent vehicle, the fire in the previous vehicle is already declining. Therefore, the application of the fire growth characteristics as fire severity component into the fire risk analysis will significantly reduce the peak heat release rates as compared to the previous assumption of linear accumulation of peak heat release rates as the

number of vehicles increases which indicates a steady linear increase resulting higher peak heat release rates (Figure 13-3).

It was also found in the analysis that the probability of fire spread to all vehicles in a cluster gradually decreases as the number of vehicles in a cluster increases. The decrease follows the equation of $y = -0.0099x + 0.88$ where y is the probability of fire to spread and x is the number of vehicles in a cluster. This means that there is zero probability of fire to spread to all vehicles if there are 89 or more vehicles in a cluster (Figure 13-4). This is as opposed to the findings in Chapter 4 where the vehicle involvement probability is using the power law correlation from the statistics which shows significant decrease in the order of magnitude as the number of vehicles in a cluster increases.

This chapter has shown that from the analyses, there is no simple answer to determine the most suitable vehicle fire scenario for the purpose of design of car parking building. It was found that the vehicle cluster size probability component is important in determining vehicle fire scenario. This component is dependent on two parameters; the parking occupancy and tendency factor weightage. It was found in the analyses that the variation of these two parameters will eventually change the vehicle cluster size probability, hence will affect the fire risk level.

As for example for parking occupancy analysis, with the case of 100 parking spaces car park, 10,000 iterations for the parking simulation model, two-row parking arrangement, tendency weightage of 0.7, and all of the assumptions in order to run the simulation e.g. the parking pace width and length, fixed distance between vehicles, etc. The highest fire risk level from the previous work in Chapter 4 is 4.90×10^{-4} which is for a single vehicle. This was due to the fire risk analysis is highly governed by the vehicle involvement probability which decreases significantly as the number of vehicles in a cluster increases. The highest fire risk level obtained from this chapter is 5.50×10^{-3} which is for 51 vehicles. It seems that from the current analysis, the cluster size probability becomes a substantial parameter in determining the fire risk level.

For parking occupancy bigger than 75%, the fire risk level depends heavily on vehicles cluster size probability, where larger parking occupancy will more likely to produce higher probability of bigger cluster size. However, for parking occupancy of less or equal to 75%,

the tendency of vehicles to be grouped in smaller clusters increases, thus the fire risk level is much more reliant on the fire severity component. It was found that for the example analysis that at 70% and 75% parking occupancy, the reasonable worst case scenario is for seven vehicles in a cluster. This is interestingly somewhat similar to the one of the design fire scenario from the literature i.e. Scenario 5 which has seven vehicles parked in a single row (Figure 1-1).

For the tendency factor weightage sensitivity analysis, it can be concluded that the higher the weightage, the higher the probability of having cluster size for larger number of vehicles in a cluster, hence the high fire risk level.

It is arguable whether one would design a car park with full occupancy of the spaces available and not for lesser occupancy but it can be proposed that to design a car park, an average parking occupancy or the most likely parking occupancy is used. This though is subject to further research in which will not be undertaken in this study. Similar for the tendency factor weightage, this factor was initially based on an empirical assumption where it was assumed that vehicles tend to park at one end of the model to represent a distance variable. This also is subject to further analysis in which will not be undertaken in this study.

As a conclusion, given a specific design of a car park with known number of parking spaces, expected parking occupancy, and tendency factor weightage, one will be able to determine the suitable vehicle fire scenario using the fire risk analysis model.

Chapter 14 CONCLUSIONS AND RECOMMENDATIONS FOR FUTURE WORK

14.1 Conclusions

The main objective of the research project was to formulate an approach that is able to develop appropriate design fire scenarios for vehicles in car park buildings using the risk-based approach. The approach has been formulated after series of analyses from past experiments, analyses of various statistics, and simulations of vehicle fires were conducted.

14.1.1 Design fire scenario for car parking buildings

A simple probabilistic risk analysis model to determine appropriate fire scenarios for car parking buildings was introduced in Chapter 4. The approach introduces a dimensionless measurement defined as fire risk level by multiplying probability by consequence. The model is able to develop of vehicle fire scenarios for car parking buildings given the key variables for the fire risk analysis are known. The key variables are vehicle cluster size probability, vehicle classification, vehicle fire involvement probability, and the severity of vehicle fires.

An analysis initially done in Chapter 4 assumed that all vehicles in a scenario catch fire simultaneously. The work also uses the statistics from literature for the estimation of the vehicle fire involvement probability. These two components then are enhanced through several analyses in Task 2. With the enhanced components available, analysis is performed in Chapter 13.

It was found from the parking occupancy analysis in Chapter 13, with the case of 100 parking spaces car park, 10,000 iterations for the parking simulation model, two-row parking arrangement, tendency weightage of 0.7 and all of the assumptions in order to run the simulation e.g. the parking pace width and length, fixed distance between vehicles, etc. The highest fire risk level from Chapter 4 is 4.90×10^{-4} which is for a single vehicle. This was due to the fire risk analysis is highly governed by the vehicle involvement probability which decreases significantly as the number of vehicles in a cluster increases. The highest fire risk level obtained from Chapter 13 is 5.50×10^{-3} which is for 51 vehicles. It seems that from the analysis in Chapter 13, the cluster size probability becomes a substantial parameter in determining the fire risk level.

In the same example (work in Chapter 13), for parking occupancy bigger than 75%, the fire risk level depends heavily on vehicles cluster size probability, where larger parking

occupancy will more likely to produce higher probability of bigger cluster size. However, for parking occupancy of less or equal to 75%, the tendency of vehicles to be grouped in smaller clusters increases, thus the fire risk level is much more reliant on the fire severity component. It was found that for the example analysis that at 70% and 75% parking occupancy, the reasonable worst case scenario is for seven vehicles in a cluster. This is interestingly somewhat similar to the one of the design fire scenario from the literature i.e. Scenario 5 which has seven vehicles parked in a single row (Figure 1-1).

It was found from the analyses in Chapter 13 that the vehicle cluster size probability component is an important component in determining vehicle fire scenario. This component is dependent on two parameters; the parking occupancy and tendency factor weightage. It was found in the analyses that the variation of these two parameters will eventually change the vehicle cluster size probability, hence will affect the fire risk level.

As a conclusion, given a specific design of a car park with known number of parking spaces, expected parking occupancy, and tendency factor weightage, one will be able to determine the suitable design fire scenario using the fire risk analysis model. Overall, the development of the probabilistic method from this thesis gives a strategic approach of obtaining design fire scenarios for different parameters.

14.1.2 Flow diagram of the process of developing design fire scenarios

This section provides the information on the overall outcome of the research. The outcome is presented in a flow diagram which explains the process of developing appropriate design fire scenarios for vehicles in car park buildings in stages. The flow diagram is shown in Figure 14-1 and followed by Figure 14-2.

From the flow diagram of the process, it infers that the process integrates numbers probability distributions. Therefore, the likelihood of getting similar results for each iteration is smaller. The layer of integration of the probability distributions involved in the process is shown in Figure 14-3. There are three main layers of the probability distributions at this stage i.e. the first layer; the vehicle parking distribution, the second layer; vehicle types distribution, and the third layer; design fire distribution where it has three separate distributions to construct a design fire for a single vehicle.

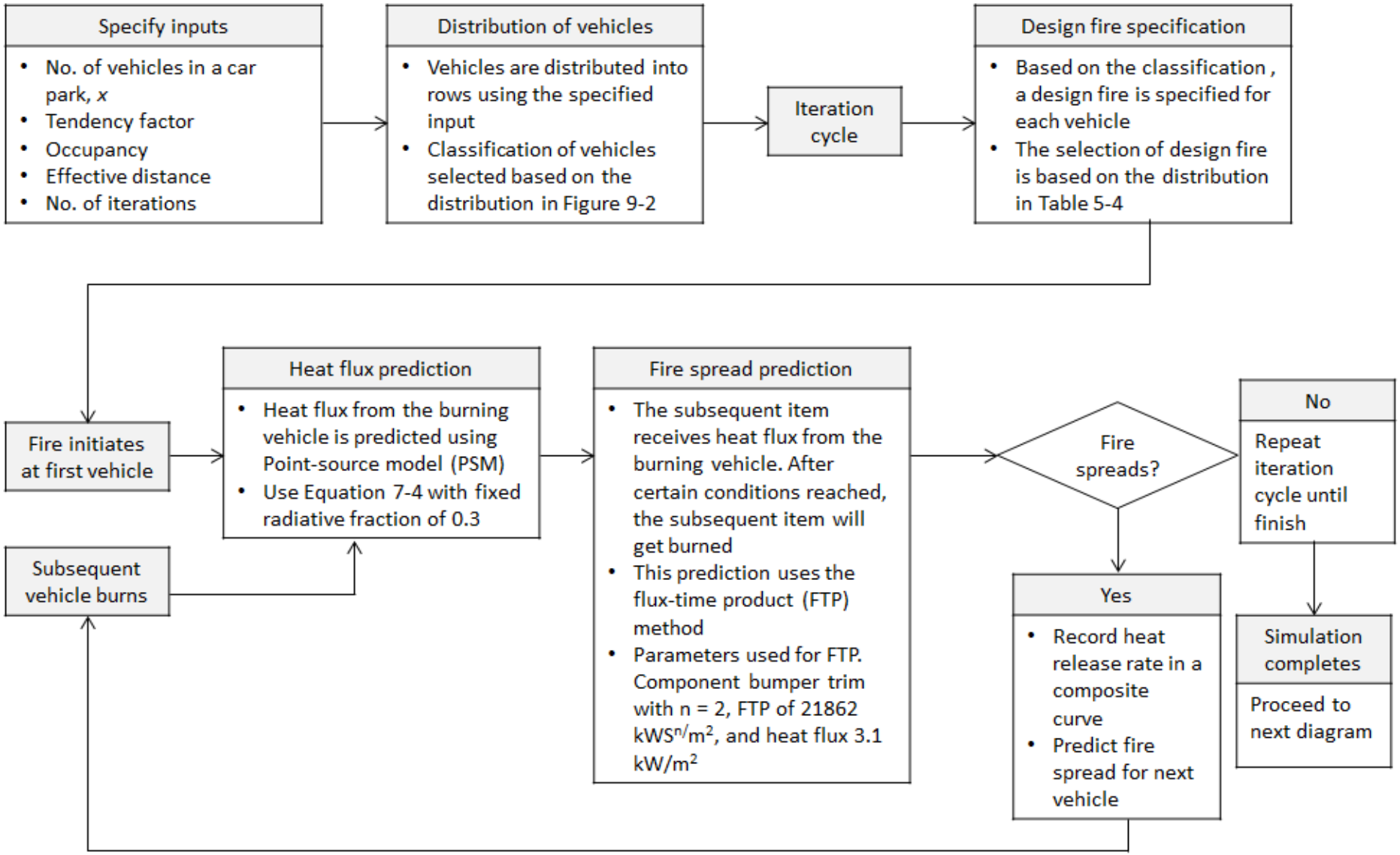

Figure 14-1: Flow diagram of the process of developing design fire scenarios

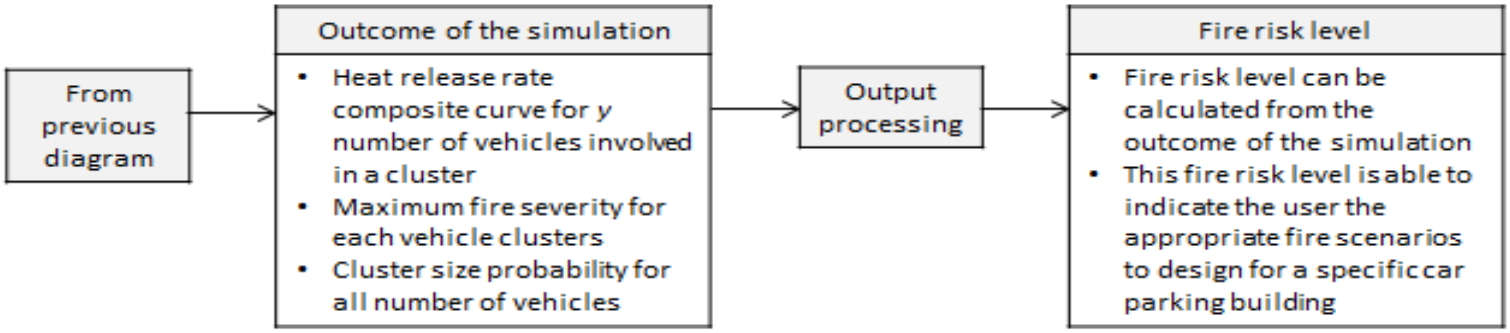

Figure 14-2: Flow diagram of the process of developing design fire scenarios

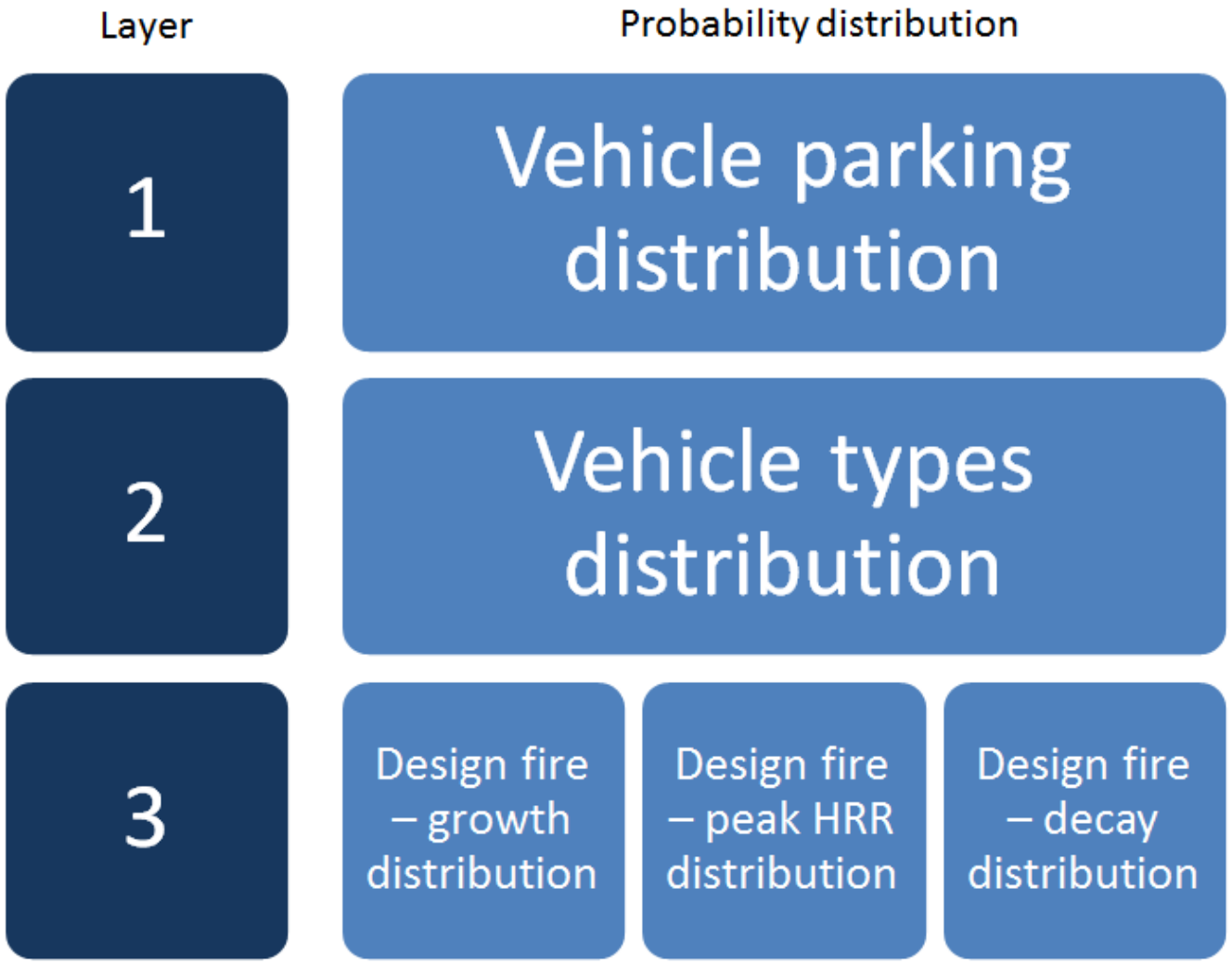

Figure 14-3: Layer of probability distributions during the process.

14.2 Other conclusions

In addition to the conclusion for the design fire scenario, the following conclusions have been reached as an outcome of this research project. These conclusions can be used straightaway for the purpose of vehicle fire research, car parking building research, design fire research, structural fire research, and fire spread research.

In terms of practicality for the design of car parking buildings, Section 14.2.6 and Section 14.2.7 give two of the most important findings. Car parking designers and practitioners are able to use the information obtained from the findings straightaway to design a car parking building.

14.1.1 Fire severity characteristics probability distributions

Experimental data for single passenger vehicles have been obtained from the literature. Grouping these experiments by the curb weight of the vehicles forms a useful classification system that can be related to vehicle population and severity where the severity is defined here as the peak heat release rate, the time to reach peak heat release rate and total energy released.

Weibull distribution functions have been obtained for the curb weights up to the Passenger car: Medium classification and the combination of these classes. Due to lack of data for analysis, the user may use the extrapolation technique from the lighter curb weight classes to obtain the probability distributions characteristics for Passenger car: Heavy classification. The summary of the distributions are given as follows;

Table 14-1: The summary distributions for fire severity characteristics

		Peak heat release rate (kW)		Time to peak (min)		Total energy released (MJ)	
Curb weight class	Distribution parameter	κ	θ	κ	θ	κ	θ
	Mini	5.19	3809	2.79	19.1	4.02	3222
	Light	1.66	5078	3.03	22.0	2.93	5009
	Compact	2.40	4691	2.60	42.8	7.49	5591
	Medium	3.18	7688	6.55	39.9	14.53	6648
	Combined	2.03	5256	2.12	31.3	3.23	5233

These distributions can be used to assess single-vehicle peak heat release rate, time to reach peak heat release rate and total energy released in a probabilistic manner which can aid designers wishing to perform probabilistic assessment analysis for cost-risk-optimized fire protection design.

14.2.1 Characterisation of design fire for multiple vehicle fires

This thesis has used published experimental data from single vehicle experiments to determine the combination of a growth and a decay functions that best characterise the rate of heat release curves for single passenger vehicles to be used in multiple vehicle fires.

The analysis in Chapter 5 suggests separate growth and decay curves be used. For the growth phase the Peak method such that $\dot{Q}(t) = \alpha_{peak} t^2$ up until the peak heat release rate $\dot{Q}_{max}$ at time t_{max} is recommended. For the decay phase the Exponential method such that $\dot{Q}(t) = \dot{Q}_{max} e^{\beta_{exp}(t-t_{max})}$ until the heat release rate reaches 50 kW is recommend.

For a risk-based fire engineering design approach this work provides a designer the flexibility to use three probability distributions (peak heat release rate, fire growth coefficient, and fire decay coefficient) as a function curb weight classifications to construct design fire for a single passenger vehicle using the Peak growth and Exponential decay method. The distributions are given as;

Table 14-2: Summary of the distributions to construct a Peak-Exponential design fire curve.

		Peak heat release rate, $\dot{Q}_{max}$ (kW)		**Fire growth coefficient, α_{peak} (kW/min²)**		**Fire decay coefficient, β_{exp} (min^{-1})**	
	Distribution shape	Weibull		Gamma		Weibull	
	Distribution parameters	**κ**	**θ**	**κ**	**θ**	**κ**	**θ**
Class	**Mini**	5.19	3809	1.39	11.86	0.93	0.17
	Light	1.66	5078	1.23	14.78	1.21	0.11
	Compact	2.40	4691	1.18	5.14	3.93	0.08
	Medium	3.18	7688	2.24	2.75	1.38	0.11
	Heavy	3.11	8723	1.51	1.82	1.86	0.11
	Minivan/MPV	4.25	4588	0.36	159.18	2.51	0.08

14.2.2 Prediction of time of ignition in a multiple vehicle fire spread simulation

The thesis also demonstrates that by using the combination of PSM and FTP methods, time of ignition of a subsequent vehicle can be predicted after receiving enough heat flux from a prior burning object. This finding is useful for the application of multiple vehicle fire simulation.

The analysis suggests that In order to get a single set of conditions that can reasonably predict the time to ignition for a two-vehicle scenario the analysis suggests that radiative fraction of 0.3 and the '2-Far' heat source position for the burning item can be applied to the PSM for the prediction of the heat flux to the target vehicle. The analysis also suggests that a power law index, n = 2 corresponding to a thermally thick material component that is equivalent to bumper trim with a FTP value of 21862 $\frac{kW \cdot s^n}{m^2}$, and critical heat flux of 3.1 kW/m² can be selected as the first component to ignite on a vehicle.

14.2.3 FLED for risk-based design of car parking buildings

The thesis also demonstrates how a probabilistic approach to obtaining FLED values can be applied by bringing together a number of recent studies related to car parking buildings. The application of the Monte Carlo model allows for a future reassessment of FLED values for car parking buildings should there be new energy content measurements for cars or changes in the composition of a vehicle fleet. The approach could also be modified to account for the occupancy of car parking spaces as a function of the time of day.

From the example analysis it was found that the 80% fractile FLED is 260 MJ/m^2 (rounded up to the nearest 10 MJ/m^2). It is interesting to compare the FLED values from the Monte Carlo model to values quoted in the literature given this work has used energy content values from vehicles subsequent to the 1980s and also adjusts for the apparent higher percentage of heavier vehicles in modern fleets. Thomas [126] gives an average FLED value for 'Garaging, maintenance and exploitation of vehicles' as 190 MJ/m^2 and 200 MJ/m^2 for 'Parking buildings' which are of the order of 20% less than median values obtained in this study. However the method proposed by Thomas to obtain 80% fractile values means values of 270 MJ/m^2 for 'Garaging, maintenance and exploitation of vehicles' and 250-300 MJ/m^2 for 'Parking buildings' are comparable with the 260 MJ/m^2 value suggested in this study.

14.2.4 Multiple vehicle fire simulation tool

A multiple vehicle fire simulation tool is able to be programmed by the combination of what have been learned in Chapter 3, Chapter 5, Chapter 6, and Chapter 7. This tool is able to simulate multiple vehicle fire scenarios although with numbers of limitations. The main output of the tool is presented in the form of a plot of family of heat release rate curves for a desired number of iterations. While the main objective of the tool is created is for the design of car parks, this tool also has shown to be useful for fire investigation as what has been presented in Chapter 12.

14.2.5 Probability of fire spread between vehicles in car parks

A study was undertaken to quantitatively assess the probability of fire spread from a burning vehicle to another vehicle within its vicinity, given no interruption of the fire by fire fighters and/or fire suppression systems. It was found from the study that the probability of fire spread from a vehicle to another vehicle in car parks was able to be calculated for two scenarios.

Using the specified inputs, this study has shown that, for Scenario 1 i.e. a vehicle parked next to burning vehicle, the probability of fire spreading to the neighbouring vehicle is 0.63 – 0.90, depending on the effective distance.

For Scenario 2 i.e. a vehicle parked a space away from burning vehicle, the highest probability of fire spreading for the shortest effective distance is 0.23, and probability for the longest effective distance (6.4 m) is 0. It is also found that the empty space between two vehicles is able to reduce the probability by at least 0.40.

Using the combination of results for Scenario 1 and 2, an equation of $y = 0.045x^2 - 0.62x + 2.11$ is obtained to estimate the probability of fire spread for different effective distance between 2.2 – 6.4 m.

14.2.6 Fire growth characteristics

It was found from the research that it was evident that as the number of vehicles in a cluster increases the average peak heat release rate also increases in logarithmic trend. The logarithmic trend shows that it agrees with the hypothesis of a travelling fire that by the time fire spreads to the subsequent vehicle, the fire in the previous vehicle is already declining. This is demonstrated in Figure 14-4. This finding defies the earlier assumption of as the

number of vehicles in a cluster increases the peak heat release rate increases linearly. Therefore, this finding would be a very useful information for future design of car parking buildings.

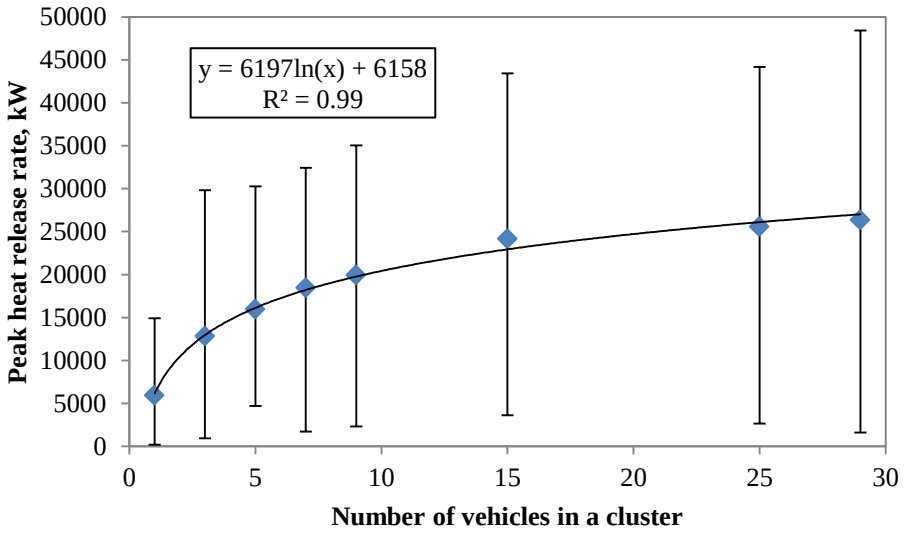

Figure 14-4: Results from series of simulations for fire spread probability analysis

14.2.7 Fire spread probability

It was also found from the research that as number of vehicles in a cluster increases, the number of probability distributions involved in the simulation increases, thus decreasing the probability of fire to spread to all vehicles. The probability is able to be obtained by using Equation 14-1 where *y* is the probability and *x* is the number of vehicles.

$$y = -0.0099x + 0.88$$

Equation 14-1

Since there is no negative probability, the equation is only true to up until 88 of vehicles in a cluster. In other words, there is zero probability of fire to spread to all vehicles if there are 89 or more vehicles in a cluster. This in itself is an important finding where it is impossible to have 89 vehicles to be involved in a fire according to this model, thus this becomes the maximum limit of the number of vehicles for design fire scenario in a car park.

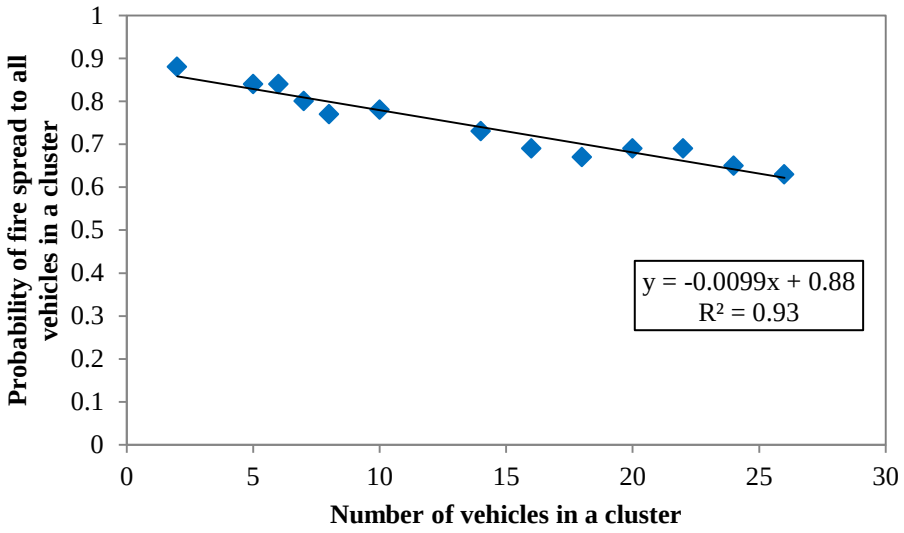

Figure 14-5: Results from series of simulations for fire spread probability analysis

14.3 Recommendations for future work

There are still much room for research in the area of vehicle fires in car parking buildings. One of the areas are;

14.3.1 Single passenger vehicle fire experiments

Although there were already numbers of experiments conducted in the past, there is a need on conducting single passenger vehicle fire experiments in the future to account for the current and future materials in automotive construction. It was found that currently vehicles use more lighter-weight materials e.g. polymer/composite than the year 1977 [121]. Also, there is also the need of conducting vehicle fire experiments since there are more vehicles with new types of fuels e.g. battery powered vehicle and solar powered vehicle.

There is also a value if single passenger vehicle fire experiments can be conducted according to its curb weight classifications. By performing these experiments, the results can be integrated into the series of data collation presented in Chapter 2 and a new analysis can be made.

A number of suggestions that could be made while conducting experiments are:

- Record the whole the experiment from the beginning until the end with proper video cameras installed at several different angles. This is for the better observation of the experiment, hence better understanding of the behaviour of the fire.
- Repeat experiments for at least three times for an identical model and similar ignition method and location for better output results.
- Collect results for heat release rate measurements by oxygen depletion and mass loss rate, temperature readings, and heat flux measurements at different points.

14.3.2 Multiple vehicle fire experiments

There is also a need on conducting more multiple vehicle fire experiments. Currently there were scarce of such experiments conducted, reported and available for analysis. Therefore, there is a need of conducting a systematic multiple vehicle fire experiments in the future for the purpose of analysing the fire spreads between vehicles in enclosed condition.

14.3.3 Vehicle parking behaviours

One of the components in the probabilistic risk analysis model is the vehicle cluster size probability. This component is somehow implicitly related to how people parked their vehicles in a car park. This is also subject to different type and function of car parks as well as a function of time of the day.

A potential research area for future work related to the vehicle cluster size probability component is to look at the distribution of classifications of vehicles in different type and function of car parking buildings. There are very few extensive studies have been done previously on this particular topic.

As opposed to a random vehicle parking distribution, there is also a possibility of having a fixed distribution. This fixed vehicle parking distribution usually occurs for example in office parking areas where parking for staff vehicles is pre-determined.

These potential studies could provide inputs to the current probabilistic risk analysis model. It would be interesting to know from whatever the outcome from these studies suggest, would it change the current assumptions have been made on the current probabilistic risk analysis model or not?

14.3.4 Effects of vehicle fires on structure, fire suppression systems, and life safety

Since the output of the simulation is the heat release rate history of a particular incident there is a potential project to study the effects of vehicle fires on structure, fire safety systems, and/or life safety of occupants using probabilistic approach introduced in this thesis. As for example in this thesis, the probabilistic FLED values found from this thesis can be used as input for time-equivalence method as to calculate the fire severity.

Another example of the application of the research is the possibility of predicting the activation time of fire sprinkler systems in the event of fire in car parking buildings. Next is the incorporation of Fire Brigade Intervention Model (FBIM) into the current research model is also a possibility. FBIM is an event-based methodology, which quantifies fire brigade responses employed during a structure fire from time of notification through to control and

extinguishment [142, 143]. All of the examples mentioned are not limited to deterministic approach but also can be applied using probabilistic input as demonstrated in this research.

14.3.5 Enhancement of B-RISK software

It is suggested that including probabilistic design fire as input can further enhance the ability of B-RISK as a probabilistic fire tool. B-RISK can also be enhanced by adding the databases of vehicles found from this thesis.

Chapter 15 REFERENCES

[1] Building Research Establishment. (2010). Fire Spread in Car Parks. Building Research Establishment (BRE), Eland House Bressenden Place London SW1E 5DU United Kingdom, BD2552.

[2] Li, Y. and Spearpoint, M. (2007). Analysis of Vehicle Fire Statistics in New Zealand Parking Buildings. *Fire Technology*, vol. 43(2), pp. 93-106. http://dx.doi.org/10.1007/s10694-006-0004-2

[3] Albrektsson, J. and Mattsson, I. (2012) Assessment of a parking garage after a major fire. *Brandposten*, 45.

[4] Pratt, C. (2015). Auckland mall shoppers evacuated because of van fire. *Stuff NZ*, http://www.stuff.co.nz/national/66735453/Auckland-mall-shoppers-evacuated-because-of-van-fire

[5] Austroads. (2008). Guide to Traffic Management Part 11: Parking. Sydney, Australia.

[6] New Zealand Transport Agency. (Accessed: 1 April 2015). Vehicle class classification. Available: http://www.nzta.govt.nz/vehicle/classes-standards/class.html

[7] International Code Council. (2012). International Building Code.

[8] ECCS. (1993). Fire Safety in Open Car Parks, Modern Fire Engineering.

[9] Jaspart, J.-P., Demonceau, J.-F., Cheng, F., Izzuddin, B., Elghazaouli, A., Nethercot, D., Zhao, B., Dhima, D., Gens, F., de Ville, V., Santiago, A., Da Silva, L., and Obiala, R. (2009). Robustness of car parks against localised fire. Univeristy of Coimbra, RFS-PR-07039-Car_Parks-v1(11).

[10] Department of Building and Housing. (2012). Building Regulations 1992.

[11] Department of Building and Housing. (2012). C/VM2 Verification Method: Framework for Fire Safety Design.

[12] Department of Building and Housing. (2012). C/AS7 Acceptable Solution for Buildings Used for Vehicle Storage and Parking (Risk Group VP).

[13] Fleischmann, C. M. (2011). Is Prescription the Future of Performance-Based Design? in *Fire Safety Science 10*, University of Maryland, College Park, MD, pp. 77 - 94. http://dx.doi.org/10.3801/IAFSS.FSS.10-77

[14] Joyeux, D., Kruppa, J., Cajot, L.-G., Schleich, J.-B., de Leur, P. V., and Twilt, L. (2002). Demonstration of Real Fire Tests in Car Parks and High Buildings. CTICM, Metz, France, No. 7215 PP 025.

[15] Zhao, B., Joyeux, D., and Kruppa, J. (2004). Guide pour la vérification du comportement au feu de parcs de stationnement largement ventilés en superstructure métallique. CTICM, France, INSI - 03/233d - BZ/PB.

[16] Cheong, M. K., Spearpoint, M., and Fleischmann, C. (2008). Using Peak Heat Release Rate to Determine the Fire Risk Level of Road Tunnels. *Journal of Risk and Reliability*, vol. 222, pp. 595-604. http://dx.doi.org/10.1243/1748006XJRR169

[17] Babrauskas, V. and Peacock, R. D. (1992). Heat Release Rate: The Single Most Important Variable in Fire Hazard. *Fire Safety Journal*, vol. 18, pp. 255 - 272. http://dx.doi.org/10.1016/0379-7112(92)90019-9

[18] Wade, C., Baker, G. B., Frank, K., Harrison, R., Spearpoint, M., and Fleischmann, C. M. (2013). B-RISK user guide and technical manual.

[19] Li, Y. (2004). Assessment of Vehicle Fires in New Zealand Parking Buildings. Master's thesis, Department of Civil & Natural Resources Engineering, University of Canterbury.

[20] Butcher, E. G., Langdon-Thomas, G. J., and Bedford, G. K. (1968). Fire and Car-park Buildings - Fire Note 10. Fire research station, London.

[21] Gewain, R. G. (1973). Fire Experience and Fire Tests in Automobile Parking Structures. *Fire Journal*, vol. 67(4), pp. 50 - 54.

[22] Bennetts, I. D., Proe, D., Lewins, R., and Thomas, I. R. (1985). Open-Deck Car Park Fire Tests. BHP Steel International Group, Whyalla, South Australia.

[23] Schleich, J. B., Cajot, L. G., Pierre, M., and Brasseur, M. (1999). Development of Design Rules for Steel Structures Subjected to Natural Fires in Closed Car Parks. European Commission, Luxembourg.

[24] Burgi, H. (1971). Swiss Tests on Fire Behaviour in Enclosed and Underground Car Parks. *Fire International*, vol. 33, pp. 64 - 77.

[25] BHP. (1987). Fire and Unprotected Steel in Closed Carparks. BHP Melbourne Research Laboratories, Melbourne, VIC.

[26] Bennetts, I. D., Thomas, I. R., Proe, D., and Lewins, R. (1990). Fire safery in car parks. BHP Steel, Structural and Development Group, Melbourne, VIC.

[27] Kitano, T., Sugawa, O., Masuda, H., Ave, T., and Uesugi, H. (2000). Large Scale Fire Tests of 4-Story Type Car Park Part 1: The Behavior of Structural Frame Exposed to the Fire at the Deepest Part of the First Floor. in *4th Asia-Oceania Symposium on Fire Science and Technology*, Tokyo, Japan, pp. 527 - 538.

[28] van der Heijden, M. G. M. (2010). Heat and smoke removal in semi-open car parks. Master's thesis, Eindhoven University of Technology, Eindhoven, Netherlands.

[29] van Oerle, N. J., Lemaire, A. D., and van de Leur, P. H. E. (1999). Effectiviteit van stuwkrachtventilatie in gesloten parkeergarages. TNO, Delft, Netherlands, 1999-CVB-RR1442.

[30] Collier, P. C. R. (2011). Car parks - Fires involving Modern Cars and Stacking Systems. Building Research Association New Zealand (BRANZ), New Zealand, BRANZ Study Report 255.

[31] Wade, C. (2004). BRANZFIRE Technical Reference Guide. Building Research Association of New Zealand (BRANZ), Judgeford, New Zealand, BRANZ Study Report 92.

[32] Deckers, X. (2007). Simulatie van rookafvoer bij brand in grote overdekte parkeergarages. Bachelor's degree dissertation, Universiteit Gent.

[33] Tilley, N. (2007). Studie van brand in kleine ondergrondse parkeergarages. Bachelor's degree dissertation, Universiteit Gent.

[34] Jansen, D. (2010). Autobranden in parkeergarages - brandscenario's, brandsimulaties en de gevolgen voor constructies. Postgraduate thesis, Universiteit Gent.

[35] Baert, L. (2011). Evaluatie en ontwikkeling van methoden voor een brandveilig ontwerp van RWA installaties in ondergrondse parkeergarages. Master's thesis, Universiteit Gent.

[36] Bureau for Standardisation. (2010). Brandbeveiliging in gebouwen Ontwerp van rook- en warmteafvoersystemen in gesloten parkeergebouwen., NBN S21-208-2/pr A1:2010.

[37] Joyeux, D. (1997). Natural Fires in Closed Car Parks – Car Fire Tests. CTICM, Metz, France, INC 96/294d DJ/NB.

[38] Merci, B. and Shipp, M. (2013). Smoke and heat control for fires in large car parks: Lessons learnt from research? *Fire Safety Journal*, vol. 57(Special), pp. 3-10. http://dx.doi.org/10.1016/j.firesaf.2012.05.001

[39] Annerel, E., Taerwe, L., Merci, B., Jansen, D., Bamonte, P., and Felicetti, R. (2013). Thermo-mechanical analysis of an underground car park structure exposed to fire. *Fire Safety Journal*, vol. 57(Special), pp. 96-106. http://dx.doi.org/10.1016/j.firesaf.2012.07.006

[40] Noordijk, L. and Lemaire, T. (2005). Modelling of fire spread in car parks. *HERON*, vol. 50(4).

[41] Jug, A., Petelin, S., and Bukovec, P. (2010). Designing an Underground Car Park Fire Scenarios on a Probabilistic Basis. *Acta Chimica Slovenica*, vol. 57, pp. 136 - 143.

[42] Olthof, P. and Scheerder, R. (2011). 'Brandscenario's Geparkeerd?' Onderzoek naar brandscenario's in ondergrondse parkeergarages. Deel 1: Rapport. Instituut voor Engineering, Brede Bachelor of Engineering, Uitstroomprofiel Fire Safety Engineering.

[43] de Feijter, M. P. and Breunese, A. J. (2007). Investigation of fire in the Lloydstraat car park, Rotterdam. Efectis Nederland BV, Postbus, Netherlands, 2007-Efectis-R0894(E).

[44] Tohir, M. Z. M. and Spearpoint, M. (2013). Distribution analysis of the fire severity characteristics of single passenger road vehicles using heat release rate data. *Fire Science Reviews*, vol. 2(5). http://dx.doi.org/10.1186/2193-0414-2-5

[45] Fleischmann, C. (2008). Proposed Framework for Performance Based Fire Engineering Design in the Next Generation New Zealand Building Code: Specification of the Design Fire. in *SFPE Conference on Performance-Based Codes and Fire Safety Design*.

[46] Opland, L. (2007). Size classification of passenger cars. Pre-study on how to size classify passenger cars by inventorying the existing classification models. Master's thesis, Chalmers University of Technology, Göteborg, Sweden.

[47] American National Standard. (2007). Manual on Classification of Motor Vehicle Traffic Accidents: ANSI D16.1-2007.

[48] Shintani, Y., Kakae, N., Harada, K., Masuda, H., and Takahashi, W. (2004). Experimental Investigation of Burning Behavior of Automobiles. in *Proceedings Of The Asia-Oceania Symposium On Fire Science & Technology*, pp. 618 - 629.

[49] European Union. (Accessed: 5 December 2012). Eurostat: Regional transport statistics. Available: http://epp.eurostat.ec.europa.eu/portal/page/portal/transport/data/database

[50] Swift, K. (2012). Chemistry and Light Vehicle Annual Report. Economics & Statistics Department, American Chemistry Council.

[51] Ingason, H. (2006). Design Fires in Tunnels. in *Safe & Reliable Tunnels. Innovative European Achievements*.

[52] Janssens, M. (2008). Development of a database of full-scale calorimeter tests of motor vehicle burns. Fire Technology Department, Southwest Research Institute.

[53] Palisade Corporation. (2010). Guide to Using @RISK: Palisade Corporation.

[54] Autofiles. (Accessed: 20 February 2015). Car technical specifications. Available: http://www.autofiles.org

[55] Carfolio. (Accessed: 20 February 2015). Automobile and Car Specifications. Available: http://www.carfolio.com

[56] Carspector. (Accessed: 20 February 2015). Automotive technical specifications. Available: http://www.carspector.com

[57] Steinert, C. (2000). Experimental Investigation of Burning and Fire Jumping Behaviour of Automobiles. *Vereinigung zur Förderung des Deutschen Brandschutzes e. V. (VFDB)*, vol. 49, pp. 163 - 172.

[58] Carvel, R. O. (2004). Fire Size in Tunnels. Doctoral thesis, Division of Civil Engineering, Heriot-Watt University.

[59] Mangs, J. and Keski-Rahkonen, O. (1994). Characterization of the Fire Behaviour of a Burning Passenger Car. Part I: Car Fire Experiments. *Fire Safety Journal*, vol. 23, pp. 17 - 35. http://dx.doi.org/10.1016/0379-7112(94)90059-0

[60] Shipp, M. and Spearpoint, M. (1995). Measurements of the severity of fires involving private motor vehicles. *Fire and Materials*, vol. 19(3), pp. 143-151. http://dx.doi.org/10.1002/fam.810190307

[61] Okamoto, K., Watanabe, N., Hagimoto, Y., Chigira, T., Masano, R., Miura, H., Ochiai, S., Satoh, H., Tamura, Y., Hayano, K., Maeda, Y., and Suzuki, J. (2009). Burning behavior of sedan passenger cars. *Fire Safety Journal*, vol. 44, pp. 301 - 310. http://dx.doi.org/10.1016/j.firesaf.2008.07.001

[62] Marlair, G., Lemaire, T., and Ohlin, M. (2008). Fire scenarios and accidents in the past. Workpackage 2 Fire development and mitigation measure D211, UPTUN.

[63] Santrock, J. (2003). Evaluation of Motor Vehicle Fire Initiation and Propagation, Part 12: Propagation of an Underbody Gasoline Pool Fire in a 1998 Front-Wheel Drive Passenger Vehicle. National Highway Traffic Safety Administration (NHTSA), Warren, Michigan, United States of America, NHTSA 1998-3588-201.

[64] Santrock, J. (2003). Evaluation of Motor Vehicle Fire Initiation and Propagation, Part 13: Propagation of an Engine Compartment Fire in a 1998 Front-Wheel Drive Passenger Vehicle. National Highway Traffic Safety Administration (NHTSA), Warren, Michigan, United States of America, NHTSA 1998-3588-203.

[65] Santrock, J. (2002). Evaluation of Motor Vehicle Fire Initiation and Propagation, Part 6: Propagation of an Underbody Gasoline Pool Fire in a 1997 Rear Wheel Drive Passenger Car. National Highway Traffic Safety Administration (NHTSA), Warren, Michigan, United States of America, NHTSA 1998-3588-158.

[66] Santrock, J. (2002). Demonstration of Enhanced Fire Safety Technology-Fire Retardant Materials-Part 1: Full Scale Vehicle Fire Tests of a Control Vehicle and a Test Vehicle containing an HVAC Module Made from Polymers Containing Flame Retardant Chemicals. National Highway Traffic Safety Administration (NHTSA), Warren, Michigan, United States of America, NHTSA 1998-3588-190.

[67] Santrock, J. (2002). Evaluation of Motor Vehicle Fire Initiation and Propagation, Part 7: Propagation of an Engine Compartment Fire in a 1997 Rear Wheel Drive Passenger Car. National Highway Traffic Safety Administration (NHTSA), Warren, Michigan, United States of America, NHTSA 1998-3588-178.

[68] Santrock, J. (2002). Evaluation of Motor Vehicle Fire Initiation and Propagation, Part 10: Propagation of a Mid-Underbody Gasoline Pool Fire in a 1998 Sport Utility Vehicle. National Highway Traffic Safety Administration (NHTSA), Warren, Michigan, United States of America, NHTSA 1998-3588-189.

[69] Santrock, J. (2002). Evaluation of Motor Vehicle Fire Initiation and Propagation, Part 9: Propagation of a Rear-Underbody Gasoline Pool Fire in a 1998 Sport Utility Vehicle. National Highway Traffic Safety Administration (NHTSA), Warren, Michigan, United States of America, NHTSA 1998-3588-188.

[70] Santrock, J. (2002). Evaluation of Motor Vehicle Fire Initiation and Propagation, Part 4: Propagation of an Underbody Gasoline Pool Fire in a 1996 Passenger Van. National Highway Traffic Safety Administration (NHTSA), Warren, Michigan, United States of America, NHTSA 1998 3588-143.

[71] Santrock, J. (2001). Evaluation of Motor Vehicle Fire Initiation and Propagation, Part 3: Propagation in an Engine Compartment Fire in a 1996 Passenger Van. National Highway Traffic Safety Administration (NHTSA), Warren, Michigan, United States of America, NHTSA 1998 3588-119.

[72] Stroup, D. W., DeLauter, L., Lee, J., and Roadarmel, G. (2001). Passenger Minivan Fire Test. Building and Fire Research Laboratory, National Institute of Standards and Technology (NIST), Gaithersburg, Maryland, United States, FR 4011.

[73] Steinert, C. (1994). Smoke and heat production in tunnel fires. in *International Conference on Fires in Tunnels*, Borås, Sweden, pp. 123 - 137.

[74] Lönnermark, A. and Blomqvist, P. (2006). Emissions from an Automobile Fire. *Chemosphere,* vol. 62, pp. 1043 - 1056.

[75] Biteau, H., Steinhaus, T., Schemel, C., Simeoni, A., Marlair, G., Bal, N., and Torero, J. L. (2008). Calculation Methods for the Heat Release Rate of Materials of Unknown

Composition in *Fire Safety Science 9*, Karlsruhe, Germany, pp. 1165-1176. http://dx.doi.org/10.3801/IAFSS.FSS.9-1165

[76] Drysdale, D. (2011). An Introduction to Fire Dynamics: Wiley.

[77] Anonymous. (2004). CTICM Fire Tests on Cars. CTICM, Metz, France.

[78] Okamoto, K., Otake, T., Miyamoto, H., Honma, M., and Watanabe, N. (2013). Burning behavior of minivan passenger cars. *Fire Safety Journal*, vol. 62, Part C(0), pp. 272-280. http://dx.doi.org/10.1016/j.firesaf.2013.09.010

[79] Tohir, M. Z. M. and Spearpoint, M. (2014). Development of Fire Scenarios for Car Parking Buildings using Risk Analysis. in *Fire Safety Science 11 (in press)*, Christchurch, New Zealand.

[80] Roosefid, M. and Zhao, B. (2011). Fire safety engineering of an open car park. CTICM, Saint-Aubin, France.

[81] Watts, J. M. and Hall, J. R. (2008). Introduction to Fire Risk Analysis. in *The SFPE Handbook of Fire Protection Engineering* P. J. DiNenno, 4th ed: NFPA.

[82] Waerden, P. V. D., Borgers, A., and Timmermans, H. (2007). Travelers Micro-Behavior at Parking Lots: A Model of Parking Choice Behavior. presented at the 82nd Annual Meeting of the Transportation Research Board, Washington DC.

[83] Subramaniam, R. (2006). Passenger Vehicle Occupant Fatality Rates by Type and Size of Vehicle. Traffic Safety Facts. Research Note.

[84] Challands, N. (Personal communication, 2012).

[85] Chen, M., Hu, C., and Chang, T. (2011). The Research on Optimal Parking Space Choice Model in Parking Lots. in *Computer Research and Development (ICCRD) 2011 3rd International Conference*, pp. 93 - 97.

[86] Stern-Gottfried, J. and Rein, G. (2012). Travelling fires for structural design–Part I: Literature review. *Fire Safety Journal*, vol. 54(0), pp. 74-85. http://dx.doi.org/10.1016/j.firesaf.2012.06.003

[87] Australian Building Codes Board. (2005). International Fire Engineering Guidelines: ABCB for the Australian Government, State and Territories of Australia.

[88] Society of Fire Protection Engineers. (2007). SFPE Engineering Guide to Performance-Based Fire Protection Analysis and Design of Buildings

[89] Babrauskas, V. and Walton, W. D. (1986). A simplified characterization of upholstered furniture heat release rates. *Fire Safety Journal*, vol. 11(3), pp. 181-192. http://dx.doi.org/10.1016/0379-7112(86)90061-5

[90] Mowrer, F. W. and Williamson, R. B. (1990). Methods to characterize heat release rate data. *Fire Safety Journal*, vol. 16(5), pp. 367-387. http://dx.doi.org/10.1016/0379-7112(90)90009-4

[91] Numajiri, F. and Furukawa, K. (1998). Mathematical expression of Heat Release Rate Curve and proposal of 'Burning Index'. *Fire and Materials*, vol. 22(1), pp. 39-42. http://dx.doi.org/10.1002/(SICI)1099-1018(199801/02)22:1<39::AID-FAM629>3.0.CO;2-H

[92] Ingason, H. (2005). Fire Development In Large Tunnel Fires. *Fire Safety Science 8*, pp. 1497-1508. http://dx.doi.org/10.3801/IAFSS.FSS.8-1497

[93] Ingason, H. (2009). Design fire curves for tunnels. *Fire Safety Journal*, vol. 44(2), pp. 259-265. http://dx.doi.org/10.1016/j.firesaf.2008.06.009

[94] Hansen, R. and Ingason, H. (2011). An engineering tool to calculate heat release rates of multiple objects in underground structures. *Fire Safety Journal*, vol. 46(4), pp. 194-203. http://dx.doi.org/10.1016/j.firesaf.2011.02.001

[95] Li, Y. Z. and Ingason, H. (2015). A New Methodology of Design Fires for Train Carriages Based on Exponential Curve Method. *Fire Technology*, pp. 1-16. http://dx.doi.org/10.1007/s10694-015-0464-3

[96] Ingason, H. (1995). Design fires in tunnels. presented at the Asiaflam 95, Hong Kong, pp. 77 - 86.

[97] Anderson, C. M. and Bell, N. M. (2014). Analysis of vehicle distribution in parking buildings. presented at the Civil and Natural Resources Engineering Research Conference, University of Canterbury, New Zealand,vol. 2 pp. 65 - 72.

[98] Baker, G., Collier, P. C. R., Wade, C., Spearpoint, M., Fleischmann, C. M., Frank, K., and Sazegara, S. (2013). A comparison of a priori modelling predictions with experimental results to validate a design fire generator submodel. in *13th International Fire and Materials Conference*, San Francisco, CA, pp. 449 - 460.

[99] Tohir, M. Z. M. and Spearpoint, M. (2014). Simplified approach to predict heat release rate curves from multiple vehicle fires in car parking buildings. in *3rd International Conference on Fires in Vehicles*, Berlin, Germany.

[100] Peacock, R. D., Reneke, P. A., D. Davis, W., and Jones, W. W. (1999). Quantifying fire model evaluation using functional analysis - some comparisons with experimental data from Australia. *Fire Safety Journal*, vol. 33(3), pp. 167-184. http://dx.doi.org/10.1016/S0379-7112(99)00029-6

[101] Baker, G. B., Spearpoint, M. J., Fleischmann, C. M., and Wade, C. A. (2011). Selecting an ignition criterion methodology for use in a radiative fire spread submodel. *Fire and Materials*, vol. 35(6), pp. 367-381. http://dx.doi.org/10.1002/fam.1059

[102] Fleury, R., Fleischmann, C. M., and Spearpoint, M. (2011). Evaluation of thermal radiation models for fire spread between objects. in *Fire and Evacuation Modelling Technical Conference*, Baltimore, MD.

[103] Ohlemiller, T. J. and Shields, J. R. (2001). Burning Behavior of Selected Automotive Parts From a Sports Coupe. NIST, NISTIR 6313.

[104] Smith, E. E. and Satija, S. (1983). Release Rate Model for Developing Fires. *Journal of Heat Transfer*, vol. 105(2), pp. 281-287. http://dx.doi.org/10.1115/1.3245575

[105] Smith, E. E. and Green, T. J. (1987). Release rates for a mathematical model. American Society for Testing and Materials, Philadelphia.

[106] Toal, B. R., Silcock, G. W. H., and Shields, T. J. (1989). An examination of piloted ignition characteristics of cellulosic materials using the ISO ignitability test. *Fire and Materials*, vol. 14(3), pp. 97-106. http://dx.doi.org/10.1002/fam.810140304

[107] Shields, T. J., Silcock, G. W., and Murray, J. J. (1993). The effects of geometry and ignition mode on ignition times obtained using a cone calorimeter and ISO ignitability apparatus. *Fire and Materials*, vol. 17(1), pp. 25-32. http://dx.doi.org/10.1002/fam.810170105

[108] Shields, T. J., Silcock, G. W., and Murray, J. J. (1994). Evaluating ignition data using the flux time product. *Fire and Materials*, vol. 18(4), pp. 243-254. http://dx.doi.org/10.1002/fam.810180407

[109] Silcock, G. W. H. and Shields, T. J. (1995). A protocol for analysis of time-to-ignition data from bench scale tests. *Fire Safety Journal*, vol. 24(1), pp. 75-95. http://dx.doi.org/10.1016/0379-7112(95)00003-C

[110] Mikkola, E. and Wichman, I. S. (1989). On the thermal ignition of combustible materials. *Fire and Materials*, vol. 14(3), pp. 87-96. http://dx.doi.org/10.1002/fam.810140303

[111] Janssens, M. L. (1991). A Thermal Model For Piloted Ignition Of Wood Including Variable Thermophysical Properties. in *Fire Safety Science 3*, pp. 167-176. http://dx.doi.org/10.3801/IAFSS.FSS.3-167

[112] Heskestad, G. (2008). Fire plumes, flame height, and air entrainment. in *The SFPE Handbook of Fire Protection Engineering*, 4th ed Quincy, MA: National Fire Protection Association.

[113] Lush, E. J. (2008). A 'Reflection' of Quality. *Metalfinishing*, vol. 36.

[114] Miller, M. A., Janssens, M. L., and Huczek, J. P. (2004). Development of a new procedure to assess the flammability of materials used in motor vehicles. Southwest Research Institute, San Antonio, TX.

[115] Bajus, M. and Olahova, N. (2011). Thermal conversion of scrap tyres. *Petroleum and Coal*, vol. 53(2), pp. 98-105.

[116] Sullivan, J. P. (2006). An Assessment of Environmental Toxicity and Potential Contamination from Artificial Turf using Shredded or Crumb Rubber. Ardea Consulting.

[117] Helps, I. (2001). Plastics in European Cars, 2000-2008: A Rapra Industry Analysis Report: RAPRA Technology.

[118] New Zealand Transport Agency. (2013). New Zealand motor vehicle registration statistics 2013. NZ Transport Agency, New Zealand.

[119] Leffin, W. W., Henderson, G. L., Van Beck Voelker, M., and Janusek, F. C. (1998). Introduction to Technical Mathematics: With Problem Solving. 3rd ed.: Waveland Press.

[120] Davis, W. D. (2002). Comparison of Algorithms to Calculate Plume Centerline Temperature and Ceiling Jet Temperature with Experiments. *Journal of Fire Protection Engineering*, vol. 12(1), pp. 9-29. http://dx.doi.org/10.1177/1042391502012001850

[121] Taub, A. I. (2006). Automotive Materials: Technology Trends and Challenges in the 21st Century. *MRS Bulletin*, vol. 31(04), pp. 336-343. http://dx.doi.org/10.1557/mrs2006.74

[122] Mark, J. E. (2007). Physical Properties of Polymers Handbook: Springer New York.

[123] Spearpoint, M., Tohir, M. Z. M., Abu, A., and Xie, P. (2015). Fire load energy densities for risk-based design. *Case Studies in Fire Safety*. http://dx.doi.org/10.1016/j.csfs.2015.04.001

[124] CEN. (2002). Eurocode 1: Actions on Structures - Part 1.2: General actions - Actions on structures exposed to fires. European Committee for Standardisation, Brussels, Belgium.

[125] Wade, C., Gerlich, J. T., and Abu, A. (2014). The relationship between fire severity and time-equivalence. BRANZ, New Zealand.

[126] Thomas, P. H. (1986). Design guide: Structure fire safety CIB W14 Workshop report. *Fire Safety Journal*, vol. 10(2), pp. 77-137. http://dx.doi.org/10.1016/0379-7112(86)90041-X

[127] Department of Building and Housing. (2005). Compliance document for New Zealand Building Code clauses C1, C2, C3, C4 fire safety (C/AS1). New Zealand.

[128] Stern-Gottfried, J., Rein, G., Bisby, L. A., and Torero, J. L. (2010). Experimental review of the homogeneous temperature assumption in post-flashover compartment fires. *Fire Safety Journal*, vol. 45(4), pp. 249-261. http://dx.doi.org/10.1016/j.firesaf.2010.03.007

[129] Nigro, E., Cefarelli, G., Ferraro, A., Manfredi, G., and Cosenza, E. (2011). Fire safety engineering for open and closed car parks: C.A.S.E. project for L'Aquila. *Applied Mechanics and Materials*, vol. 82, pp. 746 - 751. http://dx.doi.org/10.4028/www.scientific.net/AMM.82.746

[130] Moss, P. J., Abu, A., and Dhakal, R. P. (2014). Incremental fire analysis (IFA) for probabilistic fire risk assessment. in *23rd Australasian Conference on the Mechanics of Structures and Materials (ACMSM23)*, Byron Bay, Australia, pp. 707 - 712.

[131] Chrest, A. P., Smith, M. S., Bhuyan, S., Iqbal, M., and Monahan, D. R. (2000). Parking structures: planning, design, construction, maintenance, and repair. 3rd ed. New York: Chapman and Hall.

[132] Hill, J. (2005). Car Park Designers' Handbook: ICE Publishing.

[133] Li, Y. and Spearpoint, M. (2006). Cost-benefit analysis of sprinklers for property protection in New Zealand parking buildings. *Journal of Applied Fire Science*, vol. 12(3), pp. 223 - 243.

[134] Department of Planning and Land Use. (2013). Parking design manual.

[135] Asphalt Paving Association of Iowa. (1990). Parking lot design. in *Asphalt paving design guide*, Iowa, USA.

[136] City of Los Angeles - City Council. (2010). Parking design. P/ZC 2002-001.

[137] US Air Force. (1998). Parking areas. in *USAF Landscape Design Guide*.

[138] Fife Council. (2006). Parking Design Standards. in *Development Guidelines*, Fife, Scotland.

[139] Rochford District Council. (2010). Parking Standards Design and Good Practice Supplementary Planning Document.

[140] Precast Concrete Institute. (1997). Parking Structures: Recommended Practice for Design and Construction.

[141] Ponziani, F. A., Tinaburri, A., and D'Angelo, C. (2011). Investigation on a car park fire. in *12th International Fire and Materials Conference*, San Francisco, USA.

[142] Claridge, E. and Spearpoint, M. (2013). New Zealand fire Service Response Times to Structure Fires. *Procedia Engineering*, vol. 62, pp. 1063-1072. http://dx.doi.org/10.1016/j.proeng.2013.08.162

[143] Buckley, G., Bradborn, W., Edwards, J., Machant, R., Terry, P., and Wise, S. (1999). The Fire Brigade Intervention Model. in *Fire Safety Science 6*, Poitiers, France.

Appendix A

A.1 Probability distributions

This section presents the probability distributions for heat release rate, time to reach peak heat release rate, and total energy released from the experiments. The probability distributions are shown corresponds to its vehicle classification.

A.1.1 Heat release rate

A.1.1.1 Mini classification

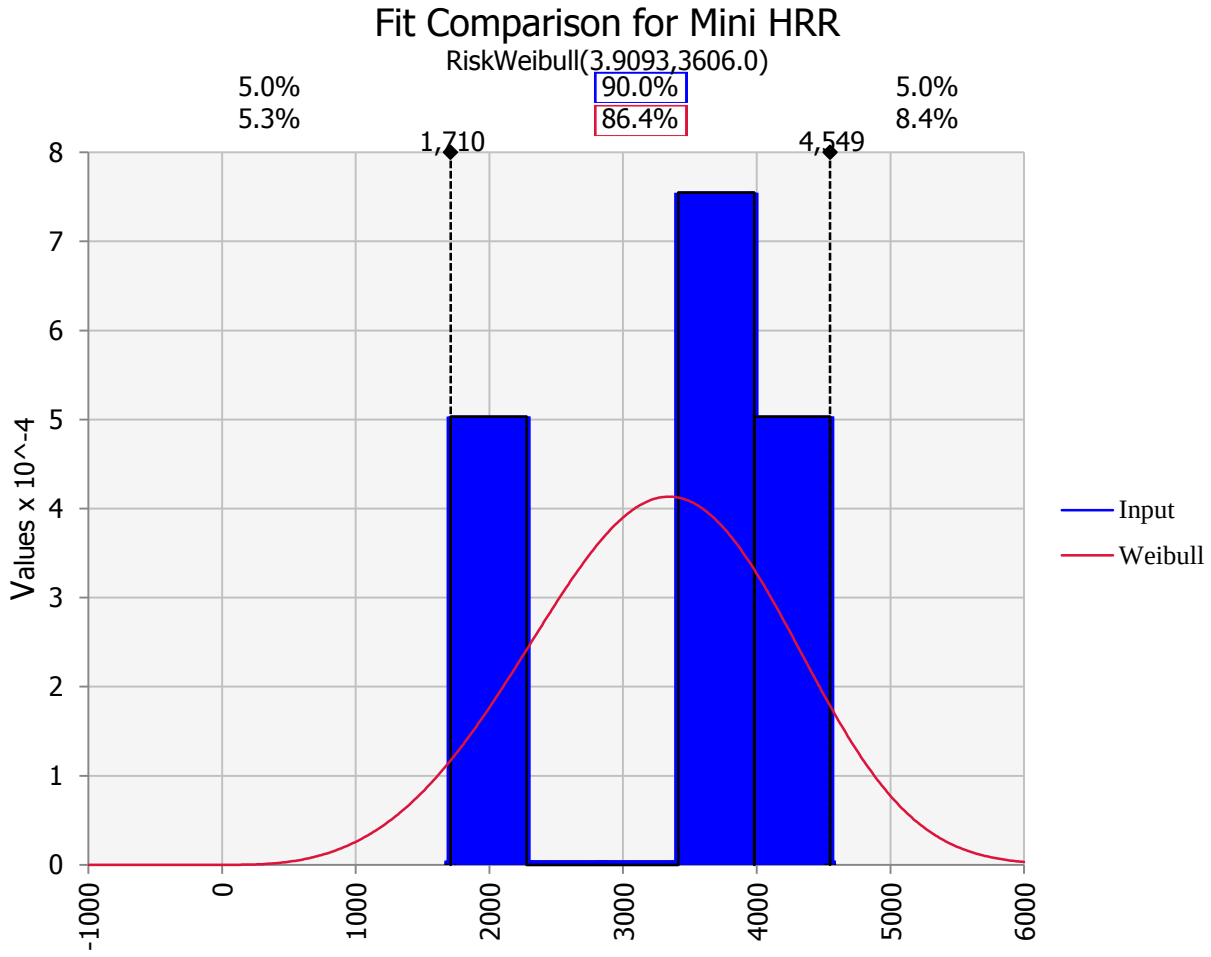

A.1.1.2 Light classification

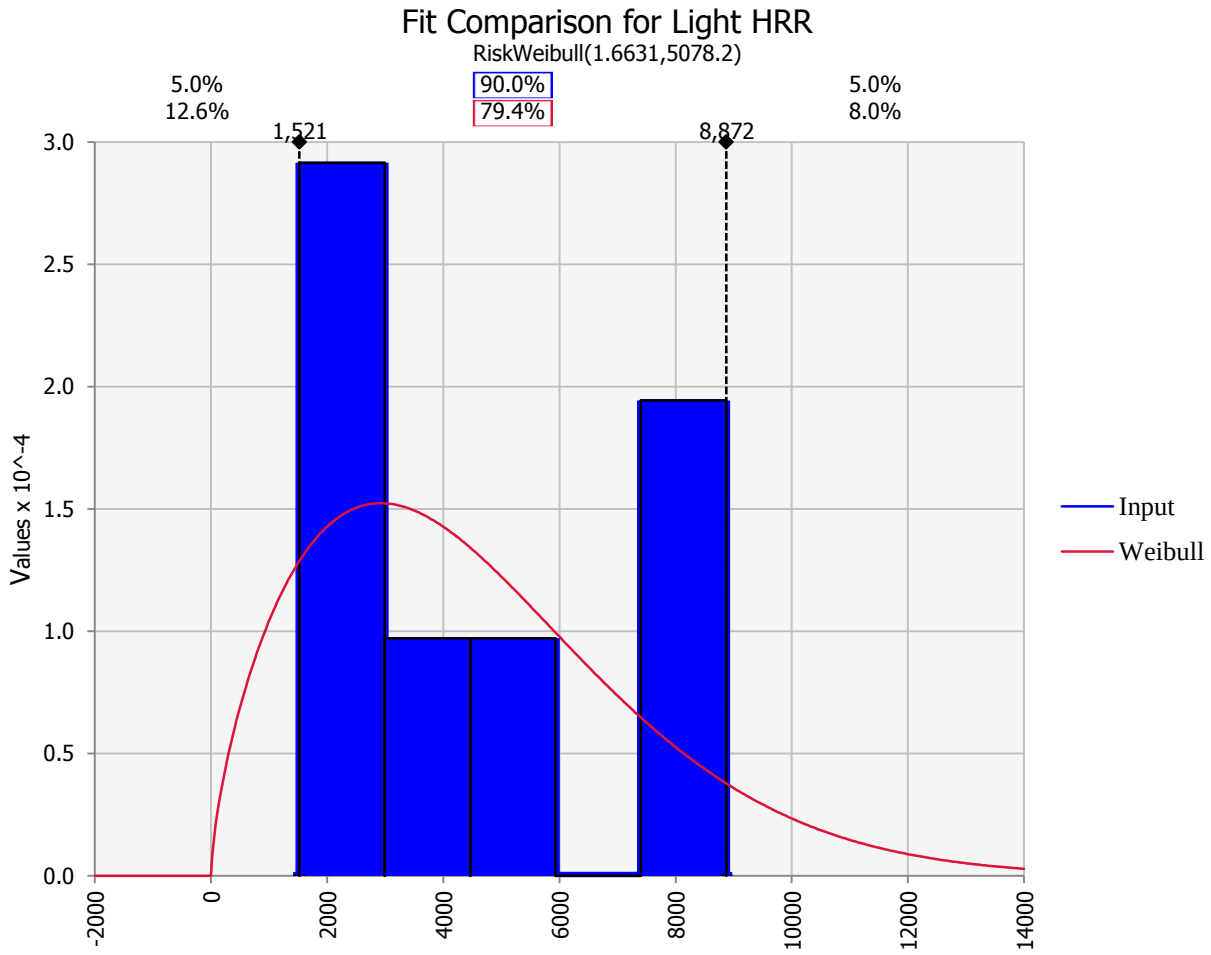

A.1.1.3 Compact classification

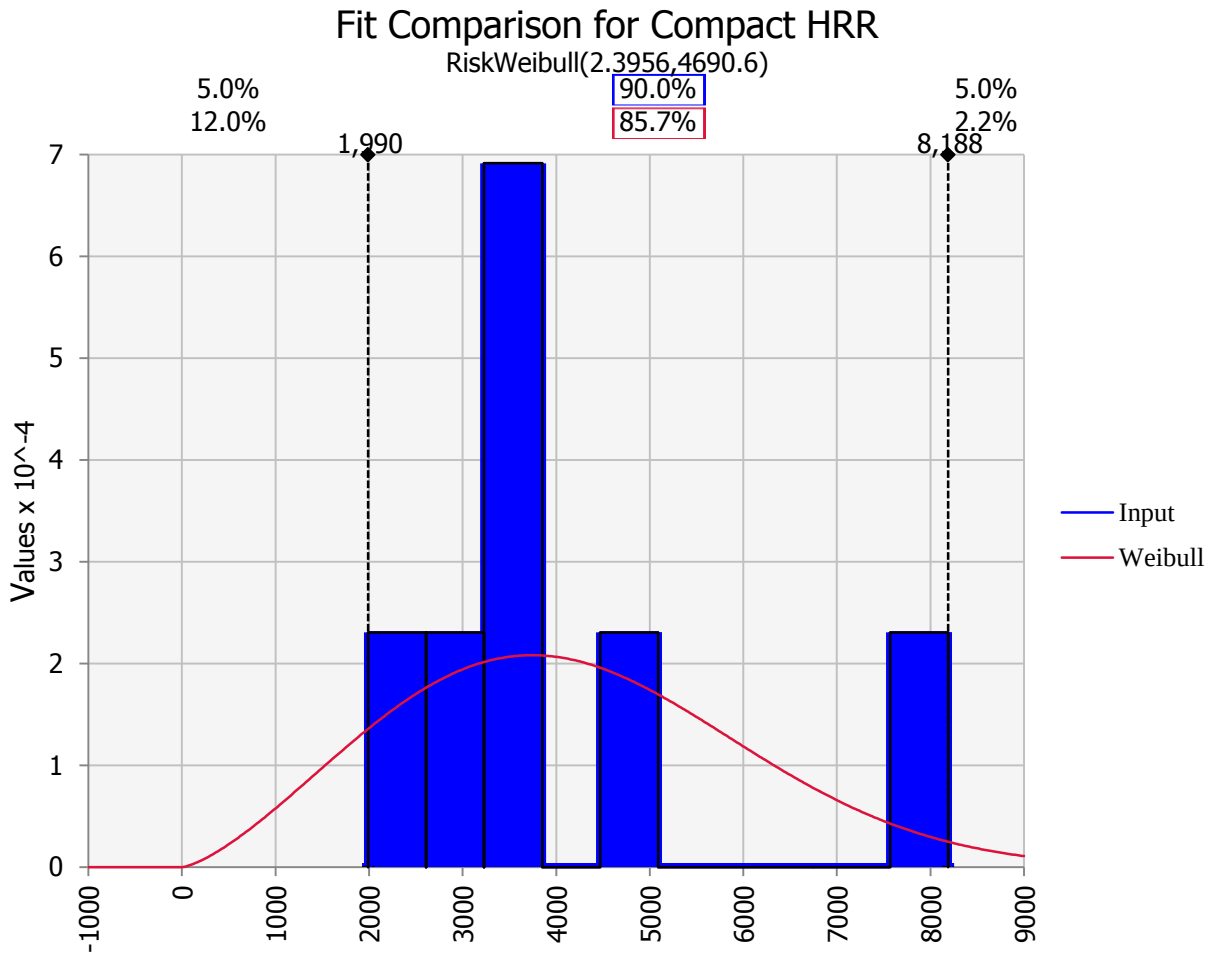

A.1.1.4 Medium classification

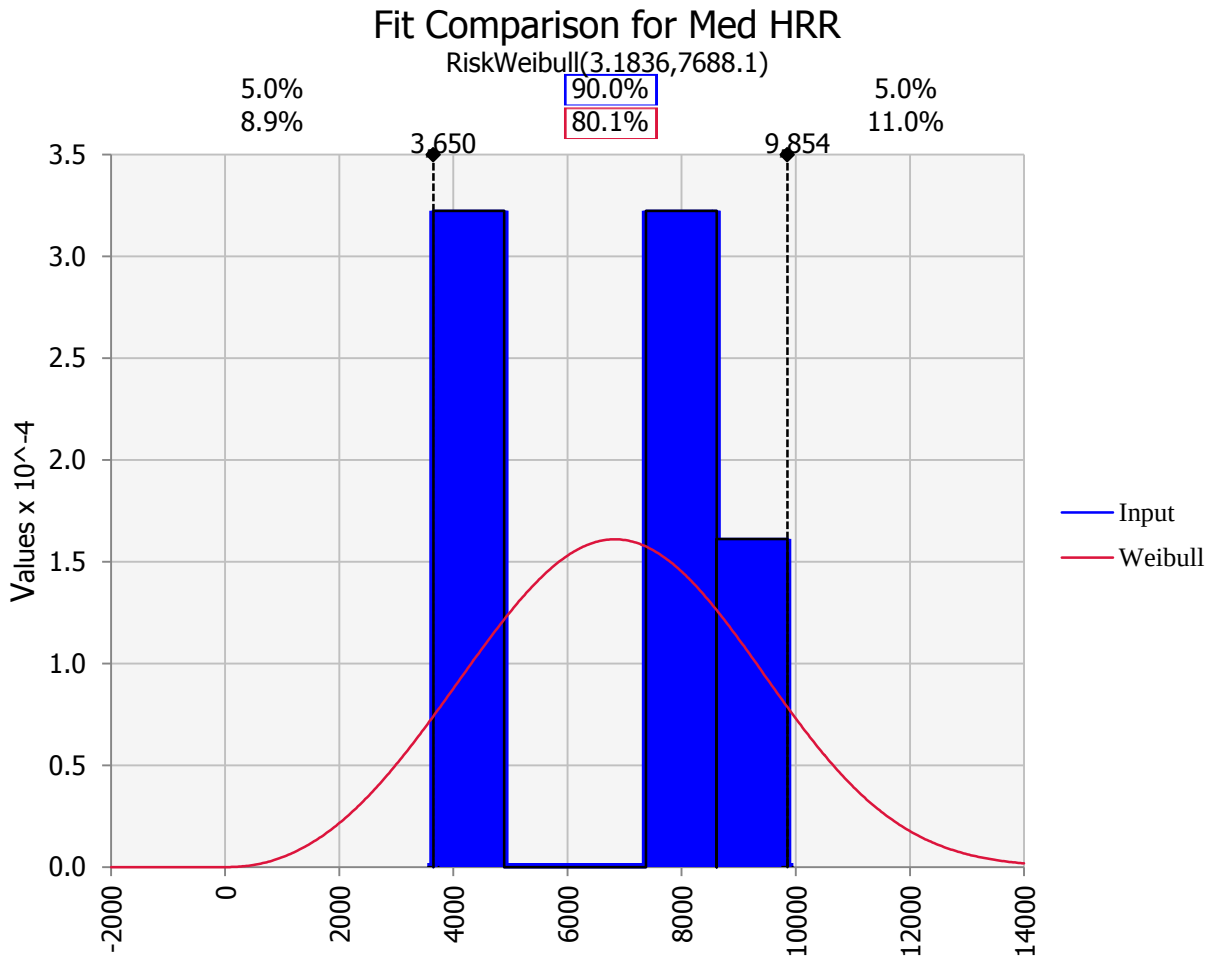

A.1.2 Time to reach peak heat release rate

A.1.2.1 Mini classification

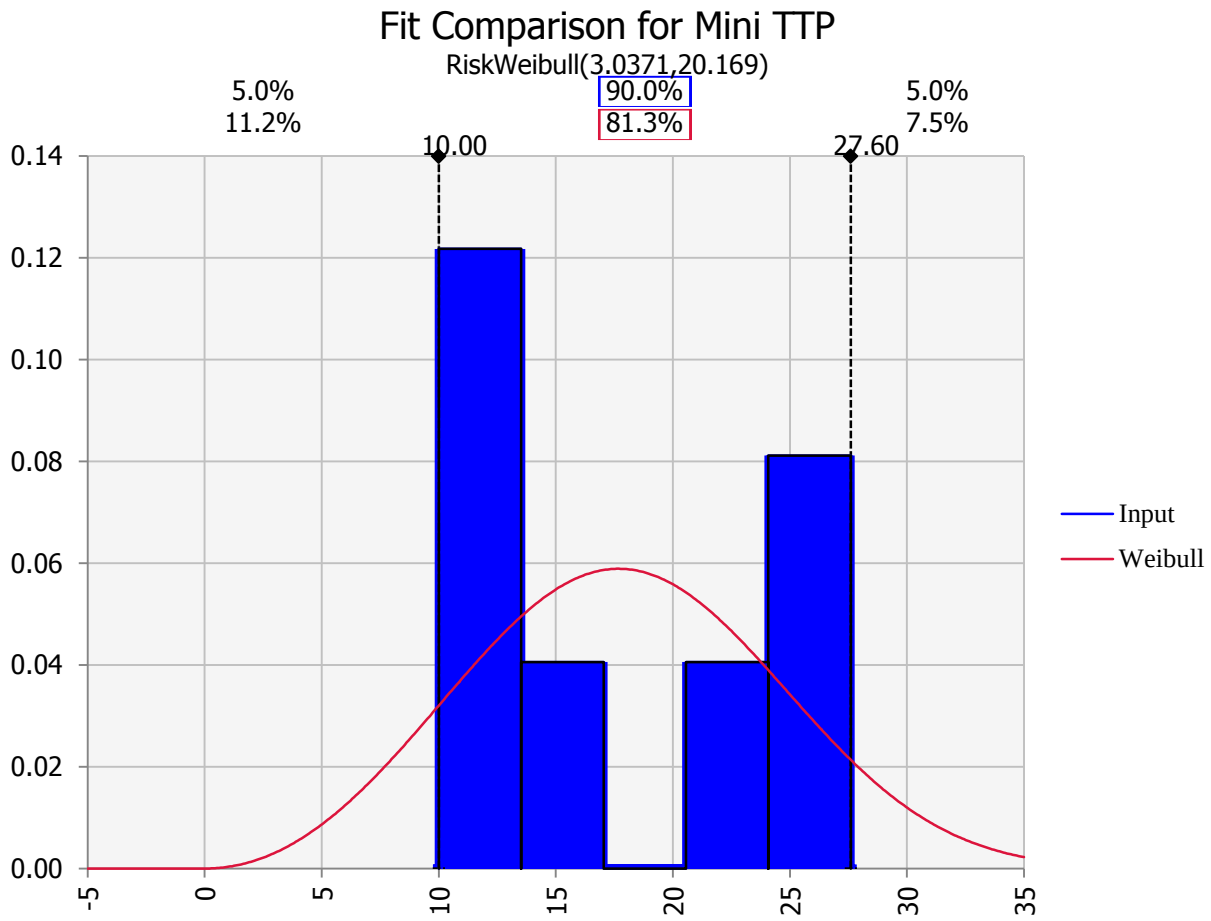

A.1.2.2 Light classification

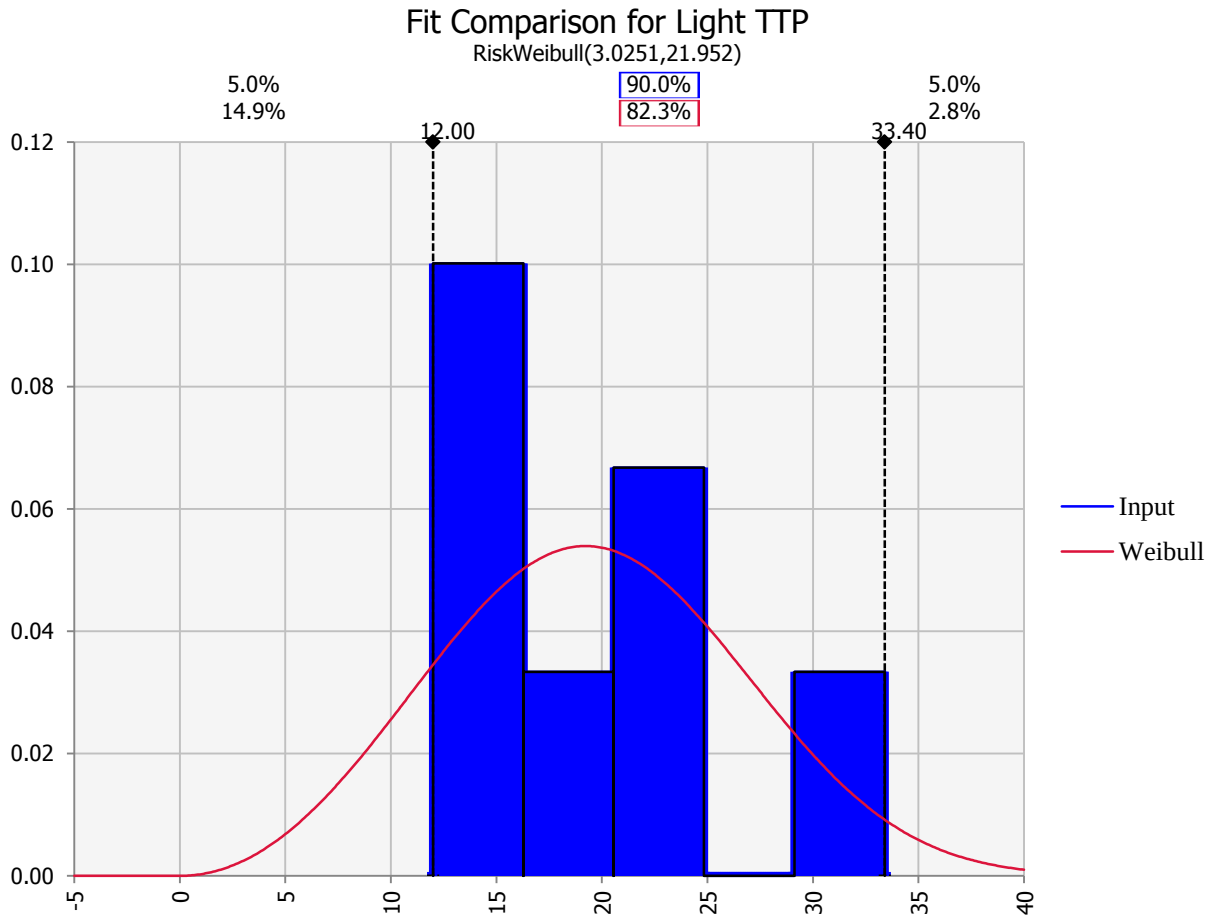

A.1.2.3 Compact classification

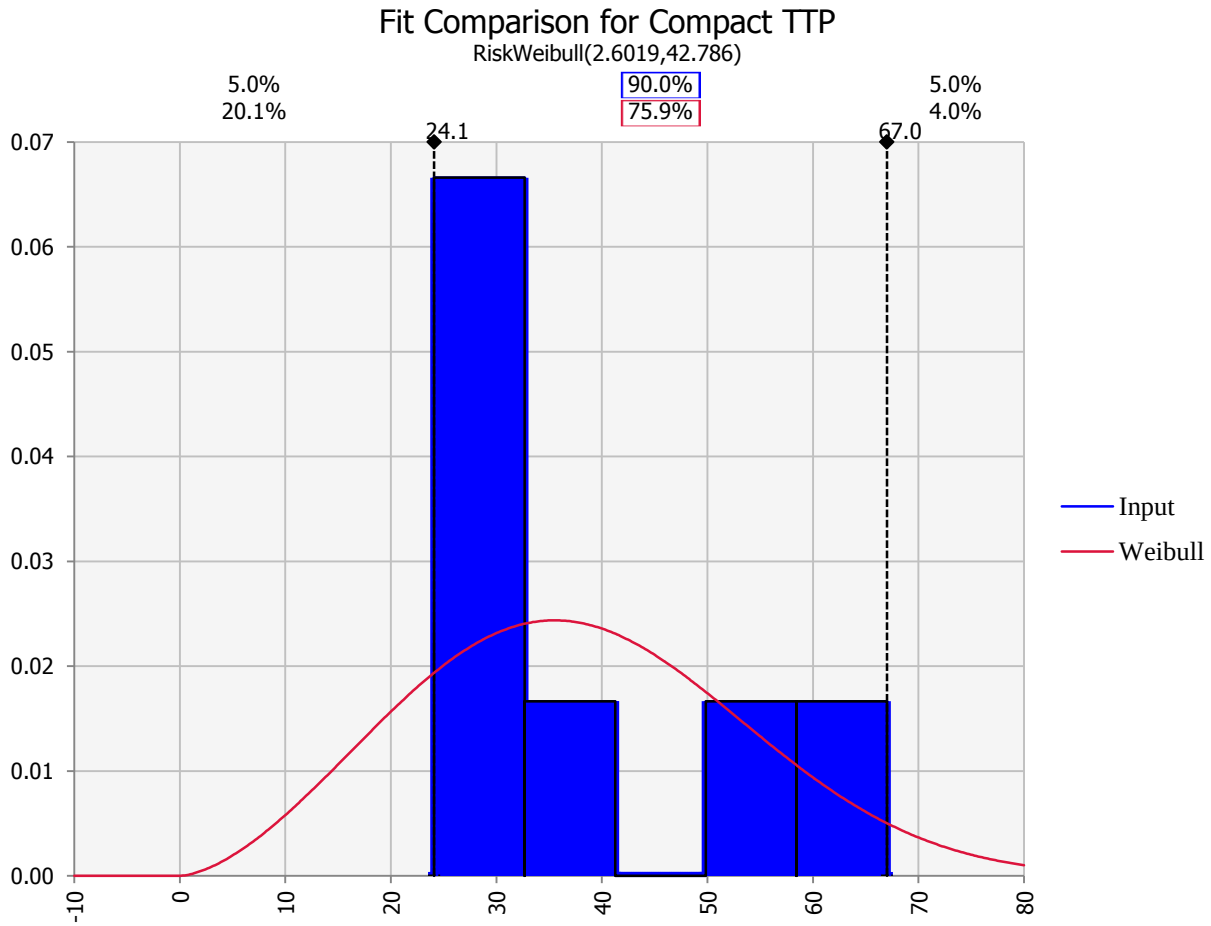

A.1.2.4 Medium classification

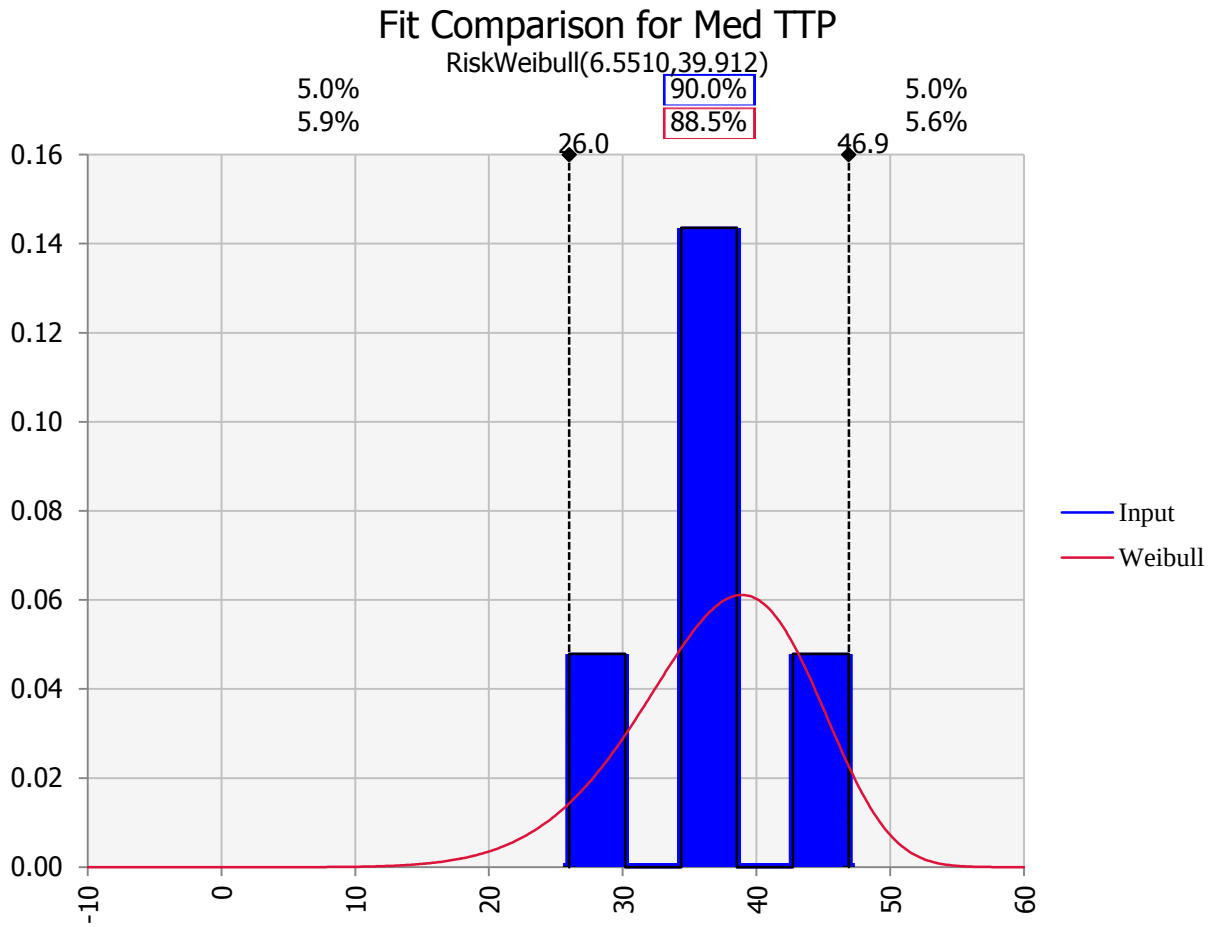

A.1.3 Total energy released

A.1.3.1 Mini classification

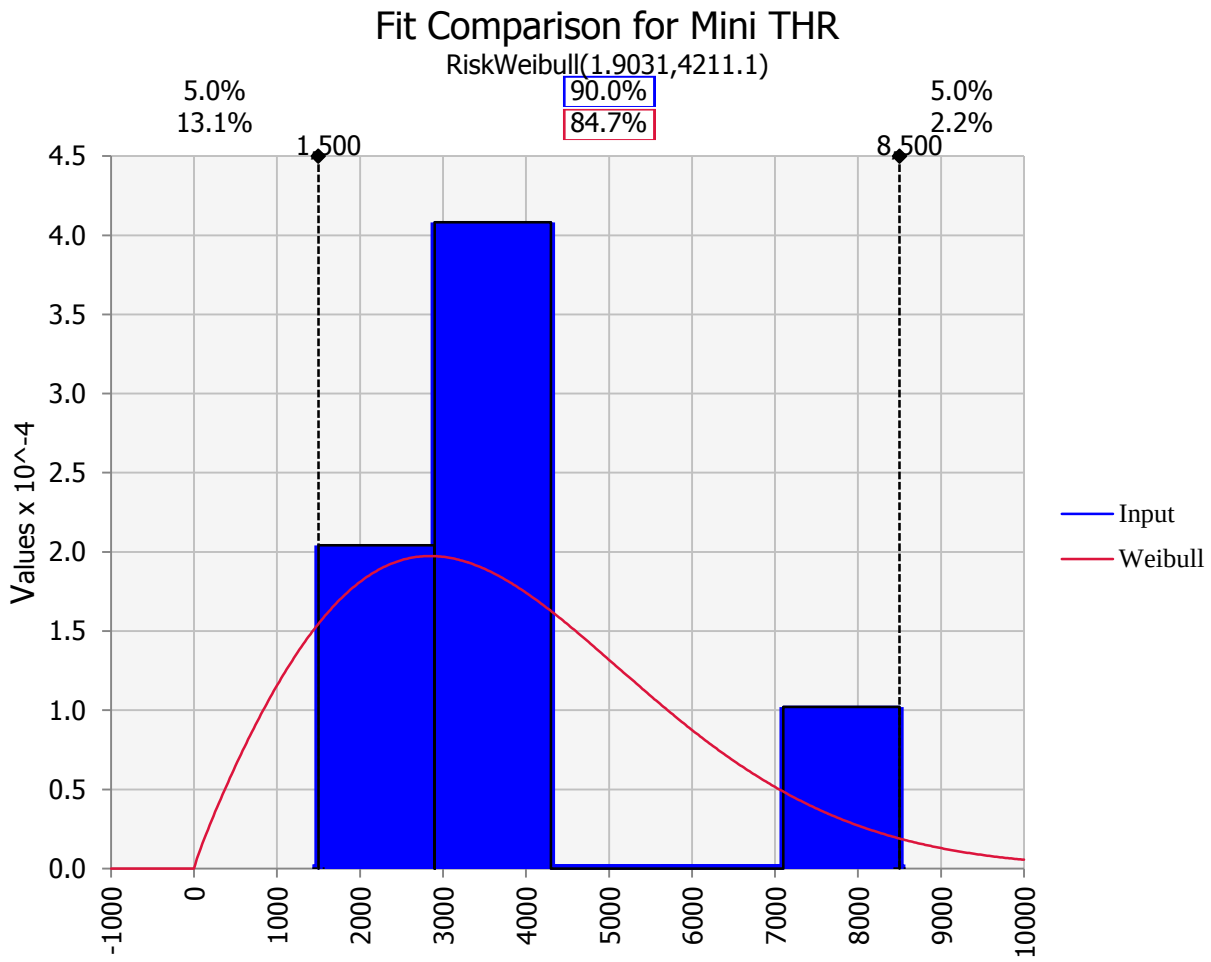

A.1.3.2 Light classification

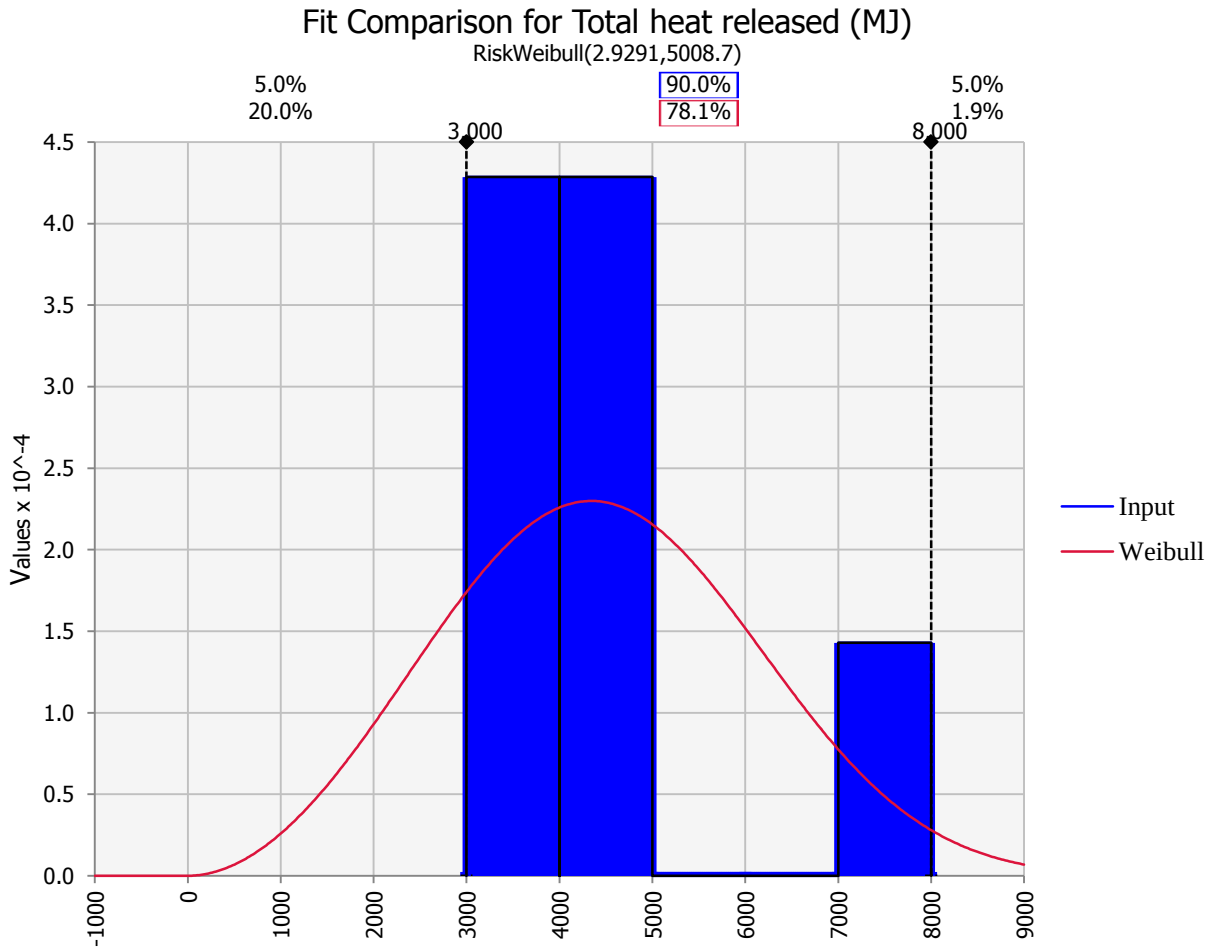

A.1.3.3 Compact classification

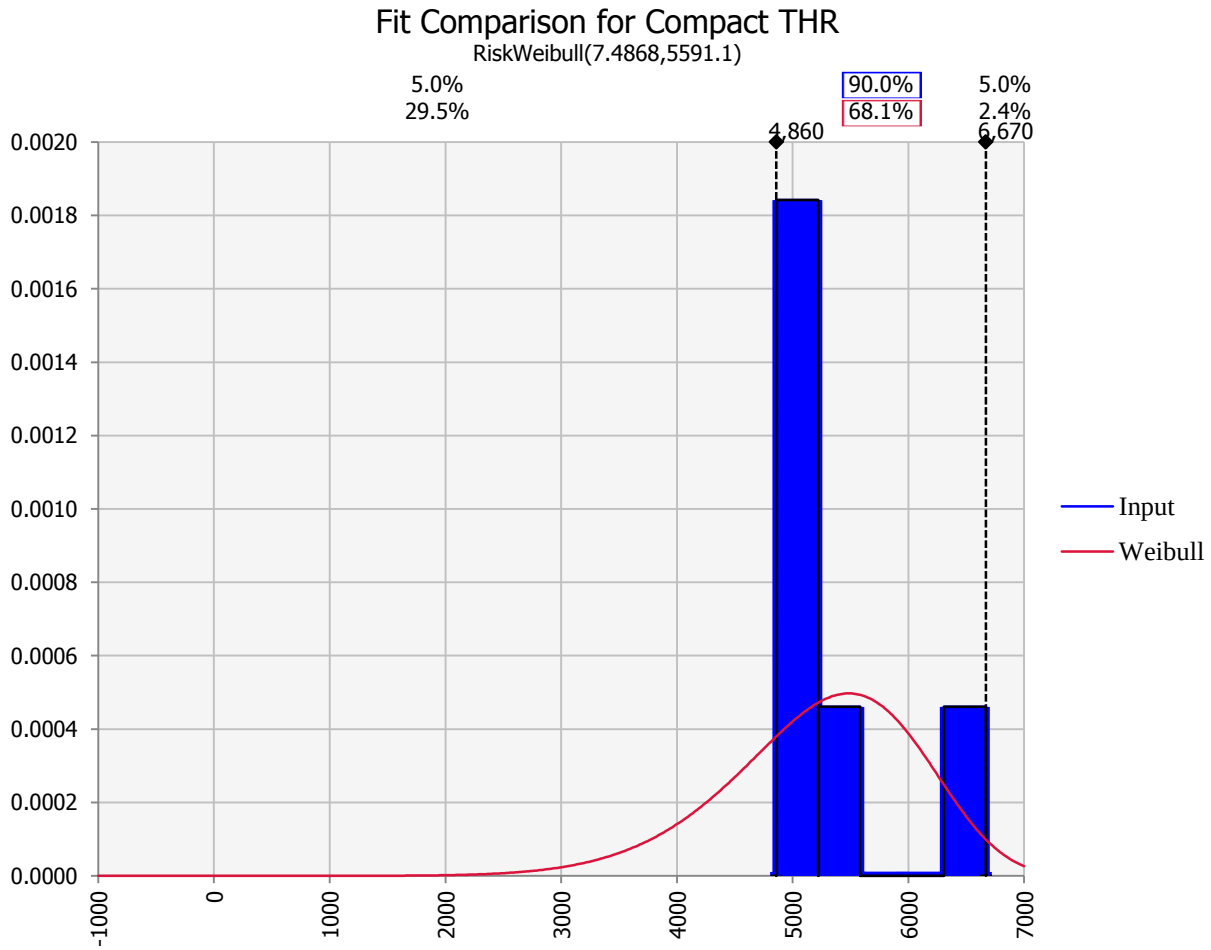

A.1.3.4 Medium classification

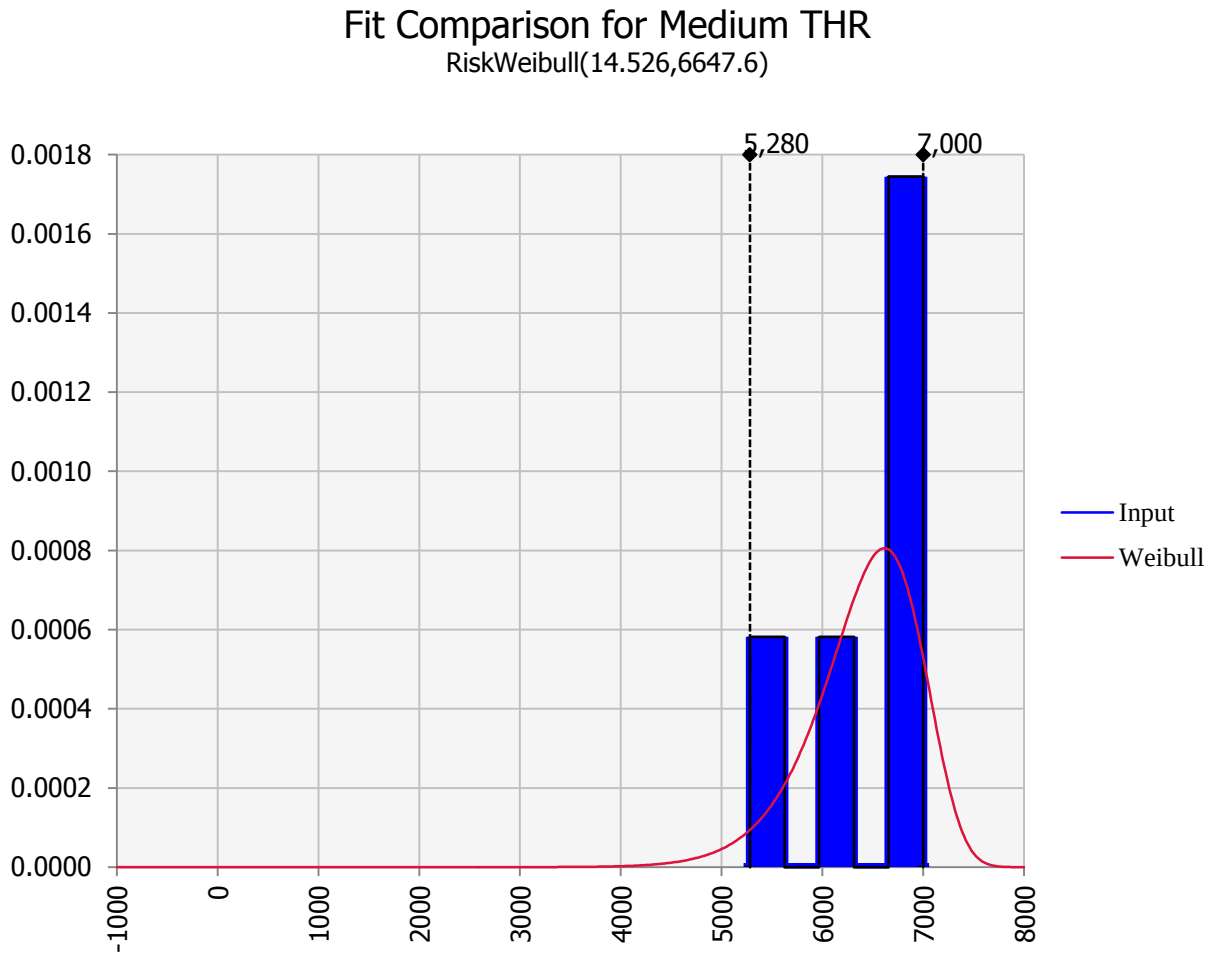

Appendix B

B.1 Vehicle fleet statistics

This section presents the statistics of the vehicle fleet statistics that have been used to estimate the composition of vehicle on the road.

B.1.1 European Union statistics

This set of data has been obtained from

http://epp.eurostat.ec.europa.eu/portal/page/portal/transport/data/database

	< 1000kg	1000 - 1249 kg	1250 - 1499 kg	> 1500 kg
Netherlands	33.7	31	24.8	10.4
Estonia	8.1	31.5	32.3	28.1
Spain	22.6	34.1	31.8	11.5
Finland	11.7	28.9	36.4	23.1
Cyprus	27.4	33.6	23.8	15.1
Latvia	7.4	30.7	32.9	29.1
Norway	10.1	27.6	36.2	26.1
Switzerland	8.6	23.5	30.6	37.4
Poland	33.3	31	20	15.7
Portugal	0.6	5.7	28	65.7
Average, %	**16.3**	**27.8**	**29.7**	**26.2**

B.1.2 United States of America statistics

Type and Size	1997	1998	1999	2000	2001	2002	2003	2004
Passenger Vehicles	191,960,390	195,749,209	200,012,521	203,913,482	207,719,870	211,992,662	216,729,606	223,213,958
Cars	124,672,920	125,965,709	126,868,744	127,740,420	128,874,299	130,196,812	131,549,941	133,275,377
Subcompact	30,275,524	29,180,185	27,979,452	26,760,764	25,619,810	24,571,274	23,148,380	21,851,909
Compact	36,139,144	36,913,085	37,094,457	37,323,021	37,554,060	37,781,267	38,297,173	38,318,494
Midsize	29,531,161	31,369,741	33,390,540	35,580,282	37,470,777	39,229,025	40,793,931	42,654,513
Full-size	28,727,091	28,502,698	28,404,295	28,056,742	28,069,375	28,325,231	28,832,982	29,642,017
Vans	16,159,473	16,718,727	17,323,154	17,890,186	18,226,000	18,382,607	18,555,362	18,931,753
Minivans	10,312,124	10,992,409	11,723,593	12,431,565	12,882,988	13,221,220	13,491,379	13,856,151
Large Vans	5,844,175	5,723,193	5,596,603	5,455,819	5,340,375	5,158,902	5,061,582	5,072,354
SUVs	14,531,850	16,247,573	18,401,488	20,726,979	22,995,533	25,521,939	28,354,796	31,415,143
Midsize	10,128,214	11,369,629	13,265,658	14,991,841	16,726,433	18,736,041	20,871,314	23,246,926
Full-size	3,601,079	4,092,926	4,655,935	5,298,616	5,880,436	6,438,417	7,168,909	7,875,001
Pickup Trucks	34,314,455	34,819,388	35,653,344	36,118,236	36,389,196	36,792,345	37,288,653	38,557,291
Compact	13,679,034	13,675,186	13,826,540	13,766,295	13,550,444	13,248,588	13,245,677	13,426,656
Standard	20,635,421	21,144,202	21,826,804	22,351,941	22,838,752	23,543,757	24,042,976	25,124,684

Figure B-1: Vehicle fleet statistics (Reproduced from Subramaniam, 2006)

B.2 Event tree for vehicle fires in NZ car parking buildings

B.2.1 From 1996 – 2003 (Taken from Li (2004))

Average registered vehicles in NZ from 1996 - 2003 = 2,636,579 licensed vehicle per year.

Annual Vehicle Fire Frequency per Number of Vehicle Registered = 3371 / 2,636,579 = 1.28 $\times 10^{-3}$ per year

Average number of vehicle fire in parking building = 12.6 per year

Probability of vehicle fire in parking building = 4.74×10^{-6} per year

Fire risk for a single vehicle in New Zealand			
Event probability	Fire spread	Vehicle involvement	Outcome

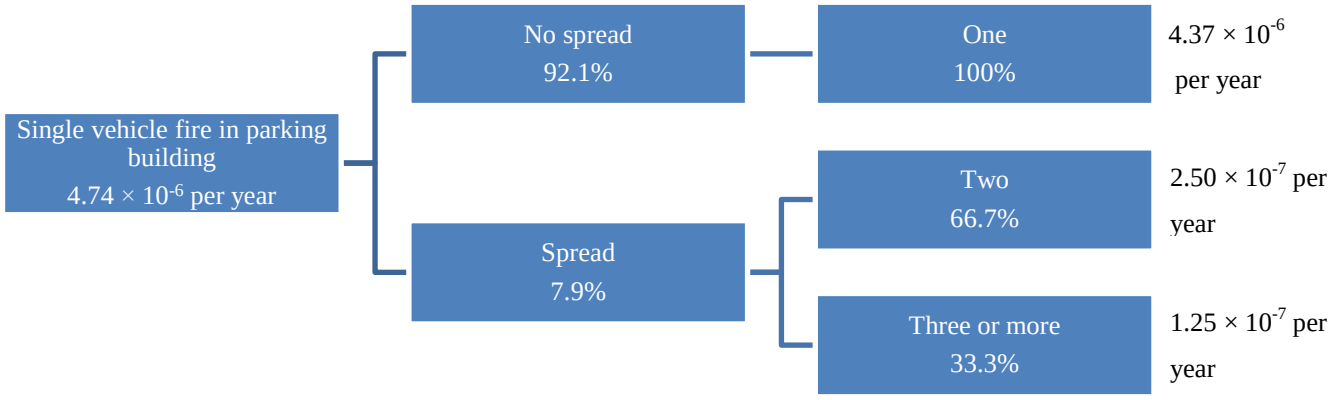

B.2.2 From 2004 – 2011

Average mobile property vehicle fire : 2987.6 fires per year

Average registered vehicles in NZ from 2004 – 2011 = 26253760 / 8 years = 3,281,720 licensed vehicle per year

Annual Vehicle Fire Frequency per Number of Vehicle Registered = 2987.6 / 3,281,720 = 9.10×10^{-4} per year

Average number of vehicle fire in parking building = 3.75 per year

Probability of vehicle fire in parking building = 3.75 / 2987.6 = 1.26×10^{-3}

$= 9.10 \times 10^{-4}$ per year $\times 1.26 \times 10^{-3}$

$= 1.15 \times 10^{-6}$ per year

Fire risk for a single vehicle in New Zealand			
Event probability	Fire spread	Vehicle involvement	Outcome

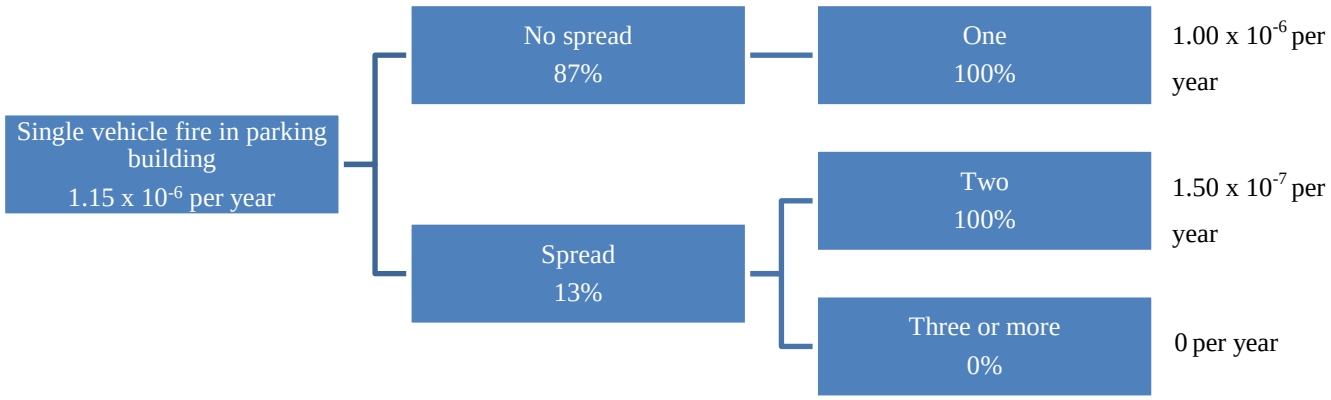

B.2.3 Combined statistics from 1996 – 2011

Average registered vehicles in NZ 1996 - 2011 = 2,959,150 licensed vehicle per year

Annual Vehicle Fire Frequency per Number of Vehicle Registered = 3179.3 / 2,959,150 = 1.07×10^{-3} per year

Average number of vehicle fire in parking building = 8.2 per year

Probability of vehicle fire in parking building = 2.58×10^{-3}

$= 1.07 \times 10^{-3}$ per year x 2.58×10^{-3}

$= 2.76 \times 10^{-6}$ per year

Fire risk for a single vehicle in New Zealand			
Event probability	Fire spread	Vehicle involvement	Outcome

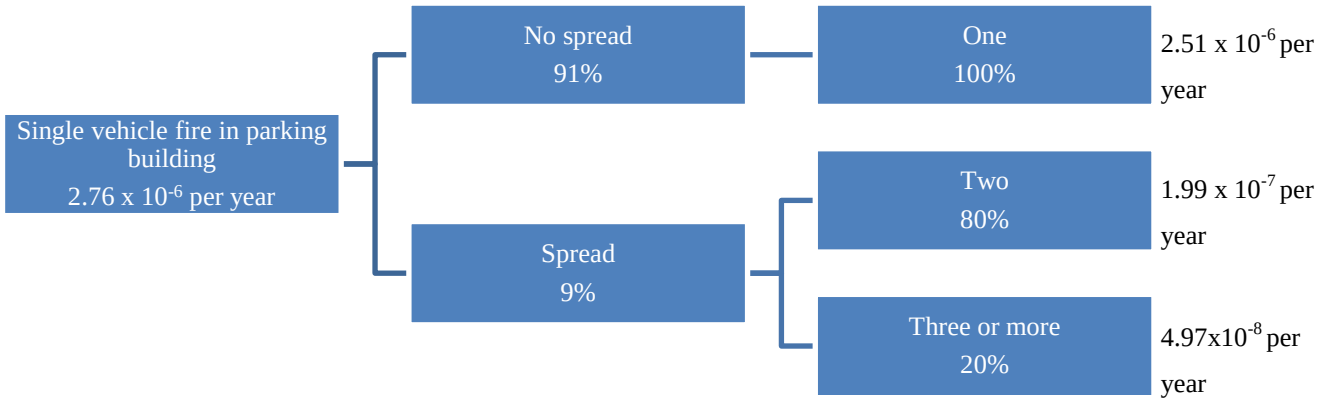

B.3 Vehicle fire statistics summary in New Zealand from the year 1996 – early 2012

B.3.1 Vehicle fires by year

	1996	1997	1998	1999	2000	2001	2002	2003	2004
Private fleet carpark: Car, Bus, Truck (Single level - covered)	*9*	*11*	*11*	*11*	*9*	*3*	*1*	*6*	2
Public carpark: Multi-storied above ground	*5*	*1*	*1*	*1*	*0*	*0*	*3*	*3*	4
Public carpark: Single level - covered	*0*	*2*	*2*	*4*	*2*	*1*	*0*	*1*	0
Public carpark: Multi-storied below ground	*1*	*0*	*3*	*0*	*1*	*1*	*1*	*0*	0
Public carpark: Multi-storied above and below ground	*1*	*4*	*1*	*0*	*1*	*0*	*0*	*0*	0
TOTAL	*16*	*18*	*18*	*16*	*13*	*5*	*5*	*10*	6

	2005	2006	2007	2008	2009	2010	2011	2012	TOTAL
Private fleet carpark: Car, Bus, Truck (Single level - covered)	1	2	0	1	3	3	0	0	73
Public carpark: Multi-storied above ground	1	0	2	1	2	0	3	1	28
Public carpark: Single level - covered	1	1	0	0	1	0	0	0	15
Public carpark: Multi-storied below ground	1	0	1	0	0	0	0	0	9
Public carpark: Multi-storied above and below ground	0	0	0	0	0	0	0	0	7
TOTAL	4	3	3	2	6	3	3	1	132

B.3.2 Causes of fire

Causes of fire	Total
Deliberately lit	36
Electrical faults	33
Mechanical failure or malfunction	23
Carelessness	17
Unknown	12
Others	11
TOTAL	132

B.3.3 Vehicles involved

Vehicles involved	Total
Single	120
Multiple	12
All	132

B.3.4 Types of vehicles involved

Types of vehicles involved	Total
Car, Taxi, Ambulance	81
Unknown	24
Other Vehicles	20
Bus	7
TOTAL	132

B.3.5 Vehicle by day of week

Vehicle by day of week	Total
Sunday	15
Monday	23
Tuesday	12
Wednesday	17
Thursday	27
Friday	16
Saturday	22
TOTAL	132

B.3.6 Heat sources

Heat sources	Total
Short circuit arc	45
Match, lighter & cigarettes	24
Exposure fire	22
Hot object	23
Flame	9
Not Recorded	9
TOTAL	132

B.3.7 Object first ignited

Object first ignited	Total
Unknown	32
Electrical components	36
Flammable liquid and gases (not aerosols or propellants)	19
Others	20
Upholstery and soft goods	16
Structure components	9
TOTAL	132

B.3.8 Materials first ignited

Materials first ignited	Total
Unknown	35
PVC: Floor tiles, Guttering, Pipes, Plastic bags, Electrical	36
Insulation	1
Upholstery and soft goods	19
Flammable liquid	19
Others	22
TOTAL	132

B.4 Parking characteristics

Shown in this appendix are weekly parking characteristics for other car parking buildings processed from the data obtained from the internet.

B.4.1 Santa Monica, USA - Library

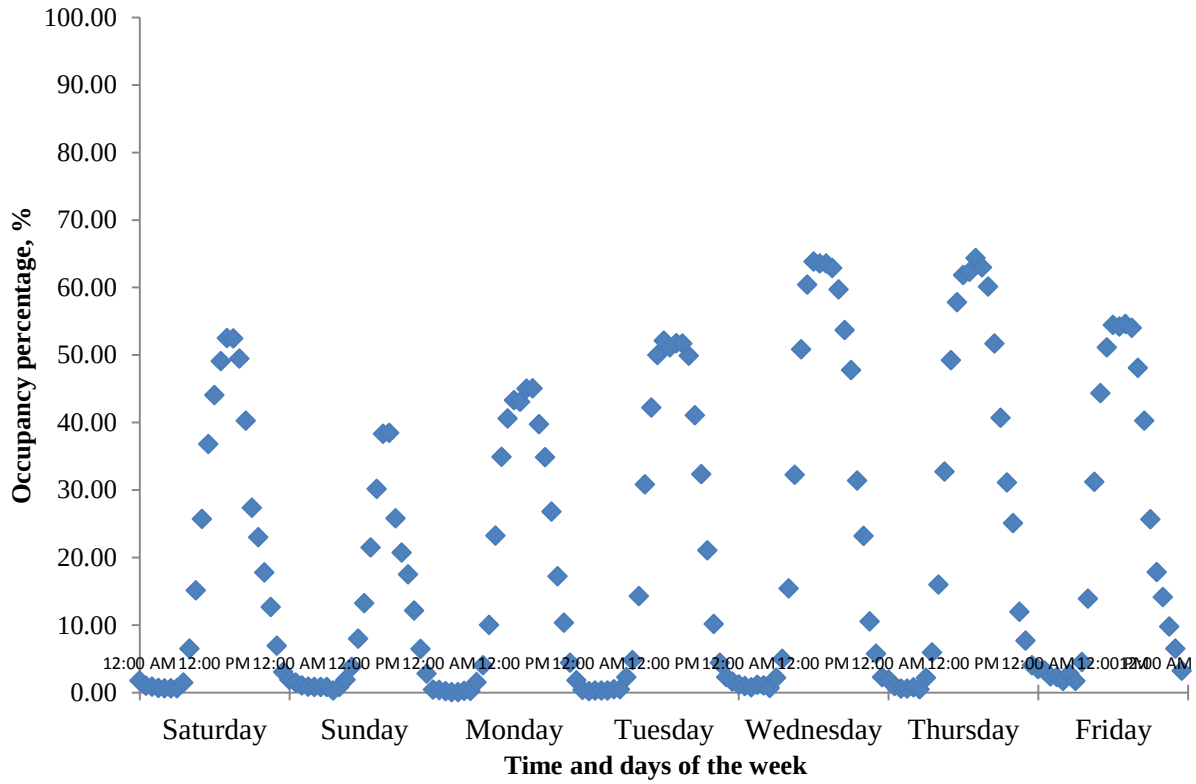

B.4.2 San Francisco, USA – Fifth & Mission car parking building

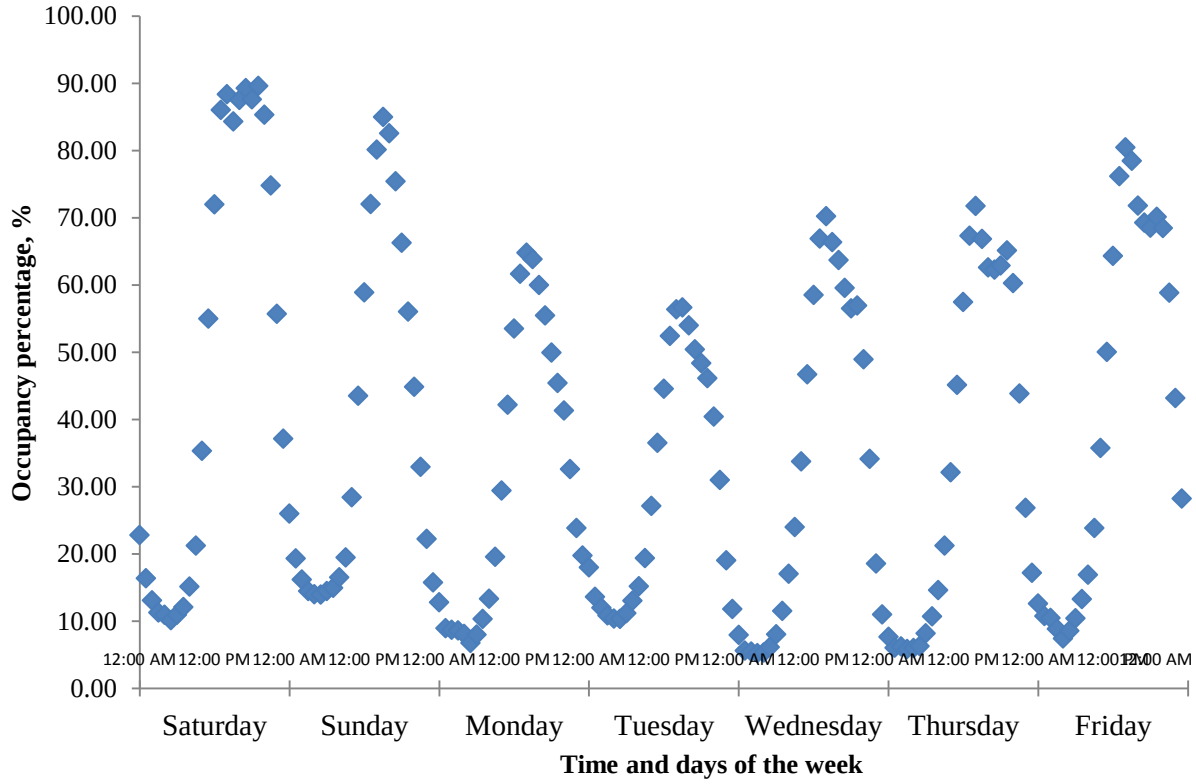

B.4.3 San Francisco, USA – Performing Arts car parking building

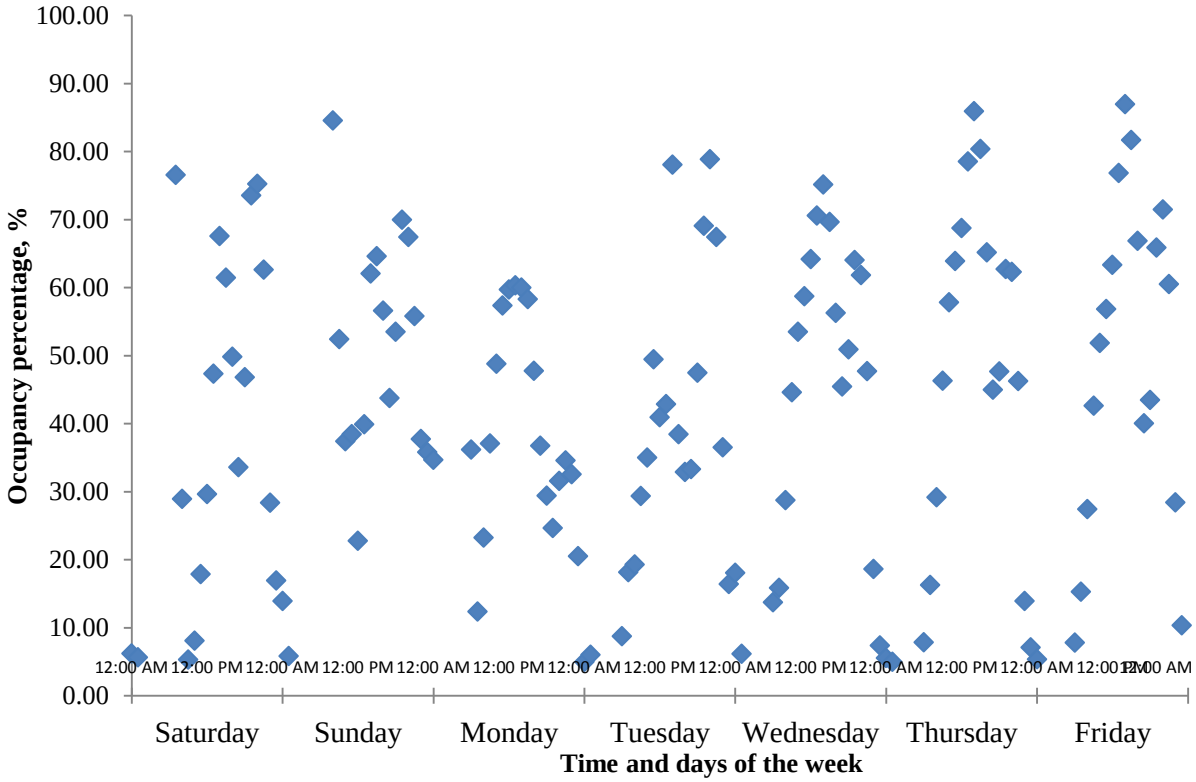

Appendix C

C.1 Fire growth and decay coefficient determination

The characterised design fire can only be constructed with sufficient data for the fire growth rate, peak heat release rate and decay rate coefficients. The proposed distribution values of peak heat release rate for each curb weight classification are obtained from the work in Chapter 3. This section provides the coefficients for the fire growth and decay for the purpose of characterising a design fire. In this work, the approach of forming a boundary line plot is presented by using the P.e combination fire growth and decay coefficients presented as a scatter plot. Table C-1 - Table C-6 shows the Peak method fire growth and Exponential decay coefficients for each of the experiments in their corresponding classifications.

Table C-1: Fire growth and decay coefficients for Passenger Car: Mini

Classification ID	Peak growth (kW/min^2)	Exponential decay (min^{-1})
M1	23.7	-0.088
M2	34.3	-0.201
M3	7.0	-0.071
M4	3.1	-0.009
M5	2.2	-0.062
M6	23.0	-0.131
M7	22.3	-0.643

Table C-2: Fire growth and decay coefficients for Passenger Car: Light

Classification ID	Peak growth (kW/min^2)	Exponential decay (min^{-1})
L1	3.2	-0.035
L2	1.4	-0.046
L3	15.5	-0.066
L4	13.6	-0.025
L5	36.7	-0.320
L6	21.0	-0.091
L7	35.6	-0.122

Table C-3: Fire growth and decay coefficients for Passenger Car: Compact

Classification	Peak growth	Exponential

ID	(kW/min²)	decay (min^{-1})
C1	6.5	-0.058
C2	12.9	-0.071
C3	5.3	-0.043
C4	12.9	-0.040
C5	0.6	-0.081
C6	1.0	-0.097
C7	3.4	-0.084

Table C-4: Fire growth and decay coefficients for Passenger Car: Medium

Classification ID	Peak growth (kW/min²)	Exponential decay (min^{-1})
MED1	2.8	-0.082
MED2	6.1	-0.161
MED3	7.3	-0.207
MED4	1.7	-0.011
MED5	12.9	-0.066

Table C-5: Fire growth and decay coefficients for Passenger Car: Heavy

Classification ID	Peak growth (kW/min²)	Exponential decay (min^{-1})
H7	2.8	-0.067

Table C-6: Fire growth and decay coefficients for Minivan/MPV

Classification ID	Peak growth (kW/min²)	Exponential decay (min^{-1})
MPV4	84.7	-0.084
MPV5	2.1	-0.135
MPV6	248.2	-0.043
MPV7	1.2	-0.069
MPV8	1.2	-0.061
MPV9	10.1	-0.046

C.2 Boundary line plot approach

Figure C-1 shows the scatter plot for the Peak method fire growth coefficients against the vehicle curb weight. The ANSI Minivan/MPV classification does not specify a particular curb weight range, hence not included in this analysis.

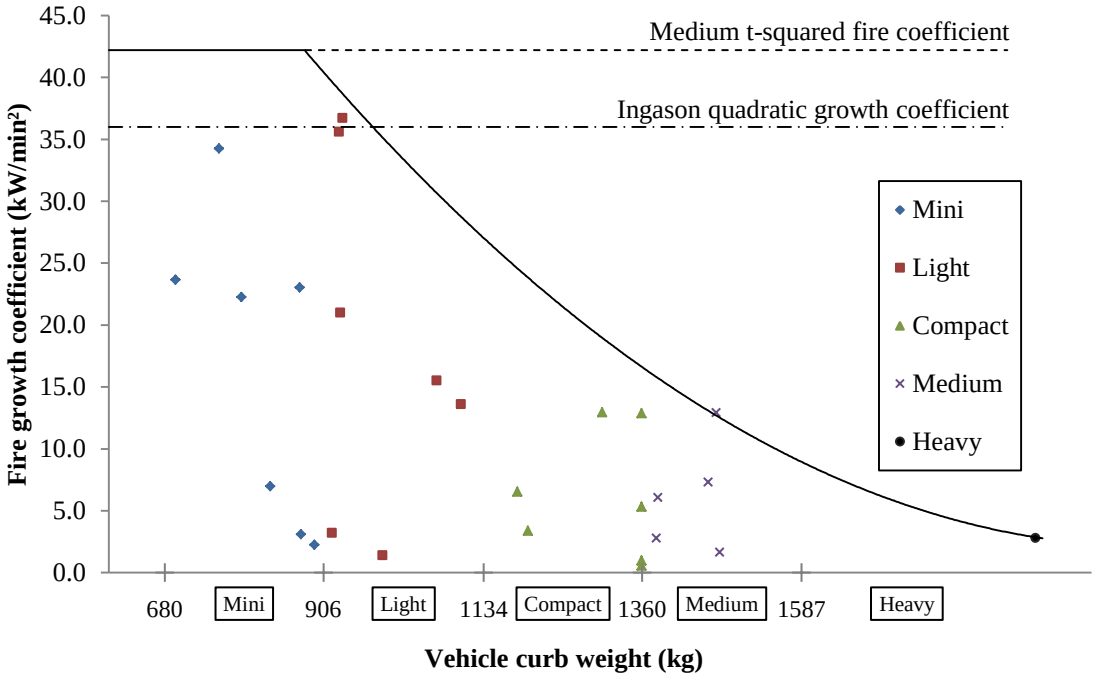

Figure C-1: Scatter plot for Peak method fire growth coefficients against vehicle classifications.

The horizontal straight line at 42.19 kW/min² indicates the medium t-squared fire growth coefficient and it can be seen that 94% of the fire growth coefficients lie below this line when considering the two excluded points. This suggests that the medium t-squared fire growth for the design fire of a car parking building is a conservative on the assumption that the faster the growth, the greater the hazard. In addition, another horizontal straight line at 36 kW/min² indicates the fire growth coefficient suggested by Ingason [93].

The curved line in the plot is the boundary of fire growth coefficient values constructed based on the scatter data in the plot. Using the maximum data of each curb weight classification to be the boundary, a quadratic line of $\alpha_{peak} = 2.75 \times 10^{-5} w^2 - 0.1148w + 121.8$ is able to be formed, where α_{peak} is the growth coefficient in kW/min² and w is the curb weight in the range 907 kg to 2000 kg and a sensitivity assessment for the appropriate number of significant figures used for the coefficients in the quadratic equation has been completed. The maximum data points are used as to represent the worst case scenario for a design fire.

Though, it is decided to start the curved line at the border of Passenger Car: Mini and Light since the maximum data point for Passenger Car: Mini is lower than Passenger Car: Light and the line ends at Passenger Car: Heavy with curb weight of around 2000 kg. Thus, it is suggested for Passenger Car: Mini to use the medium t-squared fire growth as the boundary. Based on the current data, the solid line (a combination of the curved and straight lines discussed above) implies that generally the fire growth coefficient decreases as the vehicle curb weight increases and this line is used to determine a design value for the fire growth coefficient.

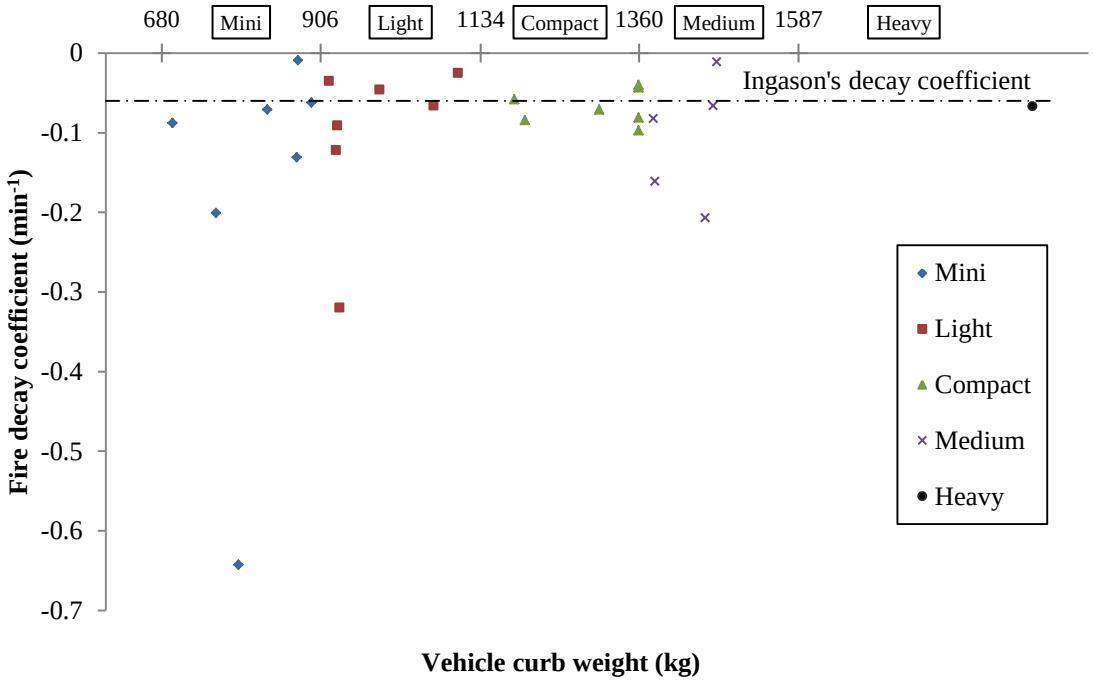

Figure C-2: Scatter plot for fire decay coefficient against vehicle classifications.

Figure C-2 shows the scatter plot for Exponential method fire decay coefficient against vehicle curb weight. In this figure, each of the Exponential method fire decay coefficient data for all classifications are plotted and a horizontal line at -0.06 min^{-1} indicates the exponential decay given by Ingason (2006). For the decay phase, most of the data points are distributed in between -0.207 min^{-1} and -0.009 min^{-1} while M7 and L5 have quicker decay rates of -0.643 min^{-1} and -0.320 min^{-1} respectively. Thus an average decay value of -0.08 min^{-1} is obtained

excluding experiments M7 and L5 and the average value is -0.11 min^{-1} if experiments M7 and L5 are included.

Table C-7: Total energy released for each vehicle classification with different decay coefficients.

Vehicle classification	Maximum and minimum growth coefficients (kW/min^2)	Total energy released, MJ			
		-0.11 min^{-1} decay	-0.08 min^{-1} decay	-0.06 min^{-1} decay (Ingason)	Avg. from experiments ± standard deviation
Mini	42.0	2550	3260	4080	2900 ± 945
Light	42.0	3485	4405	5530	4471 ± 1677
	27.0	3700	4635	5755	
Compact	27.0	4850	6000	7420	5288 ± 692
	16.5	5300	6490	7900	
Medium	16.5	6680	8020	9700	6386 ± 695
	8.8	7990	9040	10730	
Heavy	8.8	9565	10910	12890	No data
	2.3	11700	15470	17345	

Table C-7 shows the comparison of the total energy released for maximum and minimum possible fire growth coefficients for each vehicle classification combined with the different decay coefficients discussed previously. The growth coefficients are obtained from the boundary line given in Figure C-1 using the upper and lower curb weights for a given classification. Also shown in the table is average and standard deviation total energy released for each classification obtained from Section 3.4.3. From Table C-7, it can be seen that the results with -0.11 min^{-1} decay coefficient lie within the standard deviation range of the experimental results for each classification except for Passenger Car: Heavy which has no data. When the -0.08 min^{-1} decay coefficient is used the total energy released lies within the standard deviation range except for Passenger Car: Medium classification where the minimum possible total energy released over-predicts the upper standard deviation by 13%. The calculated total energy released using -0.06 min^{-1} for the decay coefficient, as suggested by Ingason, over-predicts for all classification apart from Passenger Car: Light.

It is important to ensure the total energy released using the design curves are similar to values expected in reality. If rapid decay rates (i.e. smaller coefficients) are used then the total energy release from the design curves would give values much less than are considered to be reasonable. If a boundary line approach had been used for the decay, similar to the approach used for the growth coefficients then the total energy released would have been unreasonably small thus for the decay a fixed coefficient of -0.11 min^{-1} is selected irrespective of classification as it gives reasonable total energy released for a passenger car.

Appendix D

D.1 Growth and decay coefficients distribution plots

This section presents the fire growth and decay coefficients for Mini – Medium classification probability distribution plots obtained using @RISK statistical software.

D.1.1 Fire growth coefficients

The best distribution shape found for fire growth coefficients is Gamma.

D.1.1.1 Mini classification

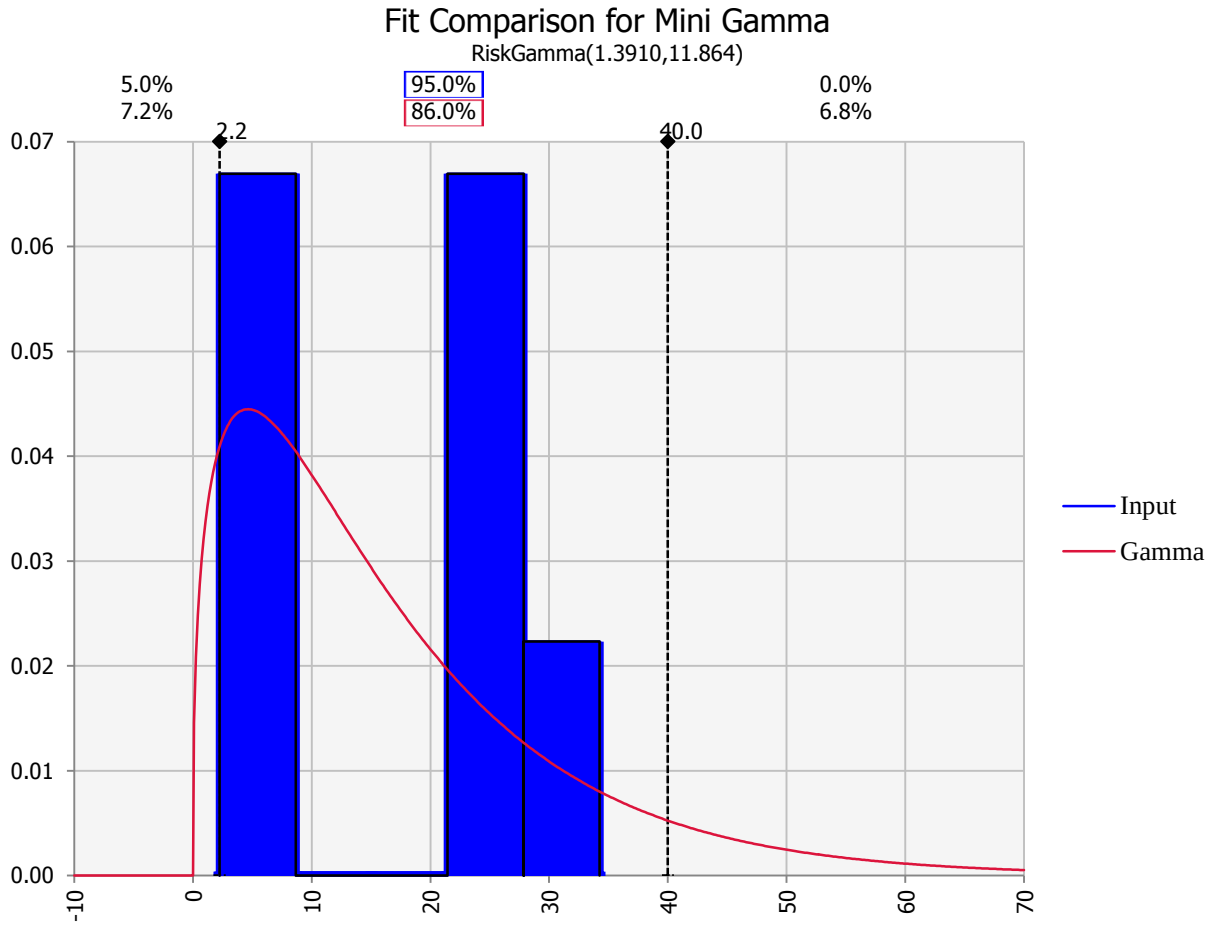

D.1.1.2 Light classification

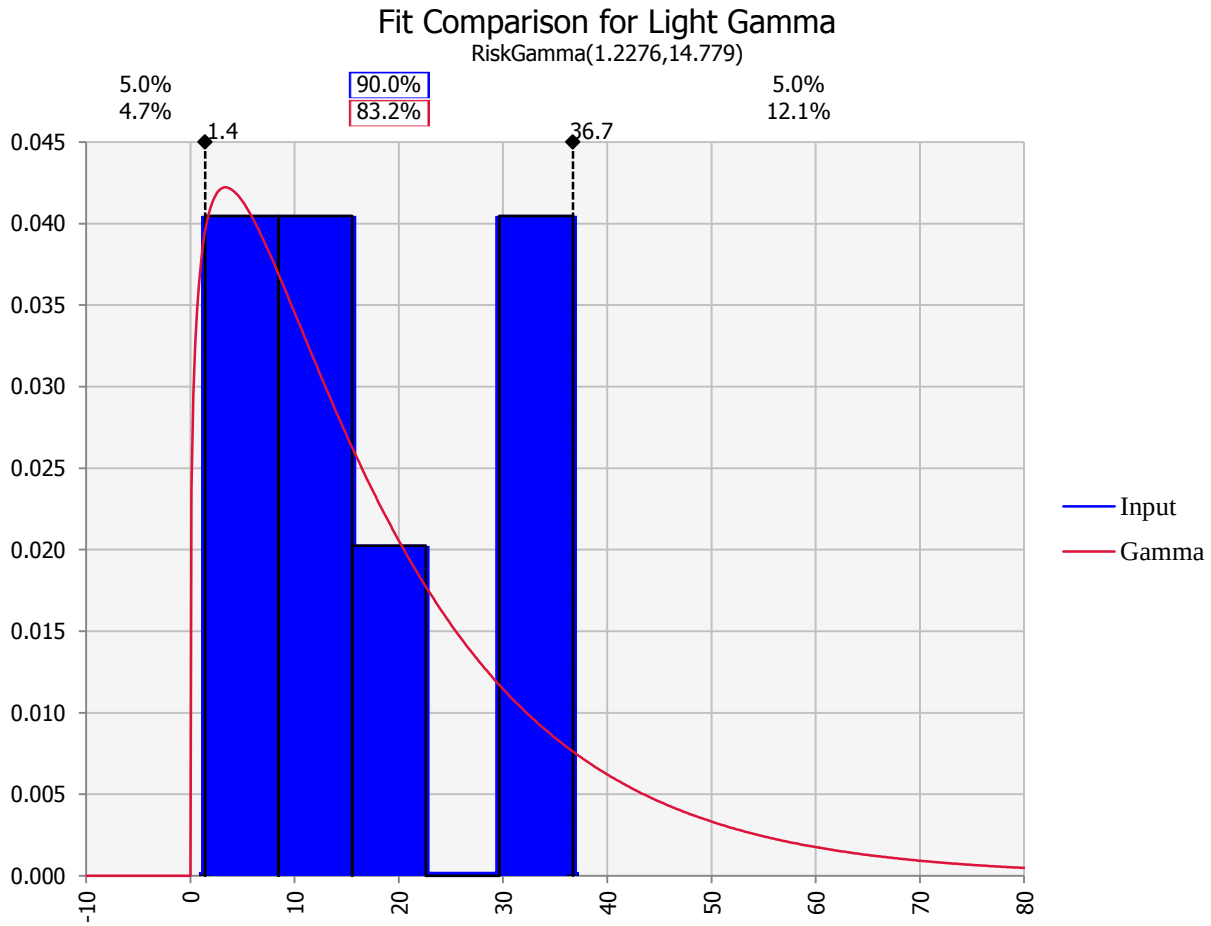

D.1.1.3 Compact classification

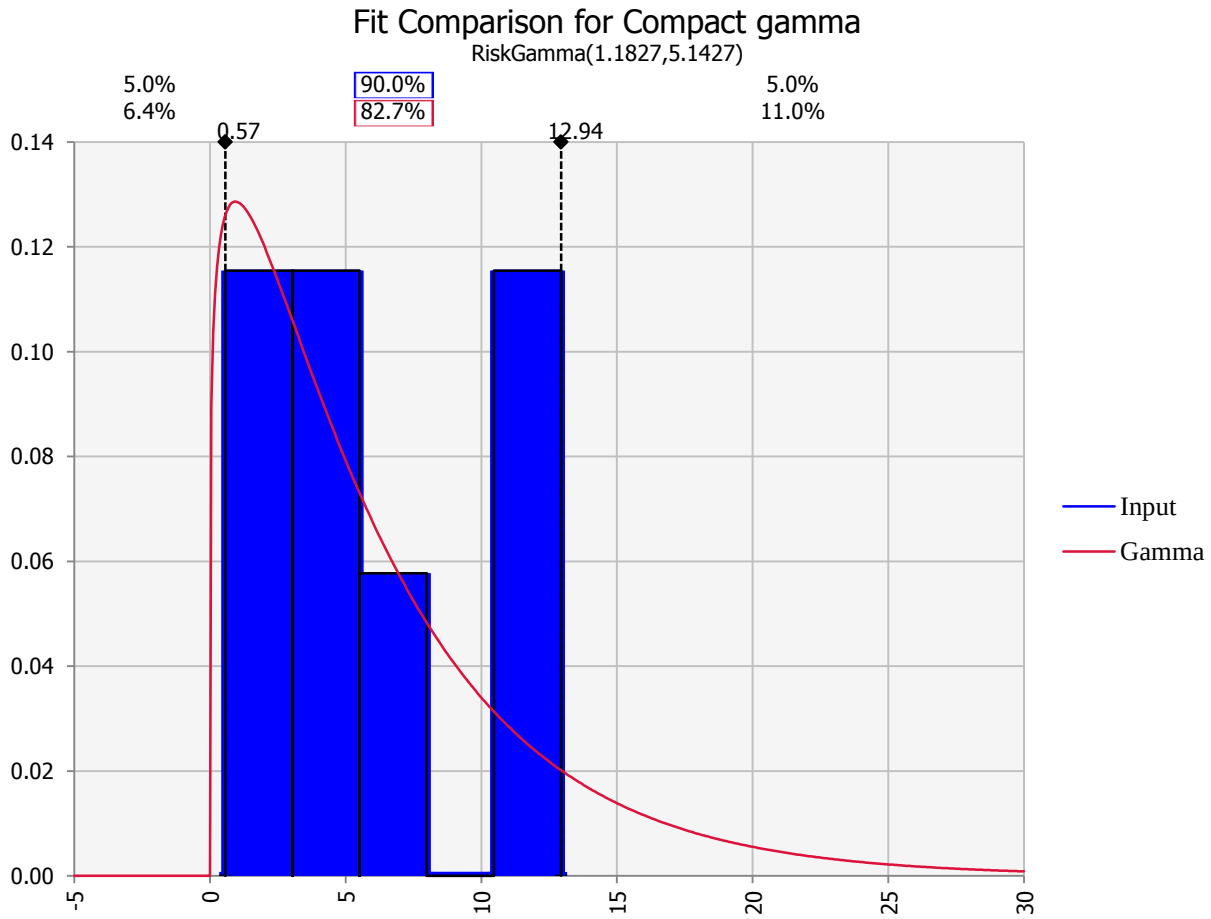

D.1.1.4 Medium classification

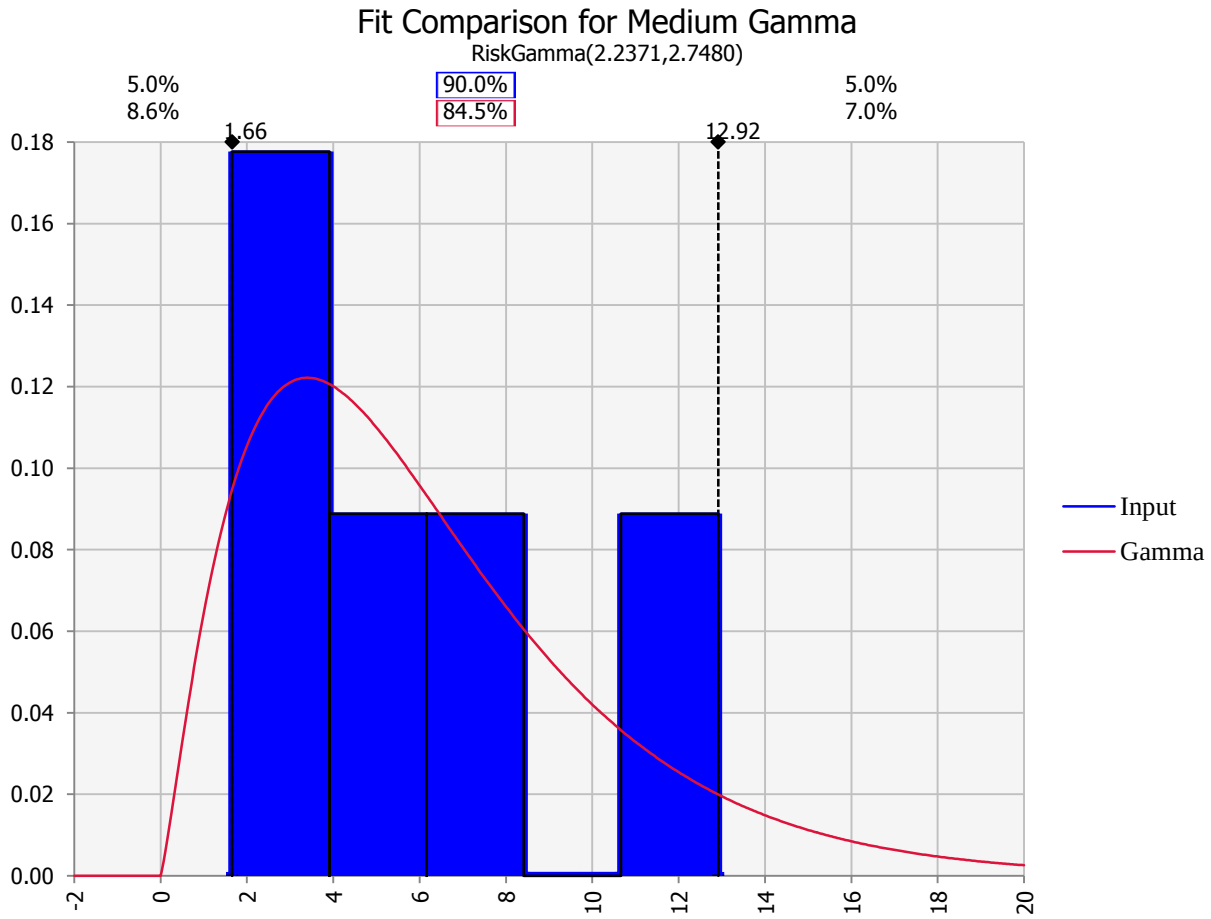

D.1.2 Fire decay coefficient

The best distribution shape found for fire decay coefficients is Weibull.

D.1.2.1 Mini classification

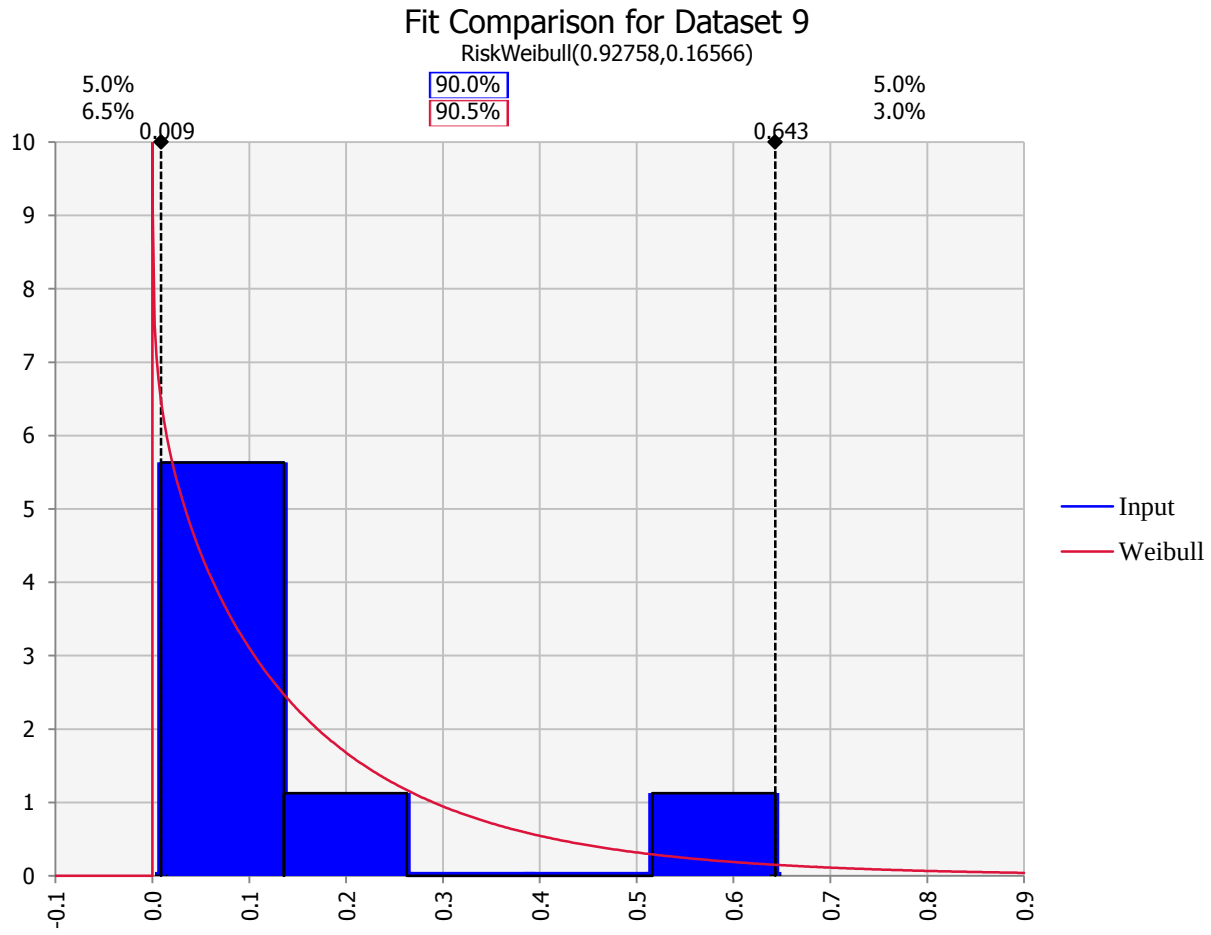

D.1.2.2 Light classification

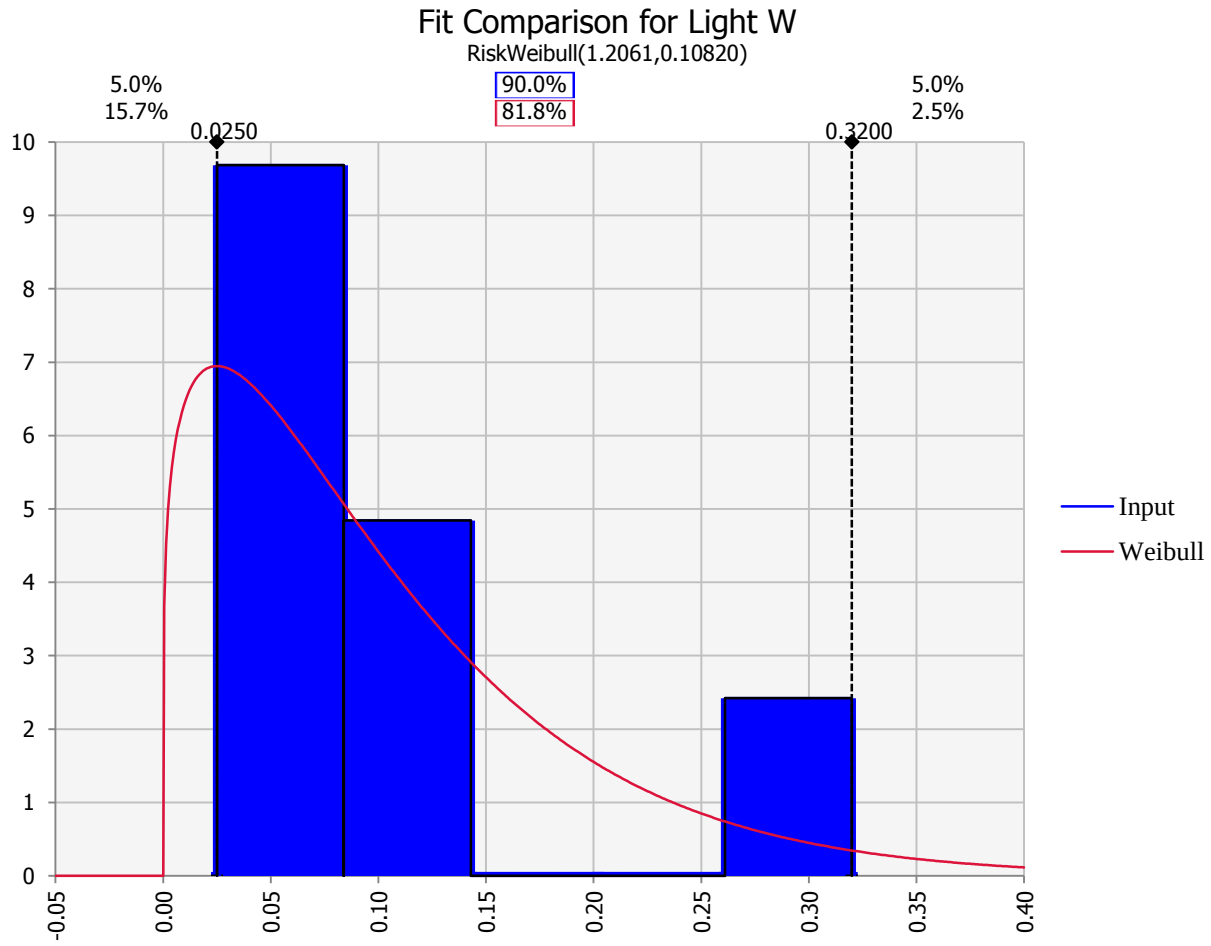

D.1.2.3 Compact classification

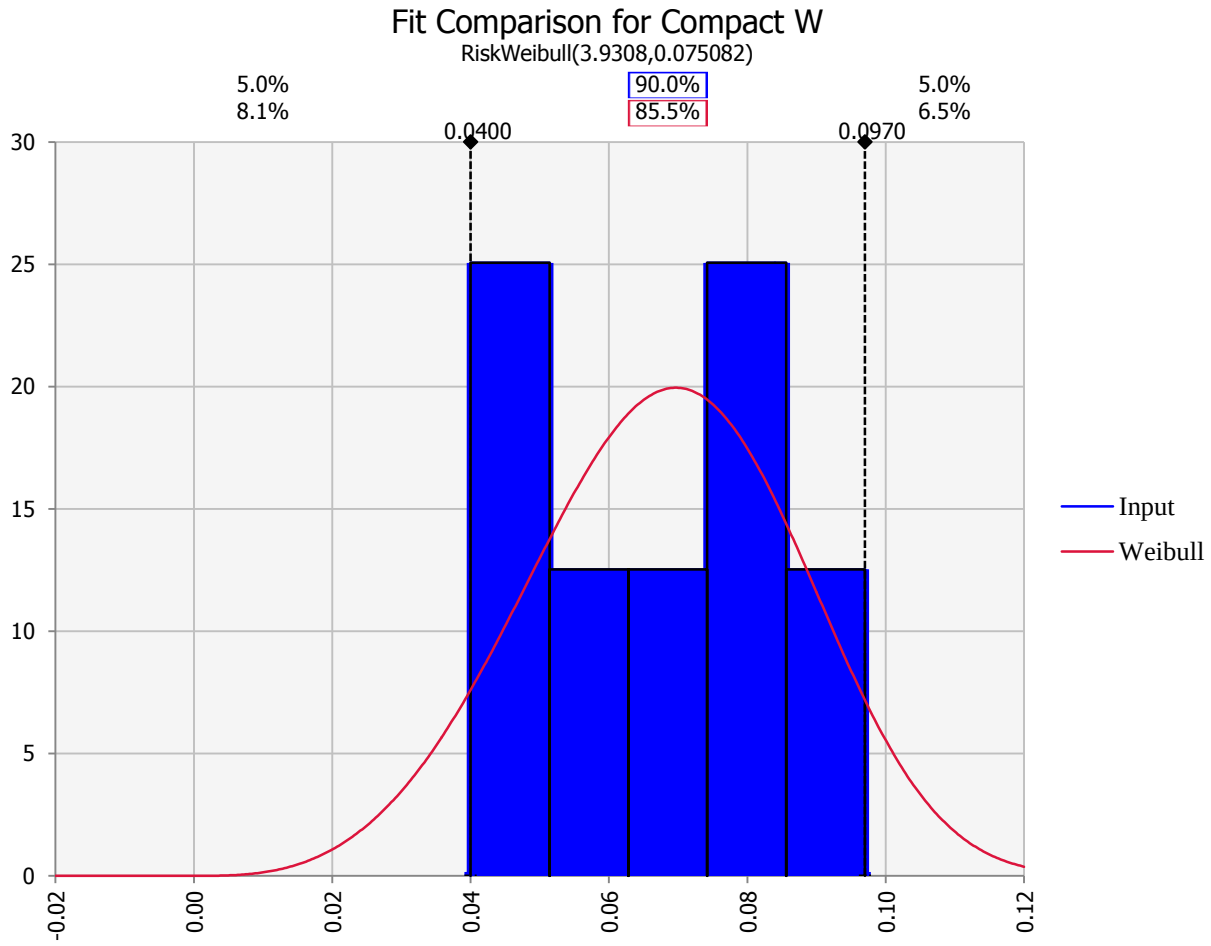

D.1.2.4 Medium classification

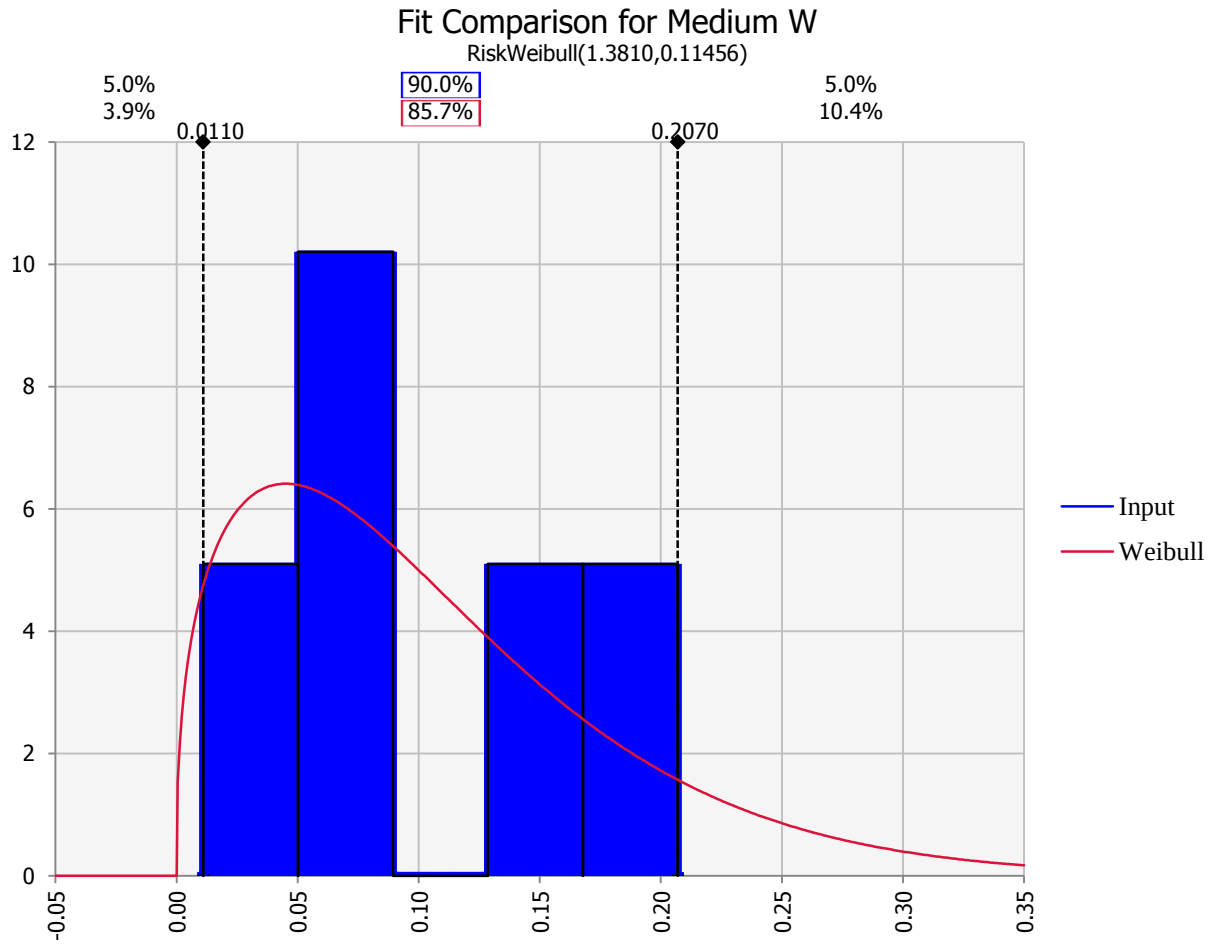

D.2 Application of simplified approach multiple vehicle experiments

D.2.1 Standard deviation boundary lines

This section presents application of simplified approach using standard deviation boundary lines.

D.2.1.1 Experiment B

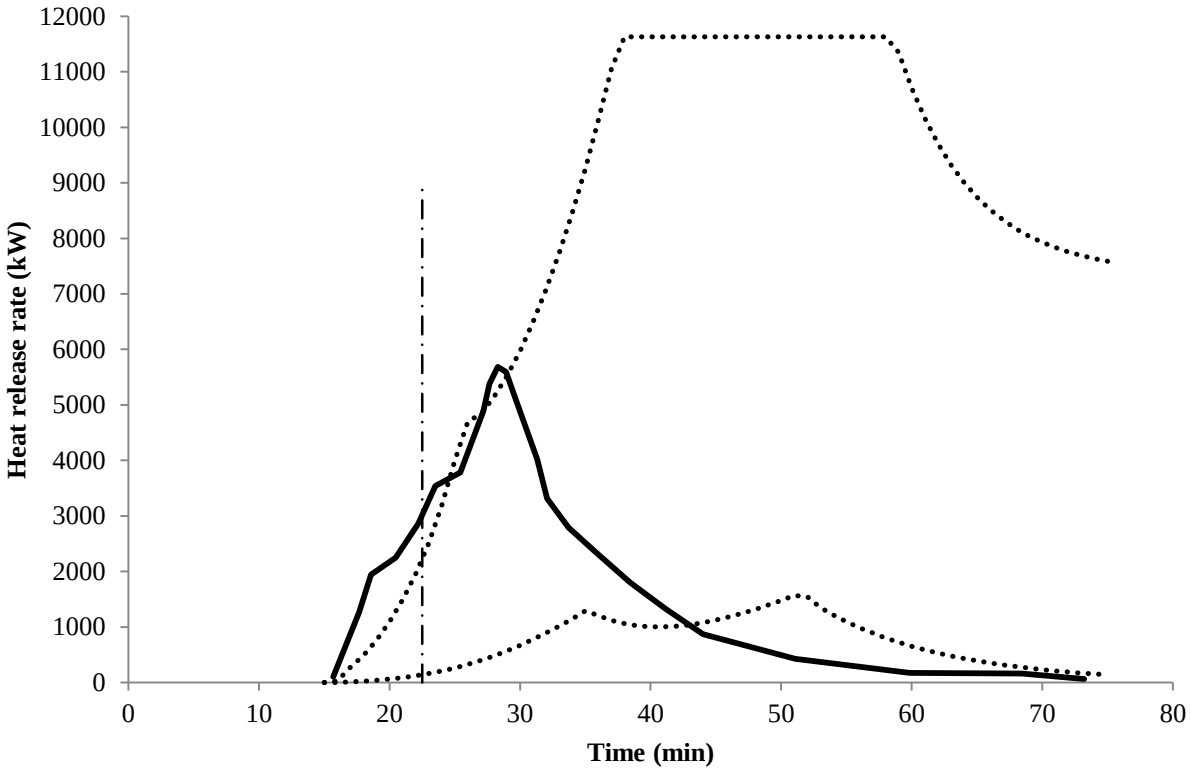

D.2.1.2 Experiment C

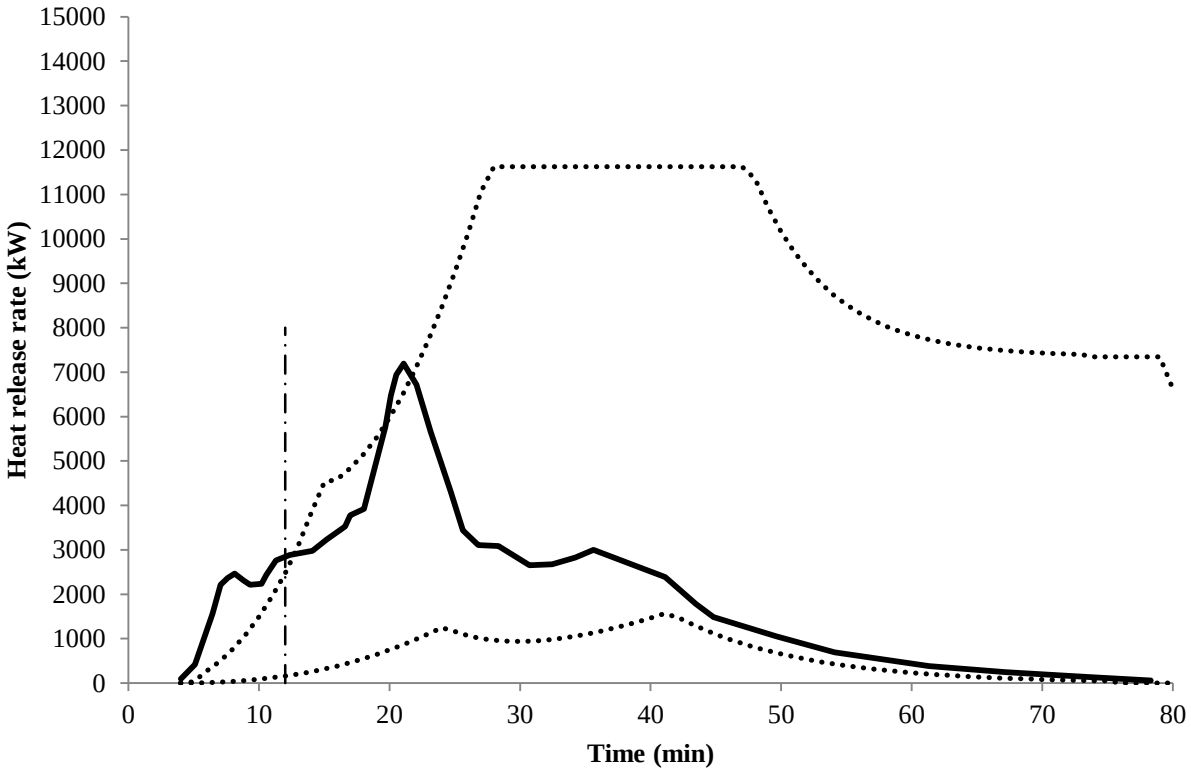

D.2.1.3 Experiment E

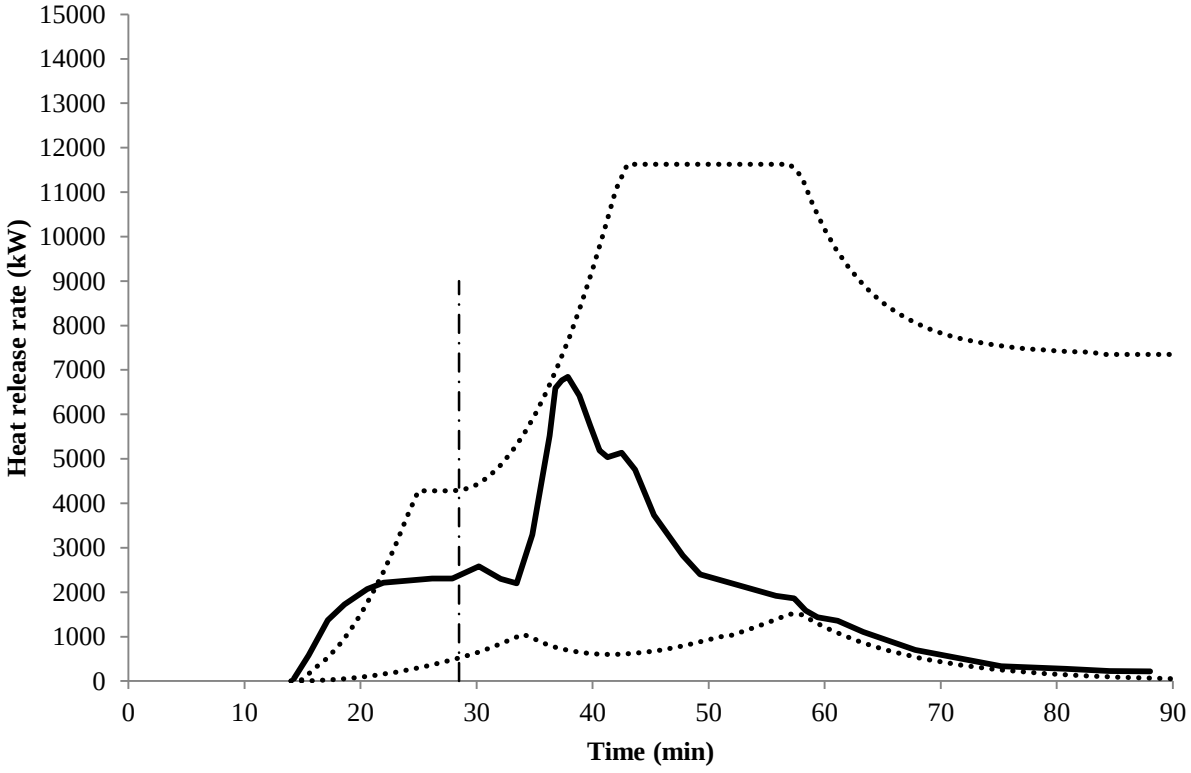

D.2.1.4 Experiment G

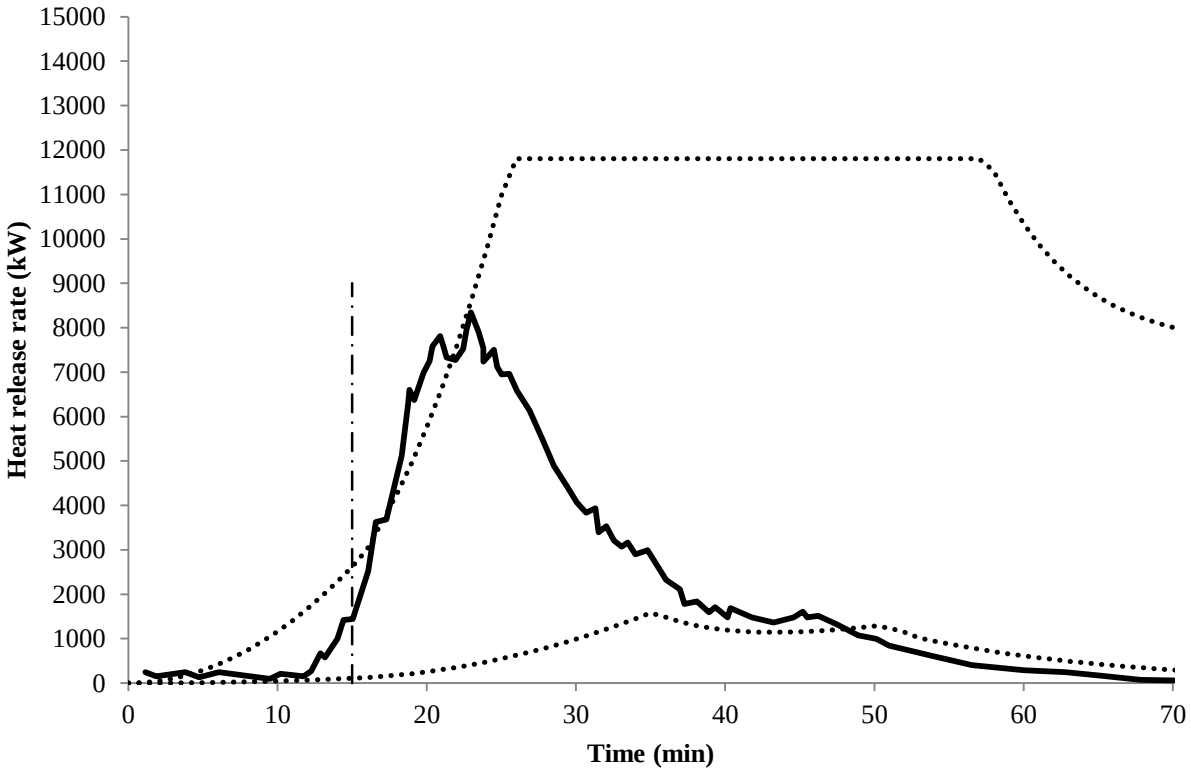

D.2.2 Standard deviation and 95th/5th percentile boundary lines

This section presents application of simplified approach using standard deviation and 95th/5th boundary lines.

D.2.2.1 Experiment A

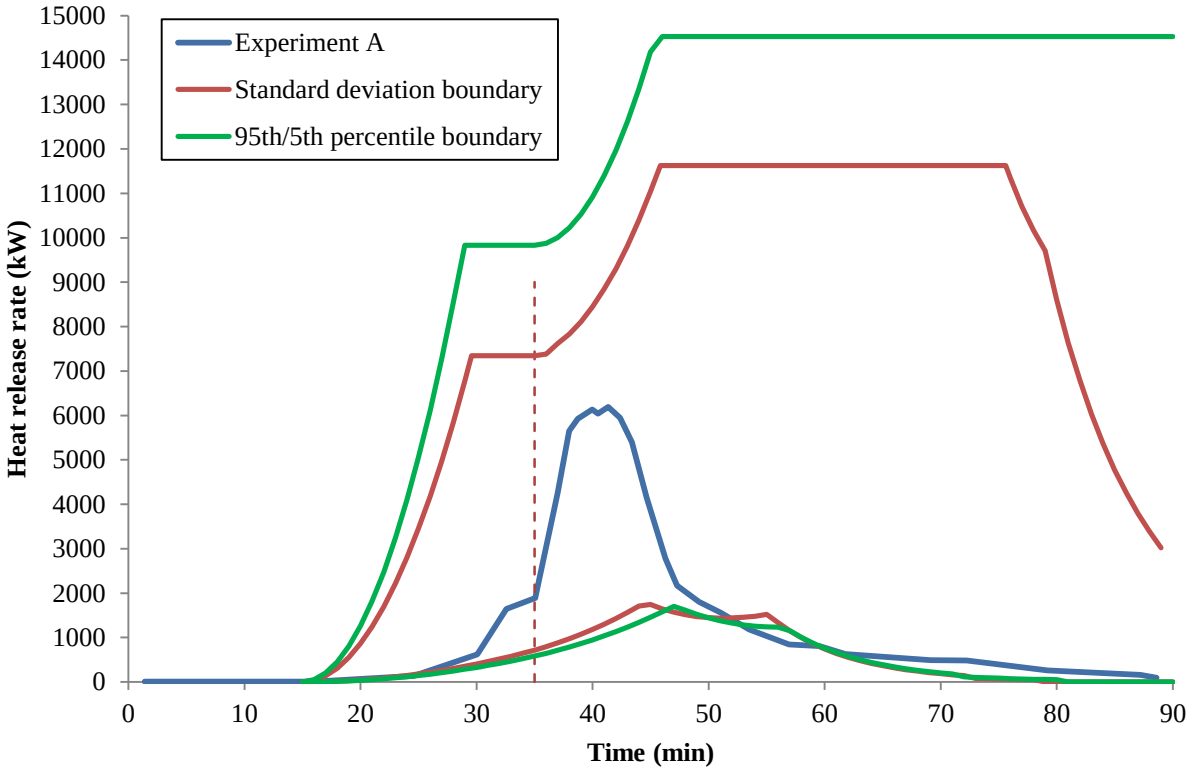

D.2.2.2 Experiment B

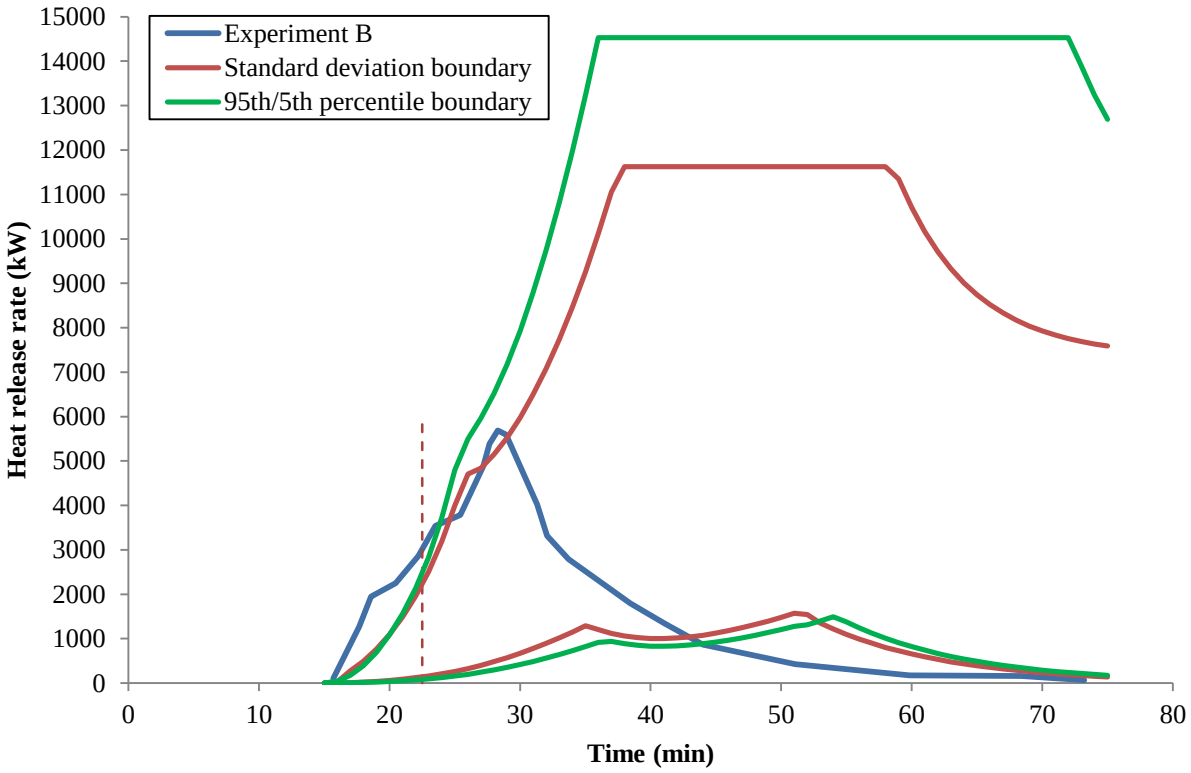

D.2.2.3 Experiment C

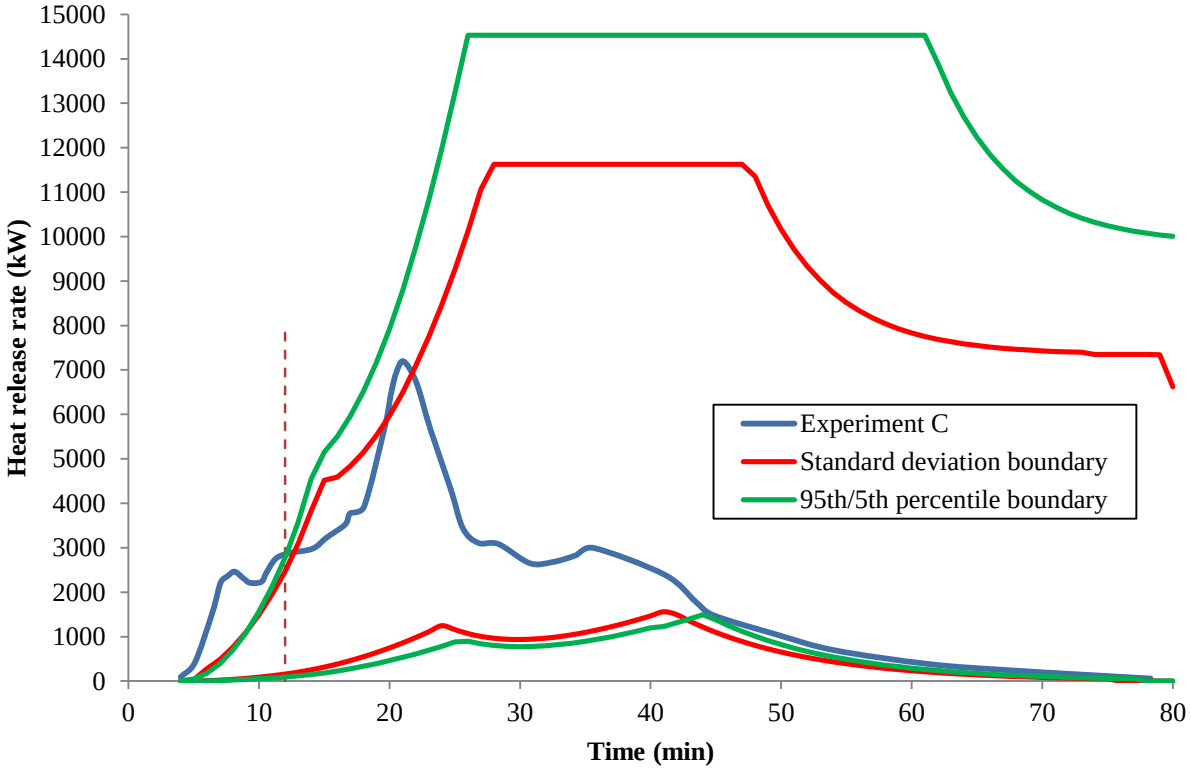

D.2.2.4 Experiment D

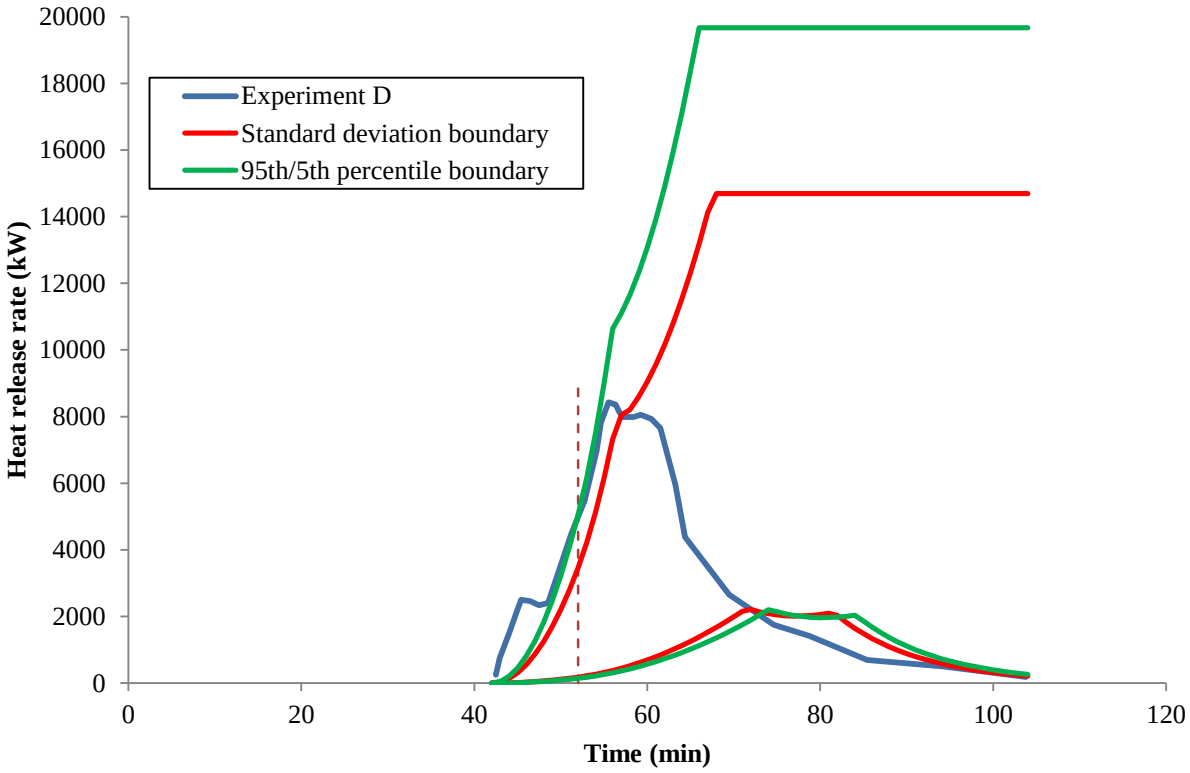

D.2.2.5 Experiment E

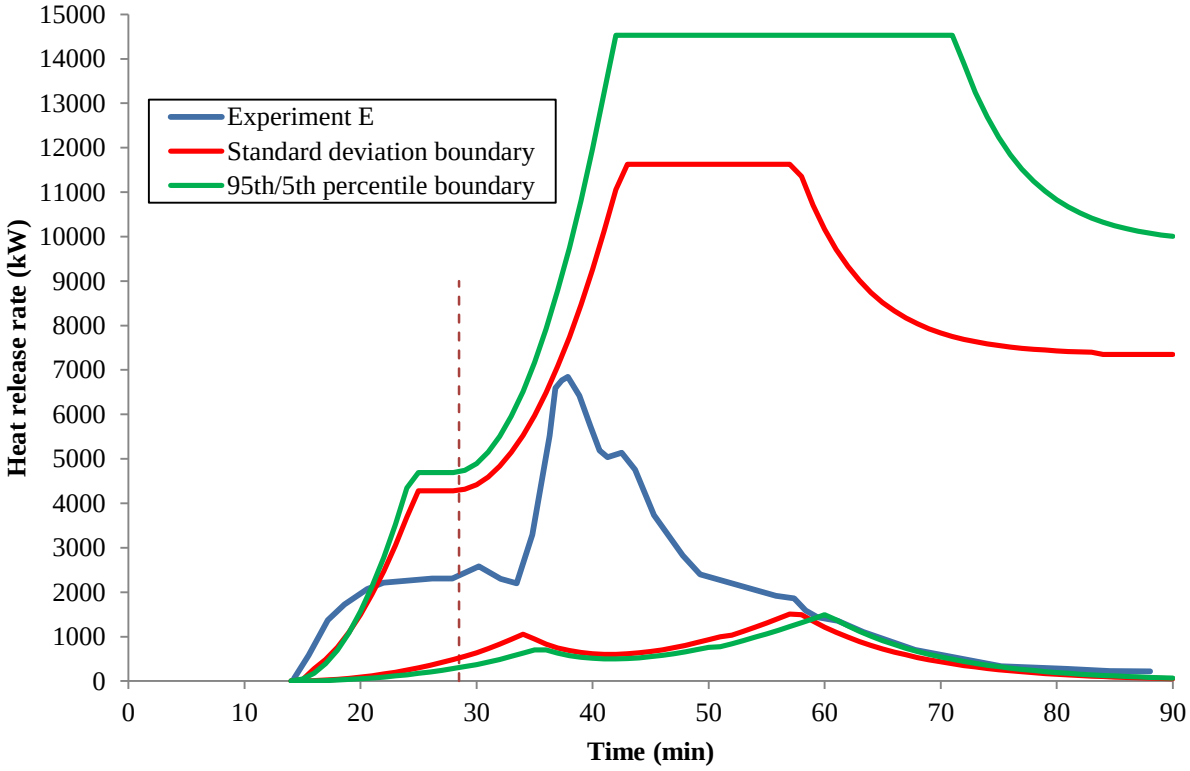

D.2.2.6 Experiment F

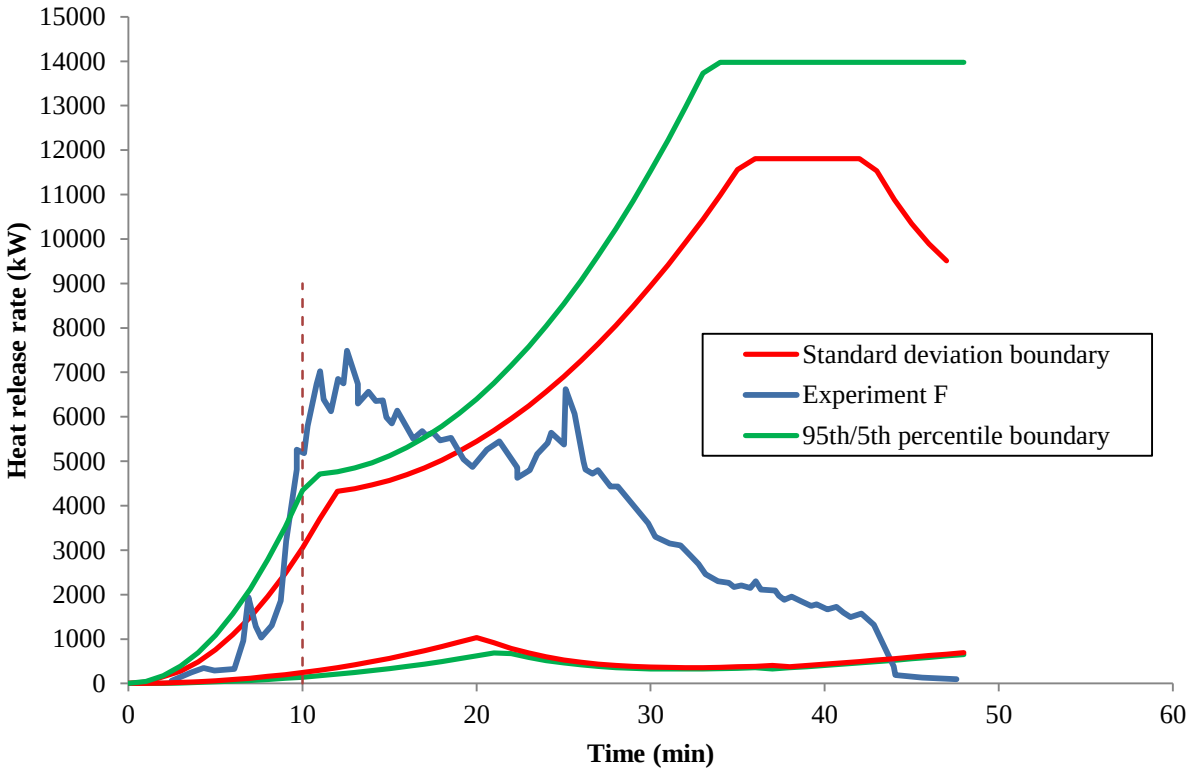

D.2.2.7 Experiment G

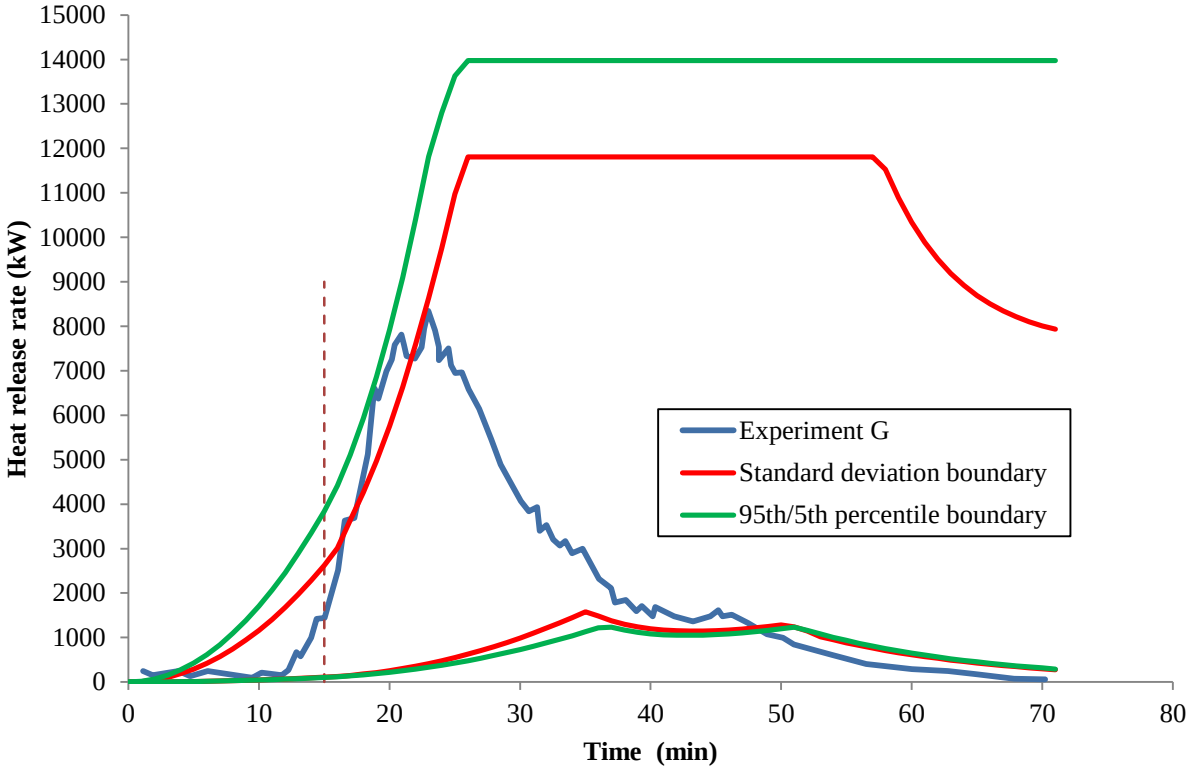

Appendix E

E.1 Alternative estimation of power law index

Alternatively, the power law index of the component/material can be calculated using thermal penetration time equation. Referring to the results from BRE cone calorimeter tests a power law index analysis is conducted on each material to estimate which power law index is suitable for each component. A thermal penetration time equation is used in order to decide whether a component should be treated as thermally thick, thermally thin or thermally intermediate. The equation is essentially the time required for a thermal pulse to reach the back face of the sample and is approximately equal to;

$$t_p = \frac{l^2}{16\alpha}$$

Equation E-1

where $\alpha = \frac{k}{\rho c}$, thermal diffusivity with k is the thermal conductivity, ρ is the density, c is the specific heat, and l is the material thickness.

The challenge in performing the analysis is that the information provided by the BRE cone calorimeter tests does not provide the exact composition of the materials. Thus, for mudflap and rubber tyre, properties for both natural and synthetic rubber are examined here, while for bumper trim and wheel arch, two different types of PVC; rigid and flexible are used. Table E-1 shows the assumed equivalent thermal properties for the materials in each of the components from the BRE cone calorimeter tests obtained from literature.

Table E-1:Thermal properties for materials

Material	***k*, W/m.K**	**ρ, kg/m³**	***c*, kJ/kg.K**	**α, m²/s × 10^{-7}**
Synthetic rubber	0.13	920	1.96	0.72
Natural rubber	0.14	920	1.55	0.98
PVC (rigid)	0.17	1255	1.38	0.98
PVC (flexible)	0.19	1415	0.98	1.34

Also, to perform the power law index analysis, the material thicknesses of each component are required. However, in the literature source, the material thicknesses of each of the components were not given. Therefore, assumed material thicknesses have to be made for each component. In this work, the thickness of a component was estimated by measuring the thickness for an assumed identical component in a regular passenger vehicle. However, to account for possible variation of thicknesses, measurements were done for several different vehicles of different make and models.

The results of the power law index analysis are shown in Table E-2. Using the different types of rubber for mudflap and rubber tyre, show minor differences in the range of penetration time where natural rubber is quicker in both cases. However, the difference in the range of penetration time does not change the fact that both can be considered as thermally intermediate (n = 1.5) due to the range of the estimated times taken to penetrate through the material. For the bumper trim and wheel arch, the use of different materials gives almost 40 s difference. Despite the 40 s difference, it is evident that both materials result in longer penetration times and hence, both can be considered as thermally thick (n = 2).

Table E-2: Power law index analysis

Component	**Estimated material thickness range, l (m)**	**Range of penetration time (s)**
Mudflap - Synthetic rubber	0.004 - 0.005	13.9 - 21.7
Mudflap - Natural rubber	0.004 - 0.005	10.2 - 15.9
Rubber tyre - Synthetic rubber	0.005 - 0.006	21.7 - 31.3
Rubber tyre - Natural rubber	0.005 - 0.006	15.9 - 23.0
Bumper trim - PVC (rigid)	0.01 - 0.015	63.8 - 143.5
Bumper trim - PVC (flex)	0.01 - 0.015	46.6 - 104.9
Wheel arch - PVC (rigid)	0.01 - 0.015	63.8 - 143.5
Wheel arch - PVC (flex)	0.01 - 0.015	46.6 - 104.9

As a result of the power law index and FTP analyses Table E-3 summarises the attributes for the components which are likely to be ignited first on a vehicle and these are used for the further evaluation of time to ignition.

Table E-3: FTP, power law index and critical heat flux values for selected components.

Component	**Power law index**	**FTP ($\frac{kW \cdot s^n}{m^2}$)**	**$\dot{q}''_{cr}$ (kW/m²)**
Mudflap	1.5	3258	5.7
Rubber tyre	1.5	9828	8.0
Bumper trim	2.0	21862	3.1
Wheel arch	2.0	50234	0.0

Appendix F

F.1 UCVFire simulation tool

This section presents the interfaces of the tool and the source code of the tool using Microsoft Visual Basic Application (VBA).

F.1.1 Interface of the tool

F.1.1.1 Front page of the tool

This is the page where the user enters all the important parameters.

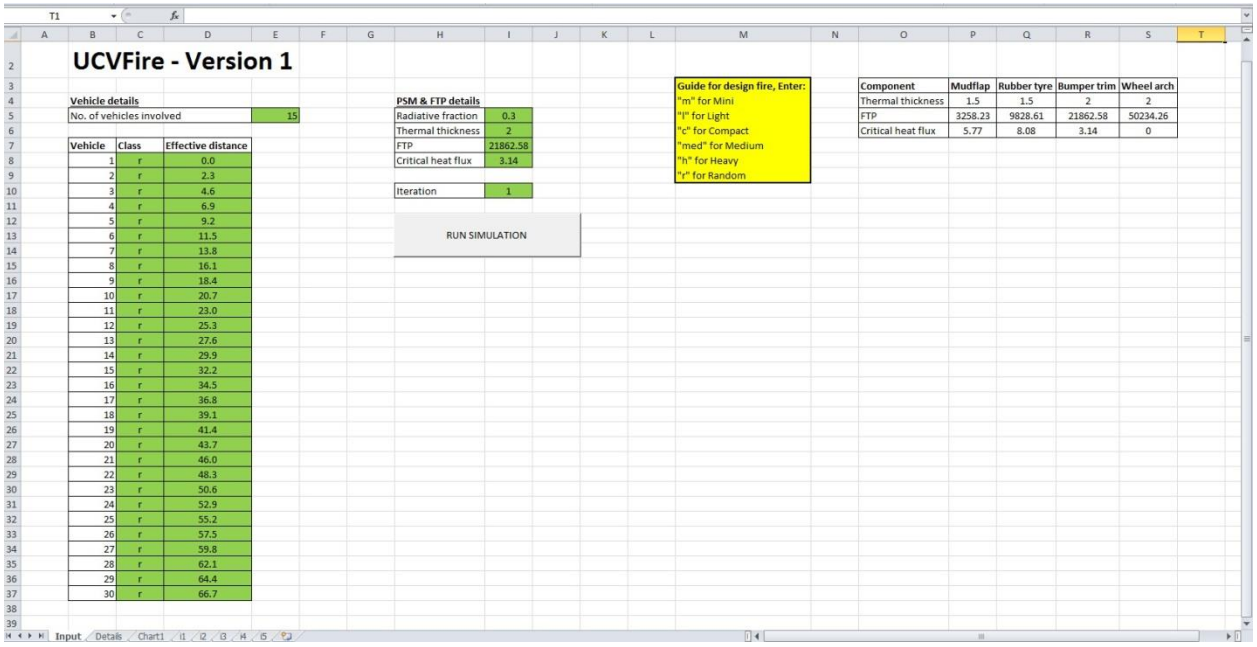

F.1.1.2 Details page of the tool

This is the page where the algorithm runs showing the random selection of fire growth coefficients, peak heat release rates, and fire decay coefficients for all vehicles involved.

Vehicle	Effective distance	Classification	Growth coefficient (kW/min²)	Peak HRR (kW)	Decay coefficient (min⁻¹)
1	0.0	Medium	0	0.0	0
2	2.3	Heavy	0	0.0	0
3	4.6	Light	0	0.0	0
4	6.9	Heavy	0	0.0	0
5	9.2	Compact	0	0.0	0
6	11.5	Heavy	0	0.0	0
7	13.8	Mini	0	0.0	0
8	16.1	Light	0	0.0	0
9	18.4	Medium	0	0.0	0
10	20.7	Mini	0	0.0	0
11	23.0	Compact	0	0.0	0
12	25.3	Heavy	0	0.0	0
13	27.6	Compact	0	0.0	0
14	29.9	Light	0	0.0	0
15	32.2	Medium	0	0.0	0
16	34.5		0	0.0	0
17	36.8		0	0.0	0
18	39.1		0	0.0	0
19	41.4		0	0.0	0
20	43.7		0	0.0	0
21	46.0		0	0.0	0
22	48.3		0	0.0	0
23	50.6		0	0.0	0
24	52.9		0	0.0	0
25	55.2		0	0.0	0
26	57.5		0	0.0	0
27	59.8		0	0.0	0
28	62.1		0	0.0	0
29	64.4		0	0.0	0
30	66.7		0	0.0	0

Input | Details | Chart1 | i1 | i2 | i3 | i4 | i5 | Result

F.1.1.3 Example output from a simulation run

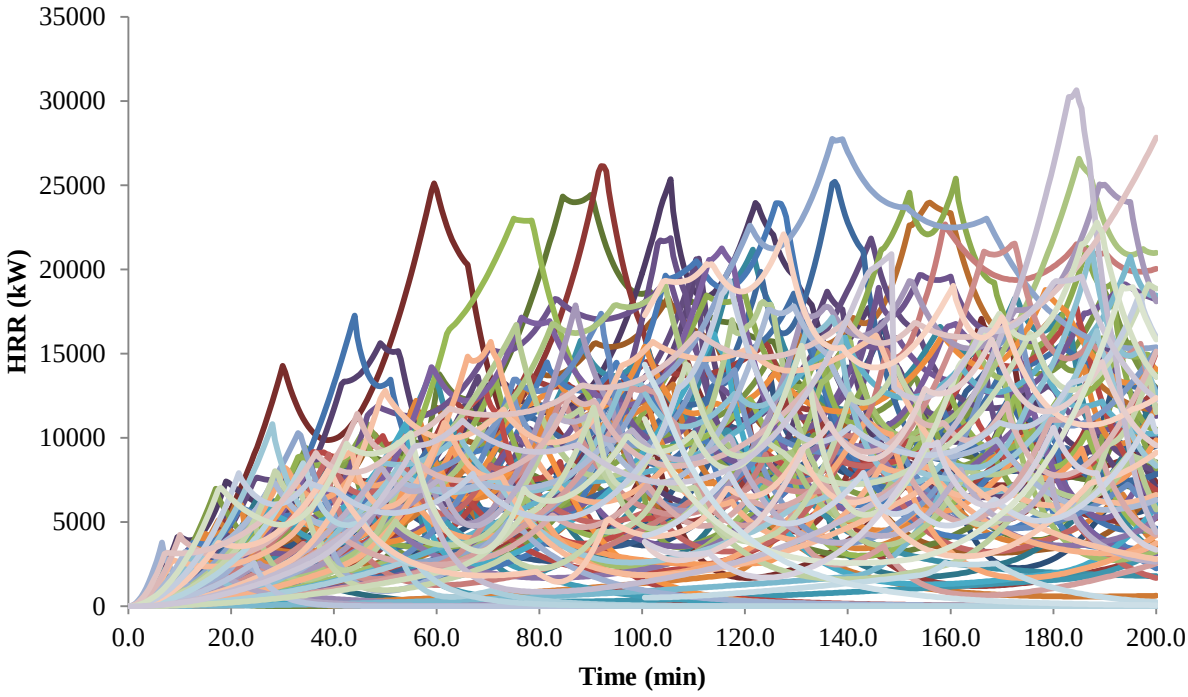

F.1.2 Source code of the tool

This section presents the source code of the UCVFire Simulation Tool.

```
Sub run_tool()

'******************** UCVFire Simulation Tool **********************

'*** Declaration ***
'All the variables in the program are declared in this section

Dim vehicles As Integer                 'No. of vehicles involved
Dim random As Integer                   'Random number for classification
selection
Dim iteration as integer                        'Iteration procedure

Dim growth                                'Growth coefficient variable
Dim peak                                  'Peak heat release rate variable
Dim decay                                 'Decay coefficient variable

'Clear the sheets from previous simulation

Worksheets("Details").Range("D3:G32").Value = ""
Worksheets("Details").Range("N3:T32").Value = 1

'*** Determine design fire for vehicles ***

'--- Iteration procedure ---
iteration_input = Worksheets("Input").Cells(10,9)      'No. of iterations
entered in the 'Input' page.

For iteration = 0 to iteration_input
```

```
vehicles = Worksheets("Input").Cells(5, 5) - 1

For eachveh = 0 To vehicles                         '

'-- Get the classification from the INPUT sheet --

Class = Worksheets("Input").Cells(8 + eachveh, 3)

If Class = "m" Then

        growth = Risk.Sample("RiskGamma(1.39,11.86)")
            peak = Risk.Sample("RiskWeibull(5.19,3809)")
            decay = Risk.Sample("RiskWeibull(0.93,0.17)")

        Worksheets("Details").Cells(3 + eachveh, 4) = "Mini"

ElseIf Class = "l" Then

        growth = Risk.Sample("RiskGamma(1.23,14.78)")
        peak = Risk.Sample("RiskWeibull(1.66,5078)")
        decay = Risk.Sample("RiskWeibull(1.21,0.11)")

        Worksheets("Details").Cells(3 + eachveh, 4) = "Light"

ElseIf Class = "c" Then

        growth = Risk.Sample("RiskGamma(1.18,5.14)")
        peak = Risk.Sample("RiskWeibull(2.4,5879)")
        decay = Risk.Sample("RiskWeibull(3.93,0.08)")

        Worksheets("Details").Cells(3 + eachveh, 4) = "Compact"

ElseIf Class = "med" Then

        growth = Risk.Sample("RiskGamma(2.24,2.75)")
        peak = Risk.Sample("RiskWeibull(3.18,7688)")
        decay = Risk.Sample("RiskWeibull(1.38,0.11)")

        Worksheets("Details").Cells(3 + eachveh, 4) = "Medium"

ElseIf Class = "h" Then

        growth = Risk.Sample("RiskGamma(1.51,1.82)")
        peak = Risk.Sample("RiskWeibull(3.11,8723)")
        decay = Risk.Sample("RiskWeibull(1.86,0.11)")

        Worksheets("Details").Cells(3 + eachveh, 4) = "Heavy"

ElseIf Class = "r" Then

random = Int((100) * Rnd)

        Select Case random

        Case 0 To 8

        growth = Risk.Sample("RiskGamma(1.39,11.86)")
            peak = Risk.Sample("RiskWeibull(5.19,3809)")
            decay = Risk.Sample("RiskWeibull(0.93,0.17)")

        Worksheets("Details").Cells(3 + eachveh, 4) = "Mini"
```

```
        Case 9 To 30

        growth = Risk.Sample("RiskGamma(1.23,14.78)")
        peak = Risk.Sample("RiskWeibull(1.66,5078)")
        decay = Risk.Sample("RiskWeibull(1.21,0.11)")

        Worksheets("Details").Cells(3 + eachveh, 4) = "Light"

        Case 31 To 57

        growth = Risk.Sample("RiskGamma(2.24,2.75)")
        peak = Risk.Sample("RiskWeibull(3.18,7688)")
        decay = Risk.Sample("RiskWeibull(1.38,0.11)")

        Worksheets("Details").Cells(3 + eachveh, 4) = "Compact"

        Case 58 To 84

        growth = Risk.Sample("RiskGamma(2.24,2.75)")
        peak = Risk.Sample("RiskWeibull(3.18,7688)")
        decay = Risk.Sample("RiskWeibull(1.38,0.11)")

        Worksheets("Details").Cells(3 + eachveh, 4) = "Medium"

        Case 85 To 99

        growth = Risk.Sample("RiskGamma(1.51,1.82)")
        peak = Risk.Sample("RiskWeibull(3.11,8723)")
        decay = Risk.Sample("RiskWeibull(1.86,0.11)")

        Worksheets("Details").Cells(3 + eachveh, 4) = "Heavy"
        End Select

End If

'*** Show Distribution properties for fire growth coefficient, peak heat
release rate, and decay coefficients in Details sheet ***

Worksheets("Details").Cells(3 + eachveh, 5) = growth
Worksheets("Details").Cells(3 + eachveh, 6) = peak
Worksheets("Details").Cells(3 + eachveh, 7) = decay

Next eachveh

'*** Collecting results from the iteration sheets to construct whole design
fire ***

For iteration2 = 0 To 600                                    'Collecting
results up to 600 minutes

Worksheets("Result").Cells(3 + iteration2, 2 + iteration) =
Worksheets("i5").Cells(9 + iterasisi, 16)

Next iteration2

Next iteration                                                'Next
iteration

End Sub
```

Appendix G

G.1 UCVFire simulation results

This section presents the results of each iteration (100 iterations) from the simulation of UCVFire for Scenario 1 and 2. The results shown here are the time between the arrivals of fire brigade until the time the fire boat start extinguishing the sixth vehicle (Vehicle 7). The observed time was 26 minutes.

G.1.1 Results for Scenario 1

Iteration	Time (min)
1	26.5
2	37.5
3	46.5
4	45.5
5	66.5
6	59.5
7	26.5
8	32.5
9	26.5
10	48.5
11	62.0
12	27.0
13	N/A
14	14.0
15	26.0
16	18.0
17	21.0
18	32.0
19	17.5
20	N/A
21	27.0
22	22.5
23	49.5
24	34.5
25	33.0
26	21.0
27	28.5
28	47.0
29	51.0
30	24.0
31	33.5

32	34.0
33	24.0
34	N/A
35	27.5
36	58.0
37	29.0
38	71.5
39	16.0
40	30.0
41	63.5
42	33.0
43	24.5
44	36.0
45	34.0
46	36.0
47	N/A
48	22.5
49	36.0
50	41.5
51	60.0
52	68.5
53	N/A
54	36.5
55	33.0
56	24.5
57	N/A
58	1.5
59	56.0
60	34.0
61	N/A
62	31.0
63	N/A
64	48.5
65	N/A
66	N/A
67	5.0
68	34.5
69	23.0
70	48.5
71	11.0
72	23.0
73	22.5
74	N/A
75	N/A
76	39.0

77	N/A
78	30.0
79	33.5
80	41.0
81	14.0
82	27.0
83	37.0
84	26.0
85	25.0
86	11.5
87	17.5
88	43.0
89	19.0
90	56.0
91	31.0
92	33.5
93	40.0
94	23.0
95	37.0
96	24.5
97	27.0
98	28.5
99	32.0
100	41.0

*N/A indicates that no result recorded probably due to fire was not able to spread

G.1.2 Results for Scenario 2

Iteration	Time (min)
1	44.0
2	40.5
3	40.0
4	33.5
5	48.5
6	N/A
7	39.0
8	43.0
9	33.0
10	38.5

11	N/A
12	63.0
13	49.5
14	58.5
15	34.5
16	53.0
17	N/A
18	32.5
19	47.5
20	56.0
21	41.5
22	38.0
23	61.5
24	40.0
25	28.5
26	49.0
27	54.5
28	35.0
29	46.0
30	47.5
31	53.5
32	42.0
33	31.5
34	41.5
35	35.0
36	53.5
37	47.0
38	45.0
39	41.0
40	N/A
41	40.5
42	41.5

43	N/A
44	38.0
45	44.0
46	42.0
47	N/A
48	N/A
49	48.5
50	48.0
51	33.5
52	32.5
53	N/A
54	51.0
55	40.5
56	66.0
57	44.0
58	63.5
59	40.0
60	43.0
61	N/A
62	53.0
63	46.0
64	32.5
65	44.0
66	35.5
67	44.5
68	51.5
69	46.0
70	44.0
71	35.5
72	61.5
73	46.5
74	N/A

75	N/A
76	31.5
77	N/A
78	47.0
79	N/A
80	43.5
81	35.0
82	37.0
83	54.0
84	45.5
85	35.0
86	40.5
87	46.0
88	34.5
89	47.5
90	46.5
91	45.5
92	35.0
93	45.0
94	39.0
95	46.0
96	39.0
97	44.0
98	38.5
99	39.0
100	34.0

*N/A indicates that no result recorded probably due to fire was not able to spread

Appendix H

H.1 Additional results for sensitivity analysis

This section presents the additional results for the sensitivity analysis that is not shown in Chapter 13.

H.1.1 Variation of parking occupancy as a function of tendency factor weightage

As a guide to look at the figures, in the figure legend ’70 wt’ means 70% tendency factor weightage ’80 wt’ means 80% tendency factor weightage, and ’90 wt’ means 90% tendency factor weightage.

H.1.1.150% parking occupancy

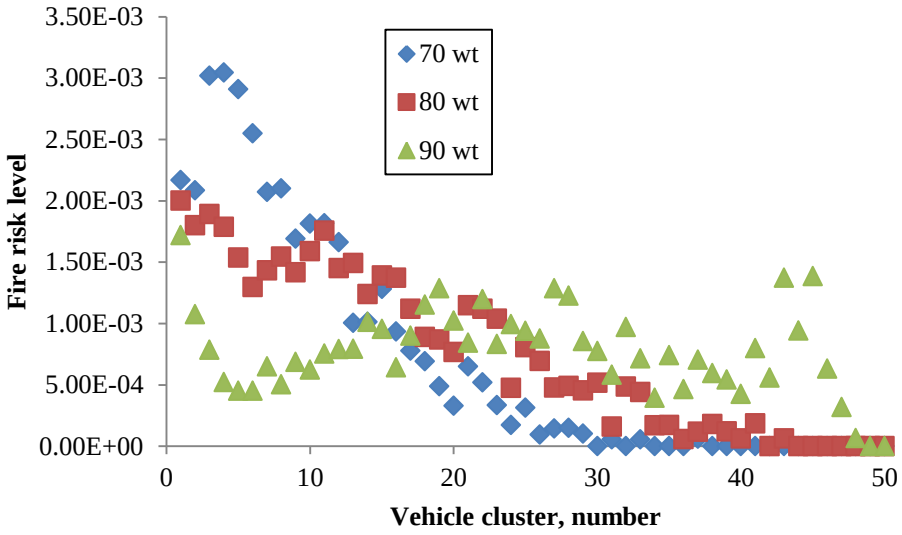

H.1.1.255% parking occupancy

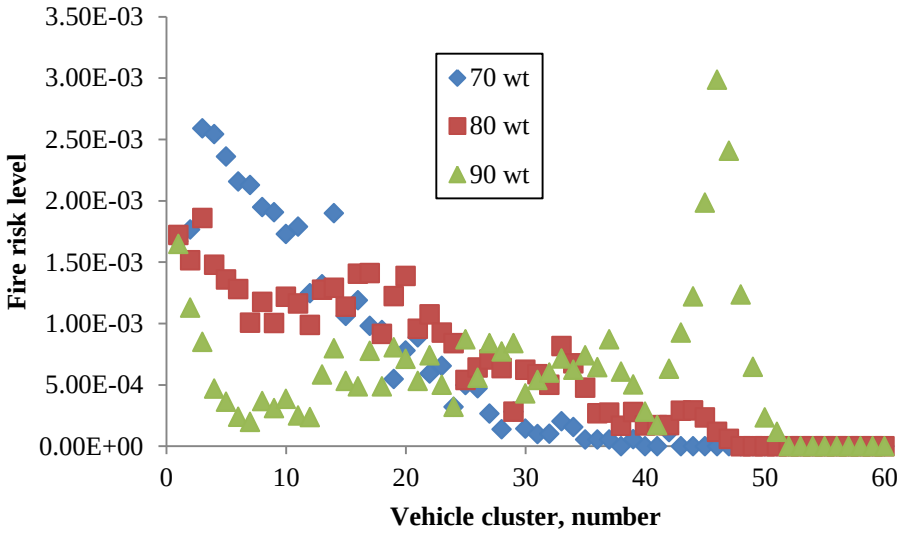

H.1.1.360% parking occupancy

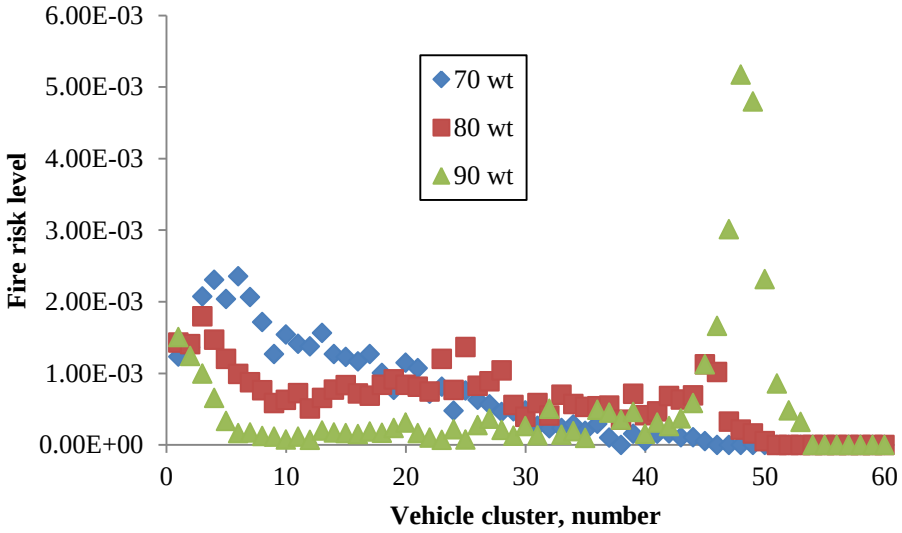

H.1.1.465% parking occupancy

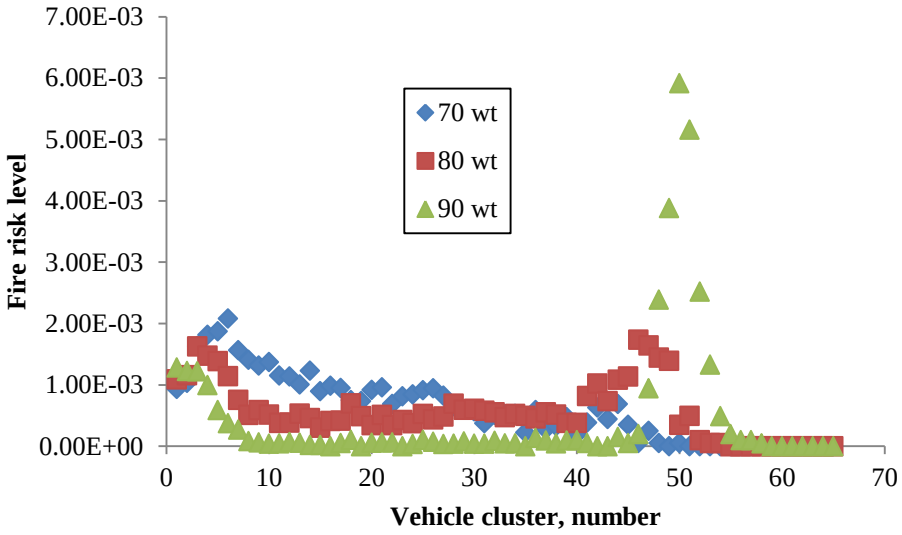

H.1.1.570% parking occupancy

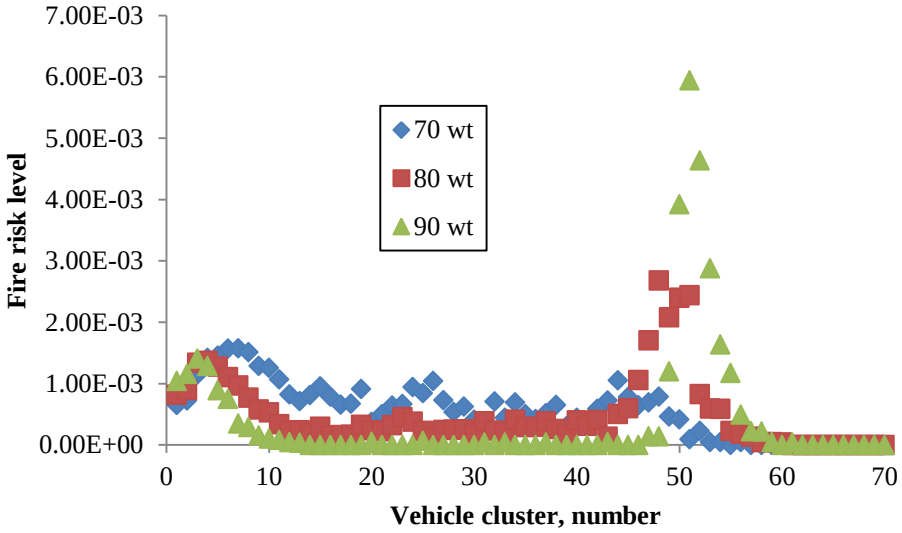

H.1.1.675% parking occupancy

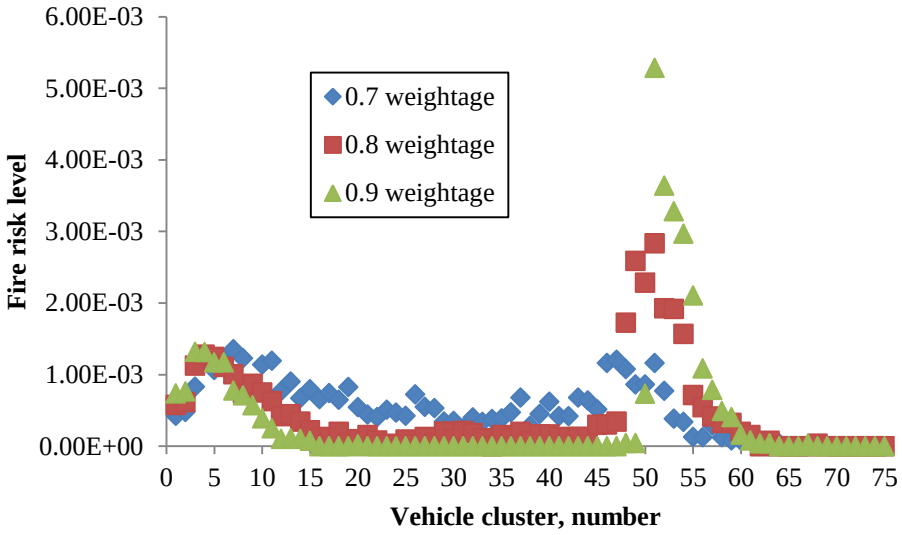

H.1.1.776% parking occupancy

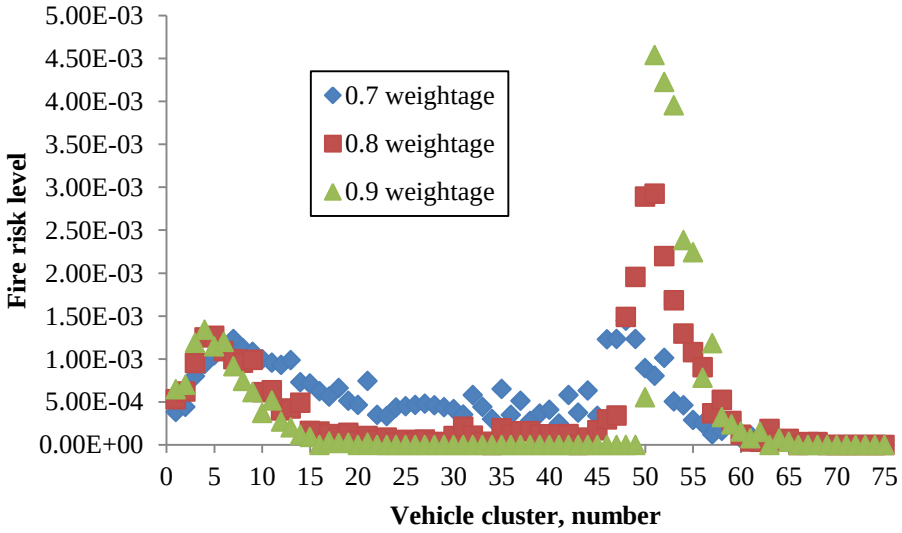

H.1.1.880% parking occupancy

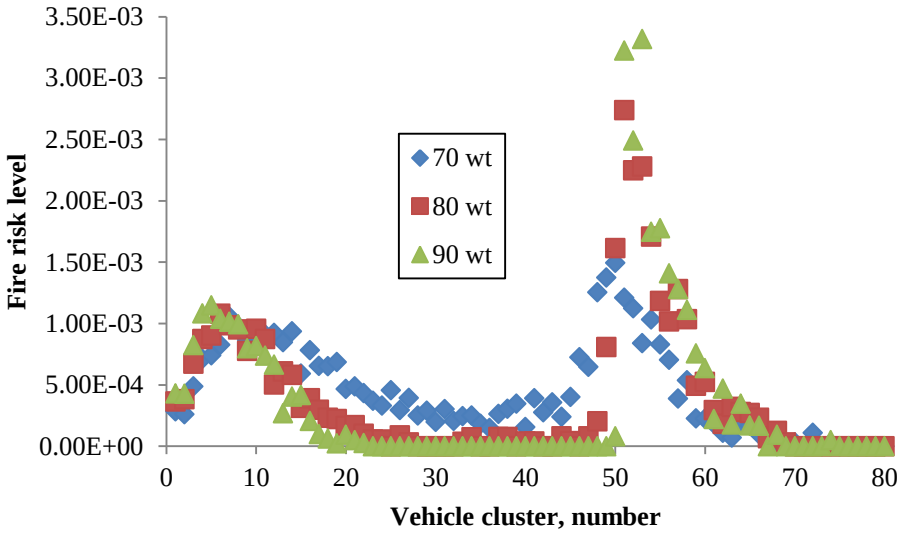

H.1.1.985% parking occupancy

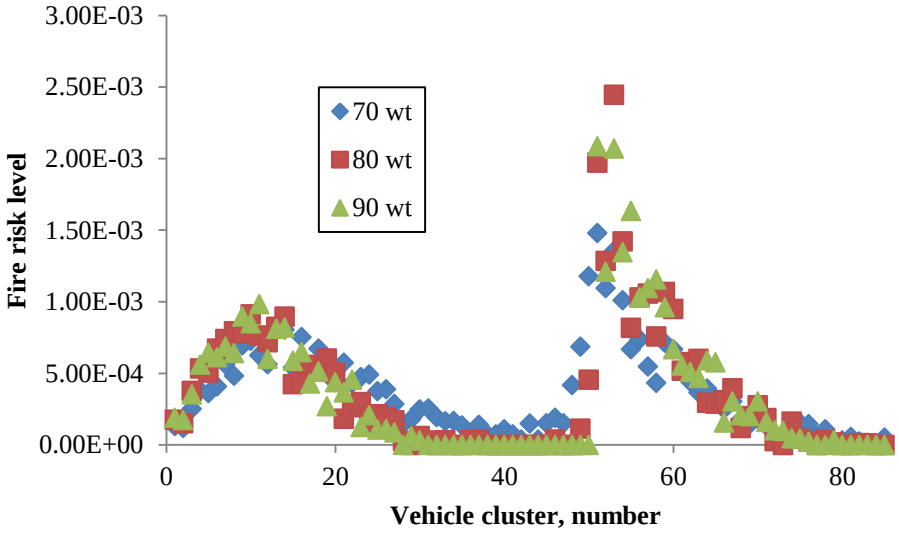

H.1.1.10 90% parking occupancy